Cranfield University

School of Water Sciences

PhD

2004

Peter Jarvis

The Impact of Natural Organic Matter on Floc Structure

Supervisors: Dr Simon A. Parsons and Dr Bruce Jefferson

October 2004

©Cranfield University, 2004. All rights reserved. No part of this publication may be reproduced without the written permission of the copyright holder.

This thesis is submitted in partial fulfilment of the requirements for the Degree of Doctor of Philosophy.

ABSTRACT

The removal of natural organic matter (NOM) at water treatment works (WTW) is essential in order to prevent toxic compounds forming during subsequent disinfection. Coagulation and flocculation processes remain the most common way of removing NOM. The properties of the resulting flocs that form are fundamental to the efficient removal of organic material. Periods of elevated NOM loads at WTW can lead to operational problems as a result of the deterioration in floc structural quality. Assessment of floc physical characteristics can therefore be a crucial tool in order to determine and predict solid-liquid removal performance at WTW. Here the growth, size, breakage, strength, re-growth, fractal dimension and settling velocity were measured for flocs formed from a NOM rich water source. NOM floc structural characteristics were measured and evaluated over a one year period in order to monitor the seasonal variation in floc structure. The results showed that a significant improvement in floc size and strength was seen during autumn and summer months. It was subsequently shown that as the organic fraction in the floc increases the floc size, settling velocity and fractal dimension all decrease. A model was proposed showing how these changes were dependent upon the adsorption of NOM onto primary particle surfaces. A range of different chemical coagulant treatment options were applied for NOM removal and the resulting floc structure compared. Considering both floc structure and optimum NOM removal the treatment systems were of the following order (best to worst): MIEX® + Fe > Fe > Fe + polymer > Al > polyDADMAC. NOM floc re-growth was shown to be limited for all the treatment systems investigated. The practical implications of the results were:

(1) The requirement for careful coagulant dosing or order to achieve optimum floc characteristics.

(2) The use of a pre-treatment anionic ion-exchange stage prior to coagulation.

(3) A comparison of alum and ferric based coagulants suggested the ferric coagulants gave better floc structure and improved NOM removal rates.

ACKNOWLEDGEMENTS

The work contained in this thesis was kindly sponsored by the UK Engineering and Physical Sciences Research Council (EPSRC), the American Water Works Association Research Foundation (AWWARF), Fort Collins Water (USA), Scottish Water, Severn Trent Water, Thames Water, United Utilities, Yorkshire Water and the University of Melbourne, without whom this thesis project would not have been possible. Special thanks go to Derek Wilson, Jenny Banks and Peter Hillis for their support and advice.

A big thank you to my supervisors Dr Simon Parsons and Dr Bruce Jefferson for their continued encouragement, positivity and opportunity to become the 'most travelled PhD student to date'! I would also like to thank Professor Peter Scales and Dr Dave Dixon for looking after me on my trip down under and teaching the benefits of a 'cleansing ale' and I'm sure Carlton will make the grand final one day!

Also, I would like to thank Aurelien Barbarit, Steve Wilson, Christina Schrewe and Jonathan Foong for their practical help during the crucial development stage of this work, the technicians and everyone in Team NOM and the School of Water Sciences for some good times.

A big thanks to my friends at Cranfield, especially: Adam and Amanda (for letting me stay), Pete H (for bringing the joy of chillies into my life), Simon (for providing a 'balanced' opinion and many James Bond thrashings) and also to Dave, Robin and Mike.

Special thanks to my mum and dad for their continual support and trips home to get away from it all and to my brother for sharing the travails of LFC over the past few years (it will get better soon). Also, to Digby for entertaining me for all these years.

Finally, to Amy for helping me through thick and thin and for putting up with me!

TABLE OF CONTENTS

LIST OF FIGURES

List of figures

LIST OF TABLES

ABBREVIATIONS AND NOTATION

Abbreviations

2D – Two dimensional

3D – Three dimensional

AOM – Aquagenic organic matter

AWWARF – American water works association research foundation

CCD – Close coupled device

CFD – Computational fluid dynamics

CFP – Central focusing point

Da – Daltons

DAF – Dissolved air flotation

DBP – Disinfection by-product

df – degrees of freedom

DI – De-ionised

DLVO – Deryagin Landau Verwey Overbeek

DOC – Dissolved organic carbon

FAF – Fulvic acid fraction

FI – Flocculation index

HPLC – High performance liquid chromatogram

HPSEC – High performance size exclusion chromatography

HRT – Hydraulic retention time

ID – Internal diameter

IEP – Isoelectric point

MIEX® – Magnetic ion exchange resin

MW – Molecular weight

NOM – Natural organic matter

NTU – Nephelometric turbidity units

PACl – Polyaluminium chloride

PC – Personal computer

PDA – Photometric dispersion analyser

polyDADMAC – Polydiallyldimethylammonium chloride

POM – Pedegenic organic matter

Abbreviations and notation

PSD – Particle size distribution

rpm – revolutions per minute

SALLS – Small angle laser light scattering

SUVA – Specific ultraviolet absorbance

THM – Trihalomethane

UV_{254} – Ultraviolet absorbance at 254 nm

WTW – Water treatment works

WWTW – Wastewater treatment works

Notation

α – Collision efficiency factor

δ – Floc binding strength, J m^{-2}

γ – Floc size exponent

σ – Floc strength, N m^{-2}

χ – Fundamental parameter for floc scattering (Lorenz-Mie theory)

ϕ – Power of ultrasonic field per floc volume and time, W m^{-3} s^{-1}

θ – Scattered angle, °

λ – Wavelength of incoming light/laser beam, m

γ – Floc size exponent

$\Delta\tau$ – Ultrasonification time, s

μ – Dynamic viscosity, kg m^{-2} s^{-1}

A – Floc projected area, m^2

$A(\beta)$ – Correction factor accounting for advection floc through floc

C – Floc strength coefficient

C' – Adapted floc strength coefficient

C_s – Cantilever stiffness, N m^{-1}

d – Floc diameter, m

D – Impeller diameter, m

$d(1)$ – Floc size after breakage, m

$d(2)$ – Floc size before breakage, m

$d(3)$ – Floc size after re-growth, m

d_{10} – 10 percentile equivalent diameter floc size, m

Abbreviations and notation

d_{50} – 50 percentile equivalent diameter floc size, m

d_{90} – 90 percentile equivalent diameter floc size, m

d_{95} – 95 percentile equivalent diameter floc size, m

d_a – Projected area diameter in stable orientation, m

d_{av} – Average floc diameter, m

d_c – Collector diameter, m

d_F – Feret's diameter, m

D_f – Floc fractal dimension

d_f – Free falling diameter, m

d_{fo} – Floc size before sonification, m

d_{hor} – Floc longest dimension in horizontal plane, m

d_i – Inscribing diameter, m

d_j – Floc size after sonification, m

d_l – Perimeter diameter, m

d_M – Martin's diameter, m

d_{max} – Maximum floc diameter, m

d_p – Primary particle diameter, m

d_{pr} – Projected area diameter in random orientation, m

d_s – Surface diameter, m

d_{sc} – Circumscribing diameter, m

d_{sv} – Surface-volume diameter, m

d_v – Volumetric diameter, m

d_{vert} – Floc longest dimension in vertical plane, m

F – Floc rupture force, N

f – Focal length of receiving lens, m

G – Velocity gradient, s^{-1}

G_{av} – Average velocity gradient, s^{-1}

G_{init} – Initial velocity gradient, s^{-1}

G_{max} – Maximum velocity gradient, s^{-1}

H – Cantilever deflection, m

h – Fitting constant for floc shear, s

i – Number of primary particles

$I(Q)$ – Intensity of scattered radiation

k – Proportionality constant, kg m^{-D}

Abbreviations and notation

K – Sensitivity of force transducer, N V^{-1}

L – Floc length, m

M – Floc mass, kg

m – Refractive index of particles

N – Impeller speed, rps

n – Refractive index of suspending medium

P – Floc perimeter, m

P_0 – Impeller power number

Q – Wave number, m^{-1}

R – Radial distance in focal plane, m

R_{agg} – Radius of floc, m

R_{br} – Rate of particle breakage

R_{col} – Rate of particle collision

R_{floc} – Rate of floc growth

R_{part} – Radius of primary particle, m

v – Kinematic viscosity, m s^{-1}

V – Volume, m^3

V_f – Volume of floc, m^3

V_l – Volume of liquid in floc, m^3

v_s – Terminal settling velocity, m s^{-1}

V_s – Volume of solids in floc, m^3

W – Voltage of force transducer, V

W_0 – Baseline voltage of the force transducer, V

X – Fundamental parameter for floc scattering (Fraunhofer theory)

y – Fitting parameter

ϵ – Energy dissipation, N m s^{-1} kg^{-1}

ζ – Zeta potential, mV

η – Kolmogoroff's microscale of turbulence, m

η_I – Filtration interception transport

ρ_f – Density of floc, kg m^{-3}

ρ_l – Density of liquid, kg m^{-3}

ρ_s – Density of solid in floc, kg m^{-3}

CHAPTER 1

INTRODUCTION

1 INTRODUCTION

1.1 Project background

Natural organic matter (NOM) removal is an essential requirement during water treatment in order to provide safe drinking water. Whilst NOM in itself is generally considered an innocuous mixture of compounds, it is the reaction of organic molecules with disinfection chemicals that can give rise to potentially harmful substances (Bolto *et al.*, 2004). Disinfection is necessary in order to kill pathogens and prevent their re-growth during mains water distribution. The reaction of NOM with chlorine (the most common water disinfectant) can lead to the formation of disinfection by-products (DBP's). The main groups of DBP's are the trihalomethanes and haloacetic acids which have been shown to be carcinogenic in animals (Dalvi *et al.*, 2000; Kimbrough and Suffet, 2002). For this reason, DBP levels are strictly controlled in drinking water in the UK and across the world by agencies such as the World Health Organisation, the Drinking Water Inspectorate (UK) and the United States Environmental Protection Agency. The main preventative measure against the formation of DBP's at water treatment works (WTW) is the removal of NOM prior to disinfection. Whilst a number of alternative treatment options have been employed, coagulation using metal salts remains the conventional treatment method for NOM removal (Odegaard *et al.*, 1999).

The addition of coagulant chemicals during water treatment removes pollutants from a water source by one or a number of the following: destabilisation; adsorption and entrapment. The resulting aggregates that form are composed of a complex matrix of coagulant and pollutants. These aggregates are known as flocs and are of non-uniform shape and composition whilst also being inherently fragile and therefore easy to break (Huang, 1994; Kim *et al.*, 2001). This makes measuring fundamental floc properties such as size, strength and settling rate difficult. However considerable effort has been made in this field using a range of techniques. A broad overview of some of these is shown in Table 1.1. As can be seen most research in this field has concentrated on activated sludge and turbidity dominated flocs. The work carried out on organic flocs has been generally limited to investigation of model humic acid solutions,

consequently there is a need to further evaluate organic dominated flocs from real NOM rich raw water sources.

Table 1.1 An overview of the methods used for evaluating floc structures.

Floc Parameter	Method	Floc type investigated	Reference
Size	Microscopy	Activated sludge Aluminium hydroxide Alum-latex beads	LI and Ganczarczyk (1986) Cornellissen *et al.* (1997) Spicer and Pratsinis (1996)
	Light scattering	Alum-latex beads Activated sludge	Spicer *et al.* (1998) Biggs and Lant (2000)
	Video/image analysis	Alum-latex beads	Chakraborti *et al.* (2003)
	Photometric dispersion analyser	Coagulants-kaolin Alum-raw water	Yukselen and Gregory (2004) McCurdy *et al.* (2004)
Settling velocity/density	Settling column	Alum-kaolin Estuarine sediment Activated sludge	Tambo and Watanabe (1979) Dyer and Manning (1999) Wu and Lee (1998)
Strength	Applied velocity gradient to floc suspension	Alum-kaolin Activated sludge Alum-organic	Francois (1987) Wu *et al.* (2003) Bache and Rasool (2001)
	Microscopic force for breakage	Calcium carbonate Latex	Yeung and Pelton (1996) Zhang *et al.* (1999)
Fractal dimension	Settling	Calcium phosphate Activated sludge	Tang *et al.* (2002) Wu *et al.* (2002)
	Microscopy	Activated sludge	Bellouti *et al.* (1997)
	Laser diffraction	Aluminium oxide Activated sludge	Waite *et al.* (1999) Guan *et al.* (1998)

1.2 Motivation for work

The work presented in this thesis forms part of a wider scoping American Water Works Association Research Foundation (AWWARF) tailored collaborative project on the 'Treatment of elevated organic content waters'. The main objectives of the overall project were to:

(1) Investigate the use of conventional and alternative coagulants for organic removal from low alkalinity waters specifically at high organic loads.

(2) Evaluate treatment strategies at pilot scale.

(3) Investigate the effect of organic content, coagulant & coagulation conditions on floc size, structure, strength, growth and break up.

The focus of this study concentrated on point (3) through the evaluation of NOM floc structural characteristics. A raw water source from the Albert reservoir on the outskirts of Halifax in the north of England was used as the representative water for the majority of coagulation experiments in this work. This water is typically of a high organic content and highly coloured and of low alkalinity and low turbidity. The character of the water changes seasonally with an increase in dissolved organic carbon (DOC) and ultra violet light absorbance at 254 nm (UV_{254}) absorbance during autumn and early winter (Figure 1.1). For example, during the summer months the DOC remains between 6-9 mg L^{-1} whilst in autumn this can increase up to 15 mg L^{-1}.

During periods of elevated organic concentration significant operational difficulties are seen at WTW. In addition to poor NOM removal and increased DBP formation, anecdotal evidence suggests that deterioration in floc structure is seen such that weak fragile flocs form that are poorly removed during solid-liquid separation processes. This leads to increased floc breakage and high solids loading on downstream filters and short filter run times. By providing a quantitative analysis of NOM flocs a more thorough knowledge of floc structure can be found. This will provide important understanding and validation of the operational problems seen whilst also providing potential solution options.

1.3 Project aims and objectives

The thesis aims to contribute to the field of floc structural characterisation with particular emphasis on NOM flocs. Initially the project looked at the development of techniques for quantifying floc structures. Once this had been achieved, the project focused on the:

(1) Seasonal variation in floc characteristics from a NOM rich water source.

(2) Impact of the ratio of coagulant to organic concentration on floc structure.

(3) Effect of different treatment options on NOM floc structure.

(4) The re-growth of NOM flocs.

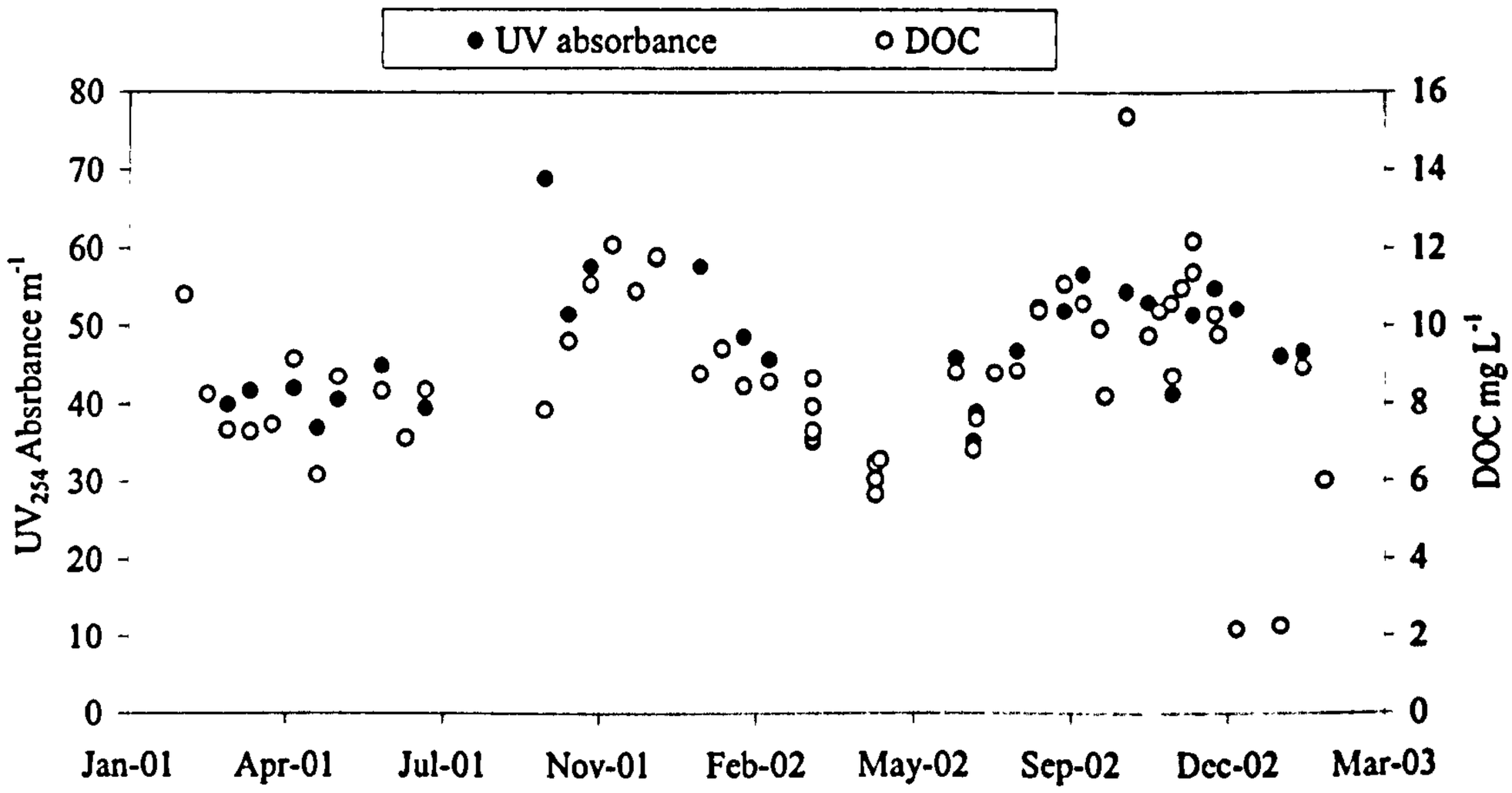

Figure 1.1 The seasonal change in UV_{254} absorbance and DOC of the raw water used in this study.

1.4 Thesis plan

The thesis is presented in paper format. An outline of each paper objective and the floc parameters reviewed or measured to meet each objective is shown in Table 1.2. The work begins with a review of the literature. This section was split into two sections with firstly an initial review of current knowledge on floc formation,

breakage and strength (Chapter 2(A) – submitted: *Jarvis, P., Jefferson. B., Gregory, J. and Parsons, S. A., A Review of Floc Strength and Breakage. Water Research*). The second section reviewed floc properties and how they can be measured (Chapter 2(B) – submitted: *Jarvis, P., Jefferson, B. and Parsons, S. A., Measuring Floc Structural Characteristics. Re/Views in Environmental Science and Bio/Technology*).

The technical content of the thesis is included in Chapters 3-7. Chapter 3 introduces the methods developed to analyse flocs in terms of floc size, breakage/strength, re-growth, settling velocity and fractal dimension. The first paper in Chapter 3 was published in: *Jarvis, P., Jefferson, B., Jarvis, and Parsons, S. A. (2004) The duplicity of floc strength. Water Science and Technology*. The second paper was published in: *Jarvis, P., Jefferson, B. and Parsons, S. A. (2003) The use of diagnostic tools to determine the operational properties of organic flocs. Proceedings of the AWWA Water Quality and Technology Conference, Philadelphia, USA*. Whilst the two papers in this chapter offered some explanation for the observations seen, their principal aim was showing development of methods to analyse floc structures. Once these methods had been developed, similar experimental protocols were used in the proceeding work in order to investigate the impact of a number of variables on NOM floc properties. Chapter 4 investigated the impact on floc structure of seasonal changes in the raw NOM rich water source (published in: *Jarvis, P., Jefferson, B. and Parsons, S. A. (2004) Characterising natural organic matter flocs. Water Science and Technology*). This was achieved by taking water samples over a year period and investigating the floc properties formed at coagulant doses used by the WTW. Following the findings of this study, Chapter 5 explored the effect on floc structure of increasing the proportion of NOM within the floc matrix by incrementally increasing the ratio of NOM to coagulant. This paper has been submitted: *Jarvis, P., Jefferson, B. and Parsons, S. A., How the Natural Organic Matter to Coagulant Ratio Impacts on Floc Operational Properties. Journal of Colloid and Interface Science*. Chapter 6 looked at how changing the treatment options impacted on floc structure. The first paper in this chapter investigated the use of a floc aid on floc structure and has been submitted: *Jarvis, P., Jefferson, B. and Parsons, S. A., Floc structural characteristics using conventional coagulation for a high doc, low alkalinity surface water source. Water Research*. The second paper examined the use of a range of coagulants and pre-treatment options and the findings have been submitted: *Jarvis, P., Jefferson, B.,*

Dixon, D. and Parsons, S. A., The Impact on NOM Floc Structure Using Different Treatment Options. Journal of the American Water Works Association. Finally, Chapter 7 attempted to compare NOM flocs with other types of floc through comparison of size, breakage, re-growth and fractal dimension (published in *Jarvis, P., Jefferson, B. and Parsons, S. A. (IN PRESS) The breakage, re-growth and fractal nature of different coagulated systems. Environmental Science and Technology*). The combined findings of the papers are then summarised in Chapter 8.

It should be noted that whilst each paper investigated specific impacts on floc structure, a common theme through a number of the papers was the coagulant precipitate. This was deemed important to include because it offered an 'absence of NOM' control for a number of the experiments presented. The work presented in the Appendix shows method validation and the repeatability of floc experimental work.

Table 1.2. The main objectives of the papers of the thesis and how they fit together.

	Chap. 2(A) Paper 1	Chap 2(B) Paper 2	Chap 3(A) Paper 3	Chap 3(B) Paper 4	Chap 4 Paper 5	Chap 5 Paper 6	Chap 6(A) Paper 7	Chap 6(B) Paper 8	Chap 7 Paper 9
Principle objective of paper	Review of literature – floc strength and breakage	Review of literature – measuring floc structure	Method development	Method development	Seasonality impacts	DOC:Fe ratio	Treatment options – Floc aid	Treatment options – Different coagulants	Floc breakage, re-growth and fractal dimension
Floc parameters investigated									
Size		✓	✓	✓	✓	✓	✓	✓	✓
Settling		✓	✓	✓	✓	✓	✓	✓	
Fractal dimension		✓	✓	✓		✓	✓		✓
Strength/breakage	✓		✓	✓	✓		✓	✓	✓
Re-growth	✓		✓				✓		✓
Organic in floc matrix					✓	✓			

1.5 References

Bellouti, M., Alves, M. M., Novais, J. M. and Motta, M. (1997) Flocs vs Granules: Differentiation by Fractal Dimension. *Water Research* **31** 1227-1231.

Biggs, C. A. and Lant, P. A. (2000) Activated Sludge Flocculation: On-Line Determination of Floc Size and the Effect of Shear. *Water Research* **34** 2542-2550.

Bolto, B., Dixon, D. and Eldridge, R. (2004) Ion Exchange for the Removal of Natural Organic Matter. *Reactional and Functional Polymers* **60** 171-182.

Chakraborti, R. K., Gardner, K. H., Atkinson, J. F. and Van Benschoten, J. E. (2003) Changes in Fractal Dimension During Aggregation. *Water Research* **37** 873-883.

Cornelissen, A., Burnett, M. G., McCall, R. D. and Goddard, D. T. (1997) The structure of hydrous flocs prepared by batch and continuous flow water treatment systems and obtained by optical, electron and atomic force microscopy. *Water Science and Technology* **36** (4), 41-48.

Dalvi, A. G. I., Al-Rasheed, R. and Javeed, M. A. (2000) Haloacetic Acids (HAAs) Formation in Desalination Processes from Disinfectants. *Desalination* **129** (3), 261-271.

Dyer, K. R. and Manning, A. J. (1999) Observation of the Size, Settling Velocity and Effective Density of Flocs and their Fractal Dimensions. *Journal of Sea Research* **41** 87-95.

Guan, J., Waite, T. D. and Amal, R. (1998) Rapid Structure Characterisation of Bacterial Aggregates. *Environmental Science and Technology* **32** 3735-3742.

Huang, H. (1994) Fractal Properties of Flocs Formed by Fluid shear and Differential Settling. *Physical Fluids* **6** (10), 3229-3234.

Kim, S. H., Moon, B. H., and Lee, H. I. (2001) Effects of pH and Dosage on Pollutant Removal and Floc Structure During Coagulation. *Microchemical Journal* **68** 197-203.

Kimbrough D. E. and Suffet, I. H. (2002) Electrochemical Removal of Bromide and Reduction of THM Formation Potential in Drinking Water. *Water Research* **36** 4902-4906.

Li, D. H. and Ganczarczyk, J. J. (1986) Physical Characteristics of Activated Sludge Flocs *CRC Critical Reviews in Environmental Control* **17** (1), 53-87.

McCurdy, K., Carlson, K. and Gregory, D. (2004) Floc Morphology and Cyclic Shearing Recovery: Comparison of Alum and Polyaluminium Chloride Coagulants. *Water Research* **38** 486-494.

Ødegaard, H., Eikebrokk, B. and Storhaug, R. (1999) Processes for the Removal of Humic Substances from Water - an Overview Based on Norwegian Experiences. *Water Science and Technology* **40** (9), 37–46.

Spicer, P. T., Pratsinis, S. E., Raper, J., Amal, R., Bushell, G., and Meesters, G. (1998) Effect of Shear Schedule on Particle Size, Density and Structure During Flocculation in Stirred Tanks. *Powder Technology* **97** 26-34.

Spicer, P. T. and Pratsinis, S. E. (1996) Shear-Induced Flocculation: the Evolution of Floc Structure and the Shape of the Size Distribution at Steady State. *Water Research* **3** 1049-1056.

Tambo, N. and Watanabe, Y. (1979) Physical Characteristics of Flocs – I. The Floc Density Function and Aluminium Floc. *Water Research* **13** 409-419.

Tang, P., Greenwood, J. and Raper, J. A. (2002) A Model to Describe the Settling Behavior of Fractal Aggregates. *Journal of Colloid and Interface Science* **247** 210-219.

Waite, T. D., Cleaver, J. K. and Beattie, J. K. (2001) Aggregation Kinetics and Fractal Structure of γ-Alumina Assemblages. *Journal of Colloid and Interface Science* **241** 333-339.

Wu, C. C., Wu, J. J., and Huang, R. Y. (2003) Floc Strength and Dewatering Efficiency of Alum Sludge. *Advances in Environmental Research* **7** 617-621.

Wu, R. M. and Lee, D. J. (1998) Hydrodynamic Drag Force Exerted on a Moving Floc and its Implication to Free-Settling Tests. *Water Research* **32** 760-768.

Wu, R. M., Lee, D. J., Waite, T. D. and Guan, J. (2002) Multilevel Structure of Sludge Flocs. *Journal of Colloid and Interface Science* **252** 383-392.

Yeung, A. K. C. and Pelton, R. (1996) Micromechanics: A New Approach to Studying the Strength and Breakup of Flocs. *Journal of Colloid and Interface Science* **184** 579-585.

Yukselen, M. A. and Gregory, J. (2004) The Reversibility of Floc Breakage. *International Journal of Mineral Processing* **73** 251-259.

CHAPTER 2

LITERATURE REVIEW:

2(A) A REVIEW OF FLOC STRENGTH AND BREAKAGE

Submitted to *Water Research.*

2(B) MEASURING FLOC STRUCTURAL CHARACTERISTICS

Submitted to *Re/Views in Environmental Science and Bio/Technology.*

2(A) A REVIEW OF FLOC STRENGTH AND BREAKAGE

PETER JARVIS[1], BRUCE JEFFERSON[1], JOHN GREGORY[2] and SIMON A. PARSONS[1]

[1]*School of Water Sciences, Cranfield University, Cranfield, Bedfordshire, MK40 0AL, UK.*

[2]*Dept. of Civil and Environmental Engineering, University College London, Gower Street, London, WC1E 6BT, UK*

Abstract

The main focus of the paper is to review current understanding of floc structure and strength. This has been done by reviewing current theoretical understanding of floc growth and breakage and an analysis of different techniques used for measuring floc strength. An overview has also been made of the general trends seen in floc strength analysis. The rate of floc formation is a balance between breakage and aggregation with flocs eventually reaching a steady state size for a given shear. The steady state floc size for a particular shear can therefore be a good indicator of floc strength. This has resulted in the development of a range of techniques to measure floc size at different applied shear levels using a combination of one or more of the following tools: light scattering and transmission; microscopy; photography; video and image analysis software. Floc strength may be simply quantified using the initial floc size for a given shear and the floc strength factor. More complex techniques have used theoretical modelling to determine whether flocs break by large scale fragmentation or smaller scale surface erosion effects, although this interpretation is open to debate. Impeller based mixing, ultrasound and vibrating columns have all been used to provide a uniform, accurate and controllable dissipation of energy onto a floc suspension to determine floc strength. Other more recent techniques have used sensitive micromanipulators to measure the force required to break or compress individual flocs, although these techniques have been limited to the measurement of only a few hundred flocs. General trends emerge showing that smaller flocs tend to have greater strength than larger flocs, whilst the use of polymer seems to give

increased strength to only some types of floc. Finally, a comparison of the strength of different types of floc (activated sludge flocs, organic matter flocs, sweep flocs and charge neutralised flocs) has been made highlighting differences in relative floc strength.

Keywords

Floc, breakage, growth, re-growth, shear, strength

2(A).1 Introduction

Floc strength is a particularly important operational parameter in solid/liquid separation techniques for the efficient removal of aggregated particles. Unit processes at water treatment works (WTW) are generally designed to minimise floc breakage, however in reality often this is not the case, with regions of high shear being prevalent (McCurdy *et al.*, 2004). This may include regions around the impeller zone of flocculating tanks, processes such as dissolved air flotation (DAF) or transfer over weirs and ledges and through pumps. Flocs are therefore exposed to a range of stresses. Flocs must resist these stresses if they are to prevent being broken into smaller particles. In an operational sense, this is important because small particles generally have lower removal efficiencies (Boller and Blaser, 1998). Smaller particles will generally settle more slowly than larger particles of similar density. Flocs formed for removal in dissolved air flotation that subsequently break up into many smaller parts may be captured less efficiently by air bubbles. In addition, flocs that are removed using membrane filtration will foul membranes if small pieces of floc break off and plug membrane pores.

Floc strength is dependent upon the interparticle bonds between the components of the aggregate (Parker *et al.*, 1972; Bache *et al.*, 1997). This includes the strength and number of individual bonds within the floc. Therefore a floc will break if the stress applied at its surface is larger than the bonding strength within the floc (Boller and Blaser, 1998). Increased floc compaction is considered to increase floc strength due to an increase in the number of bonds holding the aggregate together. Leentvaar and Rebhun (1983) also list the size and shape of floc microparticles as being an important consideration for floc strength.

However, the development of a satisfactory technique to quantify floc strength has proven to be difficult. This is partly due to the inherent complexity, fragility and variation in floc size, shape and composition and also due to a generally accepted view that there are two modes of floc rupture (Parker *et al.*, 1972; Francois, 1987; Yeung and Pelton, 1996; Mikkelsen and Keiding, 2002). These have been classified as **surface erosion** and **large-scale fragmentation.** Surface erosion is the removal of small particles from the floc surface resulting in an increase in the small particle size

ranges. Large scale fragmentation is the cleavage of flocs into pieces of a similar size without an increase in primary particle concentration. The problem of describing strength arises from the fact that these two rupture modes are thought to be caused by different stresses (Yeung and Pelton, 1996). Fragmentation is thought to occur from tensile stress acting normally across the whole floc, whilst erosion is due to the shearing stress acting tangentially to the floc surface (Figure 2(A).1). The shortcomings of the proposed model being that there seems no obvious reason as to why shear stress cannot result in breakage into large fragments and conversely why tensile stress does not pull flocs apart at floc margins resulting in small 'erosion' type fragments. However, there are complex interpretations of floc strength data arising from relative eddy size and the resulting stress on the flocs, these are discussed in later sections [*see papers 3(B) and 6*].

A review of the literature shows there to be no established standardised floc strength test, although a number of techniques have been evaluated. Floc strength may be broadly considered in terms of the energy required to break flocs under tension, compression or shear (Zhang *et al.*, 1999). However, finding ways of quantifying the energy input for floc breakage has not been easy. There is therefore a need for a more thorough understanding of how floc strength can be measured and what information can be found from floc strength tests. This paper aims to review current knowledge on floc formation and breakage, the different techniques used to measure floc strength with particular emphasis on applied shear, since most previous research has been concerned with this aspect, and finally look at the interpretation of floc strength information.

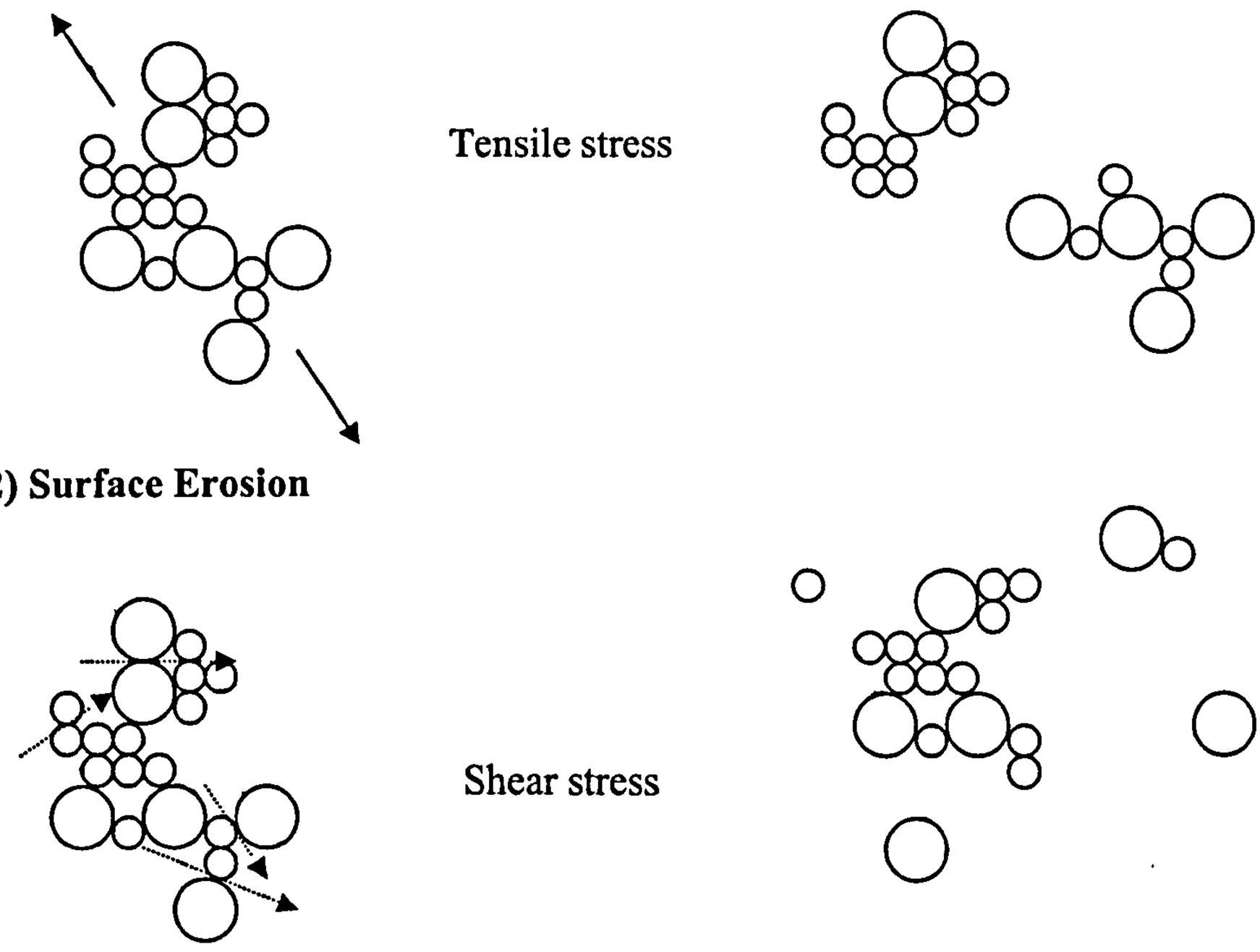

Figure 2(A).1. Two proposed mechanisms for the breakage of flocs under different shear conditions.

2(A).2 Floc formation and breakage

Floc strength is directly related to floc structure and is therefore highly dependent upon the floc formation process. The combined processes of coagulation and flocculation aim to increase particle size for increased removal efficiency of very small particles, colloids and micro-pollutants. Coagulation is the process of chemically changing colloids so that they are able to form bigger particles by coming close to one another. This may be achieved by particle destabilisation by double layer compression or physical enmeshment of colloids within coagulant precipitates or chemical reaction or chemical sorption (Cornwell and Bishop, 1983). Flocculation is the process of transferring coagulated colloids into contact with each other to form larger aggregates (Klimpel and Hogg, 1991; Gregor *et al.*, 1997). The exact process of particle destabilisation and the subsequent colloid aggregation is complex. It is generally considered to be a two stage process of particle transport and particle attachment (Armirtharajah and O'Melia, 1990). Agglomerating particles must firstly collide with each other and secondly must adhere upon collision. Gregory (1988)

treats these steps as being independent and separate from one another. However, flocs do not continue growing and reach a steady state size for a given shear condition. It has been generally accepted that floc growth is held in check by floc breakage so that the rate of aggregation is considered a balance between floc formation and floc breakage (Parker *et al.*, 1972; Francois, 1987; Spicer and Pratsinis, 1996; Ducoste and Clark, 1998; Biggs and Lant, 2000). The stability of flocs in suspension is therefore dependent upon how easy they are to break with aggregate breakage being directly related to the strength and number of the bonds holding the floc together. During the rapid initial formation of microflocs aggregation dominates over floc breakage, however the importance of breakage increases as floc size increases until a steady state floc size distribution is reached. Thus the steady state floc size is governed by the prevailing shear/stress conditions within the containing vessel. The rate of particle collision and the nature of the particle interactions are fundamental to the rate of floc growth (R_{floc}) and may be summarised as in Equation 2(A).1 as the difference between the the rate of aggregation and the rate of floc breakage (R_{br}). The former can be written as the rate of particle collision, R_{col} and a collision efficiency factor, α. The factor α is the fraction of collisions which result in attachment. Thus the overall rate of floc growth may be written as:

$$R_{floc} = \alpha R_{col} - R_{br} \qquad \text{Equation 2(A).1}$$

When the two terms on the right hand side of Equation 2(A).1 are equal, the net rate of floc growth is zero and the floc size attains a limiting value. The collision efficiency is not constant, but depends on the effective shear rate and particle size. For given shear conditions α decreases as the particle (floc) size increases, which is another reason why flocs reach a limiting size (Brakalov, 1987). Another important consideration is that floc breakage may be irreversible to some extent, so that broken fragments do not readily re-form (Francois, 1987; Spicer *et al.*, 1998; Gregory and Dupont, 2001). For irreversible breakage the collision efficiency will be reduced and, for completely irreversible breakage $\alpha = 0$.

Gregory and Dupont (2001) have compared a number of different coagulants and monitored the effect of shear on grown floc suspensions using a photometric dispersion analyser (PDA) – a technique that determines aggregation rate based upon transmitted light developed by Gregory and Nelson (1986). Suspensions were

coagulated for 11 minutes at a stirring rate of 30 rpm which was then increased to 300 rpm for 50 seconds and then reduced back to 30 rpm for 5 minutes. For the coagulation of kaolin using alum, the flocculation index (FI) - a combined measure of both particle size and number - was 3.0 at the end of the slow stir period. This was reduced to an FI of 0.5 after the increased shear. After 5 minutes at the original 30 rpm, the FI had increased and reached a plateau at an FI of 1.0 suggesting the original floc size was unattainable. The same effect was observed for three polyaluminium chloride (PACl) commercial polymer products. Similar work has shown the same behaviour for the breakage and re-growth of a coagulated natural water using alum, PACl and a combination of the two (McCurdy *et al.*, 2004). Alum and PACl had poor floc re-growth, whilst using both coagulants together showed a higher degree of recovery. Mono-disperse polystyrene beads coagulated with alum have been shown to have between 60 and 80 % recovery depending upon the intensity of the breakage shear (Spicer *et al.*, 1998). A number of mechanisms have been proposed to explain the phenomenon of irreversible floc breakage. Spicer *et al.* (1998) suggest that when inter-particle bonds within a floc are broken they lose some of their 'stickiness' such that when subsequent collisions with other particles occur, the attachment efficiency is much reduced. Yeung *et al.* (1997) use a similar analogy of re-using adhesive tape on a dirty surface for the reduction in re-flocculation. This may be due to floc re-structuring during exposure to increased shear, such that bonds previously linking parts of a larger floc are broken and are then able to re-form or re-structure within the smaller aggregate producing a more compact floc. However, irreversible breakage may also be indicative of chemical bonds being broken that are then unable to reform. In the case of polymeric coagulants, bridging flocculation is the main binding mechanism holding the particles together. High shear is likely to change the organisation of the polymer to prevent new bonds forming. A less likely explanation is that high shear causes scission of polymer chains (Yukselen and Gregory, 2004).

Irreversibility in floc breakage has not always been seen. Certain coagulated systems appear to have better re-growth when compared to others. For the coagulation of a kaolin suspension, poly(diallyldimethylammonium) chloride (polyDADMAC) showed 80 % recovery in floc size whilst a copolymer of acrylamide and cationic monomer showed complete recovery in floc size (Yukselen and Gregory, 2004). In the case of particle destabilisation by charge neutralisation as the coagulation

mechanism irreversible floc breakage is not seen. For example, when latex suspensions are destabilised with an ionic salt the original floc size can be reached after being broken by an increased shear and then subsequently returned to the original shear (Spicer *et al.*, 1998). As may be expected, physical attractive forces like van der Waals bonds can be broken and reformed without a reduction in the strength and number of bonds formed. This is supported by evidence showing that a combination of PACl and alum has better re-growth than either one of these coagulants when used alone due to a likely increase in the formation of strongly charged species for the promotion of charge neutralisation mechanisms for coagulation (McCurdy *et al.*, 2004). Chaignon *et al.* (2002) have shown that activated sludge flocs have similar reversible breakage behaviour for continuous breakage/re-growth cycles, suggesting the principal mechanism involved in bonding microbial flocs is charge neutralisation. For organic polymers it has already been mentioned that most high molecular weight polymeric flocculants are thought to work through bridging mechanisms. However, some high charge density polymers are thought to operate by an 'electrostatic patch' effect (Gregory, 1989). In these cases, patches of charged polymer form dense regions of charge on primary particle surfaces. Strong attractive forces can then occur between regions of opposite charge on the particle surface and on the adsorbed polymer. These patches are somewhat akin to charge neutralisation type mechanisms, which may help to explain improved re-growth potential for some polymers.

To summarise floc formation and breakage, flocculating suspensions are governed by the prevailing shear conditions and will reach a steady state. When the shear increases above a critical level flocs will break until a new steady state is reached. In some cases, because of the irreversible nature of floc breakage, flocs are unable to re-grow if broken at a higher shear level. Measuring the shear energy required to break individual flocs or those in a suspension is therefore of high operational importance.

2(A).3 Measuring floc strength

Two fundamental approaches have been taken in measuring floc strength; a **macroscopic** measure of the energy required in a system for floc breakage and a **microscopic** approach that measures the inter-particle forces within individual flocs. A brief summary of these techniques is shown in Table 2(A).1. Due to the fact that the applied shear determines floc size, most work on floc strength has been in the macroscopic field, using applied shear techniques.

2(A).3.1 Macroscopic floc strength tests

Macroscopic floc strength tests have arisen from the relationship between the applied hydrodynamic shear and the resulting floc size. Under low shear conditions, particles may be encouraged to aggregate, but, under increased shear, aggregate break-up is observed (Mikkelsen and Keiding 2002). Gregory (2003) stated that when comparing different flocs, the size (or flocculation index) for a given shear level indicates floc strength. Whilst this is the case for the given shear condition under which the flocs were formed, it does not give an indication of how flocs will behave upon exposure to an increased shear, as could occur at a WTW when flocs are transferred from flocculators or to higher shear treatment processes such as DAF or high rate filtration. For this reason, floc strength can be measured by applying an increased shear or a normal stress to the formed aggregates and relating the energy dissipation or velocity gradient applied to the maximum or average floc size remaining (Yeung *et al.*, 1997; Boller and Blaser, 1998; Lee and Liu, 2001).

Table 2(A).1 A review of the techniques used for determining floc strength.

Strength technique		Description	Strength calculation
Macroscopic techniques	Impeller	Exposure of floc to single level of increased shear within a containing vessel and compare the ratio of the floc size before and after breakage (Francois, 1987; Fitzpatrick *et al.*, 2003)	$Strength\ factor = \frac{d(2)}{d(1)} \times 100$ Equation 2(A).2 $d(1)$ is the average floc size of the plateau before breakage (m) and $d(2)$ is the floc size after the floc breakage period (m).
		Exposure of the floc to increased levels of shear at a controllable rate within a containing vessel and measure the energy input for floc breakage (Leentvaar and Rebhun, 1983; Francois, 1987).	$\log d_{max} = \log C - \gamma \log G$ Equation 2(A).3 d_{max} is the maximum floc diameter (m); C is the floc strength co-efficient; G is the average velocity gradient (s^{-1}) and γ is the stable floc size exponent, an exponent dependent upon floc break-up mode and the size of eddies that causes the breakage. A plot of the maximum floc size remaining against the average velocity gradient gives a line with a characteristic slope indicative of floc strength and break-up mode.
Ultrasonics		Application of a controllable ultrasonic field to a floc suspension and observe floc erosion (Wen and Lee, 1998; Chu *et al.*, 2001).	$\frac{\delta}{\phi} = \frac{-0.78k^{0.5}\Delta\tau}{d_{fo}^{-D_f/3} D_f \left.\frac{dy}{dj}\right\|_{j\to 0}}$ Equation 2(A).4 δ is the floc binding strength (J m^{-2}), ϕ is the power of the ultrasonic field per floc's volume and time (W m^{-3} s), $\Delta\tau$ is the ultrasonic time (s), d_{fo} is the floc size before sonification (m), d_f is the floc size after sonification (m), k is the proportionality constant (the ratio of the floc's cross-sectional area and $d_f^{2D/3}$), D_f is the floc fractal dimension and j is the time of ultrasonification (s).
Multigrid mixer		Flocs exposed to hydrodynamic stress from a controllable oscillatory mixer (Bache *at al.*, 1999). Flocs placed in a vibrating column and subjected to varying amounts of oscillation. The vibration is converted into an energy input for the system.	$\sigma \approx \frac{\rho_w \varepsilon^{3/4} d^{1/3}}{\nu^{1/4}}$ Equation 2(A).5 σ is the floc strength (N m^{-2}), ρ_w is the density of water (kg m^{-3}), ε is the energy dissipation at height of floc rupture (m^2 s^{-3}), d is the floc diameter (m).

Strength technique		Description	Strength calculation
Microscopic techniques	Micromechanics	The breaking force required to pull apart a single floc in the tensile mode (Yeung and Pelton, 1996).	$\sigma = \frac{F}{\frac{\pi}{4}d^2}$ Equation 2(A).6 σ is the floc strength (N m^{-2}) and d is the floc diameter (m), where F is the floc rupture force (N): $F = C_s H$ Equation 2(A).7 F is the floc rupture force (N), C_s is the cantilever stiffness (N m^{-1}) and H is the cantilever deflection (m).
	Micromanipulation	The squeezing of a single aggregate in suspension between a glass slide and a fibre optic probe until floc breakage using a force transducer (Zhang *et al.*, 1999).	$F = K(W - W_0)$ Equation 2(A).8 F is the floc breaking force (N), K is the sensitivity of the force transducer (N V^{-1}), W is the voltage output (V) and W_0 is the baseline voltage of the force transducer (V)

The majority of macroscopic floc strength tests have used impeller-based systems whereby a known shear is applied to a grown floc suspension within a vessel of between 1-4 L volume. However the geometry of the vessel and impeller type varies between the techniques (Table 2(A).2). The breakage behaviour of flocs is monitored by following changes in floc size over a range of shear values. As can be seen, the range of shear levels investigated varies from study to study. The method of floc size determination is crucial and varies between techniques. It is important to ensure that the technique used to measure floc size does not act to damage the aggregates due to their highly fragile nature. Most of the techniques listed are non-destructive *in situ* measurements, although some rely upon taking flocs from the containing vessel and observation using microscopy and image analysis (Wu *et al.*, 2003). However it is difficult to imagine that removing flocs in this manner cannot damage and break the floc particles. The remaining methods have been with commercial particle size instruments that use light scattering to determine particle size (Francois, 1987; Spicer *et al.*, 1998; Biggs and Lant, 2000) or from analysis of video frames or photographs using image analysis (Leentvaar and Rebhun, 1983; Bache *et al.*, 1999; Bouyer *et al.*, 2001; Bache and Rasool, 2001).

The light scattering instruments measure particle size by passing a laser beam through a suspension of particles. These techniques rely upon a constant flow of the suspension through the instrument during the measurement cycle (Farrow and Warren, 1993). This feature has been harnessed to allow the development of a non-destructive methodology for measuring floc size (Spicer *et al.*, 1998; Biggs and Lant, 2000). These methods have a stirred vessel containing the aggregate suspension and are connected to the particle sizing device by plastic tubing. Intrinsic to this type of system is a requirement to pump the suspension through the optical unit of the size analyser. Spicer *et al.* (1998) compared 3 types of pumping techniques for delivery to the optical cell: a peristaltic pump, a syringe pump and a hand pipette. They concluded that a continuous recycle using a peristaltic pump on the return side of the measuring cell was the least severe technique on the flocs and allowed easy continuous monitoring of the suspension. However, the problems of pumping can be removed by sending the suspension to waste after making a measurement to overcome any issues involved in a continuous recycle system (Francois, 1987). This in itself is problematic as the volume of the suspension is continuously decreasing

and will affect the velocity gradients within the containing vessel, which will therefore not be constant over the duration of the experiment, so most workers have favoured a continuous loop.

Similar dynamic systems have been employed using the PDA to give an indication of floc size (Burgess *et al.*, 2000; Gregory and Dupont, 2001; Yukselen and Gregory, 2004; McCurdy *et al.*, 2004). In this technique, a narrow light beam is passed through a flowing suspension. The transmitted light intensity (dc value) is measured along with the root mean square value of the fluctuating component (rms). A ratio of the rms:dc gives a very sensitive indication of particle aggregation and is known as the previously mentioned flocculation index. The PDA is reported to be a very good and simple comparative tool showing qualitative changes in floc aggregation (Gregory and Nelson, 1986). However, the instrument is unable to give an absolute particle size for comparison with other techniques. In addition, the FI is an indicator of both particle size and particle number and as such there is no way of knowing the precise contribution of each of these components in the final FI value. However, aggregate size is probably the over-riding factor as the previously mentioned work has shown that when flocs grow larger the FI value always increases.

A combination of photography/video and image analysis has also been widely used to monitor floc suspensions, such that a flocculated suspension can be observed by capturing images of a stirred suspension by focusing on a plane a short distance (0.3 – 1 cm) behind the wall of vessel containing the suspension (Leentvaar and Rebhun; 1983; Ducoste and Clark, 1998; Chakraborti *et al.*, 2000; Bache and Rasool, 2001). Calibration is achieved by focusing on a graticule suspended into the tank prior to flocculation experiments. The advent of powerful digital and CCD cameras and an almost inexhaustible number of different floc size measurements to be made from floc samples (Wang *et al.*, 2002).

For measuring floc size, no particle size method can be considered ideal. Aggregates are highly irregular and porous and so their scattering patterns are likely to be very different than for equivalent solid spheres of the same material in light scattering devices. Although the light scattering properties of aggregates have yet to be fully

quantified, Farrow and Warren (1993) concluded that, similar to the PDA device, light/laser scattering and transmission techniques are good for showing qualitative (rather than absolute) changes in floc size for aggregation systems. In addition their capability for measuring a very wide range of floc sizes (20 nm to 2 mm) makes them very suitable for monitoring flocs and colloidal systems, although the expense of these instruments limits their wide-scale application. In the previously mentioned set-ups, the inclusion of the measuring instrument will undoubtedly change the shear profile in the containing vessel and as such may inadvertently affect the floc size. Photographic techniques are good in this respect, because the flocs are only exposed to the shear of the impeller in the containing vessel and do not have to pass through a pumped system. The limitations of photography are the time and care that must be taken in preparing complex background lighting arrangements to allow for suitable contrast between floc and background. Furthermore, very small flocs may be undetected if they are beyond the detection limits of the camera being used thus biasing towards the detection of large particles (Leentvaar and Rebhun, 1983). Bache *et al.* (1999) concluded that floc sizes below 30 μm could not be reliably measured using their camera system. This limitation may prevent the detection of floc erosion mechanisms as the small eroded particles may be missed by the technique. Masking effects can also occur in very concentrated floc suspensions. Given these constraints, care must be taken when comparing floc size data obtained from different methodologies.

Table 2(A).2 A review of the different methods employed in shear based techniques for determining floc strength.

Type of flocs	Impeller system	Method of determining floc size	Shear levels investigated	Reference
Tap water + ferric chloride Tap water + ferric chloride	2 L glass tank with a turbine type impeller	Photography + image analysis Non-invasive	G_{av} 160-500 s^{-1}	Leentvaar and Rebhun (1983)
Kaolin + alum	4 L stirred vessel (unknown impeller type)	Small angle light scattering (Malvern Mastersizer 2200) *in situ* measurement. Single pass to waste.	G_{av} 30-1000 s^{-1}	Francois (1987)
Polystyrene + alum	2.8 L baffled tank with Rushton impeller	Small angle light scattering (Malvern Mastersizer E) *in situ* measurement. Continuous recycled pump loop.	100-460 rpm G_{av} 50-500 s^{-1} G_{max} 597-5969	Spicer *et al.* (1998)
Activated sludge	1.2 L baffled mixing tank with six flat blade impeller	Small angle light scattering (Malvern Mastersizer E) *in situ* measurement. Continuous recycled pump loop.	100-700 rpm G_{av} 19-444s^{-1}	Biggs and Lant (2000)
Bentonite + alum	Jar tester (unknown volume and impeller type)	Video camera + image analysis Non-invasive measurement.	30-150 rpm G_{av} 9-33 s^{-1} G_{max} 35-360 s^{-1}	Bouyer *et al.* (2001)
Humic + alum	2 L square beaker with single flat blade impeller	Video camera + image analysis. Non-invasive measurement.	G_{av} 10-400 s^{-1}	Bache and Rasool (2001)
Sewage sludge + cationic polymer	Couette flocculator powered by variable speed motor	Image analysis with flocs removed *ex situ*	G_{av} 10-400 s^{-1}	Wu *et al.* (2003)
Kaolin + alum/ polyaluminium chloride	1 L jar test beaker with single flat blade impeller	Photometric dispersion analyser (PDA). Continuous re-cycled pump loop.	50-400 rpm G_{av} 23-520 s^{-1}	Gregory and Dupont (2001) & Fitzpatrick *et al.* (2003).

2(A).3.1.1 Floc strength factor

One of the simplest evaluations of floc strength is the calculation of a floc strength factor (Francois, 1987). This is effectively the ratio of floc size after and before breakage at a particular shear level and may be calculated as shown in Equation 2(A).2 in Table 2(A).1.

The higher the value of the strength factor, the less sensitive the flocs are to breakage as a result of increased shear and are therefore considered stronger. The strength factor is not a constant and changes depending upon the applied shear during rupture and so strength factors can only be compared for similar breakage conditions. Francois (1987) noted an increase in the strength factor from 23.9 to 29.3 for kaolin flocs formed with longer rapid mix times between 0-360 s and an increase in strength factor from 17.5 to 26.5 for flocs formed with increased slow stir shear levels between 21-54 s^{-1}. A breakage shear of 1396 s^{-1} for 1.5 minutes was applied in these experiments. Fitzpatrick *et al.* (2003) compared the strength factor of kaolin flocs and observed the impact of temperature (6-29° C) on floc strength using a PDA and a breakage shear of 520 s^{-1} for 10 seconds. Whilst the PDA does not give an absolute floc size, the FI value before and after breakage can be used as a surrogate for $d(1)$ and $d(2)$. Floc strength has been seen to decrease with increasing temperature. For example, the floc strength factor decreased from 21 to 14 for alum-kaolin flocs dosed at 3.4 mg L^{-1} Al over the experimental temperature range. A general trend was seen that showed floc strength decreased with increasing floc size, such that flocs formed at the original slow stir that had a high FI value had lower floc strength factors than those of lower FI value.

A comparison of kaolin floc strength factors for a range of different coagulants has shown that hydrolysing coagulants such as alum and polyaluminium chloride (PAX XL-9) give lower floc strength than cationic polyelectrolytes (polyDADMAC and Zetag 64) (Yukselen and Gregory, 2004).

The floc strength factor allows a relatively quick and easy method of determining a floc strength value and indicates how small a floc will become relative to its previous size for a given increase in shear. However, as the breakage shear is invariably different between different studies it is hard to directly compare the results other than

for general trends. There has been little work showing how the relationship between the floc strength factor changes with increasing breakage shear levels. More work needs to be done in this area to give a better comparison of floc strength using the strength factor and on a wider range of suspensions other than kaolin in order to compare strength values between different coagulated systems for a standardised breakage shear.

2(A).3.1.2 Shear based floc strength and breakage models

Shear based floc strength models have evolved from strong empirical evidence showing that the final floc size distribution is related to the applied shear (Parker *et al.*, 1972; Spicer *et al.*, 1998). Shear has usually been characterised by the average velocity gradient as shown in Equation 2(A).9 (Camp and Stein, 1943).

$$G = \sqrt{\frac{\varepsilon}{\nu}} \qquad \text{Equation 2(A).9}$$

G is the average velocity gradient (s^{-1}); ϵ is the rate of energy dissipation per unit mass of fluid (N m s^{-1} kg^{-1}) and ν is the kinematic viscosity (m s^{-1}).

The energy dissipation term is given by Equation 2(A).10.

$$\varepsilon = \frac{P_0 N^3 D^5}{V} \qquad \text{Equation 2(A).10}$$

ϵ is the energy dissipation per unit mass of fluid (N m s^{-1} kg^{-1}); P_0 is the impeller power number; N is the impeller speed (rps); V is the stirred tank volume (m^3) and D is the impeller diameter (m).

Due to the relationship between the velocity gradient in the flocculating vessel and aggregate size, Parker *et al.* (1972) suggested an empirical expression for the stable floc size (Equation 2(A).11).

$$d = CG^{-\gamma} \qquad \text{Equation 2(A).11}$$

d is the floc diameter (m); C is the floc strength co-efficient; G is the average velocity gradient (s^{-1}) and γ is the stable floc size exponent.

Linearization of the equation allows values of γ and log C to be found from a log-log plot of floc size measurement against the average velocity gradient (Equation 2(A).12).

$$\log d = \log C - \gamma \log G \qquad \text{Equation 2(A).12}$$

There is some argument in the literature as to whether it is the maximum floc size remaining in the system that should be measured or the average floc size. The initial empirical observations relate the shear to the maximum particle size (d_{max}), as in Equation 2(A).3 (Table 2(A).1). Bache *et al.* (1999) used the 95 % floc diameter obtained using an external video camera. This was done to remove problems associated with resolution when measuring smaller floc sizes using this technique. However, both Leentvaar and Rebhun, (1983) and Francois (1987) concur that the same relationship is seen when using average floc diameters. When the values of γ have been compared for the mean, median and maximum floc size for the same coagulation conditions γ remained fairly constant – between 0.43 and 0.49 – for all three floc sizes (Leentvaar and Rebhun, 1983).

The value of Log C strongly depends upon the method used for particle size measurement and which characteristic value of d has been used. As there has been wide variation between different studies, Log C can only be used to study floc strength within specific experimental systems. However, as the value of γ remains relatively constant whichever value of d has been used it is a useful value for comparing floc strength and break-up.

The steeper the slope γ, the greater the reduction in floc size seen with increasing G. The curves shown in Figure 2(A).2 are three theoretical examples of different floc suspensions formed at a slow stir of G_{init} showing different resistance to floc break-up. One interpretation of the data is to consider the steepness of the slope as an indicator of floc strength. For example, considering line (a) the slope of the line is 0 and floc size is independent of the applied shear. The flocs do not break upon exposure shear and as such must be considered strong flocs. If the slope of the line is shallow as in line (b) then these flocs are better able to resist shear than the example in (c). Therefore flocs (b) should be considered stronger than flocs (c) as the average/maximum floc size does not decrease so rapidly. However, this is likely to be an over-simplification of the situation. Many workers ascribe the value of γ to the dominant mode of floc degradation from both theoretical and experimental analysis and increasing values of log C as an indicator of increased floc strength (Parker *et al.*,

1972; Leentvaar and Rebhun, 1983; Francois, 1987). Solving complex equations to describe floc break-up and turbulence patterns, Parker *et al.* (1972) were the first to theoretically describe the impact shear has on floc size. These types of models assume flocs are composed of mono-disperse primary particles and characterise eddy frequency and breakage capacity.

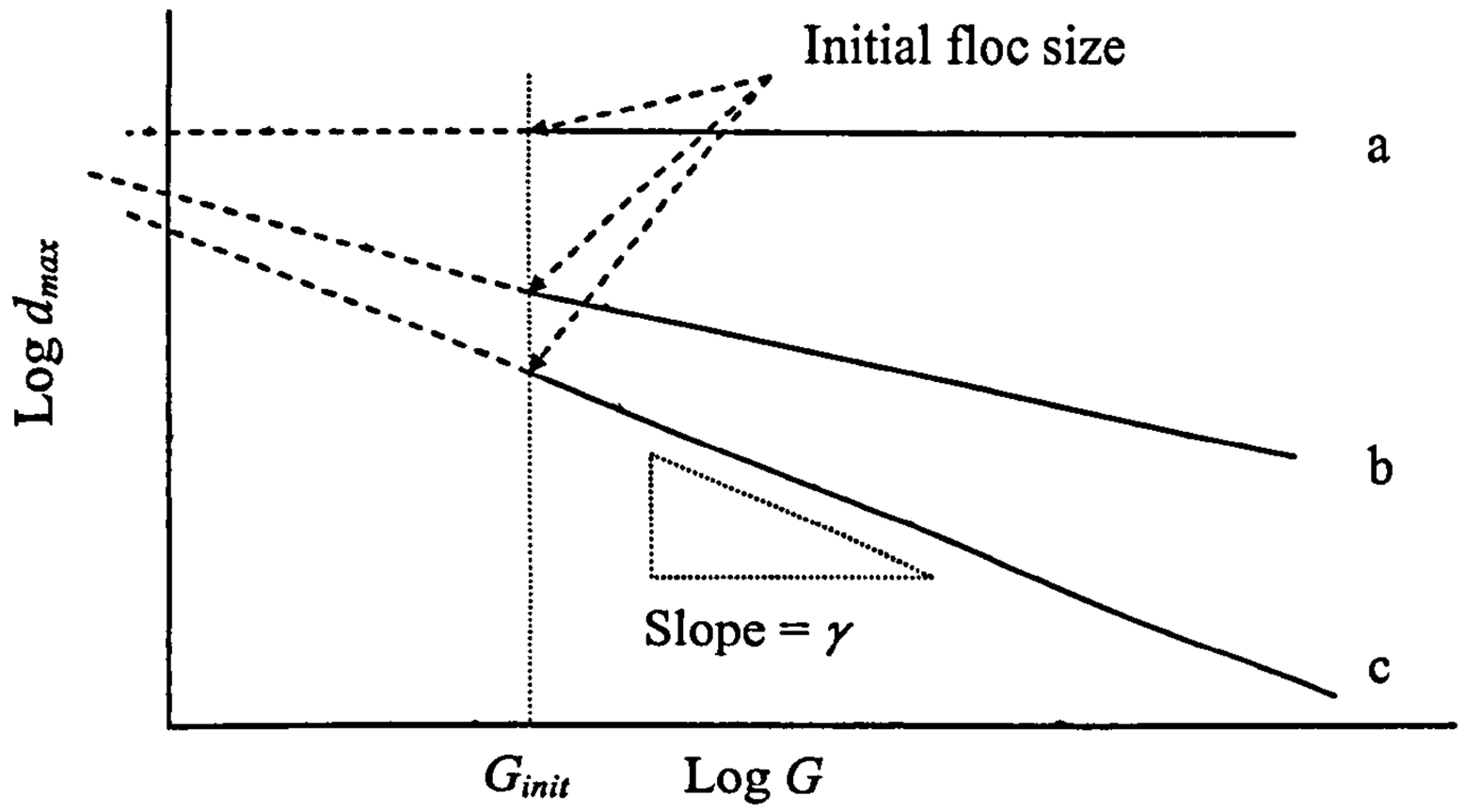

Figure 2(A).2 The relationship between the change in particle size and an increase in velocity gradient for 3 types of floc. Floc (a) is resistant to breakage, floc (b) is thought to break due to large scale fragmentation and floc (c) is thought to break by surface erosion.

The theoretical basis of the value γ may be explained by turbulent shear patterns relative to eddy size (Biggs and Lant, 2000; Bache 2004). In most flocculation processes, conditions are generally considered to be turbulent (Francois, 1987; Boller and Blaser, 1998). Eddy viscosity is the turbulent transfer of energy as a result of moving eddies, giving rise to tangential stresses. This is analogous to molecular viscosity in laminar flow where liquids resist flow as a result of intermolecular friction, therefore, when a liquid moves, energy is dissipated in a tangential direction to the moving viscous fluid. This energy is commonly referred to as viscous dissipation. Inertial convection is the release of energy in an outward direction, normal to the rotational eddy flow. Levich (1962) described turbulence using a scale whereby turbulent flow is described by the velocity and size of eddies. Very large eddies are responsible for the mixing of the system with little energy dissipation and therefore do not rupture or break flocs, whilst smaller eddies are responsible for most

of the energy dissipation. The Kolmogoroff microscale describes the length scale (η) of the energy-dissipating eddies (Equation 2(A).13).

$$\eta = \left(\frac{\mu^3}{\varepsilon} \right)^{\frac{1}{4}} \qquad \text{Equation 2(A).13}$$

η is Kolmogoroff's microscale of turbulence (m); μ is viscosity (kg m^{-2} s^{-1}) and ϵ is the energy dissipation (N m s^{-1} kg^{-1}).

Inertial convection is responsible for energy dissipation of the larger eddies within the microscale range, whilst viscous energy is responsible for the energy dissipation of the smaller eddies in this range (Figure 2(A).3).

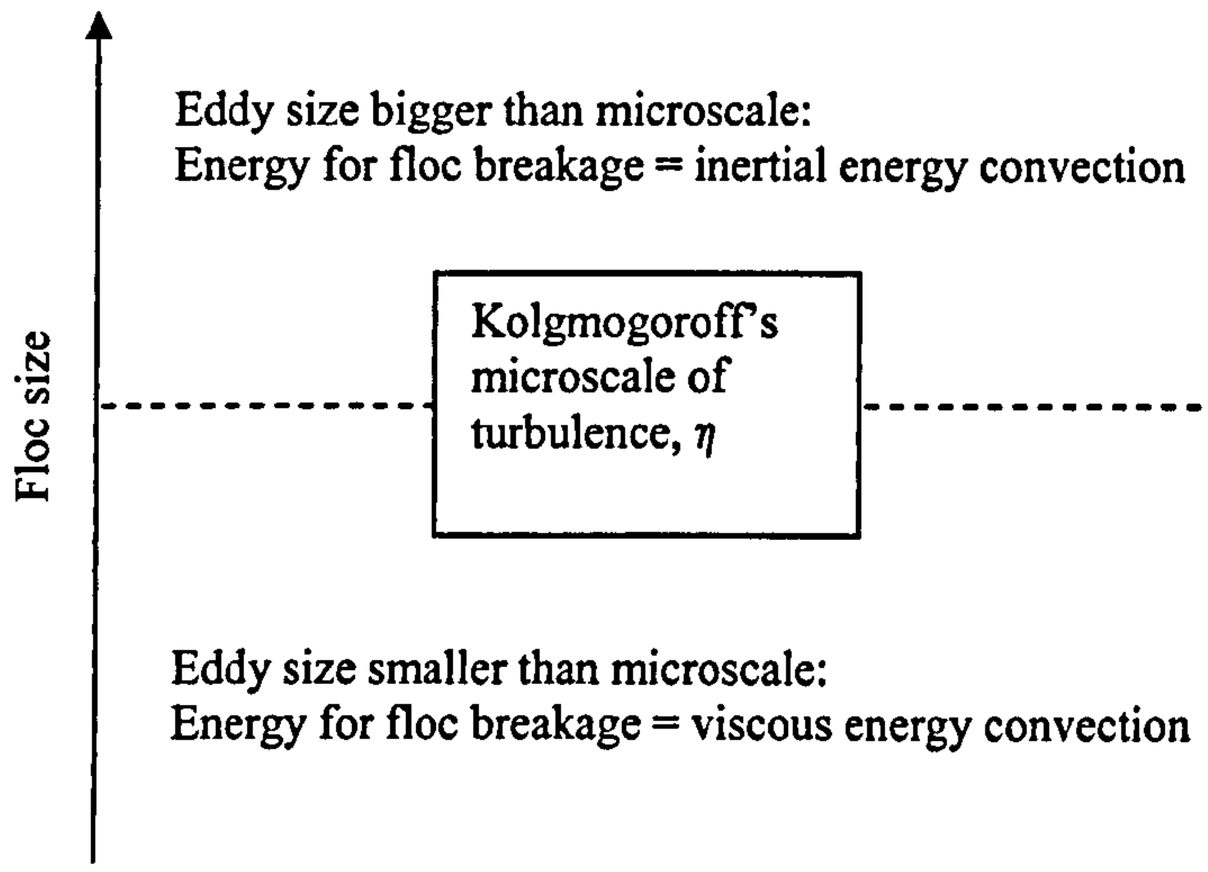

Figure 2(A).3 The importance of eddy size on floc break-up mechanism.

At high velocity gradients, the value of the micro-scale η is of a similar order of magnitude to the floc sizes whilst at low velocity gradients it is much larger, which helps to explain why flocs become more prone to breakage at high velocity gradients. Under normal flocculator conditions, viscous effects dominate (Boller and Blaser, 1998). Some authors suggest that when flocs are smaller than the micro-scale they become prone to breakage by surface erosion, whilst above the microscale flocs are thought to be more exposed to breakage by fracture (Thomas *et al.*, 1999). Other theoretical analysis suggests that when flocs are in the viscous energy region (i.e. below the critical microscale eddy size) values of γ of 0.5 have been calculated to indicate floc fragmentation, whilst erosion mechanisms are dominant if $\gamma = 1$. In the inertial convection zone a value of $\gamma = 0.5$ suggests large scale fragmentation events and $\gamma = 2$ suggests surface erosion (Parker *et al.*, 1972). The values of some of the

previous experimental work for the calculation of floc strength co-efficient (Log *C*) and constant (γ) obtained for a variety of flocs are shown in Table 2(A).3. Good linearity is always seen between floc size and shear on a log-log scale for all of the experimental studies shown in the table. For example, both Bache *et al.* (1999) and Biggs and Lant (2000) had an R^2 correlation co-efficient in excess of 0.99.

Floc strength coefficient

For a fixed shear the larger the value of log *C* the stronger the floc (Bache, 2004). As has been explained, comparing values of log *C* between studies is not possible due to the different impeller/tank geometries and different floc sizing protocols employed, however a number of trends can be seen from within individual research. Wu *et al.* (2003) saw that an increase in the polymer dose lead to an increase in the floc strength coefficient for alum sludge flocs. A comparison of ferric hydroxide flocs in tap water and sewage sludge showed an increase in log *C* from 1.5 to 1.9 with the authors stating that floc strength was higher in tap water than sewage (Leentvaar and Rebhun, 1983). For sewage flocs, it has been shown that adding polymeric flocculant doubled the floc strength co-efficient. Bache *et al.*, (1999) and Bache and Rasool (2001) have investigated alumino-humic flocs. In the latter case, a useful comparison of flocs obtained from flocculators at 7 water treatment plants treating water of high colour (50-140° Hazen) has been made. The value of log *C* was highest for flocs where polymer was used and in the instance of water that was initially of high alkalinity.

Floc strength constant

Whilst the value of log *C* provides a good indication of how strong flocs are when they are formed at a given shear, it does not provide information on how flocs will respond to subsequent increases in shear. This information can be provided by the previously mentioned floc strength factor but also by the floc strength exponent (γ). The higher the value of γ the more prone the flocs are to breakage into smaller sizes with increasing shear.

For alumino-humic flocs under low alkalinity conditions, the value of the slope varied between 0.44 and 0.64 (Bache and Rasool, 2001). Looking at the data for comparable

Al doses (2.4-2.7 mg L^{-1}), the humic floc degradation was reduced from 0.63 to 0.44 when polymer aid had been added. The value of γ was seen to increase when the water alkalinity was high suggesting that these flocs were less able to withstand increases in shear than the low alkalinity flocs. For sewage flocs, the addition of polymer has been shown to increase the degradation rate with increasing shear from 0.29 to 0.55 (Leentvaar and Rebhun, 1983). This does not concur with what has been seen for humic flocs. This is likely to be an indication of different polymer binding mechanisms occurring within different types of floc aggregate. Coagulant dose also has an impact on γ, for kaolin flocs, increasing coagulant dose from 4.02 to 5.02 mg L^{-1} Al increased the floc strength constant, whilst above this coagulant dose there was a decrease in γ (Francois, 1987). This suggests that there is an optimum coagulant dose in terms of floc strength.

For all types of floc the reported values of γ have been around 0.5 (the exception being alumino-humic flocs formed in high alkalinity water were $\gamma = 0.81$). Whilst these values of γ do not highlight major differences in degradation rate for different types of floc (e.g. sewage, kaolin and humic), the mode of breakage can be theoretically determined from the floc strength constant. If it is assumed that viscous effects are responsible for most of the energy dissipation in flocculating systems and the models of floc breakage are correct, then it appears that floc breakage is generally dominated by floc fragmentation as the value of γ remains around the theoretical value of 0.5 as derived by Parker *et al.* (1972). However, this strict theoretical interpretation is open to debate. For example fragmentation and erosion could occur simultaneously in a containing vessel. This may explain the result seen for the high alkalinity water, were the value of γ was half way between the theoretical values for fragmentation and surface erosion. In addition, large flocs in an aggregated system may be larger than the microscale (η) whilst the smaller flocs may be smaller than η. This has been shown experimentally for activated sludge flocs with the $d_{95} > \eta > d_{50}$, suggesting that the larger flocs in the system fragment and the smaller flocs erode (Biggs and Lant, 2000).

Table 2(A).3 The value of the floc strength constants and coefficients obtained from shear based techniques.

Type of floc	Coagulant type and dose	Floc strength coefficient value, log *C*	Floc strength constant, γ	Reference
Alum sludge	Cationic polymer (PL-320)			Wu *et al.* (2003)
	0 → 30 mg L^{-1}	2.4 → 5.9	N/A	
Ferric hydroxide precipitate in sewage effluent	Ferric chloride 10 mg L^{-1} as Fe	1.9	0.29	Leentvaar and Rebhun (1983)
	Ferric chloride + anionic polymer 10 mg L^{-1} as Fe + 3 mg L^{-1} polymer	4.1	0.55	
Ferric hydroxide precipitate in tap water	Ferric chloride 10 mg L^{-1} as Fe	2.5	0.51	
Alumino-humic	Al based coagulant	3.1	0.44	Bache *et al.* (1999)
Alumino-humic in low alkalinity and high colour water	Al based coagulant 2.4 mg L^{-1} as Al 2.7 mg L^{-1} as Al 4.7 mg L^{-1} as Al 5.4 mg L^{-1} as Al 2.5 mg L^{-1} as Al + 0.1 mg L^{-1} polymer	 3.8 3.4 3.6 3.6 3.8	 0.61 0.63 0.57 0.52 0.44	Bache and Rasool (2001)
	3.7 mg L^{-1} as Al + 0.1 mg L^{-1} polymer	4.0	0.64	
Alumino-humic in high alkalinity and high colour water	Al based coagulant 5.0 mg L^{-1} as Al	4.1	0.81	
Alumino-kaolin in DI water	Aluminium sulphate 4.02 mg L^{-1} as Al 4.52 mg L^{-1} as Al 5.02 mg L^{-1} as Al 5.52 mg L^{-1} as Al 6.02 mg L^{-1} as Al	N/A	 0.44 0.48 0.61 0.50 0.43	Francois (1987)
Activated sludge flocs	No coagulant dosed	2.9	0.35	Biggs and Lant (2000)

Velocity gradient term

Traditionally, the average hydraulic gradient (G_{av}) has been used as the descriptor for shear and, as has been previously described, many studies have reported a highly significant relationship between G_{av} and floc size (d). However, there is some debate as to the use of velocity gradient, and in particular the average velocity gradient, when considering floc strength and breakage. This is because G_{av} is unlikely to be able to accurately describe the complexities of turbulent flow in stirred vessels (Boller and Blaser, 1998). There is a large body of evidence suggesting that local G values are more important than the G_{av} in a stirred vessel (Francois, 1987; Essamanai and de Traversay, 2002). Maximum local G values are found close to the impeller region in a stirred vessel and are considered to be of most importance in determining floc size distributions in a tank (Francois, 1987; Bouyer *et al.* 2001). This is further supported by data showing that systems with different impellers or vessels may have the same average velocity gradient, but the resulting floc size distributions are not the same due to differences in G_{max} (Ducoste and Clark, 1998; Bouyer *et al.*, 2001).

The reported empirical relationship between G_{av} and d is valid for a given impeller and container geometry because they are directly proportional to one another. This can be shown by work by Bouyer *et al.* (2001) that has evaluated the hydrodynamic velocity profile in a jar tester using computational fluid dynamics (CFD). The relationship between the calculated G_{av} and G_{max} is very significant (Figure 2(A).4). The G value in the impeller region was shown to be four times the average velocity gradient at 30 rpm, whilst at 150 rpm the G value in the impeller region was more than 10 times the average velocity gradient. The maximum velocity gradient was seen in the area between the paddle and the vessel wall just as the paddle has passed through the region.

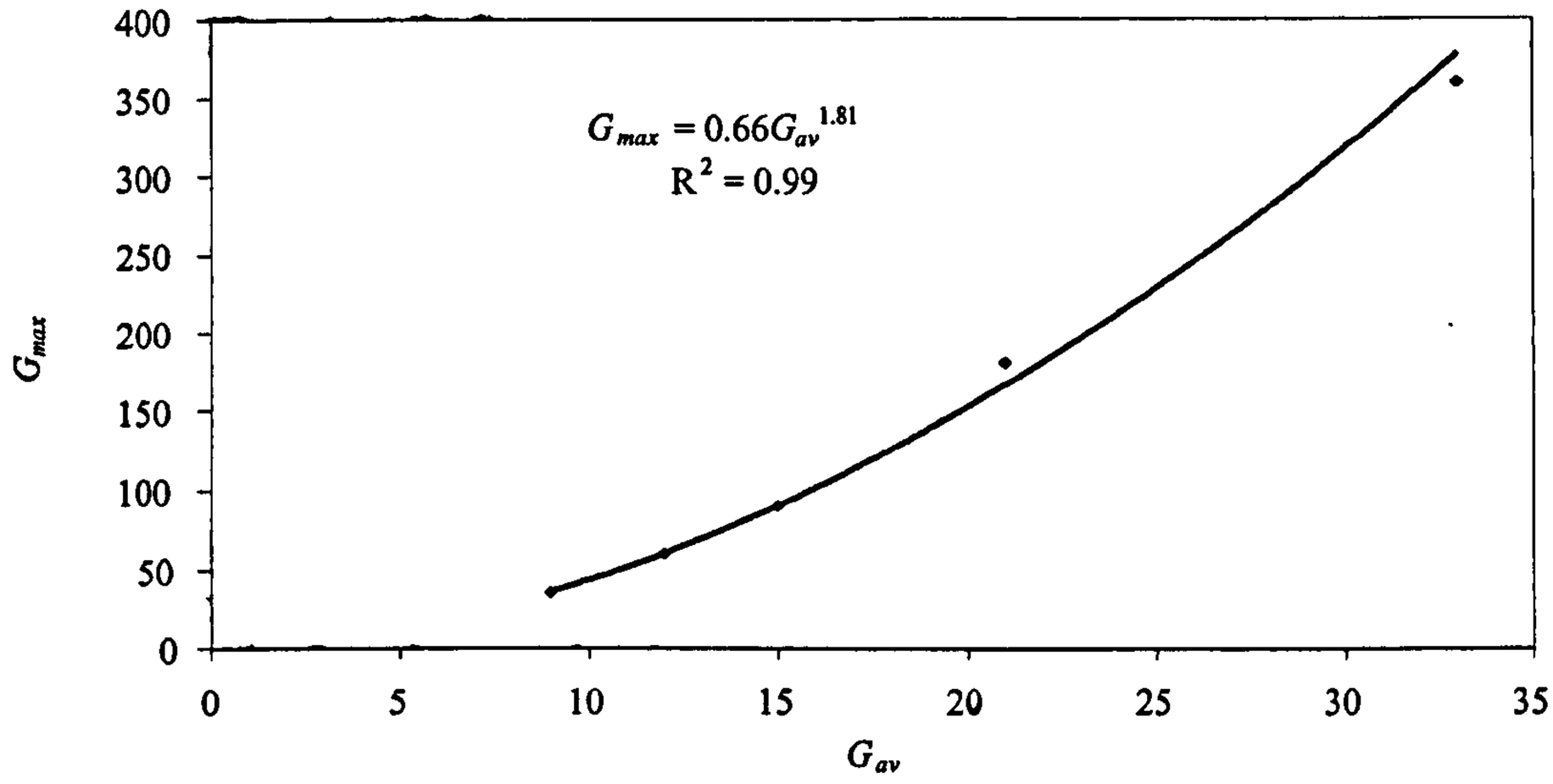

Figure 2(A).4 The relationship between G_{av} and G_{max} from data obtained using CFD (from Bouyer et al., 2001).

Essamanai and de Traversay (2002) have used a combination of CFD modelling based on Navier-Stokes equations with experimental pilot work to produce a model of the different *G* distributions in a stirred flocculator. They have found that the maximum *G* value in the impeller region to be 38,000 s^{-1}, whilst the G_{av} in the impeller zone was 5549 s^{-1} and the G_{av} in the whole flocculator was 163 s^{-1}. These large orders of magnitude differences must be considered carefully as G_{max} was only a very small volume of the flocculator. The probability that a floc passes through this region must firstly be quantified because if the majority of flocs do not become exposed to this very high shear level, flocs cannot be broken by that shear level. Secondly, if a floc does enter the very high shear the time spent there must be long enough to break aggregate bonds. Further modelling work needs to be carried out in order to quantify critical G_{max} levels for floc breakage. In addition, although G_{max} may be the controlling factor of floc size it can also be attained in different ways. For example Spicer and Pratsinis (1998) calculated the G_{max} from Equation 2(A).9 based upon the impeller swept volume (compared to the G_{av} calculated from the vessel volume), whilst Bouyer *et al.* (2001) generated G_{max} using CFD.

Because there is still much work to be done in quantifying critical G_{max} the use of the G_{av} value should not be ignored and is probably acceptable for order of magnitude purposes to describe energy dissipation (Bache and Rasool, 2001). Furthermore, the

concept of G_{av} is very well known, easy to calculate and universally used for the design of water and wastewater treatment facilities (Boller and Blaser, 1998).

Recent work by Ducoste and Clark (1998) has formulated an alternative empirical expression to that of Parker *et al.* (1972) that was satisfied regardless of variations in impeller geometry and tank size that removes the direct use of G_{av}:

$$d_{av} = \frac{h}{(P_0^{0.5} ND)^y} \qquad \text{Equation 2(A).14}$$

d_{av} is the mean particle diameter (m), h is a constant (s), P_0 is the impeller power number, N is the impeller speed (rps), D is the impeller diameter (m), y is a fitting parameter.

The data suggest that the steady state floc size was controlled by the shear in the impeller zone, however more extensive quantification of this expression is required to confirm the observed relationship as the study only evaluated two impellers (a Rushton turbine and an A310 fluid foil impeller) and three square tank volumes of 5, 28 and 560 L.

Hydrodynamic shear based techniques using impellers have been widely used because of their similarity to operational flocculators and the likelihood that hydrodynamic shear stress is probably of great importance when considering floc breakage. In addition these techniques have highlighted differences in how a floc will respond to different increased levels of shear as determined by the value of γ. However, whilst the observation of an empirical relationship between shear and floc size is widespread, the problem has been in the interpretation and application of shear based models to the data. Whilst experimental work is fitted to these models there is little direct evidence to suggest either erosion or fragmentation is definitively taking place. Ideally, the particle size distribution of a 'fragmenting' floc system needs to be compared to an 'eroding' system to show the differences in particle sizes to confirm that the models are totally accurate. A final problem with these techniques has been an accurate description of the shear energy dissipated into impeller systems. G_{av} is probably not sufficient enough whilst critical threshold values of G_{max} have not been sufficiently well modelled to directly relate to the resulting floc size. This has lead to a number of workers tackling this problem by applying a reliable, accurate and

controllable measure of the energy input and the following section will review a number of these techniques in turn.

2(A).3.1.3 Ultrasound

The use of ultrasound to condition sludge is a well known technique (Chu *et al.*, 2001). By applying a controlled ultrasonic field to a sludge suspension, flocs may be effectively 'exploded' into smaller parts to improve biodegradability. During ultrasonic treatment, pressure waves pass through a medium releasing large quantities of energy. This induces the formation and collapse of gas bubbles. The result is a release of energy in the form of temperature and turbulent eddies around the collapsing bubble. There has been some limited application of this in determining floc strength. Wen and Lee (1998) have developed a complex term for the calculation of a floc strength value from an applied ultrasonic field (see Table 2(A).1). Above a critical ultrasonic energy input it has been seen that kaolin flocs and activated sludge flocs break-up and decrease in size (Wen and Lee, 1998; Chu *et al.*, 2001). A direct measure of the ultrasonic energy per unit volume of sample can be made that reflects the flocs internal binding strength as the flocs break up. The resulting floc size can then be measured and compared to the original floc size using one of the previously mentioned techniques. For activated sludge thickened with alum, the effect of polymer addition on floc strength has been investigated (Lee and Liu, 2001). A non-ionic polymer was compared with a cationic polymer and it was seen that floc strength decreased with increasing polymer dose and that non-ionic polymer showed greater floc strength than cationic polymer. However, it was interesting to note that in all cases the sludge flocs without polymer were stronger than with polymer. The major problem associated with this technique is the impact of temperature. At an applied ultrasonic rate of 44 Watts mL^{-1} the temperature was seen to increase from 20 to 56° C in just over 1 minute. Therefore considerable temperature control needs to be applied in order to better stabilise the system conditions.

Wen and Lee (1998) investigated the strength of clay coagulated with cationic polymer for different pH and polymer dose. They found that at higher pH and polymer dose, the initial floc size was larger. The results were contradictory in that the large flocs formed at pH 7 and 10 were observed to break down at a faster rate than at pH 3 in terms of floc size. However, the binding strength based on Equation

2(A).4 was observed to increase with both polymer and pH. This is perhaps a reflection of there being two approaches of considering floc strength. The first is a measure of the maximum floc size attained at the end of the floc formation process such that larger flocs should be considered stronger than smaller flocs because they have reached a bigger size. The second considers the floc strength as a measure of the strength of floc bonds to withstand increases in energy once formed.

For activated sludge flocs the use of ultrasound is confused due to the effect of ultrasound on bacterial components of the floc. Ultrasound increases the formation of free radicals which can impact on bacterial metabolism and also cause cell lysis (Jorand *et al.*, 1995). Therefore, in these instances the applied energy may be causing other effects other than breaking apart primary particles within the floc. For water treatment flocs that are generally dominated by non-living chemical constituents, ultrasonic methods may have potential for determining the forces required to break flocs. From an operational sense it is difficult to relate the energy experienced by flocs from an ultrasonic field to the hydrodynamic shear conditions that are important in a flocculator. However, as inter-particle bonds are being broken in both techniques a comparison of the results between the different methods would be of great interest.

2(A).3.1.4. Oscillating multigrid mixer

Bache and Al-Ani (1989) developed a technique whereby flocs are exposed to stress in a vibrating settling column. An oscillating plunger was used to provide turbulent energy dissipation in the column. In this manner relatively uniform energy dissipation can be achieved in the horizontal plane with shear stress increasing as flocs pass down the column, therefore the height at which a floc ruptures in the column is proportional to a certain level of energy dissipation. A floc breaks when it passes through a region where the hydrodynamic forces are greater than the binding force at the point of rupture within the floc. The advantage of such a system is that the hydrodynamic shear stress at each point in the column may be more accurately modelled when compared to the more complex flow of impeller systems. In this technique floc size before and after breakage has been monitored using CCTV and image analysis. The underlying trend emerging from this technique is for large flocs to rupture higher in the column than smaller floc aggregates, showing the increased susceptibility of large flocs to increases in shear. This has been shown for kaolin-

alum flocs (Bache and Al-Ani, 1989) and for humic-alum flocs (Bache *at el.*, 1991). The calculation of a value for floc strength from these data is shown in Equation 2(A).5, (in Table 2(A).1). This has been derived from a force balance between accelerations across the floc at the plane of rupture where turbulent energy acceleration have been defined as $\sqrt{3}\varepsilon^{3/4}\nu^{-1/4}$ from Levich (1962):

$$\frac{1}{4}\pi d^2\sigma = 2\frac{\pi}{6}\rho_w d^3\sqrt{3}\frac{\varepsilon^{3/4}}{\nu^{1/4}} \qquad \text{Equation 2(B).15}$$

d is the size of floc sub-units (m), σ is the floc strength per unit area (N m^{-2}), ρ_w is the density of water (kg m^{-3}), ν is the kinematic viscosity (m s^{-1}) and ε the energy dissipation (N m s^{-1} kg^{-1}).

Some floc strength calculations have shown that, although flocs sheared at high G_{av} values were smaller, they had higher strength. For example, flocs sheared at 50 s^{-1} had a d_{95} of 238 μm and a strength of 0.08 N m^{-2}, whilst flocs sheared at 230 s^{-1} had a d_{95} of 120 μm and a strength of 0.42 N m^{-2}. The relative floc strength of alumino-humic flocs was found to change with coagulant dose. For doses of between 2-7 mg L^{-1} Al, an optimum was seen at 4 mg L^{-1}.

2(A).3.2 Microscopic Floc Strength Tests

Whilst macroscopic techniques rely upon complex theory of turbulence, eddy size and floc breakage models, recent work has been carried out to gain a more direct measurement of floc strength by taking individual flocs and finding the force required to pull or compress a floc until breakage (Yeung and Pelton, 1996; Zhang *et al.*, 1999). The principal advantage of such a technique being that an understanding of the mechanisms of how and where flocs break may be gleaned and a floc rupture force may be directly measured to give floc strength. This may eventually lead to a more thorough knowledge of the currently poorly-understood mechanisms of floc breakage. The following section briefly reviews two microscopic techniques.

2(A).3.2.1 Micromechanical approach

In this method, floc strength is measured by the tensile force required to break single flocs (Yeung and Pelton, 1996; Yeung *et al.*, 1997). A schematic overview of this technique can be seen in Figure 2(A).5. Calcium carbonate flocs coagulated in NaCl with polymeric floc aid were placed in a sample chamber consisting of two glass cover slips separated by 2 mm. The force required to rupture the flocs was determined

by carefully attaching single flocs onto a glass rod cantilever beam and attaching and translating an opposing pipette horizontally until the floc broke. The deflection of the cantilever may be directly converted into a floc rupture force, provided the cantilever stiffness is known, using sensitive micromanipulators. Floc size before and after breakage was determined by averaging the major and minor axis of the aggregates of the original floc and the broken floc pieces. In their first study (Yeung and Pelton, 1996) floc strength was reported as simply the force required to break apart the floc. Initial floc sizes ranged from between 5-50 μm diameter. In this instance when this force is plotted against floc size no correlation was seen between floc strength and size. A change in floc strength was seen when two polymeric flocculants were compared with the first system having an average floc strength of 64 nN and the second was 110 nN. Boller and Blaser (1998) have transformed these data into a floc rupture pressure so that floc strength is found from the ratio of the rupture force to the cross sectional area of the smaller fractured aggregate (as shown in Equation 2(A).6 in Table 2(A).1) giving floc strengths in the region of 100-1000 N m^{-2}. In this way, the size dependency of floc strength was again seen, such that smaller flocs showed increased strength. The application of this technique has been taken further to show the effect of mixing speed on floc strength (Yeung *et al.*, 1997). A range of mixing speeds between 50-2500 rpm were investigated for paper pulp with calcium carbonate flocculated with polymeric flocculant. An optimum mixing speed was determined at 500 rpm that gave optimum floc strength of 1,500 N m^{-2}.

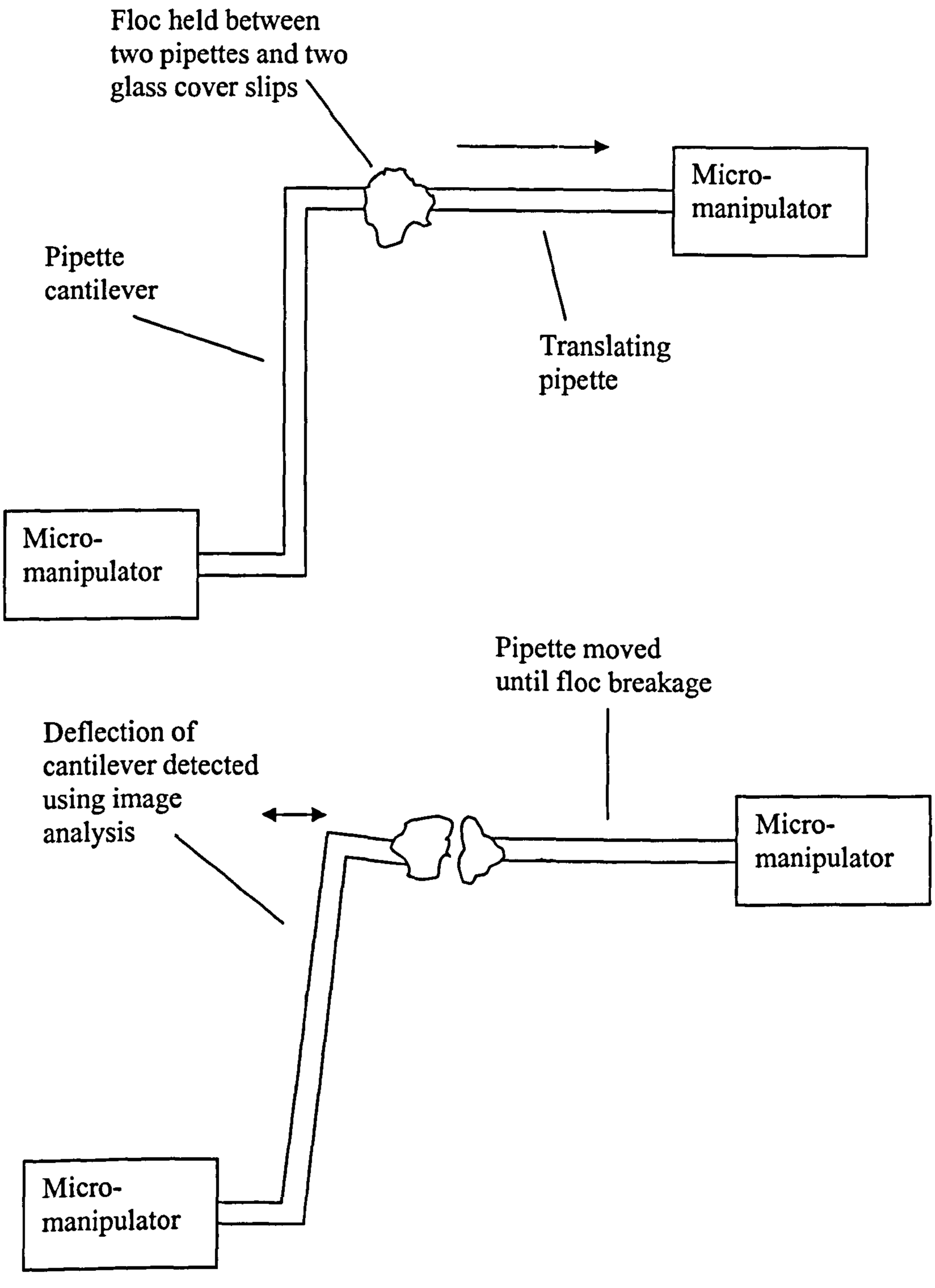

Figure 2(A).5 A schematic overview of the micromechanical floc strength technique (adapted from Yeung and Pelton, 1996).

The technique provides an interesting insight into floc breakage in the tensile mode. It was observed that not all flocs breakages resulted in large scale fragmentation. This contradicts hydrodynamic shear models that suggest tensile stress is responsible for

large scale fragmentation. It was hypothesised that flocs were breaking at their narrowest point because it is here that there are fewer attachment sites. The size ratio of floc fragments ($d(2)$) after breakage with the initial floc ($d(1)$) were compared with floc compaction (as determined by fractal dimension analysis). Values of d_2/d_1 approaching 0.5 indicate that the floc has been split into two similar sized pieces whilst near 0 and 1 a floc has been broken into a very small and large aggregate. The authors argue that the mode of floc breakage is therefore more to do with floc compaction than the differences in turbulence stresses and eddy size. Very compact flocs have fewer bonds in their margins, so surface erosion is more likely to occur. More loosely bound flocs are more likely to have weak points randomly located anywhere across their cross-section and are therefore more susceptible to large scale fragmentation. This questions one of the fundamental assumptions of the shear based floc strength characterisations based upon Equation 2(A).12 that flocs are homogenous structures composed of similar primary particle units.

The micromechanical technique has provided a useful addition to the field of floc strength quantification. However, as yet the application has been limited to the measurement of only a few hundred individual floc aggregates in total and across a relatively narrow range of floc types. More work is required in this field in order to assess its broad application to all types of floc. In addition, the importance of tensile stress as a mechanism for floc breakage in flocculators and other WTW processes has yet to have been fully quantified.

2(A).3.2.2 Micromanipulation

A further microscopic technique has measured the compression force required to break flocs between a glass slide and a fibre optic probe (Zhang *et al.*, 1999). In this technique, a sample of floc suspension was placed on a microscope slide, individual flocs could then be selected using a microscope (Figure 2(A).6). A 50 μm probe with one flattened end was mounted onto a force transducer and lowered just above a floc aggregate using a micromanipulator. The transducer then lowered the probe at a set speed until the aggregate broke from compression between the probe and slide. The applied force was then measured as the breaking force (Equation 2(A).7). The flocs under investigation were very small latex particles aggregated in a salt solution. The

mean size of flocs aggregated by vortexing was 2.5 μm and the mean floc strength was 5.3 μN. However, the experimental procedure did not measure the sizes of the residual flocs once they had been broken. This meant the results could not be normalised to a floc rupture force over the floc cross sectional area and so compared to the other techniques. This method provides an alternative microscopic measure of floc size and again needs to be assessed over a range of floc types in order to rigorously evaluate the technique. However from an operational sense it is difficult to think of a situation where flocs would be exposed to such a compression stress under normal solid/liquid separation conditions and as such this value of floc strength may not be indicative of the likelihood of floc breakage in industrial unit processes.

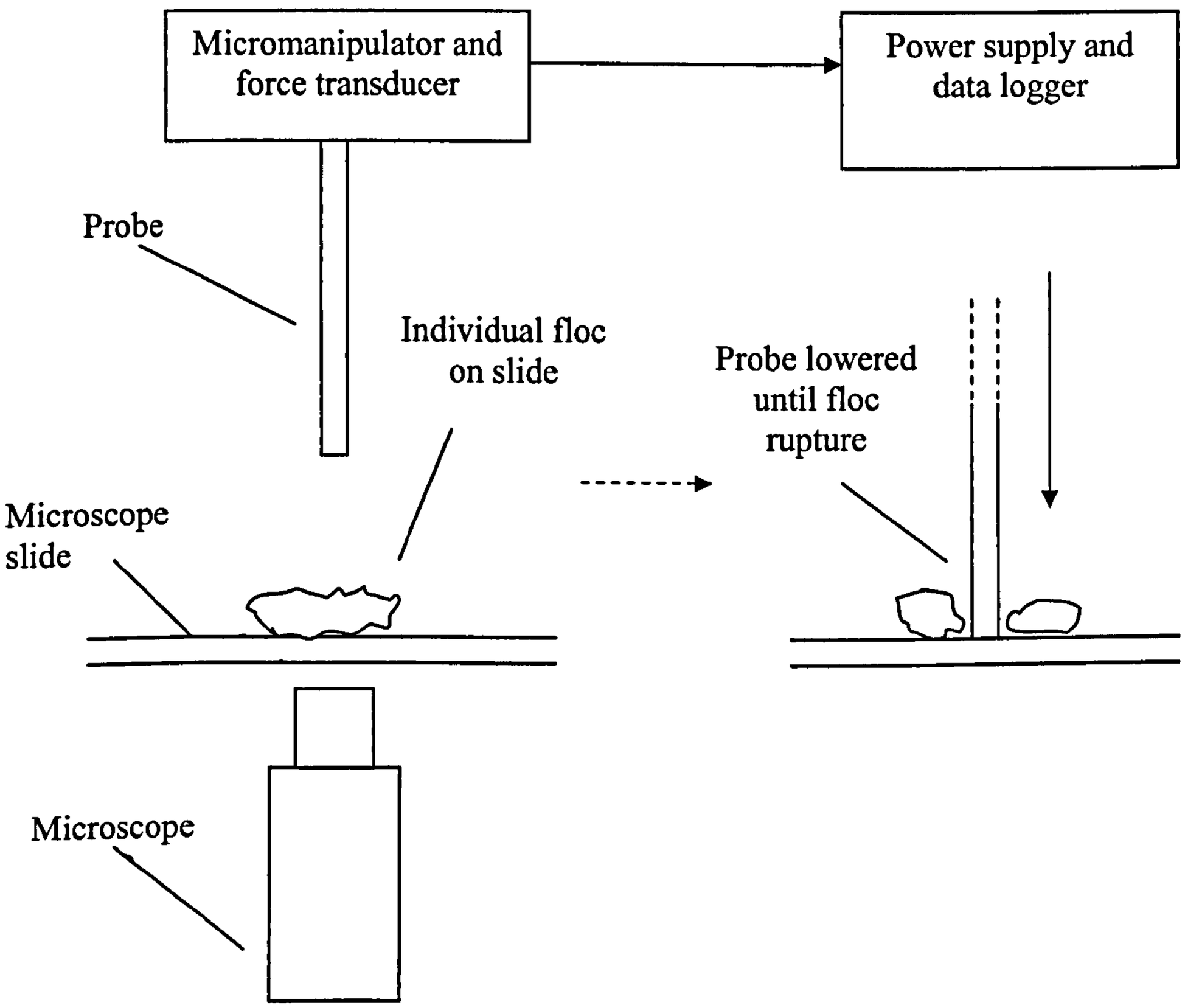

Figure 2(A).6 A schematic overview of the micromanipulation floc strength technique (adapted from Zhang et al., 1999).

2(A).4 Trends seen in floc strength techniques

Direct comparison of floc strength between the different techniques is made difficult because each technique measures floc strength in a different way giving either floc strength as a relative measure or an actual breakage force. However an attempt has been made in Table 2(A).4 to highlight the general trends that the floc strength measurements indicate. Table 2(A).5 emphasises some of these trends with a comparison of absolute values of floc strength from a number of techniques were the force per area of floc has been measured.

*Table 2(A).4 The general trends observed in floc strength tests**

Floc characteristic	Trend observed
Floc size	Floc size increases → floc strength decreases
Coagulant dose	Optimum coagulant dose for floc strength
Polymer addition	Biological flocs: Addition of polymer → floc strength decreases Chemical flocs: Addition of polymer → floc strength increases
Type of floc	Bridging particle flocs > charge neutralised particle flocs > complexation flocs (e.g. NOM/coagulant)

* for this table, the symbol '>' indicates where flocs were stronger than another type of floc.

The most significant trend to emerge from these strength tests is the increase in floc strength with a decrease in floc size. This can be clearly seen from data in Table 2(A).5 for alumino-humic flocs with an increase floc strength of over five times with a halving of the initial floc size. This is further supported by polymer-calcium carbonate flocs. Polymer A produced flocs with an average diameter of 25 μm and an average floc strength of 100 N m^{-2}, whilst polymer B produced smaller flocs of 10 μm with an increase in average floc strength to 1000 N m^{-2}. A mechanistic explanation for this relationship has not yet been fully described. However, the reasons are likely to relate to floc compaction and the number of internal bonds. In much of the strength work, flocs are grown and then exposed to an increased shear. This acts to break flocs

and therefore reduce the average floc size in the suspension. The breakage procedure breaks flocs at their weakest points, which results in smaller pieces that are smaller and more compact. This has been shown by fractal dimension analysis of polystyrene-alum flocs. There is a large amount of evidence suggesting that flocs are examples of fractal structures (Gregory, 1998; Gorczyca and Ganczarczyk, 1999; Thomas *et al.*, 1999; Bushell *et al.*, 2002). The floc fractal dimension (D_f) can indicate the openness of the internal floc structure with a higher fractal dimension indicating a more compact structure. Flocs formed at a high shear rate (G_{av} = 300 s^{-1}) were small and had a fractal dimension of 2.65 whilst floc size increased and the fractal dimension was reduced to 2.4 when the flocs were formed at a much lower shear rate (G_{av} = 50 s^{-1}) (Spicer *et al.*, 1998). More compact structures indicate that primary particles may have more attachments with one another or repulsive forces between these particles is at a minimum. Floc restructuring during breakage is one mechanism for allowing primary particles to become closer to one another so that floc internal bonds break and re-form at more favourable points within the floc where the attractive force is greater or the repulsive force lower.

Similarly, compaction is thought to explain why an optimum coagulant dose exists in terms of floc strength. For charge neutralisation coagulation mechanisms, the optimum floc characteristics should be seen when the repulsion forces between primary particles are low. However, a slight amount of charge repulsion allows attached particles to re-arrange into more compact structures rather than attaching at the first contact (Waite *et al.*, 2001). In water and wastewater treatment operations, charge neutralisation is generally achieved by the addition of charged metal ions of an opposite charge. Increasing or decreasing the ratio of the charged coagulant will therefore change the balance of the charge within the floc above or below an optimum (Bache *et al.*, 1991).

Table 2(A).5 Floc strength estimates using a variety of different methods.

Method	Type of Floc	Floc Size, μm	Floc Strength Estimate, N m^{-2}	Reference
Oscillating multigrid mixer	Alumino-humic flocs	238 182 143 120	0.08 0.16 0.29 0.42	Bache *et al.* (1999)
Oscillating multigrid mixer	Rice starch aggregated at isoelectric point (IEP)	1100	1.0	Bache *et al.* (1997)
	Latex aggregated at IEP	600	0.9	
Micromechanics	Polymer A – calcium carbonate flocs	25	100	Yeung and Pelton (1996)
	Polymer B – calcium carbonate flocs	10	1000	
Micromanipulation	Latex aggregated at IEP	2.5	5.3 μN*	Zhang *et al.* (1999)
	Latex aggregated by Brownian motion	1.7	3.1 μN*	

* data unavailable to normalise to N m^{-2}

A generally held conception within the water and wastewater industry is that the addition of polymer acts to increase floc structural characteristics by aiming to increase floc size, strength, settleability and filterability (Bratby, 1980). From the limited data presented in this review, this statement appears to be at least partially true in terms of floc strength and size. Sewage flocs and alumino-humic flocs were seen to increase in size with the addition of a polymeric floc aid. However, only the alumino-humic flocs showed improved resistance to shear, implying an increase in floc strength. The difference in floc strength with and without polymer is likely to be some reflection of the binding mechanisms of the polymer to the primary particles of the floc. For a range of polymers (anionic, cationic and non-ionic), floc strength was seen to decline for biological flocs in their response to increases in shear (Leentvaar and Rebhun, 1983; Lee and Liu, 2001). No mechanistic explanations were given although one possible hypothesis was a toxicity effect from the polymer on the

biological component of the floc. The polymer may act to kill bacteria or prevent bacterial adhesion mechanisms within the floc, thus reducing the overall bonding capacity in the floc through changes in concentration and character or extracellular polymeric substances. However, some of this previous research goes against intuitive and practical experience of polymers used in water and wastewater treatment. Much more work is required in this field to more adequately quantify the effects of polymeric flocculants.

During the removal of solid particles, enmeshment and bridging of particles within the precipitated coagulant matrix are thought to be the principal binding forces holding the floc together. These types of bond are considered much stronger than van der Waals attractive forces formed during charge neutralisation (Bache *et al.*, 1997). This is supported by the experimental data shown in Table 2(A).5. From the available data, there are considerable differences in floc strength for different types of aggregate. Flocs composed of coagulant and particles were one to two orders of magnitude stronger than charge neutralisation flocs.

Flocs formed from waters of high colour and high natural organic matter (NOM) content are widely recognised as being fragile structures when compared to other flocs (Bache *et al.*, 1997). The floc strength data available confirm this, with these flocs being weaker than flocs formed by charge neutralisation at their isoelectric point (IEP). The weakness of humic flocs is explained by Bache *et al.* (1999) to be due to the fact that charge neutralisation is the main removal route for NOM thus preventing stronger bridging bonds from forming. This in part explains the weakness of organic flocs but does not help explain why IEP flocs are considerably stronger than humic flocs. If both flocs are formed by charge neutralisation, then van der Waals forces between primary particles will dominate. The reduced floc strength of humic flocs therefore suggests an increased degree of repulsion within the floc matrix. This makes sense because organic matter is a complex mixture of different organic compounds (Goslan *et al.*, 2002). These organic molecules have differing degrees of charge and hydrophobicity (O'Melia *et al.*, 1999). Therefore, whilst some molecules and parts of molecules may be effectively charge neutralised by coagulants, regions of similar charge will exist that increase repulsion within the floc.

2(A).5 Conclusions

There have been a number of different approaches taken in measuring floc strength. Some workers consider that floc strength is indicated by the size a floc reaches at the end of its growth phase, whilst others consider the force required to break already formed flocs. Most research has concentrated on exposing flocs to increased shear in a containing vessel by the application of stirring, ultrasonification and oscillation. More recently microscopic techniques have been developed that relate the energy required to pull apart or compress individual flocs until breakage.

Whilst there is strong evidence showing an empirical relationship between the applied shear and the final floc size distribution, there are a number of problems associated with comparing the data from one study to another. The interpretations of floc breakage models need to be further analysed. These models ascribe floc breakage as either erosion or fragmentation based upon the rate of floc breakage with increasing shear relative to the eddy size in the system. These interpretations are open to debate given the incomplete understanding of how eddies interact with flocs during floc breakage. Different impeller geometries and containing vessels give rise to different shear patterns and maximum shear levels experienced by flocs that result in different floc breakage behaviour. For this reason a simple consideration of how floc size changes relative to its initial size may give the best global indication of how strong flocs are.

Some general trends have emerged from floc strength tests that show that floc strength increases with decreasing floc size. The addition of polymer decreased floc strength for biological flocs and increased floc strength for chemical flocs.

Floc strength is a difficult parameter to measure accurately due to the inherent fragility and complexity of floc structures. As yet, there is no detailed understanding of the internal composition and bonding that occurs within a floc aggregate such as the number of bonds, locations of points of attachment and internal attractive and repulsive forces within the structure. Therefore many of the floc strength and breakage models developed so far have not reached a thorough mechanistic level.

2(A).6 References

Amirtharajah, A. and O'Melia, C. R. (1990) Coagulation Processes: Destabilisation, Mixing and Flocculation. In: *American Water Works Association Water Quality and Treatment A Handbook of Community Water Supplies*. McGraw-Hill, New York.

Bache, D. H. (2004) Floc Rupture and Turbulence: a Framework for Analysis. *Chemical Engineering Science* **59** 2521-2534.

Bache, D. H. and Rasool, E. R. (2001) Characteristics of Alumino-Humic Flocs in Relation to DAF Performance. *Water Science and Technology* **43** (8), 203-208.

Bache, D. H., Johnson, C., McGilligan, J. F., and Rasool, E. (1997) A Conceptual View of Floc Structure in the Sweep Floc Domain. *Water Science and Technology* **36** (4), 49-56.

Bache, D. H., Rasool, E., Moffatt, D., and McGilligan, F. J. (1999) On the Strength and Character of Alumino-Humic Flocs. *Water Science and Technology* **40** (9), 81-88.

Bache, D. H., Hossain, M. D., Al-Ani, S. H. and Jackson, P. J. (1991) Optimum Coagulation Conditions for a Coloured Water in Terms of Floc Size, Density and Strength. *Aqua Journal of Water Supply: Research and Technology* **9** 93-102.

Bache, D. H. and Al-Ani, S. H. (1989) Development of a System for Evaluating Floc Strength. *Water Science and Technology* **21** 529-537.

Biggs, C. A. and Lant, P. A. (2000) Activated Sludge Flocculation: On-Line Determination of Floc Size and the Effect of Shear. *Water Research* **34** 2542-2550.

Boller, M. and Blaser, S. (1998) Particles Under Stress. *Water Science and Technology* **37** (10), 9-29.

Bouyer, D., Line, A., Cockx, A., and Do-Quang, Z. (2001) Experimental Analysis of Floc Size Distribution and Hydrodynamics in a Jar-test. *Transactions of the Institute of Chemical Engineers* **79** (A), 1017-1024.

Brakalov, L. B. (1987) A Connection between the Orthokinetic Coagulation Capture Efficiency of Aggregates and their Maximum Size. *Chemical Engineering Science* **42** 2373-2383.

Bratby, J. (1980) *Coagulation and Flocculation.* Uplands Press Ltd, Croydon, UK.

Burgess, M. S., Phipps, J. S. and Xiao, H. (2000) Flocculation of PCC Induced by Polymer/Microparticle Systems: Floc Characteristics. *Nordic Pulp and Paper Research* **15** (5), 2000.

Bushell, G. C., Yan, Y. D., Woodfield, D., Raper, J., and Amal, R. (2002) On Techniques for the Measurement of the Mass Fractal Dimension of Aggregates. *Advances in Colloid and Interface Science* **95** 1-50.

Camp T.R. and Stein P.C. (1943) Velocity Gradients and Internal Work in Fluid Motion. *Journal of the Boston Society of Civil Engineers* **30** 219–237.

Chaignon, V., Lartiges, B. S., El Samrani, A. and Mustin, C. (2002) Evolution of Size Distribution and Transfer of Mineral Particles Between Flocs in Activated Sludges: an Insight into Floc Exchange Dynamics. *Water Research* **36** 676-684.

Chakraborti, R. K., Atkinson, J. F. and Van Benschoten, J. E. (2003) Characterisation of Alum Floc by Image Processing. *Environmental Science and Technology* **34** (18), 3969-3979.

Chu, C. P., Chang, B. V., Liao, G. S., Jean, D. S., and Lee, D. J. (2001) Observations on Changes in Ultrasonically Treated Waste-Activated Sludge. *Water Research* **35** 1038-1046.

Cornwell, D. A. and Bishop, M. M. (1983) Determining Velocity Gradients in Laboratory and Full Scale Systems. *Journal of the American Water Works Association* **75** (9), 470-475.

Ducoste, J. J. and Clarke, M. M (1998) The Influence of Tank Size and Impeller Geometry on Turbulent Flocculation: I. Experimental. *Environmental Engineering Science* **15** (3), 215-224.

Essamiani, K. and de Traversay, C. (2002) Optimisation of the Flocculation Process Using Computational Fluid Dynamics. In: *Chemical Water and Wastewater Treatment VII: Proceedings of the 10th Gothenburg Symposium*; International Water Association: Gothenburg, June.

Farrow, J. and Warren, L. (1993) Measurement of the Size of Aggregates in Suspension. In: Coagulation and Flocculation – Theory and Applications. Dobias B. Marcel Dekker, New York.

Fitzpatrick, C. S. B., Fradin, E. and Gregory, J. (2003) Temperature Effects on Flocculation Using Different Coagulants. In: *Proceedings of the Nano and Micro Particles in Water and Wastewater Treatment Conference*; International Water Association: Zurich, September.

Francois, R. J. (1987) Strength of Aluminium Hydroxide Flocs. *Water Research* **21** 1023-1030.

Gorczyca, B. and Ganczarczyk, J. (1999). Structure and Porosity of Alum Coagulation Flocs. *Water Quality Research Journal of Canada* **34** 653-666.

Goslan, E. H., Fearing, D. A., Banks, J., Wilson, D., Hillis, P., Campbell, A.T., and Parsons, S. A. (2002) Seasonal Variations in the Disinfection By-product Precursor Profile of a Reservoir Water. *Aqua Journal of Water Supply: Research and Technology* **51** 475-482.

Gregor, J. E., Nokes, C. J., and Fenton, E. (1997) Optimising Natural Organic Matter Removal from Low Turbidity Waters by Controlled pH Adjustment of Aluminium Coagulation. *Water Research* **31** 2949-2958.

Gregory, J. (1989) Fundamentals of Flocculation. *Critical Reviews in Environmental Control* **19** 185-230.

Gregory, J. and Dupont, V. (2001) Properties of Flocs Produced by Water Treatment Coagulants. *Water Science and Technology* **44** 231-236.

Gregory, J. (1998) The Role of Floc Density in Solid-Liquid Separation. *Filtration and Separation* **35** 367-371.

Gregory, J. (2003) Monitoring Floc Formation and Breakage. In: *Proceedings of the Nano and Micro Particles in Water and Wastewater Treatment Conference*; International Water Association: Zurich, September.

Gregory, J. and Nelson, D. W. (1986) Monitoring of Aggregates in Flowing Suspension. *Colloids and Surfaces* **18** 175-188.

Jorand, F., Zartarian, F., Thomas, F., Block, J. C., Bottero, J. Y., Villemin, G., Urbain, V. and Manem, J. (1995) Chemical and Structural (2D) Linkage Between Bacteria Within Activated Sludge Flocs. *Water Research* **29** 1639-1647.

Klimpel, R. C. and Hogg, R. (1991) Evaluation of Floc Structures. *Colloids and Surfaces* **55** 279-288.

Lee, C. H. and Liu, J. C. (2001) Sludge Dewaterability and Floc Structure in Dual Polymer Conditioning. *Advances in Environmental Research* **5** 129-136.

Leentvaar, J. and Rebhun, M. (1983) Strength of Ferric Hydroxide Flocs. *Water Research* **17** 895-902.

Levich, V. G. (1962) Physico-Chemical Hydrodynamics. Prentice Hall, Englewood Cliffs, US.

McCurdy, K., Carlson, K. and Gregory, D. (2004) Floc Morphology and Cyclic Shearing Recovery: Comparison of Alum and Polyaluminium Chloride Coagulants. *Water Research* **38** 486-494.

Mikkelsen, L. H. and Keiding, K. (2002) The Shear Sensitivity of Activated Sludge: an Evaluation of the Possibility for a Standardised Floc Strength Test. *Water Research* **36** 2931-2940.

O'Melia, C. R., Becker, W. C. and Au, K. K. (1999) Removal of Humic Substances by Coagulation. *Water Science and Technology* **40** (9), 47-54.

Parker, D. S., Kaufman, W. J., and Jenkins, D (1972) Floc Breakup in Turbulent Flocculation Processes. *Journal of the Sanitary Engineering Division: Proceedings of the American Society of Civil Engineers* **SA 1** 79-99.

Spicer, P. T., Pratsinis, S. E., Raper, J., Amal, R., Bushell, G., and Meesters, G. (1998) Effect of Shear Schedule on Particle Size, Density and Structure During Flocculation in Stirred Tanks. *Powder Technology* **97** 26-34.

Thomas, D. N., Judd, S. J., and Fawcett, N. (1999) Flocculation Modelling: A Review. *Water Research* **33** 1579-1592.

Waite, T. D., Cleaver, J. K. and Beattie, J. K. (2001) Aggregation Kinetics and Fractal Structure of γ-Alumina Assemblages. *Colloid and Interface Science* **241** 333-339.

Wang, X. C., Jin, P. K. and Gregory, J. (2002) Structure of Al-Humic Flocs and their Removal at Slightly Acidic and Neutral pH. *Water Science and Technology: Water Supply* **2** (2), 99-106.

Wen, H. J. and Lee, D. J. (1998) Strength of Cationic Polymer-Flocculated Clay Flocs. *Advances in Environmental Research* **2** 390-396.

Wu, C. C., Wu, J. J., and Huang, R. Y. (2003) Floc Strength and Dewatering Efficiency of Alum Sludge. *Advances in Environmental Research* **7** 617-621.

Yan, Y. D., Burns, J. L., Jameson, G. J., and Biggs, S. (2000) The Structure and Strength of Depletion Force Induced Particle Aggregates. *Chemical Engineering Journal* **80** 23-30.

Yeung, A. K. C., Gibbs, A., and Pelton, R. P. (1997) Effect of Shear on the Strength of Polymer-Induced Flocs. *Journal of Colloid and Interface Science* **196** 113-115.

Yeung, A. K. C. and Pelton, R. (1996) Micromechanics: A New Approach to Studying the Strength and Breakup of Flocs. *Journal of Colloid and Interface Science* **184** 579-585.

Yukselen, M. A. and Gregory, J. (2004) The Reversibility of Floc Breakage. *International Journal of Mineral Processing* **73** 251-259.

Zhang, Z., Sisk, M. L., Mashmoushy, H., and Thomas, C. R. (1999) Characterisation of the Breaking Force of Latex Particle Aggregates by Micromanipulation. *Particle Particle System Characterisation* **16** 278-283.

2(B) MEASURING FLOC STRUCTURAL CHARACTERISTICS

PETER JARVIS, BRUCE JEFFERSON and SIMON A. PARSONS

School of Water Sciences, Cranfield University, Cranfield, Bedfordshire, MK43 0AL, United Kingdom

Abstract

A review is presented of a range of techniques for the structural characterisation of flocs. Flocs may be considered as highly porous aggregates composed of smaller primary particles. The irregular size and shape of flocs makes them difficult to measure and quantify. A range of different equivalent diameters are often used to define the floc size and allow comparison with other floc systems. The application of a range of floc sizing methods have been described. Microscopy is time consuming, requiring large sample size and considerable preparation but gives good information on floc shape and form. Light scattering and transmitted light techniques have been used to good effect to measure floc size on-line whilst individual particle sensors have limited applicability to measuring floc size. Fractal dimension can be measured using one of three major techniques: light scattering, settling and two dimensional (2D) image analysis. Light scattering is ideally suited for small, open flocs of low refractive index whilst settling may be applied to most floc systems of low porosity. 2D image analysis requires flocs to have good contrast between the solid in the floc and the background.

Keywords

Fractal dimension, image analysis, light scattering, microscopy, shape, size

2(B).1 Introduction

The aggregation of fine particles and colloids into larger assemblages is a process that can occur both naturally and artificially. The resulting aggregates that form are known as 'flocs' which are best described as being highly porous, irregularly structured and loosely connected aggregates composed of smaller primary particles (Dolfing, 1987; Huang, 1994; Kim *et al.*, 2001). In natural aqueous environments examples of floc formation include the transport and deposition of particulate matter in estuaries (Manning and Dyer, 1999), the assemblage of marine particles (e.g. plankton, organic matter, faecal material and minerals) into large aggregates known as marine snow (Ransom *et al.*, 1998) and the colloidal aggregates that are present in most natural surface waters (Gregory, 1997). However, industrial processes that require the separation of solids from liquids may be enhanced by an artificially induced floc formation stage. This includes bioprocess, chemical and mineral processing industries and at water treatment works (WTW) and wastewater treatment works (WWTW) (Zhang *et al.*, 1999).

The size and structure of flocs are considered fundamental to the operation of industrial unit processes (Waite, 1999). In water and wastewater treatment processes, the aim is to remove impurities from water in the form of solid particles. Once the solid particles are produced, they may be separated from water using sedimentation, flotation, filtration and thickening techniques (Rebhun and Lurie, 1993). The physical characteristics of the floc are therefore fundamental in determining their removal efficiency. For example, large compact flocs have a high settling rate that results in a treated water of low turbidity during settlement (Wilen *et al.*, 2003), whilst large and porous flocs aid filtration due to high permeability (Bushell *et al.*, 2002)

Quantifying floc characteristics is made difficult due to the highly irregular three-dimensional structure of flocs and their inherent delicate nature. In addition, the characteristics of flocculated aggregates have been shown to change depending upon the physical and chemical conditions prevailing in the flocculator (Farrow and Warren, 1989). However, a review of the literature shows there is a comprehensive amount of work on the evaluation of floc structures. The principal aim of this review is to assess how floc structural characteristics can be measured.

2(B).2 Coagulation and Flocculation

An in depth review of coagulation and flocculation theory is beyond the scope of this review, for a more rigorous and thorough treatment readers are referred to Gregory (1989) and Amirtharajah and O'Melia (1990). However, in order to understand the importance of floc structure it is firstly necessary to briefly review current knowledge of floc structure and formation. In aqueous systems, floc aggregates are composed of smaller sub-units. In most cases the primary particles are often of sizes between 1 nm and 1 μm and consequently fall into the colloidal size range.

There is some confusion in the literature as to the precise definitions of coagulation and flocculation and there appears to be a certain amount of interchanging between the two (Jefferson and Parsons, IN PRESS). However, there is some consensus that the two should be treated as separate and for the purposes of this review the following definitions are used from Cornwell and Bishop (1983) and Gregor *et al.* (1997). **Coagulation** is the process of chemically changing colloids so that they are able to form bigger particles by coming close to one another. This may be achieved by particle destabilisation through double layer compression, enmeshment, chemical reaction or chemical sorption. **Flocculation** is the process of transferring coagulated colloids into contact with each other to form larger aggregates (flocs).

The exact process of particle destabilisation and the subsequent colloid aggregation is complex. It is generally considered to be a two stage process of particle transport and particle attachment (Thomas *et al.*, 1999). The schematic in Figure 2(B).1 shows a simplified view of the steps involved. Floc formation is considered a balance between aggregation and breakage (Biggs and Lant, 2000).The rapid initial formation of microflocs is dominated by aggregation, however the importance of floc breakage increases until a steady state floc size is reached.

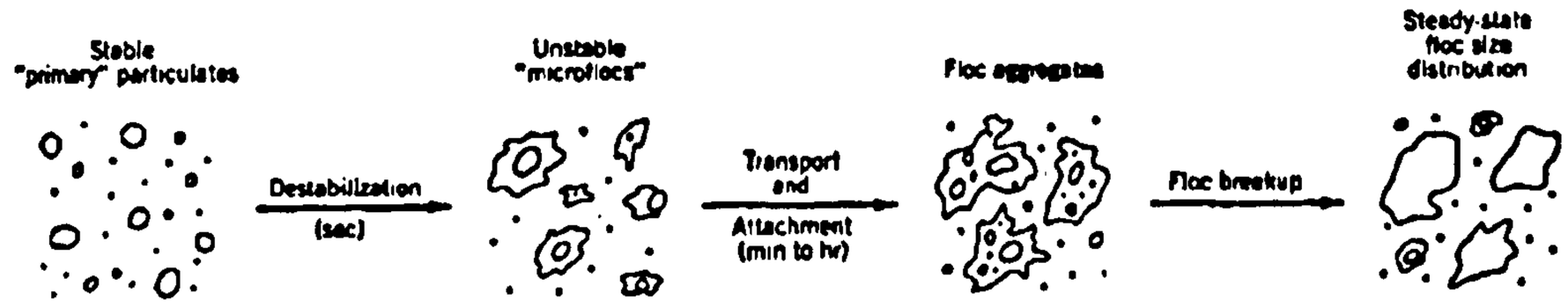

Figure 2(B).1 The steps of particle transport and attachment for aggregating particles (from Montgomery, 1985).

2(B).3 Floc structural properties and their measurement

The evaluation and quantification of floc structural characteristics is made difficult due to the highly irregular three-dimensional structure of flocs and their inherent delicate nature and porosity. However, there is a great deal of information in the literature on methods for the quantification of flocs. The following section deals in turn with measuring floc size, shape and fractal dimension.

2(B).3.1 Floc Size

Many different measurements have been chosen as the representative characterisation of floc size. A simple measure of floc size is the floc longest dimension. On its own this measurement is of limited use as it only gives an indication of floc size in one dimension. A more common approach is to find the longest dimension of the floc in both the horizontal (d_{hor}) and vertical (d_{vert}) planes as shown in Figure 2(B).2 (Farrow and Warren, 1989; Manning and Dyer, 1999). This also allows an indication of the floc height: width ratio and gives an indication of floc shape.

Typically, when referring to floc size a floc equivalent diameter measurement is made (Cousin and Ganczarcyk, 1998). The use of equivalent diameters allows the particle to be defined as a sphere or circle that is in some way equivalent to the particle. Such a standardised measurement allows a comparison to be made between very irregular forms. However, unless the particle being measured is a sphere, then each of these different diameters will take a different value for the same particle. Rather than an absolute value, equivalent diameters should be used for comparative purposes. For this reason it is important that the choice of equivalent diameter remains the same when comparing floc size. Dharmarajah and Cleasby (1986) list fifteen different characteristic diameters that are used to quantify non-spherical particles. Some of

these are not applicable to the measurement of flocs because they would damage the fragile aggregates. This precludes the use of sieve diameters, which involves passing the aggregates through a sieve and determining the smallest mesh size that will allow the particle through. The most common size measurements that are used in the literature for flocs are summarised in Table 2(B).1.

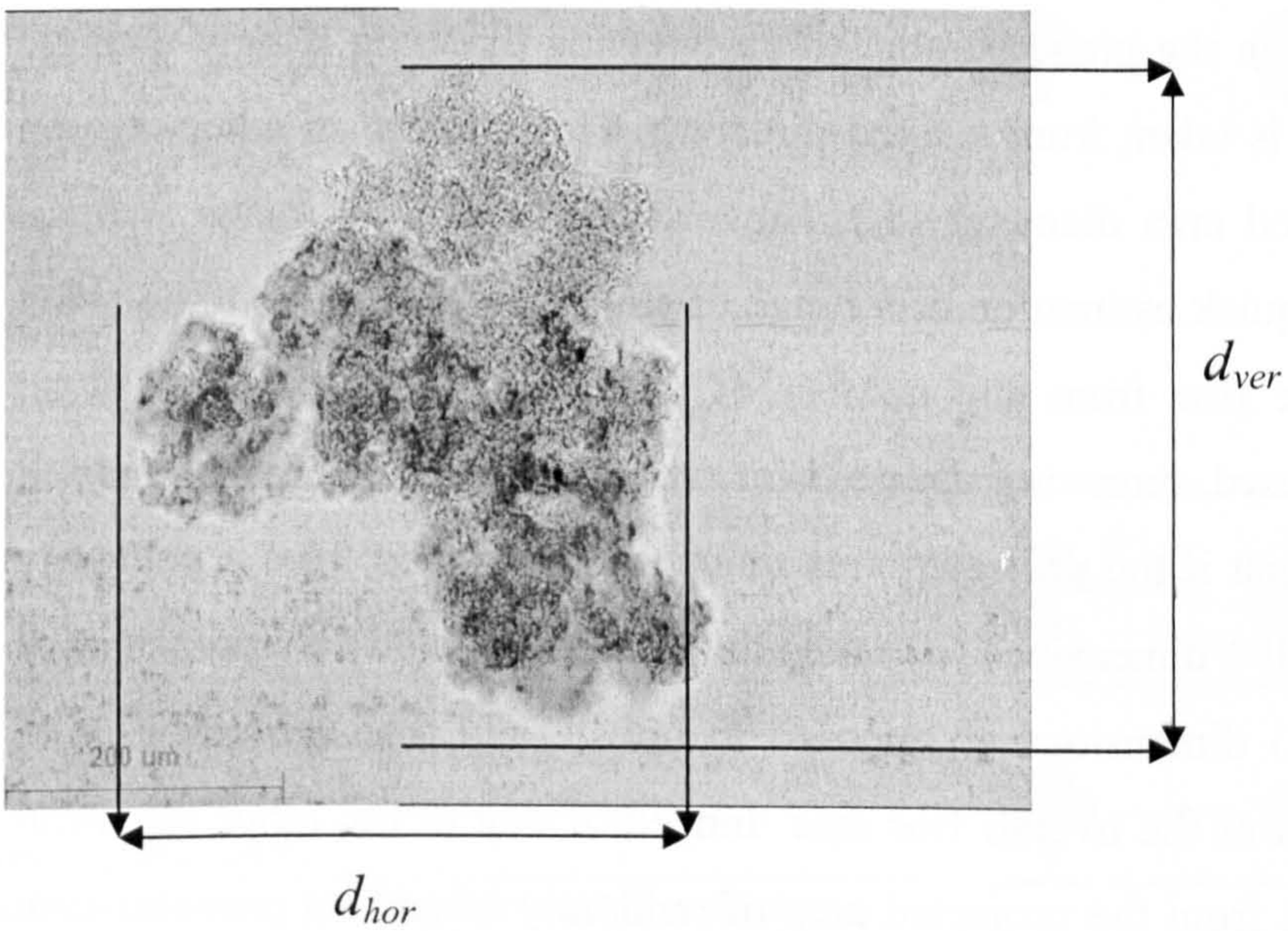

Figure 2(B).2 The maximum dimensions in the horizontal and vertical planes for a typical floc.

As microscopy has been widely applied in particle sizing (Allen, 1997; Aguillar *et al.*, 2003) most of the floc diameters in Table 2(B).1 are from two-dimensional images. As with all two dimensional measurements of complex and irregular three dimensional structures, there are difficulties in getting representative size data from a single measurement. Additionally, the results strongly depend upon the orientation of the floc presented to the researcher because a single non-uniform shape has an infinite number of linear dimensions, so it is only when these results are averaged for a large number of particles that a meaningful number can be found. The British Standard for microscope counting suggests that a minimum of 625 particles should be sized in order to get a representative size distribution (BS3406, 1963).

The diameters based upon 2 dimensional images (such as the projected area diameter (d_a), the Martin's diameter (d_M) and the Feret's diameter (d_F)) are known as statistical diameters because they are only an acceptable indication of particle size distribution if

enough measurements are made. The situation is complicated because particles have a tendency to orientate themselves on slides such that they present their maximum area (Allen, 1997). This means that the dimension perpendicular to the viewing plane is generally the smallest and is often neglected. Therefore there is a tendency for statistical diameters based upon 2 dimensional images to be larger than those based upon 3 dimensions. Martin's and Feret's diameters also rely upon the random orientation of the floc in the plane parallel to the viewing direction if only a single measurement per floc is taken from a fixed direction. This confers an advantage on the use of the projected area diameter (d_a). However the advent of image analysis tools has enabled the quick estimation of a range of single measurements to be taken from around the same floc from any number of different directions such that an average value can be used, removing the need for random orientation in this plane. It should also be noted that if the projected area diameter is obtained from a randomly orientated particle in all 3 dimensions (d_{pr}) then the diameter should be representative of the particle in all 3 dimensions as opposed to only 2 and thus provide a more accurate representation of the overall floc size. Indeed, if any of the other statistical diameters are obtained from the projected area of randomly orientated particles then they too should be representative of the three dimensional floc.

Particle size estimates based upon volume are particularly useful for settlement purposes. The settlement of flocs is a particularly important operational parameter because increased rates of floc settlement result in better solids removal in settlement tanks. In laminar flow, particles fall randomly so orientation should average out over a range of measurements. In non-laminar conditions, particles tend to orientate themselves to resist motion, so the free falling diameter found is smaller than the Stoke's diameter (Allen, 1997). It is therefore recommended that laminar conditions are applied in order to find a more representative indication of particle size.

Table 2(B).1 The most common equivalent diameters used for characterising floc aggregates (taken from Dharmarajah and Cleasby, 1986 and Allen, 1997).

Floc Diameter (m)	Description	Diagram	*Equation for Calculation*
Perimeter diameter, d_c	The diameter of a circle with the same perimeter (*P*) as the measured particle.		$d_c = \frac{P}{\pi}$
Projected area diameter 1, d_a	The diameter of a circle with the same projected cross-sectional area (*A*) as the floc measured in a stable orientation.		$d = 2\sqrt{\frac{A}{\pi}}$
Projected area diameter 2, d_{pr}	The diameter of a circle with the same projected area as the floc measured in a random orientation.		
Surface diameter, d_s	The diameter of a sphere having the same surface area (S) as the floc.		$d_s = \sqrt{\frac{S}{\pi}}$
Volumetric diameter, d_v (OR equivalent spherical diameter)	The diameter of a sphere with the same volume (*V*) as the floc measured.	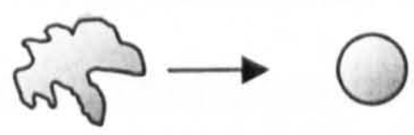	$d_v = \sqrt[3]{\frac{6V}{\pi}}$
Surface-volume diameter, d_{sv}	The diameter of a sphere with the same surface area to volume ratio as the floc.		$d_{sv} = \frac{d_v^3}{d_s^2}$
Free-falling diameter, d_f	The diameter of a sphere having the same density and free-falling speed as the floc in the same fluid at the same density and viscosity.	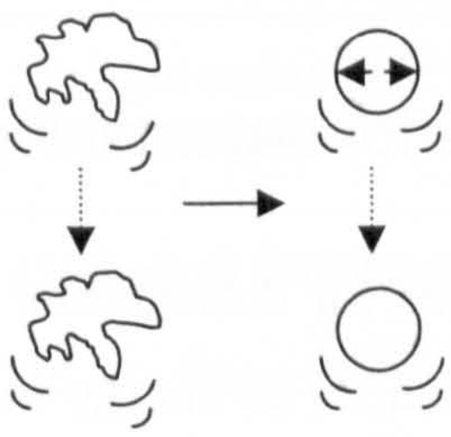	
Stoke's diameter, d_{st}	The diameter of a free falling particle in the laminar flow range (where Re < 0.2).		$d_{st} = \frac{18\mu v}{\rho_f - \rho}$
Feret's diameter, d_F	The (mean) value between pairs of parallel tangents to the projected outline of the particle.		-
Martin's diameter, d_M	The length of the chord parallel to a fixed direction which splits the floc projected area into two equal parts.	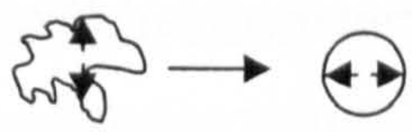	-
Circumscribing diameter, d_{sc}	The diameter of the smallest circle that circumscribes the outline of the projected floc.	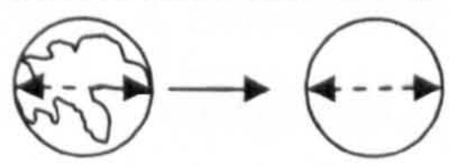	-
Inscribing diameter, d_I	*The diameter of the biggest circle that fits inside the outline of the projected floc.*		-

2(B).3.2 Floc Shape

An indication of floc shape may be provided by sphericity and circularity shape factors. The indices measure how much a particle varies from a sphere or a circle (Equations 1 and 2). The sphericity factor is a function of the volumetric diameter (d_v) and the surface area diameter (d_s).

$$Sphericity = \left(\frac{d_v}{d_s}\right)^2 \qquad \text{Equation 2(B).1}$$

$$Circularity = \frac{P^2}{4\pi A} \qquad \text{Equation 2(B). 2}$$

Circularity is related to the projected perimeter (P) and the projected area of the particle (A). A value of close to zero indicates a shape approaching a straight line, whilst a value of 1 indicates the shape is a perfect sphere or circle. The shape factors may be of use to show the change of particle shape under differing conditions. For example, Cousin and Ganczarczyk (1998) compared the affect of salinity on activated sludge flocs. A reduction in the value of the circularity shape factor with increasing salinity indicated that the flocs were becoming more elongated at higher salt concentrations.

2(B).4 Methods for determining floc size and shape

Most of the methods for determining floc strength rely upon some measurement of floc size before and after an energy input. Techniques for quantifying and measuring floc size and shape parameters are made difficult due to the inherent irregularity of floc structures in both two and three dimensions. Most efforts have been to size flocs from magnified images captured from cameras (Wang and Gregory, 2002). Two fundamental difficulties arise when using such an approach. The first is which comparable floc characteristic(s) should be measured and the second is how the flocs are prepared prior to being measured.

Farrow and Warren (1993) have divided some of the methods used for characterising aggregate particle size into a number of separate categories (Table 2(B).2). Different workers have used a variety of different methods for the determination of aggregate

size. It is important to ensure that the extraction, preparation and measuring technique:

(1) measures a representative sample or sub-sample of the original floc suspension
(2) does not damage, break or change the flocs
(3) does not encourage further aggregation

Table 2(B).2 Some of the methods used for obtaining aggregate size.

General Floc Sizing method	Floc Size found from:
Microscopy	(1) observation of static floc size (2) observation of dynamic floc size
Photography and image analysis	(1) observation of floc static size taken from suspension (2) observation of floc dynamic size under turbulent conditions (3) observation of floc dynamic size under laminar flow
Light scattering	(1) back/front scattering of light by floc particles
Transmitted light	(1) light transmitted through floc suspension
Individual particle sensors	(1) optical sensing of flocs (2) electrical sensing of flocs

2(B).4.1 Microscopy

Microscopy is one of the most widely used technique for measuring particle size (Allen, 1997; Aguillar *et al.*, 2003). Microscopy has been used for decades as a method for sizing and counting flocs (Li and Ganczaryck, 1986; Droppo *et al.*, 1996). Before the advent of image analysis gaining useful floc size data was laborious and highly dependent upon the skill of the microscopist. A non-biased selection of flocs is required that is representative of the flocs contained within the sub-sample presented to the researcher. Aggregate size is estimated by reference to a graduated eye piece graticule or by placing flocs in cells with background grids or scales of a known size

(for example a plankton counting chamber). This also requires good practice on behalf of the microscopist.

In most instances, carefully dropping a small sample of the suspension onto a microscope slide or into a measuring cell on a slide is suitable for particle size analysis under a microscope (Spicer and Pratsinis, 1996; Wang and Gregory, 2002). In some studies, a cover slip is placed over the floc sample on a flat slide without a well as this removes depth of field problems (Cornelissen *et al.*, 1997; da Motta *et al.*, 2001). However, it is difficult to accept that this approach does not change the flocs due to their delicate nature. The compression from the cover slip is likely to considerably change floc structure.

The problem associated with all techniques where flocs must be removed *ex situ* from the suspension arises from the method of aggregate extraction and preparation prior to being sized. As reported in Farrow and Warren (1993), Camp (1968) used a dipped tube technique, whereby a hollow glass tube was submerged in a flocculated suspension and sealed at the top and then removed. The tube was then placed horizontally beneath the microscope for analysis. This method provides a good representative sample of the flocs without much rupture. However, in the tube flocs can settle onto one another and cannot be distinguished from one another. Therefore this cannot be a true representation of the actual size distribution. Wang and Gregory (2002) use a similar method to withdraw flocs for analysis using a sampling tube. The contents of the tube were carefully emptied into a microscope cell previously filled with water. By ensuring the tube was large enough and the cell filled with water no floc breakage was seen. In addition, the dilution upon entering the cell should prevent the flocs from falling onto one another. In addition it is important that the technique must not allow further agglomeration to take place during the sample preparation, therefore as dilute suspensions as possible are favoured.

Cousin and Ganczarczyk (1998) and Gorczyca and Ganczarczyk (1999) have used an agar solution (1.5-4 %) to solidify activated sludge flocs and alum flocs in suspension in a Petri dish. A thin layer of the solidified suspension containing an equal distribution of flocs can then be viewed and measured under a microscope. This technique aims to ensure the flocs randomly orientate themselves in the suspension

and overcome the non-random orientation of flocs settling onto the slide surface (Farrow and Warren, 1993). Effectively a static measurement is giving a three dimensional representation of the floc. However, it is not clear what affect the agar has on floc structure. A further method from Gorczyca and Ganczarczyk (1999) embedded cubes of agar-solidified alum floc suspensions in a hardening resin. In this way, very thin sections (2 μm thick) could be cut through the cubes to allow floc internal structure to be viewed under a microscope. However, when compared to the agar technique smaller flocs were seen suggesting the hardening resin has a considerable affect on floc structure. Indeed, for both techniques there must be some question as to whether you get random orientation of flocs in the thin agar suspension of the Petri dish.

The use of wide-mouthed pipettes is a common method for floc extraction (Li and Ganczarczyk, 1986; Spicer and Pratsinis, 1996). Individual flocs may be selected in this way or a larger sub-sample of the suspension may be removed. The latter option is preferred and is more widespread because it requires no bias on behalf of the worker for a selection of a whole range of floc sizes. The use of pipettes is a widely used technique, however Manning and Dyer (1999) suggest that they are a destructive method. They explain that their use may account for differences between floc sizes generated from *in situ* and *ex situ* methods. It is therefore useful to compare *in situ* and *ex situ* techniques. Spicer *et al.* (1998) have compared the size of polystyrene-alum flocs generated from a Malvern Mastersizer (a light scattering method discussed later in the review) using three types of sample delivery mechanisms: a) a 5 mL hand pipette, b) a syringe pump and c) a peristaltic pump. The mass-mean floc diameters after 15-20 minutes of flocculation was ~150 μm using the pipette and ~250 μm using the syringe and peristaltic pumps. This would seem to confirm that hand pipettes adversely disrupt flocs. However, the authors discuss that it was actually the result of flocs settling between sampling and measurement by the Mastersizer because the rate of delivery using the measuring cell is very slow using the hand pipettes and that the pipettes did not adversely affect the floc size.

Microscopy has the advantage of allowing individual particles to be viewed, scrutinised and analysed at high magnification. This allows the researcher to get a feel

for the structure of each aggregate under investigation and give a better indication of floc shape and irregularity. In many applications, microscopy is the only method available to find floc porosity and other shape factors. In addition, microscopy is a relatively inexpensive method. Limitations of microscopy are the small depths of field possible with light microscopes such that a particle may be entirely focused due to its 3D structure projecting into the plane of view (Allen, 1997).

A can be seen from Table 2(B).3, the recommended 625 individual particle counts per sample is generally not seen for most studies using microscopy to investigate floc size distributions. This suggests that the microscopy work carried out to date should only be used as an indicator of the actual floc size or as a compliment to other sizing techniques because it does not meet the rigorous statistical criteria of the British standard.

Table 2(B).3 The number of flocs sized per sample for a number of different studies.

Type of floc under investigation	Number of flocs measured	Authors
Activated sludge	245-377	Ll and Ganczarczyk (1986)
Polystyrene beads	500+	Spicer and Pratsinis (1996)
Activated sludge	70+	da Motta *et al.* (2001)
Alum flocs	~ 100	Gorczyca and Ganczarczyk (1999)

Microscopy has been and still is a widely used technique for floc sizing. Sample extraction and preparation is key to gaining accurate knowledge of floc size distributions. Simply transferring a diluted floc sample into a shallow microscope well is the quickest and easiest and most widely used method. Considerable time and effort needs to be invested in order to achieve the necessary accuracy and a statistically significant distribution.

2(B).4.2 Photography and image analysis

Image analysis is the manipulation of information within an image to turn it into a more useful form whilst digital image analysis is the manipulation of digital images using a computer. For the purposes of this review, where the term image analysis is used this refers to digital image analysis. The basic stages and requirements of

performing image processing and analysis are shown in Figure 2(B).3. Image analysis usually requires image processing which is the conversion of one image into another. Usually this is done to improve the quality of the image for analysis. For example, if an image does not have a well defined contrast between the object and background a particle may be incorrectly sized due to a blurred boundary between the two (Chakraborti *et al.*, 2000).

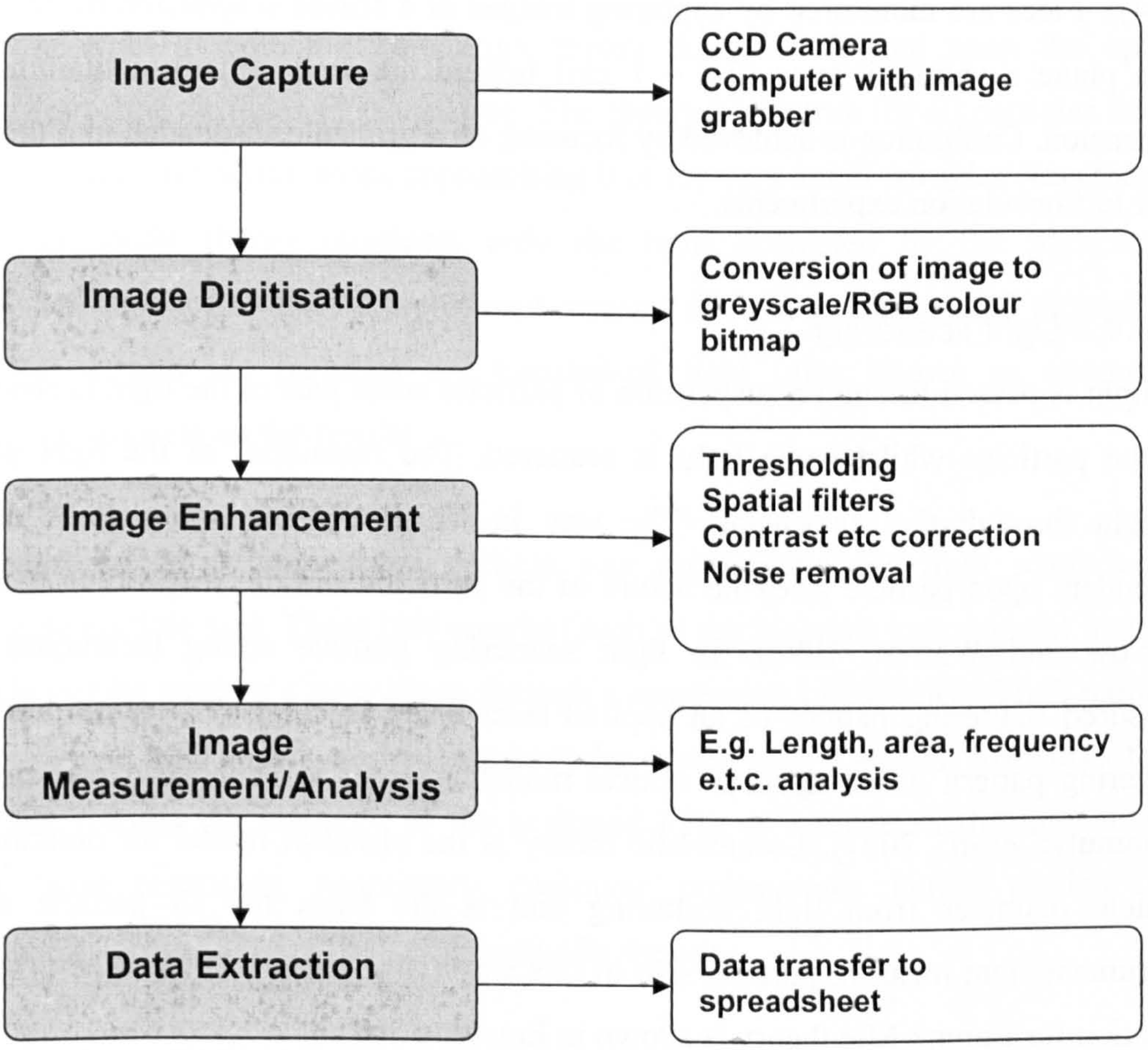

Figure 2(B).3 The steps involved in digital image analysis.

The main components of a modern image analysis system are an image capture device (usually a close-coupled device (CCD) camera) connected to a computer with an image grabber. In recent times, the widespread use of digital photography negates the need for image digitisation because the digital camera directly captures a digital image. Computer software is required for the image processing and analysis and a variety of commercial products are available. Image analysis is often combined with microscopy by mounting a CCD camera onto the microscope (Li and Ganczarczyk,

1986; Cousin and Ganczarczyk, 1998; da Motta *et al.*, 2001; Kobayashi, 2004). The advent of photography and image analysis has allowed much quicker measurements of an almost inexhaustible number of different floc size measurements to be made from floc samples when compared to traditional microscope methods (Wang and Gregory, 2002). However, it still relies upon an unbiased approach from the microscopist. Image analysis has also been used to monitor floc suspensions *in situ* (Ducoste and Clark, 1998; Chakraborti *et al.*, 2000; Bache and Papavasilopoulos, 2004)). Flocs are monitored by capturing images of a stirred suspension by focusing on a plane a short distance (0.3 – 1 cm) behind the wall of tank containing the suspension. Calibration is achieved by focusing on a graticule suspended into the tank prior to flocculation experiments.

2(B).4.3 Light scattering

As light is passed through a suspension of particles some part of the light is absorbed by the particles whilst some light is scattered. The remainder of the light passes straight through the suspension. The way in which the suspension does this is dependent upon particle size, the nature of the particles and the suspending medium (Farrow and Warren, 1993). In light scattering particle sizing techniques, the measured scattering pattern of an applied laser beam is compared to the predicted scattering pattern based upon an optical model in order to generate a particle size (Selomulya *et al.*, 2001). Lorenz-Mie theory is the classical model for determining particle diameter from light scattering and is the basis for all particle sizing instruments that measure particle size in this way (Black *et al.*, 1996). The principle equation for Lorenz-Mie theory is shown in Equation 2(B).3.

$$\chi = \frac{\pi n d}{\lambda} \qquad \text{Equation 2(B).3}$$

χ is the fundamental parameter for light scattering, d is the particle diameter (m), m is the refractive index of the particles and the λ is the wavelength of the incoming laser beam (m).

The model assumes particles are (1) spherical, (2) the laser beam illuminates particles uniformly and (3) the laser beams are plane light waves. This theory works well for particles that are smaller than the cross section of the laser beam. However, as particles get larger assumptions 2 and 3 become unreliable. For example, at a typical beam size of 100 μm, the assumptions of plane light and uniform illumination do not

hold at particle sizes above 10-20 μm (Black *et al.*, 1996). Fraunhofer diffraction theory is a modified version of Lorenz-Mie theory that takes this into account (Equation 2(B).4).

$$X = \frac{\pi d R}{\lambda f}$$ Equation 2(B).4

X is the fundamental parameter for light scattering, d is the particle diameter (m), R is the radial distance in the focal plane as measured from the optical axis (m), λ is the wavelength of the incoming laser beam (m) and f is the focal length of the receiving lens (m).

It is important to note the Fraunhofer theory does not depend upon the optical properties of the particles in suspension. The theory holds true for all particles except particles with a refractive index approaching 0 or for very small particles (less than 10 μm). Fraunhofer theory considers only the light diffracted by the particles in suspension, however where a significant amount of light is transmitted through the particles or past the particles the transmitted light (also known as anomalous scattering) impacts on the results.

The most common commercial particle size instruments use light scattering to determine particle size. These instruments (such as the Malvern instruments) measure particle size by passing a laser beam through a suspension of particles. Small particles scatter light at high angles whilst large particles scatter at low angles. An array of ring detectors records the intensity of the scattered light at a range of different angles. From these responses, proprietary computer programmes iterate particle size distributions from Lorenz-Mie and Fraunhofer theory.

A certain amount of light passes through the suspension and out of the optical system. The amount of light lost is dependent upon the size and concentration of the particles in suspension. The instrument measures this in terms of the laser beam obscuration, in other words the amount of the laser beam that is scattered or absorbed by the particles. The manufacturers recommend that between 10-30 % obscuration is achieved for reliable measurements (Guan *et al.*, 1998). The concentration required to reach this range will vary for different suspensions, however Farrow and Warren (1993) suggest that solids should be < 0.03 % solids by weight. Excessive obscuration leads to significant underestimation of the laser beam scattering.

These techniques rely upon a constant flow of the suspension through the instrument during the measurement cycle. This feature has been harnessed to allow the development of a non-intrusive methodology for measuring dynamic floc size (Spicer *et al.*, 1998; Biggs and Lant, 2000; Chaignon *et al.*, 2002). These methods have a stirred vessel containing the aggregate suspension and are connected to the particle sizing device by plastic tubing. Intrinsic to this type of system is a requirement to pump the suspension through the optical unit of the size analyser. As has been previously been discussed, Spicer *et al.* (1998) compared 3 types of pumping techniques for delivery to the optical cell. They concluded that a continuous recycle using a peristaltic pump on the return side of the particle was the least severe technique on the flocs and allowed easy continuous monitoring of the suspension. Flocs were extracted from the recirculation zone in the flocculation vessel (a distance midway between the top of the tank and the stirrer) to ensure an accurate representation of the bulk suspension was sampled. Rattanakawin and Hogg (2001) used a similar set-up without the recirculation system. The floc samples were discarded once they had passed through the size analyser. This was done to ensure that any affect of the pump on floc size was ignored. However such a method could not be used for continuous monitoring of the flocculation process as the suspending fluid would run dry.

Biggs and Lant (2000) compared the effect of pump speed on the size distribution of activated sludge flocs for a continuous system using a Malvern Mastersizer as the size analyser. They compared four different flow rates ranging from 1.7-5.5 mL s^{-1} using a peristaltic pump. They found that the optimum pump speed was at a flow of 3 mL s^{-1}, above this rate shear within the pump and tubing significantly reduced the floc size. Whilst below this flow there was a significant time lag before a representative sample was measured in the particle size analyser. Spicer *et al.* (1998) also used a flow of 3 mL s^{-1} in 6 mm internal diameter tubing (corresponding to a Reynolds number of 618) for research into flocculation of polystyrene beads. Lartiges *et al.* (1994) used a pump speed corresponding to 1.75 mL s^{-1} as this did not encourage aggregation or break-up in the pump system for research on optimising coagulation of raw river water.

2(B).4.4 Transmitted light

Another technique that has been used extensively to monitor the size and growth of floc suspensions is the photometric dispersion analyser (PDA). First described by Gregory (1985), the PDA gives a combined measurement of the particle size and frequency for a flocculating suspension. The device consists of a light source, detector and processing equipment that monitors turbidity fluctuations in the sample. Specifically the PDA measures the average light transmitted through a suspension and the rms value of the fluctuating component (Gregory and Dupont, 1997). The ratio of the two gives the flocculation index (FI), which gives a good measurement of aggregation. The PDA has been widely used in closed loop systems to measure dynamic floc size, similar to those mentioned for the light scattering techniques (Burgess and Phipps, 2000; Fitzpatrick *et al.*, 2003; Yukselen and Gregory, 2004; McCurdy *et al.*, 2004). Whilst the other sizing methods give an absolute value for floc size, the PDA gives a combined value that increases with increasing particle size and number. However, for a system containing a constant solids fraction an increase in the FI can be attributed to an increase in floc size as the larger particles have a greater signal fluctuation than smaller ones (McCurdy *et al.*, 2004). The PDA is therefore good at showing relative changes in floc size, such as during floc growth and breakage phases and giving qualitative comparisons between different treatment variables. Unlike, some of the other sizing techniques, the PDA is unable to give information on floc size distributions and the solids passing through the measuring cell must be at a high enough concentration to provide a reliable signal.

2(B).4.5 Individual particle sensors

Individual particle sensors measure single particles as they pass through an aperture onto an electric field **(electrical sensing)** or through a light beam **(optical sensing)**. In both of these techniques, the major source of problems for particle sizing comes from the break-up of floc aggregates as they pass through the aperture of the measuring cell.

In the electric field method, particles are suspended in an electrolyte solution and then passed through an electric field. The change in resistance caused by the particle is proportional to the particle size with a small correction factor (Farrow and Warren, 1993). The Coulter counter is the most common electrical sensing technique.

Leentvaar and Rebhun (1983) summarise that the Coulter counter significantly underestimates floc size when compared to optical analysis as it only measures the volume of the solid in the floc and not the effective volume of the floc including pores and water. The effect of the electrolyte solution on floc macrostructure has yet to be fully investigated at the ionic concentrations involved using electric field methods, but Cousin and Ganczarczyk (1998) have shown an increase in activated sludge floc porosity, diameter and elongation at very high salt concentration.

The optical sensing methods measure particles of a size >10 μm. The amount of light attenuated by particles as they cross a light beam is proportional to particle size. However this method is limited by a need for a low particle concentration for accurate measurement and a narrow size distribution band due to the narrow size of each aperture in these instruments and there are few examples of these instruments being used for floc sizing.

2(B).4.6 Summary

No particle sizing method is perfect for measuring floc size and each of the techniques have their own advantages and disadvantages. The tedious requirements for sample preparation and floc transfer indicate that microscopy is not the most suitable technique for finding floc size. Photography *ex-situ* gives a considerable improvement in that flocs do not need removing from the flocculating vessel but high quality images are required for accurate image analysis. Nevertheless, both photography and microscopy can give a crucial indication as to the type of particle they are dealing with and are often the only reliable method for getting floc shape factors and porosity measurements. The particle sensing instruments are not ideal due to the problems associated with only being able to measure narrow size bands at a time using electrolyte solutions in the measuring cell. On-line techniques such as those involving light scattering and the PDA allow quick measurements to be made and their non-intrusive nature and ability to monitor a wide range of particle size distributions make them ideal for showing quantitative size distributions (light scattering) and qualitative changes in floc size (PDA).

2(B).5 Fractal dimension

Since Mandlebrot introduced the concept of fractal theory in the 1970's, the application of fractal geometry is now a well established means of describing the complicated structure of particle aggregates (Gorczyca and Ganczarczyk, 1999; Thomas *et al.*, 1999; Selomulya *et al.*, 2003; Chakraborti *et al.*, 2003). Fractal objects may be defined as those objects that:

(1) show self similarity
(2) express a power-law relationship between two variables
(3) can be characterised by a non-integer fractal dimension

Self similarity is the existence of the same pattern regardless of the magnification from the which the fractal object is viewed. In many systems exact self-similarity is not observed, but a less restrictive definition of a fractal object is that it shows statistical self-similarity. This means that on average different sections of the object look similar to one another (Kaye, 1989). The second characteristic of fractal objects is a power relationship between two variables of the object and the fractal dimension (D_f). This may be a link between area (A) and length (L) as in Equation 2(B).5, or the relationship between volume (V) and area as in Equation 2(B).6.

$$A \propto L^{D_f} \qquad \text{Equation 2(B).5}$$

$$V \propto A^{D_f} \qquad \text{Equation 2(B).6}$$

Flocculated aggregates are examples of mass fractal objects. This means that both the internal structure and the surface of the aggregate exhibit fractal properties. Mass fractals are summarised by Equation 2(B).7.

$$M \propto L^{D_f} \qquad \text{Equation 2(B).7}$$

M is the mass of particles, L is a characteristic measure of size and D_f is the mass fractal dimension. Gregory (1998) summarises that the choice of measurement for the size L does not matter as the same trends are seen so long as the choice is constant. For Euclidean objects, the one dimensional value of D_f will be 1 for a linear line, 2 for a two dimensional planar shape and 3 for a compact three dimensional shape. Fractal objects take non-integer values of D_f and are therefore said to show non-Euclidean

dimensionality. Values approaching 3 for a three dimensional floc therefore indicates a high degree of compaction whilst values approaching 1 indicates a very loose and open structure. The fractal dimension can therefore give important structural information of floc compaction and the space filling nature of the aggregate. The fractal dimension of a floc may be found in a number of ways. These may be broadly categorised into techniques that use scattering (of light, neutrons or x-rays), settling and two dimensional fractal analysis using image analysis (Waite, 1999).

2(B).5.1 Scattering

The pattern in which an aggregate scatters incoming radiation gives information on the aggregate structure as a function of a length scale (Bushell *et al.*, 2002). The way in which an object scatters light can give fractal values if enough is known about the scattering properties of the material contained within the aggregate. This technique assumes:

(1) The primary particles that make up the aggregate are uniform in shape and size.

(2) The refractive index of the aggregate material is low so that the wavelength of the incident light does not become shortened.

(3) Light is only scattered once as it passes through the suspension of aggregates before hitting the detector. Multiple scattering should be minimised by ensuring the concentration of particles is low (Tang *et al.*, 2002).

Generally, finding the fractal value from scattering theories rely upon the power law based upon Rayleigh-Gans-Debye (RGD) scattering theory shown in Equation 2(B).8.

$$I(Q) \propto Q^{-D_f} \qquad \text{Equation 2(B).8}$$

$I(Q)$ is the intensity of the scattered radiation and Q is the wave number (m^{-1}) estimated from Equation 2(B).9:

$$Q = \frac{4\pi n \sin(\theta/2)}{\lambda} \qquad \text{Equation 2(B).9}$$

n is the refractive index of the suspending medium, θ is the scattered angle, λ is the wavelength (m) of the radiation in a vacuum.

The fractal dimension D_f is found from the slope of the line of a log-log plot of $I(Q)$ against Q (Wu *et al.*, 2002). For fractal objects a power law relationship exists between $I(Q)$ and Q. This dependency is only valid when:

$$\frac{1}{R_{agg}} \gg Q \gg \frac{1}{R_{part}} \qquad \text{Equation 2(B).10}$$

R_{agg} is the radius of the aggregate (m) and R_{part} is the radius of the primary particle (m).

This is because when Q approaches $1/R_{agg}$ the relationship is affected by the edges of the aggregate whilst when Q approaches the size of $1/R_{part}$, light is mainly scattered by the primary particles and not the aggregate (Guan *et al.*, 1998; Waite *et al.*, 2001). The primary particles of the flocs must also satisfy independent scattering for RGD scattering theory approximations to be obeyed. The RGD approximation is deemed applicable when:

$$|m-1| \ll 1 \qquad \text{Equation 2(B).11}$$

$$(2\pi n/\lambda)L|m-1| \ll 1 \qquad \text{Equation 2(B).12}$$

where m is the material refractive index and L is the length of the scattering body (m).

Most application of scattering has been to mono-disperse systems where information is known about primary particle size and the scattering behaviour of the particles under investigation. Examples include flocs formed from particles of latex (Tang, 1999; Selomulya *et al.*, 2001), aluminium oxide (Waite *et al.*, 2001), and iron oxyhydroxide (Waite, 1999). In these cases the assumptions mentioned above are generally valid for application to floc aggregates. Application to more complex flocs typically found during water and wastewater treatment processes has been more difficult. In these instances, information on primary particle composition can be limited with little to no knowledge of particle refractive index. Furthermore the primary particles may be non-uniform and consist of particles with different refractive indices. Therefore a number of the assumptions mentioned above may not be met when analysing complex floc structures. As a practical example of this, a mixture of iron oxyhydroxide and kaolin has a considerably distinct shaped scattering curve when compared to a pure iron oxyhydroxide system (Waite, 1999). It is unknown at present what the impact of not knowing the refractive index of material from metal hydroxide-natural organic matter has on the calculation of floc fractal dimension. In

the case of activated sludge good scattering law relationships have been seen (Guan *et al.*, 1998; Waite, 1999). This is because the very low refractive index of the bacteria in the floc allows RGD theory to be met.

A common limitation to this technique is the limited scale of investigation of the technique. Commonly, the scattering power law relationship breaks down at small floc sizes compared to the average floc size. This was seen for kaolin suspensions where the average floc sizes ranged between 200-350 μm in diameter whilst the linear portion of the linear scattering relationship applied to flocs less than 50-100 μm (Wu *et al.*, 2002). For activated sludge flocs ranging up to 400 μm in diameter, the power law cut-off was below 70 μm (Waite, 1999). The application of light scattering to larger floc systems is an area that needs further investigation to find whether the larger flocs have variable fractal dimension or interfere with the scattering.

2(B).5.2 Settlement

Using settlement as a means of determining the fractal value of aggregates is a well established technique to the more widely used small angle light scattering method. The use of sedimentation to determine floc structural characteristics takes on an extra relevance because the settling behaviour of aggregates is an important parameter for optimising the sedimentation procedure. Floc settling behaviour is dependent upon size, effective density and porosity (Tang *et al.*, 2002). The fractal nature of floc structure can have two possible consequences on floc settlement behaviour because flocs take on increasingly non-spherical forms as they grow. This may act to increase the drag on the particle when compared to a solid sphere of the same size. Conversely, the porosity of flocs can act to reduce drag by allowing advection of the suspending medium through the floc structure (Bushell *et al.*, 2002).

The following determination of floc fractal dimension from settling velocity has been taken from Miyahara *et al.* (2002) and Wu *et al.* (2002). A spherical particle at its terminal settling velocity may be summarised by Stoke's law as shown in Equation 2(B).13.

$$v_s = \frac{(\rho_p - \rho_l)gd^2}{18\mu} \qquad \text{Equation 2(B).13}$$

v_s is the terminal settling velocity (m s^{-1}), ρ_f is the density of the particle (kg m^{-3}), ρ_l is the density of the liquid (kg m^{-3}), d is the floc diameter (m), μ is the viscosity of the suspending medium (m s^{-1}) and g is acceleration due to gravity (m s^{-1}).

Whilst Stokes law may be an over-simplification to completely describe floc setting, it is generally believed that flocs settle slow enough in order for Stokes derived equations to apply (Gregory, 1998). Shape factor and drag coefficient corrections are usually added to account for the irregular shape of flocs. A fractal floc consisting of similar primary particles may be summarised from the derived expression (Wu *et al.*, 2002):

$$v_s = \frac{{d_f}^{D_f - 1} 4kg}{3A(\beta)\mu} \qquad \text{Equation 2(B).14}$$

v_s is the terminal settling velocity (m s^{-1}), k is a proportionality constant (kg m^{-D}), ρ_l is the density of the liquid (kg m^{-3}), $A(\beta)$ is a correction factor for advection through the floc, μ is the viscosity of the suspending medium (m s^{-1}) and g is acceleration due to gravity (m s^{-1}).

The slope from a log-log plot of floc settling velocity against size will therefore yield the fractal dimension (Johnson *et al.*, 1996). The fractal dimension is found from the slope of the plot with D_f being equal to the value of the slope + 1. The equation only applies when the floc Reynolds number is less than one and the flocs fall isolated at their terminal settling velocity in laminar flow. Wu *et al.* (2002) summarise that most experimental systems measuring settling rate meet the criteria for finding the floc fractal dimension. Problems may be encountered when the floc porosity is high, in these instances advection flow through the floc significantly increases the settling rate over that predicted by Stokes equations. In most practical instances, porosity effects on settling are neglected and currently far from understood. Therefore, care must be made of interpreting data when the floc fractal dimension is significantly less than 2 (Gregory, 1998). In addition, measuring floc settling requires meticulous preparation and a large sample number in order to get accurate results (Bushell *et al.*, 2002).

2(B).5.3 Image analysis

The combination of microscopy and image analysis software have has been widely used to determine floc fractal dimension (Bellouti *et al.*, 1997; Cousin and Canczarczyk, 1998; Chakraborti *et al.*, 2003). Generally, high quality images of flocs are taken and the two dimensional (2D) fractal dimension D_I found from the projected image. This may be achieved in two common ways. The first is from the relationship between floc area and length (Equation 2(B).5). A log-log plot of floc area against size as found from image analysis yields a line with a slope giving the fractal dimension (Chakraborti *et al.*, 2000). A second way of determining floc fractal dimension is the box counting method. The process begins by covering the floc image with boxes of a minimum size to just cover the floc, this is then repeated with smaller box sizes (Bushell *et al.*, 2002). Plotting the number of boxes needed to cover the object against the size of the box on a log-log scale gives a line with a slope equivalent to the fractal dimension (Bellouti *et al.*, 1997). Commercial software packages are able to do this analysis very quickly and easily.

The main requirement for projected area fractal dimension investigation using image analysis is for the image to be of suitable quality for commercial software packages to be able to distinguish the floc from the background (Chakraborti *et al.*, 2000). In practice this often requires considerable image correction prior to fractal analysis and works best with flocs that show good contrast with their background and are not transluscent.

2(B).5.4 Summary

To summarise, Table 2(B).4 highlights the major advantages and disadvantages of each of the techniques mentioned. Light scattering methods work well with small, open flocs that have low refractive indices. Bushell *et al.* (2002) stated that these are precisely the type of aggregates that settlement and image analysis techniques do not apply well to because they do not settle well, the modelling of the settling of open flocs is very difficult due to permeability effects and these particles are difficult to see because of their low refractive index. However, when analysing systems of high particle concentrations, shadowing effects and multiple light scattering invalidates the scattering models. Therefore, the calculation of fractal dimension and particle size only holds when within the obscuration threshold of the scattering instrument being

used (Guan *et al.*, 1998). Similarly, flocs composed of a number of different primary particles have scattering behaviour that is difficult to predict and should not be used in these instances. The technique is also limited in that fractal values are generally only found for the small flocs in the system. However, when using the settling technique the fractal relationship is always seen across the whole range of flocs under investigation. Settling is a reliable technique provided a large enough sample is measured which can make this technique very time consuming. Settling can be widely applied to most floc systems provided that flocs are relatively compact thus avoiding interference in settling from porosity and advection though the floc. Careful temperature control and quiescent conditions in the settling column must be provided in order to prevent disruption to the floc.

Projected area image analysis relies upon flocs that have a high degree of definition between the solid of the floc and the background. Therefore pale translucent activated sludge flocs are often not ideal for this technique. In addition sample preparation prior to image capture is an important consideration and as has been mentioned in previous sections, the preparation stage must not act to damage or interfere with the floc structure. The main advantage of the box counting method is that the fractal dimension of individual flocs are measured. This can highlight differences in floc fractal dimension within a system whilst all the other techniques report average fractal values for the whole system.

Finally, it is important to report which technique has been used to measure floc fractal dimension. This is because each technique gives a different answer and may in fact be measuring different structural properties of the floc. For example, in a comparative study by Wu *et al.* (2002) the fractal dimension of activated sludge using settling was 1.31 whilst it was 2.06 using light scattering. Furthermore, image analysis of 2D images can only give a maximum fractal value of 2 whilst the maximum is 3 for the analysis of 3D flocs in settling and scattering. However, the relationship between the projected area diameter and the mass fractal dimension may be summarised as (from Bushell *et al.*, 2002):

$$D_f[mass] < 2, \quad D_f[projected] = D_f[mass] \qquad \text{Equation 2(B).15}$$

$$D_f[mass] \geq 2, \quad D_f[projected] = 2 \qquad \text{Equation 2(B).15}$$

Therefore, so long as the mass fractal value is less than 2, the fractal found from the image analysis of the projected area should give a comparable mass fractal value. Open flocs of low dimensionality are therefore suitable for mass fractal investigation when using image analysis.

Table 2(B).4 The advantages and disadvantages of the techniques used for determining the fractal dimension of floc aggregates.

Technique	Advantages	Disadvantages
Light scattering	- Rapid, non-intrusive method - Lends itself well to dynamic, online analysis - Very good for analysis of small aggregates with an open structure and low refractive index - Takes a large number of readings from many aggregates in a few seconds	- Not good for polydisperse aggregates made from many primary particles - Choosing an appropriate model for scattering behaviour can be difficult - Results affected by contamination from dust etc. - Power-law relationship breaks down at large floc size
Settling	- Best for measuring fractals of compact flocs - Cheap and simple - Not prone to contamination issues - Good for aggregates of made from a number of different primary particles	- Time consuming - Finding an appropriate drag coefficient is difficult - Can get non-random orientation of falling aggregates - Careful regulation of settling column required
Image analysis	- Best for large, open aggregates - Not prone to contamination issues - Examination of single flocs allows detailed information on variation in floc structure within a sample	- Time consuming - Requires well defined, high contrast images for accurate analysis – which flocs generally aren't

2(B).6 Overall summary

A range of techniques for measuring floc structural characteristics of size, shape and fractal dimension have been presented. Of the sizing techniques, microscopy is the most time consuming requiring considerable sample preparation and analysis time in order to achieve satisfactory results. However, microscopy and photography can give an important feel for the type of floc under investigation and is also the only reliable method to determine floc shape characteristics. On-line light scattering and PDA devices show good capability for measuring a whole range of different floc types and size in a non-intrusive way. Fractal dimension analysis can be measured using three main techniques. Light scattering works best for small, open flocs of low refractive index whilst larger, flocs of low porosity and of high colour contrast are more suited to settling and 2D image analysis under a microscope.

Acknowledgements

The submitted manuscript has been made possible through funding from American Water Works Association Research Foundation and Co-funding Utilities. The information contained herein is based upon Intellectual Property which is jointly owned by Cranfield University and the Foundation. The Foundation retains its right to publish or produce the Jointly Owned Intellectual Property in part or in its entirety. The authors would also like to thank the EPSRC, Fort Collins Water, Scottish Water, Severn Trent Water, Thames Water, United Utilities and Yorkshire Water.

2(B).7 References

Aguilar, M. I., Saez, J., Llorens, M., Soler, A. and Ortuno, J. F. (2003) Microscopic Observation of Particle Reduction in Slaughterhouse Wastewater by Coagulation-Flocculation Using Ferric Sulphate as Coagulant and Different Coagulant Aids. *Water Research* **37** 2233-2241.

Allen, T. (1997) Particle Size Measurement. In: *Powder Sampling and Particle Size Measurement*. Chapman and Hall, London.

Amirtharajah, A. and O'Melia, C. R. (1999) Coagulation Processes: Destabilisation, Mixing and Flocculants, In: *American Water Works Association Water Quality and Treatment: a Handbook of Community Suppliers*. McGraw-Hill, New York.

Bache, D. H. and Papavasilopoulos, E. N. (2003) Dewatering of Alumino-Humic Sludge: Impacts of Hydroxide. *Water Research* **37** 3289-3298.

Bellouti, M., Alves, M. M., Novais, J. M. and Mota, M. (1997) Flocs vs Granules: Differentiation by Fractal Dimension. *Water Research* **31** 1227-1231.

Biggs, C. A. and Lant, P. A. (2000) Activated Sludge Flocculation: On-Line Determination of Floc Size and the Effect of Shear. *Water Research* **34** 2542-2550.

Black, D. L., McQuay, M. Q. and Bonin, M. P. (1996) Laser-Based Techniques for Particle Size Measurement: a Review of Sizing Methods and their Industrial Applications. *Progress in Energy and Combustion Science* **22** 267-306.

BS3406 – British Standard Methods for Determinination of Particle Size Distribution (1984).

Burgess, M. S. and Phipps, J. S. (2000) Flocculation of PCC Induced by Polymer/Microparticle Systems: Floc Characteristics. *Nordic Pulp and Paper Research Journal* **15** (5), 572-578.

Bushell, G. C., Yan, Y. D., Woodfield, D., Raper, J., and Amal, R. (2002) On Techniques for the Measurement of the Mass Fractal Dimension of Aggregates. *Advances in Colloid and Interface Science* **95** 1-50.

Chaignon, V., Lartiges, B. S. El Samrani, A. and Mustin, C. (2002) Evolution of Size Distribution and Transfer of Mineral Particles Between Flocs in Activated Sludges: an Insight into Floc Exchange Dynamics. *Water Research* **36** 676-684.

Chakraborti, R. K., Atkinson, J. F. and Van Benschoten, J. E. (2000) Characterisation of Alum Floc by Image Analysis. *Environmental Science and Technology* **34** 3969-3976.

Chakraborti, R. K., Gardner, K. H., Atkinson, J. F. and Van Benschoten, J. E. (2003) Changes in Fractal Dimension During Aggregation. *Water Research* **37** 873-883.

Cornelissen, A., Burnett, M. G., McCall, R. D. and Goddard, D. T. (1997) The Structure of Hydrous Flocs by Batch and Continuous Flow Water Treatment Systems and Obtained by Optical, Electron and Atomic Force Microscopy. *Water Science and Technology* **34** (4), 41-48.

Cornwell, D. A. and Bishop, M. M. (1983) Determining Velocity Gradients in Laboratory and Full Scale Systems. *Journal of the American Water Works Association* **75** (9), 470-475.

Cousin, C.P. and Ganczarczyk, J. (1998) Effects of Salinity on Physical Characteristics of Activated Sludge Flocs. *Water Quality Research Journal of Canada* **33** (4), 565-587.

da Motta, M., Pons, M.-N., Roche, N., and Vivier, H. (2001) Characterisation of activated sludge by automated image analysis. *Biochemical Engineering Journal* **9** (3), 165-173.

Dharmarajah, A. H. and Cleasby, J. L. (1986) Predicting the Expansion Behaviour of Filter Media. *Journal of the American Water Works Association* **78** 66-76.

Dolfing, J. Microbiological Aspects of Granular Methanogenic Sludge. PhD 1997. Agricultural University Wageningen, Netherlands.

Droppo, I. G., Flannigan, D. T., Leppard, G. G. and Liss, S. N. (1996) Microbial Floc Stabilisation and Preparation for Structural Analysis by Correlative Microscopy. *Water Science and Technology* **34** (5-6), 155-162.

Ducoste, J. J. and Clark, M. M. (1998) The Influence of Tank Size and Impeller Geometry on Turbulent Flocculation: I Experimental. *Environmental Engineering Science* **15** (3), 215-224.

Farrow, J. and Warren, L. (1993) Measurement of the Size of Aggregates in Suspension. In: *Coagulation and Flocculation – Theory and Applications*. Dobias B. Marcel Dekker, New York.

Farrow, J. and Warren, L. (1989) A New Technique for Characterising Flocculated Suspensions. In: *Dewatering Technology and Practice.* Engineering Foundation, New York.

Fitzpatrick, C. S. B., Fradin, E. and Gregory, J. (2003) Temperature Effects on Flocculation Using Different Coagulants. In: *Proceedings of the Nano and Micro Particles in Water and Wastewater Treatment Conference*; International Water Association: Zurich, September.

Gorczyca, B. and Ganczarczyk, J. (1999). Structure and Porosity of Alum Coagulation Flocs. *Water Quality Research Journal of Canada* **34** 653-666.

Gregor, J. E., Nokes, C. J., and Fenton, E. (1997) Optimising Natural Organic Matter Removal from Low Turbidity Waters by Controlled pH Adjustment of Aluminium Coagulation. *Water Research* **31** 2949-2958.

Gregory, J. (1985) Turbidity Fluctuations in Flowing Suspensions. *Journal of Colloid and Interface Science* **105** 676-684.

Gregory, J. (1989) Fundamentals of Flocculation. *Critical Reviews in Environmental Control* **19** 185-230.

Gregory, J. (1997) The Density of Particle Aggregates. *Water Science and Technology* **36** (4), 1-13.

Gregory, J. (1998) The Role of Floc Density in Solid-Liquid Separation. *Filtration and Separation* **35** 367-371.

Gregory, J. and Dupont, V. (2001) Properties of Flocs Produced by Water Treatment Coagulants. *Water Science and Technology* **44** 231-236.

Guan, J, Waite, D., Amal, R. (1998) Rapid Structure Characterization of Bacterial Aggregates. *Environmental Science and Technology* **32** 3735-3742.

Huang, H. (1994) Fractal Properties of Flocs Formed by Fluid shear and Differential Settling. Physical Fluids **6** (10), 3229-3234.

Jefferson, B. and Parsons, S. A. (IN PRESS) Agglomeration of Clay Particles. Thomas Telford, London.

Johnson, C. P., Li, X. and Logan, B. E. (1996) Settling Velocity of Fractal Aggregates. *Environmental Science and Technology* **30** 1911-1918.

Kaye, B. H. (1989) A Random Walk Through Fractal Dimensions. VCH Verlagsgesellschaft, Weinheim, Germany.

Kim, S. H., Moon, B. H., and Lee, H. I. (2001) Effects of pH and Dosage on Pollutant Removal and Floc Structure During Coagulation. *Microchemical Journal* **68** 197-203.

Kobayashi, M. (2004) Breakup and Strength of Polystyrene Latex Flocs Subjected to a Converging Cell. *Colloids and Surfaces A: Physicochemical and Engineering Aspects* **235** 73-78.

Leentvaar, J. and Rebhun, M. (1983) Strength of Ferric Hydroxide Flocs. *Water Research* **17** 895-902.

Li, D. H. and Ganczarczyk, J. J. (1986) Physical Characteristics of Activated Sludge Flocs. *CRC Critical Reviews in Environmental Control* **17** (1), 53-87.

Manning, A. J. and Dyer, K. R. (1999) A Laboratory Examination of Floc Characteristics with Regard to Turbulent Shearing. *Marine Technology* **160** 147-170

McCurdy, K., Carlson, K. and Gregory, D. (2004) Floc Morphology and Cyclic Shearing Recovery: Comparison of Alum and Polyaluminium Chloride Coagulants. *Water Research* **38** 486-494.

Miyahara, K., Adachi, Y., Nakaishi, K. and Ohtsubo, M. (2002) Settling Velocity of a Sodium Montmorillonite Floc under High Ionic Strength. *Colloids and Surfaces A: Physicochemical Aspects* **196** 87-91.

Ransom, B., Shea, K. F., Burkett, P. J., Bennett, R. H., and Baerwald, R. (1998) Comparison of Pelagic and Nephloid Layer Marine Snow: Implications for Carbon Cycling. *Marine Geology* **150** 39-50.

Rattanakawin, C. and Hogg, R. (2001) Aggregate Size Distributions in Flocculation. *Colloids and Surfaces A: Physicochemical and Engineering Aspects* **177** 87-98.

Rebhun, M. and Lurie, M. (1993) Control of Organic Matter by Coagulation and Floc Separation. *Water Science and Technology* **27**(11), 1-20.

Selomulya, C., Amal, R., Bushell, G., and Waite, T. D. (2001) Evidence of Shear Rate Dependence on Restructuring and Break-up of Latex Aggregates. *Journal of Colloid and Interface Science* **236** 67-77.

Spicer, P. T., Pratsinis, S. E., Raper, J., Amal, R., Bushell, G., and Meesters, G. (1998) Effect of Shear Schedule on Particle Size, Density and Structure During Flocculation in Stirred Tanks. *Powder Technology* **97** 26-34.

Spicer, P.T. and Pratsinis, S.E. (1996) Shear-Induced Flocculation: the Evolution of Floc Structure and the Shape of the Size Distribution at Steady State. *Water Research* **3** 1049-1056.

Tang, P., Greenwood, J. and Raper, J. A. (2002) A Model to Describe the Settling Behaviour of Fractal Objects. *Journal of Colloid and Interface Science* **247** 210-219.

Tang, S. (1999) Prediction of Fractal Properties of Polystyrene Aggregates. *Colloids and Surfaces A: Physicochemical and Engineering Aspects* **157** 185-192.

Thomas, D. N., Judd, S. J., and Fawcett, N. (1999) Flocculation Modelling: A Review. *Water Research* **33** 1579-1592.

Wang, X. C. and Gregory, J. (2002) Structure of Al-Humic Flocs and their Removal at Slightly Acidic and Neutral pH. *Water Science and Technology* **2** (2), 99-106.

Waite, T. D. (1999) Measurement and Implications of Floc Structure in Water and Wastewater Treatment. *Colloids and Surfaces A: Physicochemical and Engineering Aspects* **151** 27-41.

Waite, T. D., Cleaver, J. K. and Beattie, J. K. (2001) Aggregation Kinetics and Fractal Structure of γ-Alumina Assemblages. *Journal of Colloid and Interface Science* **241** 333-339.

Wilen, B-M., Jin, B. and Lant, P. (2003) Impacts of Structural Characteristics on Activated Sludge Floc Stability. *Water Research* **37** 3632-3645.

Wu, R. M.; Lee, D. J., Waite, T. D. and Guan, J. (2002) Multilevel Structure of Sludge Flocs. *Journal of Colloid and Interfacial Science* **252** 383-392.

Yukselen, M. A. and Gregory, J. (2004) The Reversibility of Floc Breakage. *International Journal of Mineral Processing* **73** 251-259.

Zhang, Z., Sisk, M. L., Mashmoushy, H., and Thomas, C. R. (1999) Characterisation of the Breaking Force of Latex Particle Aggregates by Micromanipulation. *Particle Particle System Characterisation* **16** 278-283.

CHAPTER 3

METHOD DEVELOPMENT:

3(A) THE USE OF DIAGNOSTIC TOOLS TO DETERMINE THE OPERATIONAL PROPERTIES OF ORGANIC FLOCS

Published in the Proceedings of the *American Water Works Association Water Quality and Technology Conference,* Philadelphia, 2003.

3(B) THE DUPLICITY OF FLOC STRENGTH

Published in *Water Science and Technology* (2004), Vol. 50 (12), pp 63-70.

3(A) THE USE OF DIAGNOSTIC TOOLS TO DETERMINE THE OPERATIONAL PROPERTIES OF ORGANIC FLOCS

PETER JARVIS, BRUCE JEFFERSON and SIMON A. PARSONS

School of Water Sciences, Cranfield University, Cranfield, Bedfordshire, MK43 0AL, United Kingdom

Abstract

Floc structural characteristics are fundamental to the efficient removal of organic material at water treatment works. Assessment of floc structure can therefore be an important tool in determining operational performance at the waterworks. Floc size, strength and settlement characteristics were assessed for three coagulant doses using an iron based coagulant. Size and strength was determined using conventional light microscopy and an on-line laser diffraction technique. Settlement characteristics were measured using a settling column with a close-coupled device (CCD) video camera and image analysis software. Significant differences in floc size, strength and settlement were observed using the above techniques. The coagulant dose as used by the waterworks at the time of abstraction gave the best floc structure. Complex interactions occur between organic material and coagulant during the coagulation process and floc structure is likely to be determined by the ratio of organic matter and coagulant within the floc structural mass.

3(A).1 Introduction

The size and structure of flocs are fundamental to the operation of water and wastewater treatment processes and the floc structural mass should be considered as a reflection of the performance of the coagulation process as removed pollutants are incorporated into this mass (Bache *et al.*, 1991). For this reason a detailed analysis of floc structure can provide information on both the treated water quality and the likely separation efficiency of the aggregates.

Whilst the removal of dissolved and colloidal natural organic matter (NOM) is well established at water treatment works using conventional coagulation and filtration processes, the impact of organic matter on floc structure is less well understood. An accurate assessment of floc structure can be a crucial tool for predicting performance under certain coagulation conditions and may be used in combination with removal data to find optimum coagulation pH and dose. No single structural parameter is able to provide all the required information necessary to determine floc operational performance. Therefore a suite of techniques should be used. In this study three structural characteristics were chosen for investigation; these were floc strength, size and settling velocity. Overall, the paper discusses the development and use of diagnostic tools to highlight the importance of considering floc structure as an indicator of WTW performance with particular emphasis on NOM removal. This paper presents structural data from flocs formed from a reservoir water of high colour and dissolved organic carbon (DOC) and of low alkalinity and conductivity for three different coagulant doses.

3(A).2 Materials and methods

All experiments were carried out on raw water obtained from a reservoir source in the uplands of Yorkshire, England obtained in March 2003. This source is typical of a moorland catchment being of high colour and DOC, low turbidity and low alkalinity. Some of the general water parameters are shown in Table 3(A).1.

Table 3(A).1 Raw water characteristics.

Parameter	Value
Dissolved organic carbon	11.2 mg L^{-1}
Turbidity	2.4 NTU
pH	6.0
Alkalinity	< 10 mg L^{-1} as $CaCO_3$
Conductivity	75 μS cm^{-1}
UV absorbance at 254 nm	52.6 m^{-1}

A pre-polymerised ferric sulphate based coagulant was used (Ferripol – Huntsman Tioxide Europe Ltd, Billingham, UK). Three coagulant doses were chosen for investigation. These were 8 and 16 mg L^{-1} as Fe and a dose that corresponded to the optimised dose as used by the water works at the time of abstraction, which in this case was 14.4 mg L^{-1} as Fe. The only other chemical used was 1M NaOH (Fisher Scientific UK, Loughborough) for pH adjustment. In all cases the coagulation pH was 4.5. This corresponds to the optimum pH for NOM removal using this iron based coagulant. Coagulation performance was evaluated in terms of DOC removal and the operational properties of the flocs formed as outlined below.

3(A).2.1 Floc size and strength

A laser diffraction instrument (Malvern Mastersizer 2000, Malvern UK) was used to measure dynamic floc size as the coagulation and flocculation process proceeded (Figure 3(A).1). A PB-900 variable speed jar tester (Phipps and Bird, Virginia USA) was used with 76 x 25 mm flat paddle impellers for coagulation experiments. A 1 litre cylindrical jar was used with holding ports for the inflow/outflow tubing secured onto the sides of the jar. The suspension was monitored by drawing water through the optical unit of the Mastersizer and back into the jar by a peristaltic pump on the return tube using 5 mm internal diameter peristaltic pump tubing at a flow rate of 1.5 L hr^{-1}. The inflow and outflow tubes were positioned opposite to one another at a depth just above the paddle in the holding ports.

Water samples were placed on the jar tester under the following conditions: 200 rpm for 1.5 minutes, followed by a slow stir phase at 30 rpm for 15 minutes. Coagulant and pH adjustment chemicals were added at the start of the rapid mix. Size measurements were taken every minute for the duration of the jar test and logged onto a PC. Each size experiment was repeated 3 times for each set of conditions.

The same set-up was used for the determination of floc strength. The jar tester was programmed as before, however after the slow stir phase the suspension was exposed to increased shear for a further 15 minutes. Separate experiments were carried out and replicated 3 times at increased shear of 30, 40, 50, 75, 100, 150 and 200 rpm. Particle size was monitored before and after exposure to each level of shear.

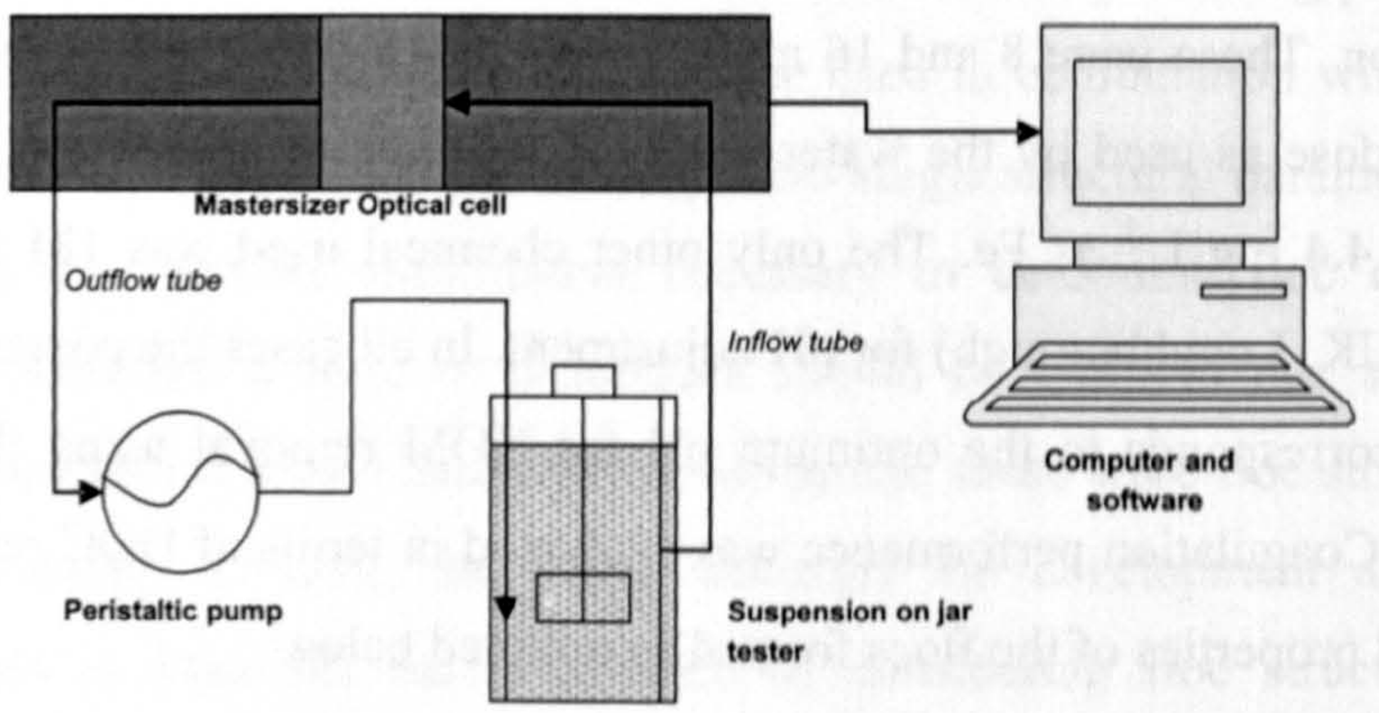

Figure 3(A).1 A schematic of the apparatus used for measuring floc size and strength.

Floc structural characteristics were additionally investigated using an Olympus BHB light microscope (Olympus European, Hamburg, Germany) and image analysis software (Image Pro Plus from Media Cybernetics, Maryland, USA).

3(A).2.2 Floc settling velocity

The settling column apparatus are shown in Figure 3(A).2. Floc aggregates were introduced into the settling column via a tapered entry port to ensure the flocs settled into the centre of the column. In order to avoid thermal currents disrupting floc settlement, the central settling column was enclosed by a water bath. The water bath was connected to a ThermoHaake K10 heat-refrigerated circulator (Hakke, Germany) to ensure a constant temperature was maintained in the column at 21.5 – 22.0 °C. The settling column was filled with de-ionised water and left to reach the required

temperature. Floc images were captured using a CV M90 colour close-coupled device (CCD) camera (JAI UK Ltd, England). The image analysis software was used to determine floc settling velocity. The image analysis system was calibrated by suspending a 1 cm microscope graticule with 100 graduations in the centre of the settling column and focusing the CCD camera on the graticule. A focused image of the graticule was captured and digitised. Calibration was then achieved by specifying the number of units the reference graticule represented and by then placing a defining line over the length specified using the software drawing tools. The graticule was removed and the tapered entry port placed in the column. A period of 2 hours was left for quiescent conditions to be reached.

Particles were then added into the settling column. Flocs were aggregated on a jar tester under the required conditions at room temperature (21-22° C). Flocs were then carefully removed from the jar using a wide mouthed pipette and re-suspended in de-ionised water held in a water bath at 21.5° C for dilution and temperature control of the flocs. Flocs could then be removed and placed in the settling column and recorded as they passed through the focused zone described above at their terminal settling velocity. Visual observation showed that little change in floc macrostructure occurred using the pipettes, however if flocs were observed to break during the transfer procedure then they were discarded.

Falling flocs were captured as image sequences. As a focused floc passed in front of the camera, the image grabber was manually triggered to take a series of 10 images. The time between each frame was set at 1 second. This meant that the distance travelled by the floc could be calculated per frame and therefore per time period, thus giving a settling velocity. The projected area of the floc presented in front of the camera was determined using the image analysis software and converted to an equivalent diameter. This standardised diameter was recorded along with its settling velocity for 100 aggregates for each set of coagulation conditions.

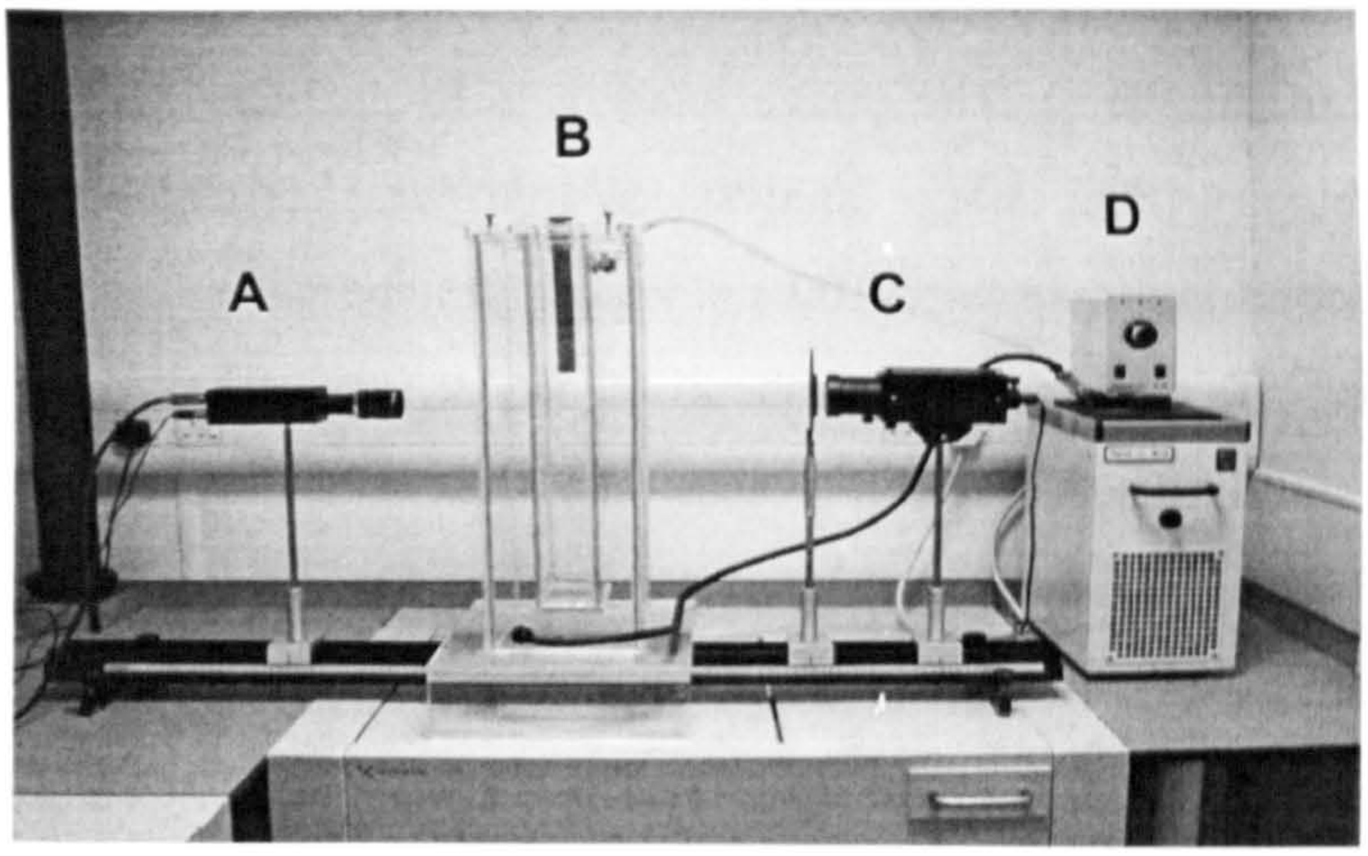

Figure 3(A).2 Settling column apparatus. A = CCD camera linked to PC and image analysis software; B = the central settling column contained within a sealed water bath; C = lamp for background lighting; D = temperature controlled-circulator for the water bath.

3(A).3 Results

The DOC removal efficiencies were similar for each of the coagulant doses (Table 3(A).2). This implies that the DOC contained within each floc mass is similar for each of the coagulation conditions, however the ratio of the coagulant precipitate to the DOC will be different for each of the coagulant doses.

Table 3(A).2 DOC concentrations and removals for the three coagulant doses (raw water filtered DOC 11.2 mg L^{-1}).

Coagulant dose, (mg L^{-1} as Fe)	Coagulated water DOC (mg L^{-1})	% Removal
8	1.7	85 %
14.4	1.6	86 %
16	1.6	86 %

3.(A).3.1 Floc size and strength

The flocs shown in Figure 3(A).3 (a-c) are typical floc examples from each of the coagulation conditions. Analysis of microscope images of a range of flocs of different size (between 30 and 40 individual flocs) formed from the 3 coagulant doses did not

highlight any differences in floc porosity, roundness and perimeter: area ratio. Whilst the flocs sampled in this manner does not constitute a statistically significant sample of the whole floc population, it gives an indication that floc macrostructure does not change for the range of coagulant dosage. This infers that any differences seen in the settling and strength tests relate to microscopic changes occurring within the floc matrix.

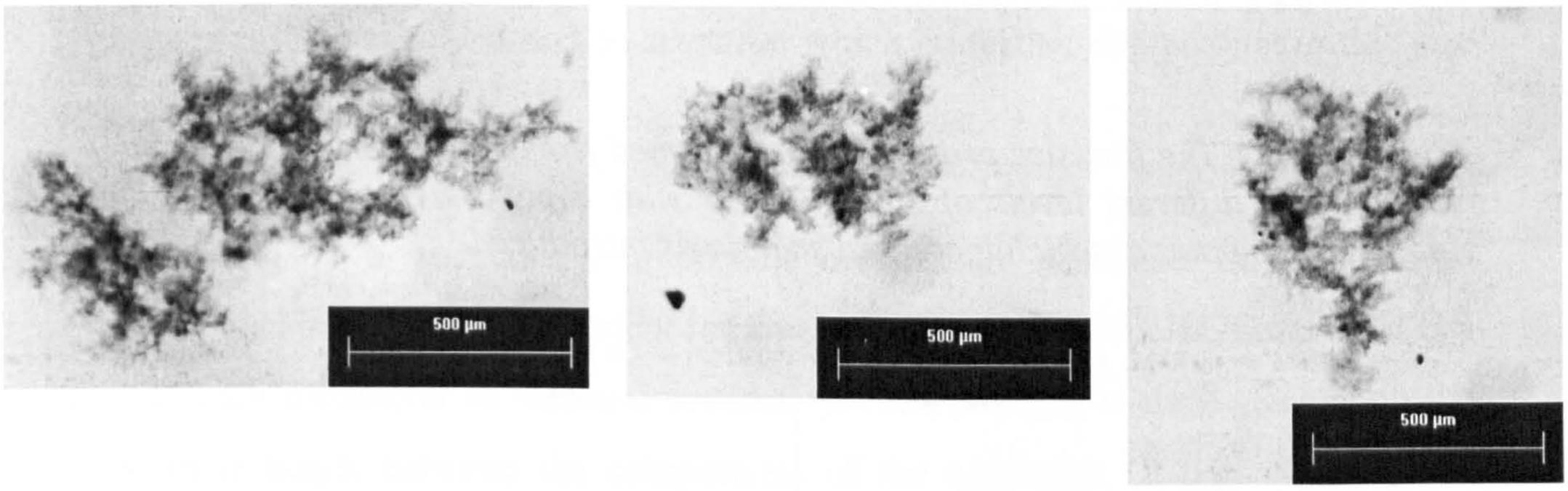

a) 8 mg L^{-1} Fe b) 14.4 mg L^{-1} Fe c) 16 mg L^{-1} Fe

Figure 3(A).3 Example floc aggregates as viewed under a light microscope at coagulant doses of a) 8 mg L^{-1} Fe, b) 14.4 mg L^{-1} Fe and c) 16 mg L^{-1}.

The growth rate of flocs for the three coagulant doses are shown in Figures 3(A).4-6. The data shows the 50 percentile floc size expressed as an equivalent volumetric diameter (d_{50}). The d_{50} was chosen as the representative size, although the same general trends were seen for other percentile floc sizes. From these profiles it is evident that the different coagulation conditions give rise to different floc sizes and growth rate. At the low coagulant dose of 8 mg L^{-1} as Fe, the rate of floc formation is slow and the maximum floc size is reached after 10 minutes (floc d_{50} ~750 µm), the two higher coagulant doses have similar profiles. The peak floc size is seen almost immediately after the end of the rapid mix phase, the floc size then decreases and reaches a stable size by 5 minutes. After 15 minutes slow stir the floc size at a coagulant dose of 14.4 mg L^{-1} Fe was ~ 650 µm, whilst at the 16 mg L^{-1} Fe dose this was ~700 µm. For sedimentation purposes floc size is important because promoting the formation of large flocs increases settling rate and will contain most of the solid volume removed even though larger flocs tend to be of lower effective density than smaller flocs (Dyer and Manning, 1998).

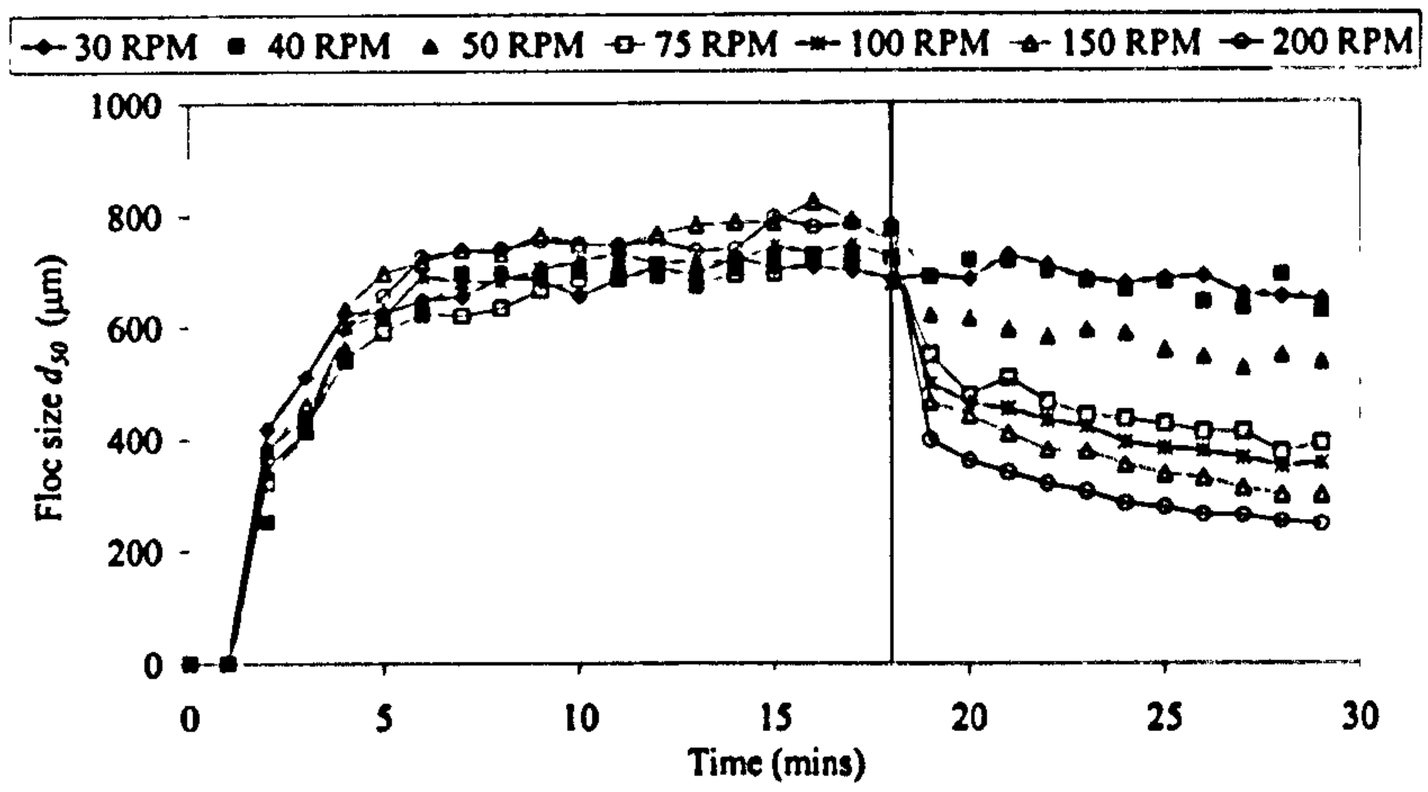

Figure 3(A).4 The floc size profile for flocs formed from raw reservoir water upon exposure to different levels of shear (dosed with 8 mg L^{-1} Fe at pH 4.5). Line indicates the point at which increased shear was introduced.

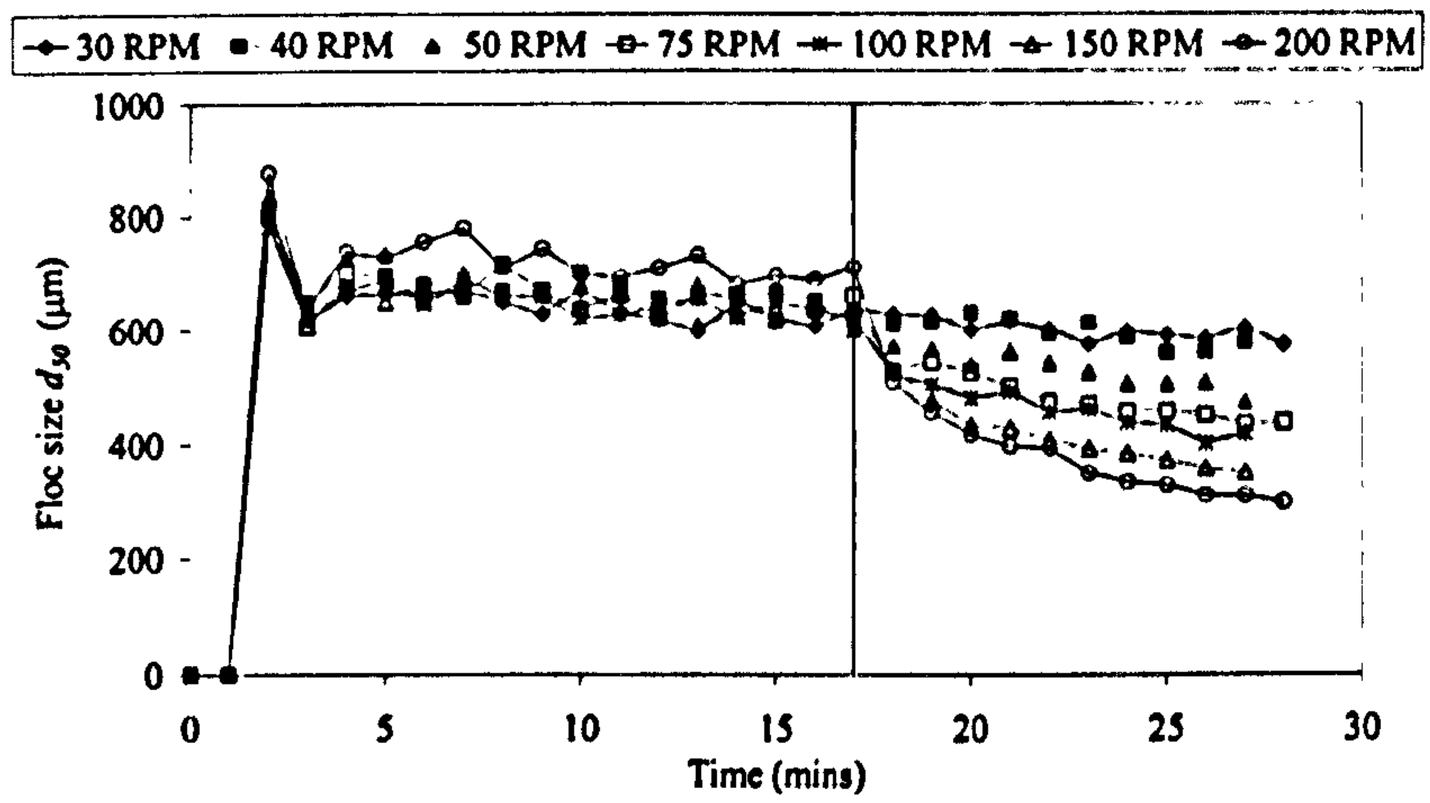

Figure 3(A).5 The floc size profile for flocs formed from raw reservoir water upon exposure to different levels of shear (dosed with 14.4 mg L^{-1} Fe at pH 4.5). Line indicates the point at which increased shear was introduced.

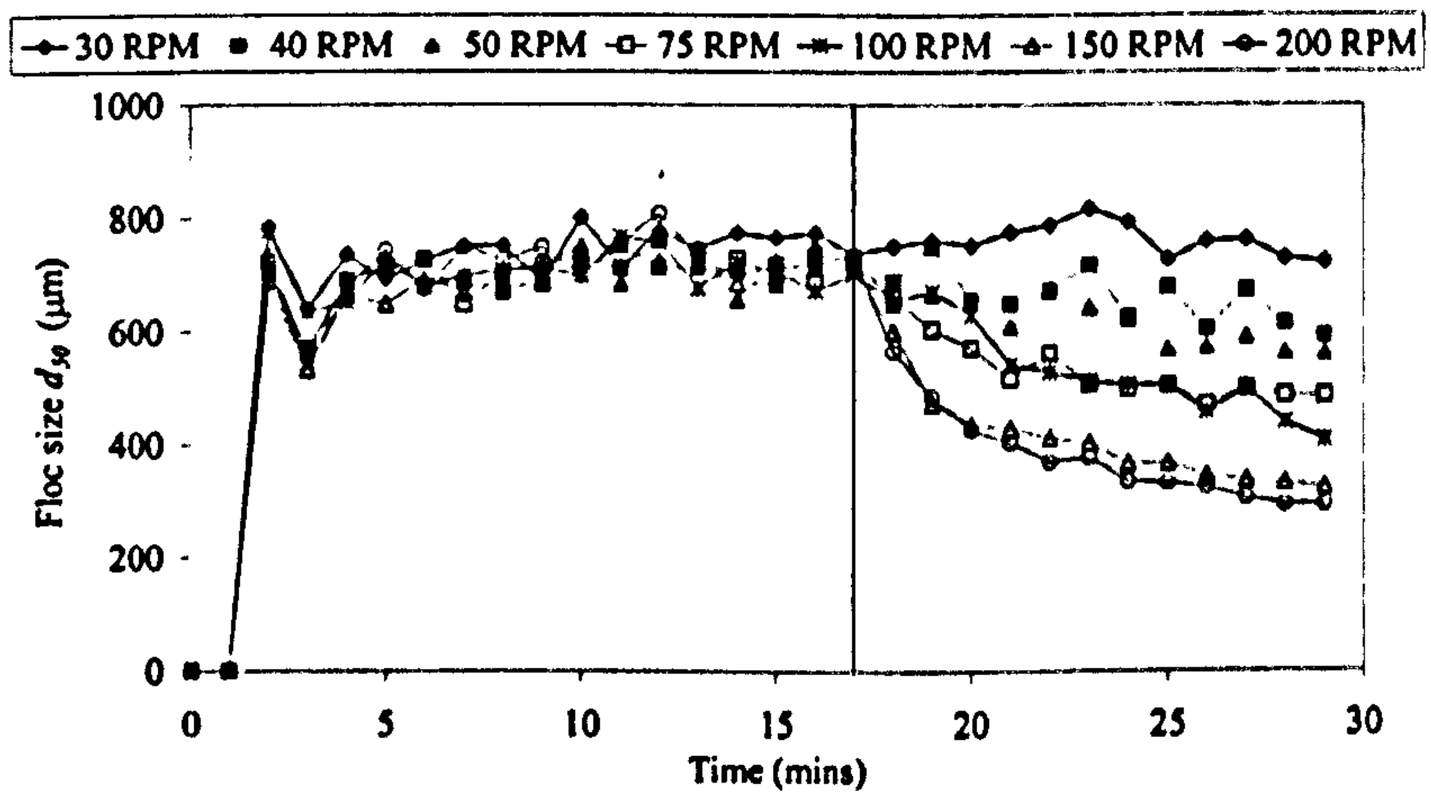

Figure 3(A).6 The floc size profile for flocs formed from raw reservoir water upon exposure to different levels of shear (dosed with 16 mg L^{-1} Fe at pH 4.5). Line indicates the point at which increased shear was introduced.

The response of the flocs to increased levels of shear after 15 minute of slow stir show that the floc d_{50} decreases with increasing shear rate. The profiles show that there is an immediate large scale decline in floc size during the two minutes after the introduction of shear at high rpm (>70 rpm), followed by a more gradual reduction in floc size. For low rpm (between 30 and 50 rpm) there is no characteristic jump in floc size, only a gradual decline. After 10 minutes exposure to the shear, the floc aggregates reach a steady state floc size after which no further degradation in floc size is seen.

Floc strength is a particularly important operational parameter in solid/liquid separation techniques for the efficient removal of aggregated particles, however it is a very difficult parameter to measure accurately. Floc strength is dependent upon the interparticle bonds between the components of the aggregate (Parker *et al.*, 1972; Bache *et al.*, 1997). From the relationship in Equation 3(A).1 developed by Parker *et al.* (1972) plotting the steady state size against shear on a log-log scale gives a degradation curve with a straight line – the slope of this line being indicative of the degree of degradation with increasing shear. Although the data represented here does not include the velocity gradient term, the rpm value is proportional to the velocity gradient and as such can be used as a surrogate for this value.

$$d = CG^{-\gamma} \qquad \text{Equation 3(A).1}$$

d is the floc diameter (m); C is the floc strength co-efficient; G is the average velocity gradient (s^{-1}) and γ is the stable floc size exponent.

The curves for the three coagulant doses are shown in Figure 3(A).7 and the values of the slopes of these lines are represented as the strength exponent (γ) in Table 3(A).3. There was a statistical difference in the slopes of the regression lines at coagulant doses of 8 and 14.4 mg L^{-1} Fe and 14.4 mg L^{-1} Fe and 16 mg L^{-1} Fe at the 99 % confidence level (two tailed t-test with 10 df).

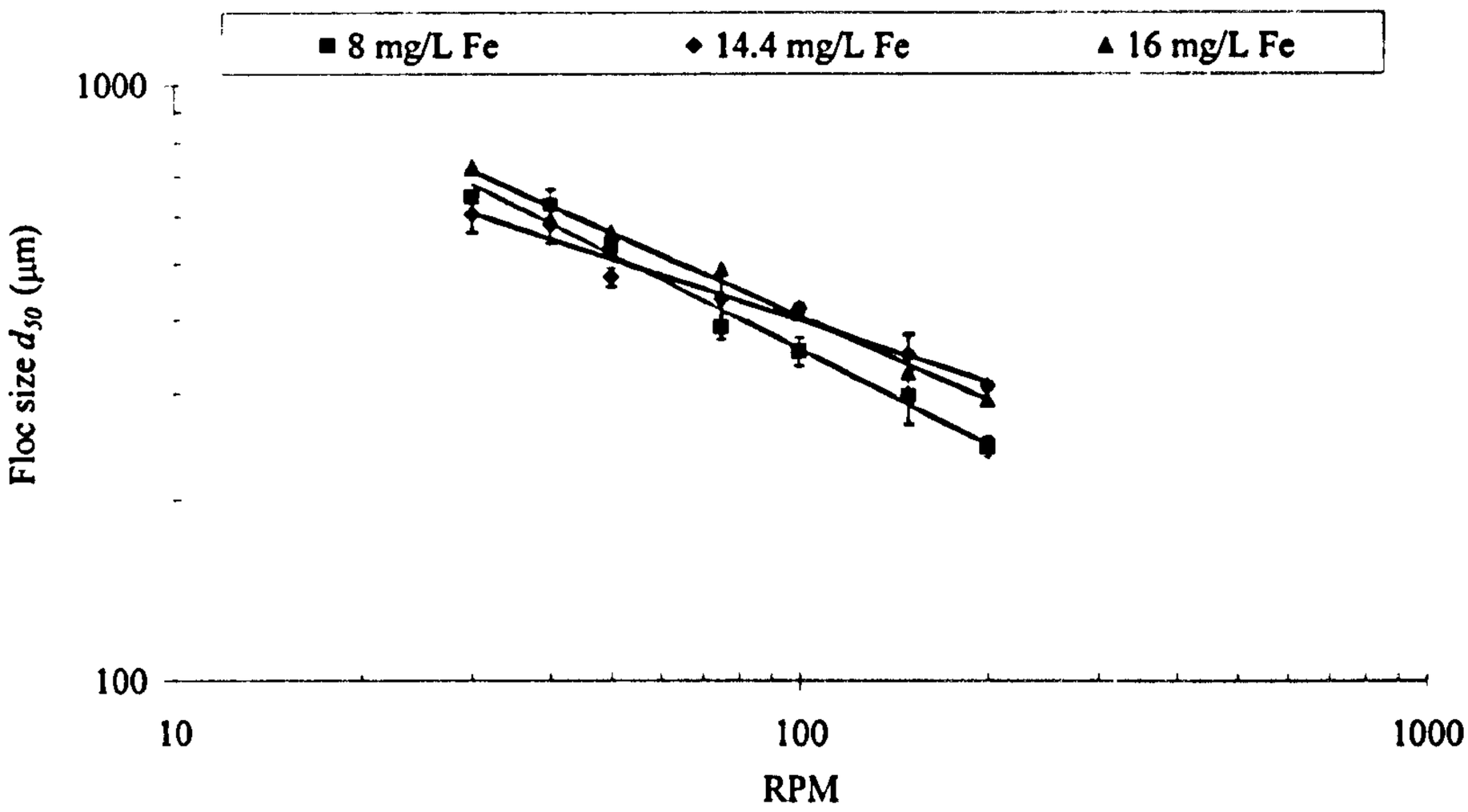

Figure 3(A).7 The degradation rate of flocs exposed to increasing levels of shear for the three coagulant doses.

Table 3(A).3 The strength exponent for the three experimental coagulation conditions.

Coagulant dose (mg L^{-1} Fe)	Floc strength exponent, γ
8	0.53
14.4	0.34
16	0.46

The interpretation of the value of this slope is open to some debate. The simple interpretation is that the steeper the slope of the line then the more affected a floc suspension will be by exposure to shear and thus should be considered a weak floc. A more subtle interpretation is that the slope of the line is more indicative of the mode of break-up. Two modes of degradation are proposed for the break-up of floc aggregates and are shown in Figure 3(A).8 (Parker *et al.*, 1972; Francois, 1987; Yeung and Pelton, 1996; Mikkelsen and Kieding, 2002). Surface erosion occurs due to the shear stress of small scale eddies that are one or two scales of magnitude smaller than the floc particles. Increasing turbulence results in bigger eddies of similar magnitude to the flocs that are more liable to fragment particle aggregates.

A large body of previous experimental and theoretical work has shown that a slope with a value around 0.5 is indicative of large scale fragmentation, whilst values of 1-2

suggest erosion type mechanisms. The evidence from the experimental work suggests that floc breakage is dominated by fragmentation type mechanisms.

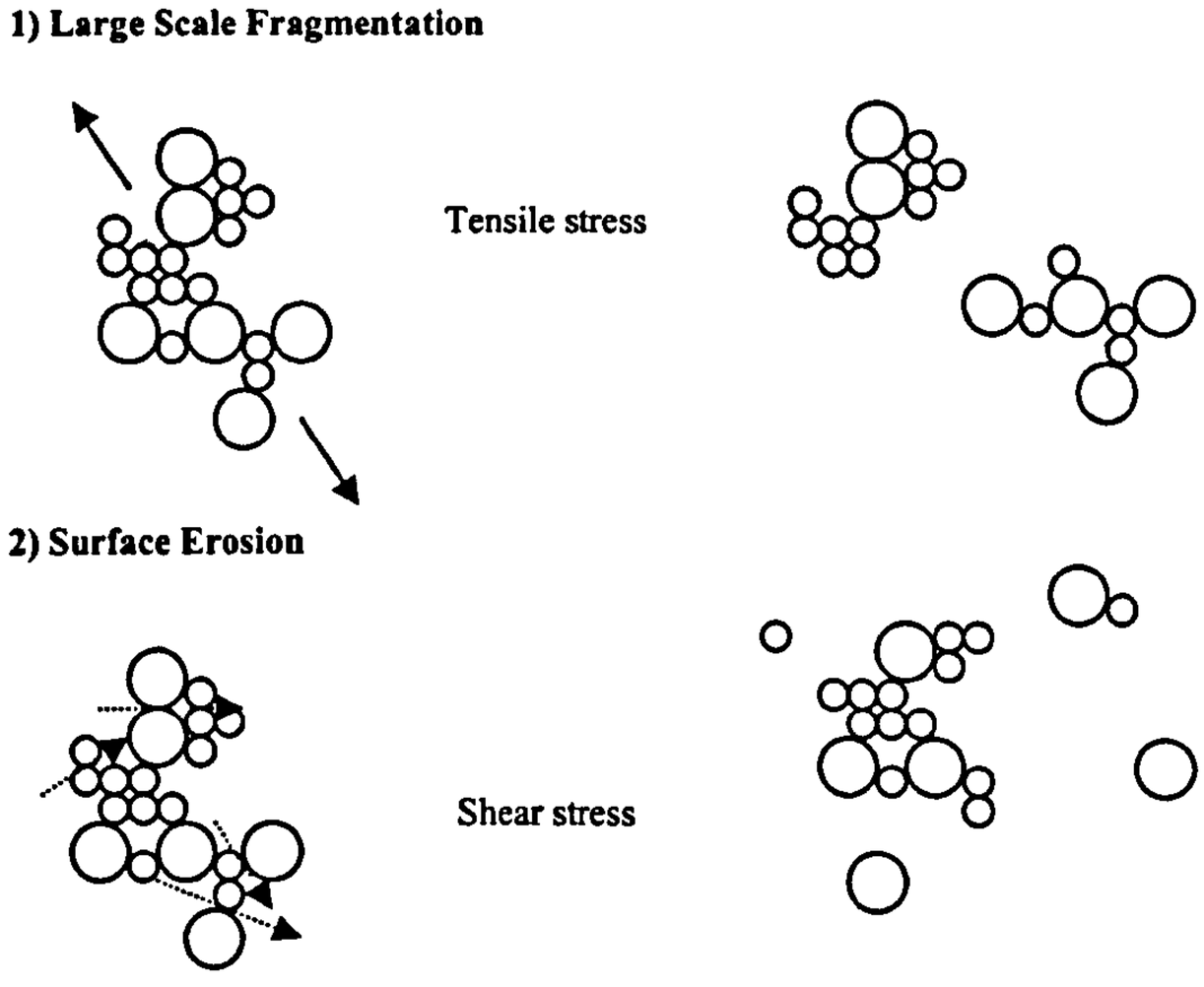

Figure 3(A).8 Two proposed mechanisms for floc breakage.

3(A).3.2 Settling velocity

An example of the settling velocities of a range of floc sizes are shown in Figure 3(A).9. Statistical analysis of the data sets implies that there is a statistical difference in the value of the slope at the 99% confidence limit for the coagulant doses of 14.4 and 8 mg L^{-1} Fe (two tailed t-test with 196 df). The difference between the values of the slopes is insignificant between the other coagulant doses. Information on the compaction of the floc structure can be found from the slope of this line. Flocs have long been recognised as being fractal objects; that is they effectively show self similarity at whatever scale they are viewed. In addition, fractal objects have a non-Euclidean fractal dimension. A normal solid particle will have a slope with a value of 2 when the settling velocity is scaled against some measure of size of the particle. For a fractal object the effective density of the particle decreases as the object gets bigger, for this reason the slope of the line takes a value of less than 2, with a value closer to 2 indicating a higher degree of compaction. There is a large body of evidence showing that the settling velocity is related to the fractal dimension for a fractal object in the following way (Dyer and Manning, 1999; Bushell *et al.*, 2002):

$$v_s \propto L^{D_f - 1}$$ Equation 3(A).2

v_s is the settling velocity; L is a characteristic length of the aggregate and D_f is the fractal dimension.

Fractal values will therefore take a fractal dimension (D_f) of <3, with more compact floc structures taking values approaching 3. The fractal values for the three coagulant doses are shown in Table 3(A).4, along with the range of settling velocities for a large and small floc.

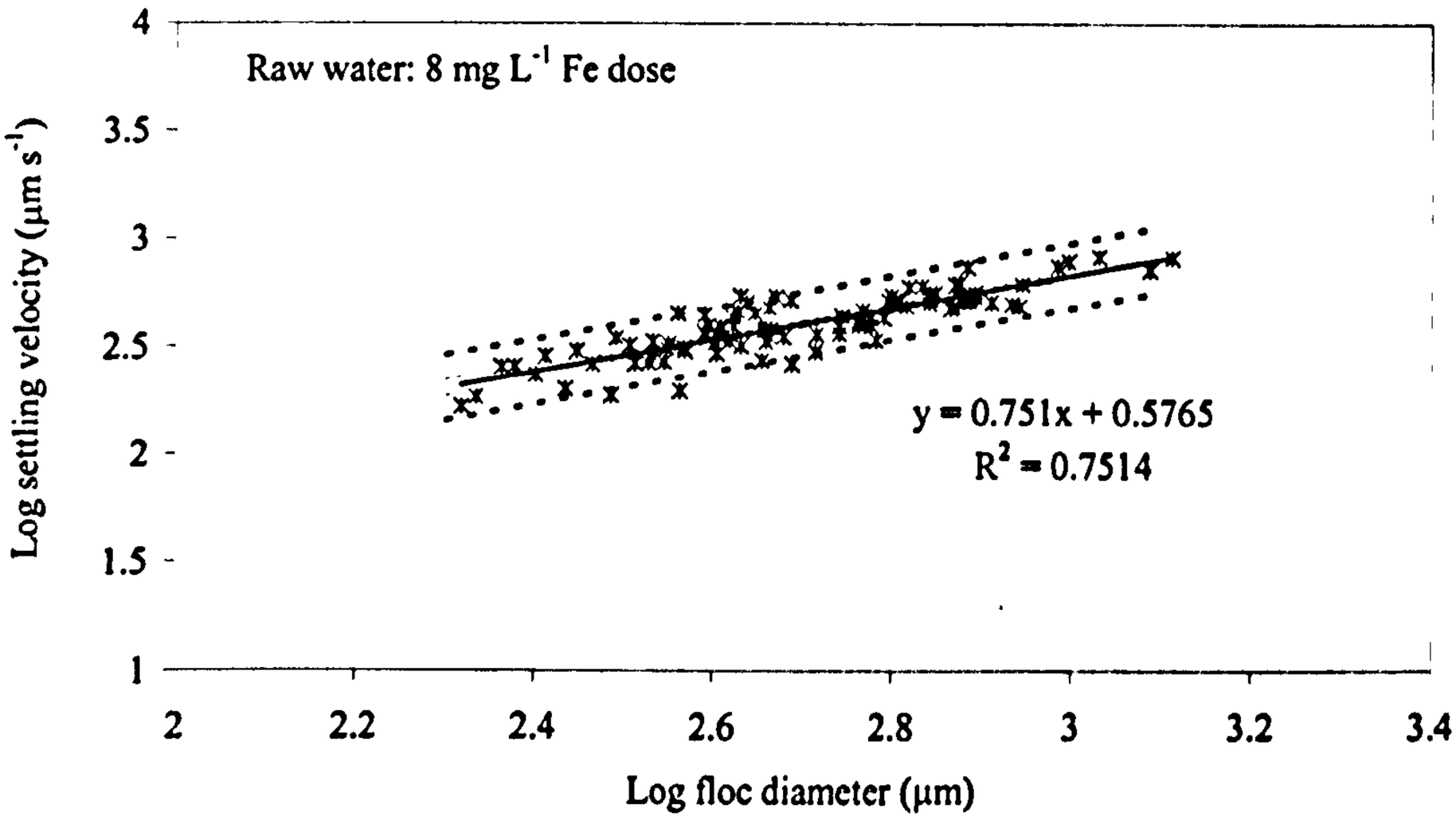

Figure 3(A).9 An example of the settling velocities of a range of different sized flocs at a coagulant dose of 8 mg L^{-1} Fe.

The fractal values for the coagulant doses suggest that the coagulant dose at 14.4 mg L^{-1} Fe produces flocs with the most compact structure, this dose also produced the flocs that were least susceptible to rupture.

Table 3(A).4 The raw water floc fractal dimensions for the three coagulant doses.

Coagulant dose	Fractal dimension	Settling velocity range (m hr^{-1})	
		Small floc (250 µm diameter)	Large floc (1000 µm diameter)
14.4 mg L^{-1} as Fe	2.00	0.66	2.62
16 mg L^{-1} as Fe	1.86	0.98	3.20
8 mg L^{-1} as Fe	1.75	0.84	2.43

3(A).4 Discussion

Whilst the DOC removals were similar for the three coagulant doses investigated, the floc structural characteristics were different. One of the main points seen from the experimental work was the better structural composition of the flocs formed from the WTW dose when compared to the two other doses chosen. Whilst the doses of 8 and 16 mg L^{-1} were arbitrarily chosen for these experiments, the WTW dose had been chosen after optimisation from in-house jar tests. Optimal coagulation conditions should be those that achieve the best DOC removals whilst also producing flocs of good quality that may be effectively removed in downstream processes. If weak and low density flocs are formed they will be poorly removed in separation stages and subsequently it is likely to put extra pressure on filters and increase finished water turbidity regardless of the DOC removal during coagulation. Similarly, if large, strong and high density flocs are formed that have excellent separation characteristics but also have a poor level of DOC removal then problems may occur in meeting colour and THM consents in the final water. This highlights the need to look at both removal efficiency and floc structure when considering jar tests and the subsequent performance of a coagulant dose at a WTW. The proposed strength technique combined with size and settling information allows a much more detailed knowledge of floc structure than simply the removal performance obtained from jar tests

The explanations for the improved floc structure must consider the complex interaction of NOM and coagulant. If adsorption is the key to NOM removal then the ratio of the metal hydroxide precipitate to the organic material will be important. If it is assumed that an increase in coagulant dose will result in an increased amount of coagulant precipitate, then there is an obvious change in the ratio of NOM to precipitate between the three doses. This may consequently have an important impact on floc structure. Previous work has shown that humic type materials can act to both stabilise and destabilise particulates depending upon the organic concentration (Amal *et al.*, 1992; Waite *et al.*, 1993). Particles totally covered in an organic layer produce flocs that have a lower fractal dimension than particles without an organic layer. This is likely to be due to steric effects and electrostatic stabilisation from the negative charge on ionised acidic groups on the organic molecules. Particles with partial coverage of organic material tend to produce more compact structures due to the

presence of more oppositely charged surface sites allowing restructuring and a more tightly bound structure. This may infer that at the low coagulant dose the adsorption coverage of the precipitate is high resulting in greater stabilisation and thus the observed more open structure when compared to the two other coagulant doses. It follows that a more open structure as a result of increased stabilisation will produce a weaker structure due to fewer and weaker attractive forces between the primary particles. However, there is a large amount of evidence in the literature suggesting that the principle mechanism for NOM removal at pH below 6 is complexation of NOM with soluble metal species into insoluble precipitates (Dempsey *et al.*, 1984; Dennett *et al.*, 1996). In which case the effect of the direct adsorption of NOM would not be as important as described above, however it is likely that NOM adsorption onto NOM-coagulant microflocs as shown in Figure 3(A).1 will still be important and affect the further agglomeration into large floc aggregates in the same manner as described above [*NOM coverage/adsorption discussed further in paper 6*].

3(A).5 Conclusions

The study has demonstrated the use of methodologies to determine differences in floc structure. The flocs formed at the WTW coagulant dose were smaller, more compact and less prone to breakage when compared to the other coagulant doses investigated in this study. These affects could not be seen using conventional optical microscopy and must therefore be due to changes in the floc microstructure.

Acknowledgements

The submitted manuscript has been made possible through funding from American Water Works Association Research Foundation and Co-funding Utilities. The information contained herein is based upon Intellectual Property which is jointly owned by Cranfield University and the Foundation. The Foundation retains its right to publish or produce the Jointly Owned Intellectual Property in part or in its entirety. The authors would also like to thank the EPSRC, Fort Collins Water, Scottish Water, Severn Trent Water, Thames Water, United Utilities and Yorkshire Water.

3(A).6 References

Amal, R., Coury, J. R., Raper, J. A., Walsh, W. P., and Waite, T. D. (1990) Structure and Kinetics of Aggregating Collooidal Haematite. *Colloids and Surfaces* **46** 1-19.

Bache, D. H., Hossain, M. D., Al-Ani, S. H., and Jackson, P. J. (1991) Optimum Coagulation Conditions for a Coloured Water in Terms of Floc Size, Density and Strength. *Aqua Journal of Water Supply: Research and Technology* **9** 93-102.

Bache, D. H., Johnson, C., McGilligan, J. F., and Rasool, E. (1997) A Conceptual View of Floc Structure in the Sweep Floc Domain. *Water Science and Technology* **36** (4), 49-56.

Bushell, G. C., Yan, Y. D., Woodfield, D., Raper, J., and Amal, R. (2002) On Techniques for the Measurement of the Mass Fractal Dimension of Aggregates. *Advances in Colloid and Interface Science* **95** 1-50.

Dempsey, B. A., Ganho, R. M., and O'Melia, C. R. (1984) The Coagulation of Humic Substances by Means of Aluminium Salts. *Journal of the American Water Works Association* **76** (4), 141-150.

Dennett, K. E., Amirtharajah, A., Moran, T. F., and Gould, J. P. (1996) Coagulation: its Effect on Organic Matter. *Journal of the American Water Works Association* **88** 129-142.

Dyer, K. R. and Manning, A. J. (1998) Observation of the Size, Settling Velocity and Effective Density of Flocs, and their Fractal Dimensions. *Journal of Sea Research* **41** 87-95.

Francois, R. J. (1987) Strength of Aluminium Hydroxide Flocs. *Water Research* **21** 1023-1030.

Mikkelsen, L. H. and Keiding, K. (2002) The Shear Sensitivity of Activated Sludge: an Evaluation of the Possibility for a Standardised Floc Strength Test. *Water Research* **36** (12), 2931-2940.

Parker, D. S., Kaufman, W. J., and Jenkins, D. (1972) Floc Breakup in Turbulent Flocculation Processes. *Journal of the Sanitary Engineering Division: Proceedings of the American Society of Civil Engineers* **SA 1** 79-99.

Waite, T. D., Amal, R., Ngo, H., and Vigneswaran, S. (1993) Effects of Adsorbed Organic Matter on Size, Structure and Filterability of Iron Oxyhydroxide Flocs. *Water Science and Technology* **27** (11), 133-142.

Yeung, A. K. C. and Pelton, R. (1996) Micromechanics: A New Approach to Studying the Strength and Breakup of Flocs. *Journal of Colloid and Interface Science* **184** 579-585.

3(B) THE DUPLICITY OF FLOC STRENGTH

PETER JARVIS, BRUCE JEFFERSON and SIMON A. PARSONS

School of Water Sciences, Cranfield University, Cranfield, Bedfordshire, MK43 0AL, United Kingdom

Abstract

The breakage of flocs is dependent upon the strength of the bonds holding the aggregate together. The present work describes the breakage and re-growth behaviour of three different types of floc, these were: 1) coagulant precipitate flocs, 2) turbidity flocs and 3) organic matter flocs. Floc aggregates were exposed to increased levels of shear on a conventional jar tester and the size of flocs were observed dynamically using a laser diffraction instrument. The organic flocs showed most resistance to breakage across the whole range of shear under investigation. The dynamic procedure provided detailed information on particle size distributions (PSD). Large and small scale degradation events could be identified from analysis of the PSD data. All of the flocs under investigation showed little re-growth potential after breakage. The precipitate and organic flocs showed slightly better re-aggregation of the small floc sizes.

Keywords

Breakage; floc; re-growth; strength

3(B).1 Introduction

The aggregation of fine particles and colloids into larger particles is a well established means of removing turbidity, colour, and pollutants at water treatment works (WTW). These larger aggregates are known as flocs. Flocs may be defined as highly porous, irregularly shaped and loosely connected aggregates composed of smaller primary particles (Huang, 1994; Kim *et al.*, 2001). The size and structure of flocs are considered fundamental to the operation of industrial unit processes. Floc strength is a particularly important structural characteristic in solid/liquid separation techniques for the efficient removal of aggregated particles. The strength of a floc is dependent upon the number and magnitude of the interparticle bonds between the components of the aggregate (Parker *et al.*, 1972; Bache *et al.*, 1997). However, the development of a proficient technique to quantify floc strength has proven to be difficult. This is partly due to the inherent complexity, fragility and variation in floc size, shape and composition and also due to a view that there are two theoretical modes of floc rupture (Parker *et al.*, 1972; Francois, 1987; Yeung and Pelton, 1996; Mikkelsen and Keiding, 2002). These have been classified as surface erosion and large-scale fragmentation. Surface erosion is the removal of small particles from the floc surface resulting in an increase in the primary particle concentration. Large scale fragmentation is the cleavage of flocs into pieces of a similar size without an increase in primary particle concentration. The problem of describing strength arises from the fact that Yeung and Pelton (1996) summarise that these two rupture modes are thought to be caused by different stresses. Fragmentation is thought to occur from tensile stress acting normally across the whole floc, whilst erosion is due to the shearing stress acting tangentially to the floc surface. The likelihood of this occurring is discussed later in the paper [*see also paper 6*]'

The rate at which a floc suspension decays upon exposure to shear is indicative of the strength of the flocs within the system as the steady state floc size is governed by the prevailing shear/stress conditions within the containing vessel. A large body of floc strength work has investigated the empirical relationship between floc size and the applied shear as shown in Equation 3(B).1 (Parker *et al.*, 1972; Leentvaar and Rhebun, 1983; Francois 1987; Bache *et al.*, 1999).

$$d = CG^{-\gamma}$$ Equation 3(B).1

d is the floc diameter (m); C is the floc strength coefficient; G is the average velocity gradient (s^{-1}) and γ is the stable floc size exponent dependent upon floc break-up mode and the size of eddies that causes the breakage

To date there has been no direct comparison of the effect of shear on different types of floc suspensions, in other words most work has concentrated on specific floc systems (e.g. turbidity, humic material or sewage flocs). The objective of this study was to compare the strength/breakage of flocs upon exposure to different levels of shear from three types of floc aggregate: 1) turbidity flocs, 2) organic matter flocs and 3) coagulant precipitate flocs. In addition, the re-growth capacity of these flocs was also investigated

3(B).2 Materials and methods

The details of the three test suspensions are outlined below:

(1) turbidity suspension – kaolin was suspended in tap water at a concentration of 80 mg L^{-1} at pH 7.5.

(2) organic matter – raw water was obtained from a reservoir source in the uplands of Yorkshire, England. This source is typical of a moorland catchment being of high colour and DOC (10 mg L^{-1} as carbon), low turbidity (2.4 NTU) and low alkalinity (< 10 mg L^{-1} as $CaCO_3$) at pH 6.0.

(3) coagulant precipitate - the iron hydroxide precipitate was formed by adding coagulant to de-ionised water containing a small amount of alkalinity in the form of $NaHCO_3$ (20 mg L^{-1}).

For all experiments a pre-polymerised ferric sulphate based coagulant was used (Ferripol – Huntsman Tioxide Europe Ltd, Billingham, UK) at a dose of 8 mg L^{-1}. A coagulation pH of 6.5 was used for the kaolin suspension, whilst the pH was 4.5 for the raw water and for the formation of the coagulant precipitate. These conditions correspond to the optimum for turbidity and organic matter removal for this iron based coagulant.

A dynamic laser diffraction instrument (Malvern Mastersizer 2000, Malvern, UK) was used to measure floc size as the coagulation and flocculation process proceeded.

A PB-900 variable speed jar tester (Phipps and Bird, Virginia, USA) was used with 76 x 25 mm flat paddle impellers for coagulation experiments. A 1 litre cylindrical jar was used with holding ports for inflow and outflow tubing secured onto the sides of the jar. The suspension was monitored by drawing water through the optical unit of the Mastersizer and back into the jar by a peristaltic pump on the return tube using 5 mm internal diameter peristaltic pump tubing at a flow rate of 1.5 L hr^{-1}. The inflow and outflow tubes were positioned opposite to one another at a depth just above the paddle in the holding ports.

Water samples were placed on the jar tester under the following conditions: 200 rpm for 1.5 minutes, followed by a slow stir phase at 30 rpm for 15 minutes. Coagulant and pH adjustment chemicals were added at the start of the rapid mix. After the slow stir phase, the suspension was exposed to increased shear for a further 15 minutes. Separate experiments were carried out at increased shear of 30, 40, 50, 75, 100, 150 and 200 rpm. Size measurements were taken every minute for the duration of the jar test and logged onto a PC. Each experiment was repeated 3 times for each set of conditions. For floc re-growth experiments, flocs were aggregated as before, however after 15 minutes of slow stir the shear was increased to 200 rpm for 15 minutes followed by a further 15 minutes slow stir at 30 rpm. Particle size was monitored as before.

3(B).3 Results and discussion

3(B).3.1 Floc strength

Floc size profiles for the three suspensions are shown in Figure 3(B).1. The floc size is expressed as the d_{50}, the median volumetric equivalent diameter. This was chosen as the representative floc size, however the same behaviour was observed for the d_{10} and the d_{90}. The figure highlights the differences in the steady state floc size. The iron hydroxide precipitate formed the largest flocs followed by the raw water with the kaolin flocs being the smallest. The breakage behaviour of the flocs followed the same pattern: exposure to increased rpm resulted in a decline in floc size until a steady state size was reached after 30 minutes. With increasing rpm, flocs became progressively smaller until a steady state size was reached. At low rpm the rate of

decline changed gradually, whilst above 50 rpm there was an initial steep rate of decline followed by a more gradual reduction in floc size.

A comparison of floc strength between the three different suspensions is shown in Figure 3(B).2. In this work, the rpm of the stirrer was used as the shear value. Traditionally, the average hydraulic gradient (G) has been used as the descriptor for shear. There is some debate as to the use of velocity gradient and in particular the average velocity gradient when considering floc breakage and strength. The average velocity gradient is an easy number to deal with and well established in the water industry but is unlikely to be able to accurately describe the complexities of turbulent flow in stirred vessels and is not sufficient to describe the shear experienced by particles (Boller and Blaser, 1998).

There is a large body of evidence suggesting that local G values are more important than the average G in a stirred vessel (Francois, 1987; Essamanai and de Traversay, 2002). Maximum local G values are found close to the impeller region in a stirred vessel (Bouyer *et al.* 2001). The G value found at the impeller zone (or the maximum G value experienced) is considered to be of most importance in determining floc size distributions in a tank (Francois, 1987). This is further supported by evidence that systems with different impellers or vessels may have the same average velocity gradient, but the resulting floc size distributions are different (Bouyer *et al.*, 2001). However, estimates of local velocity gradients in flocculating vessels can vary by several orders of magnitude. Due to this confusion and the lack of consistency between technique geometries and impeller type, a simpler indicator of shear such as the rpm of the stirrer was used in this work.

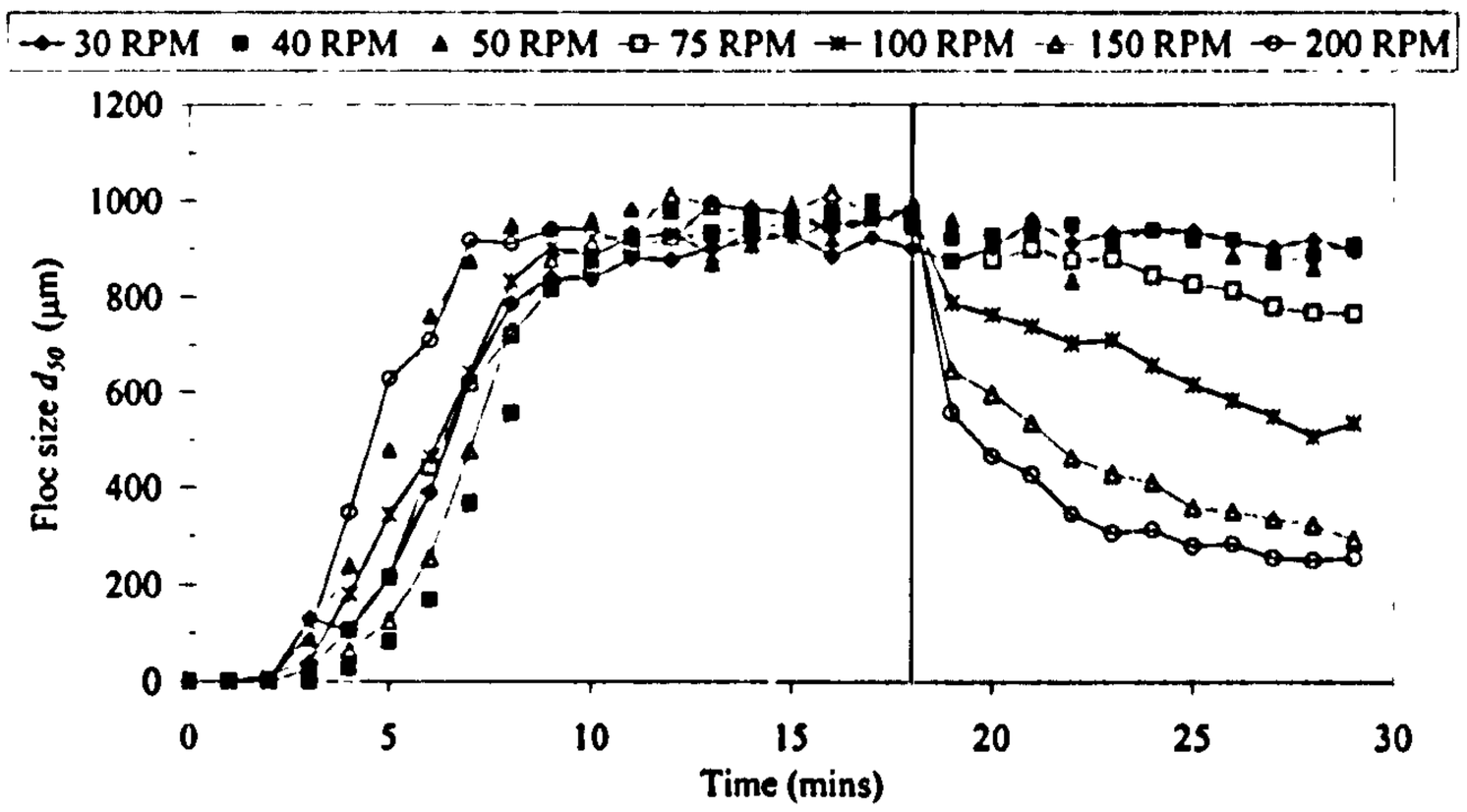

a) Iron hydroxide precipitate

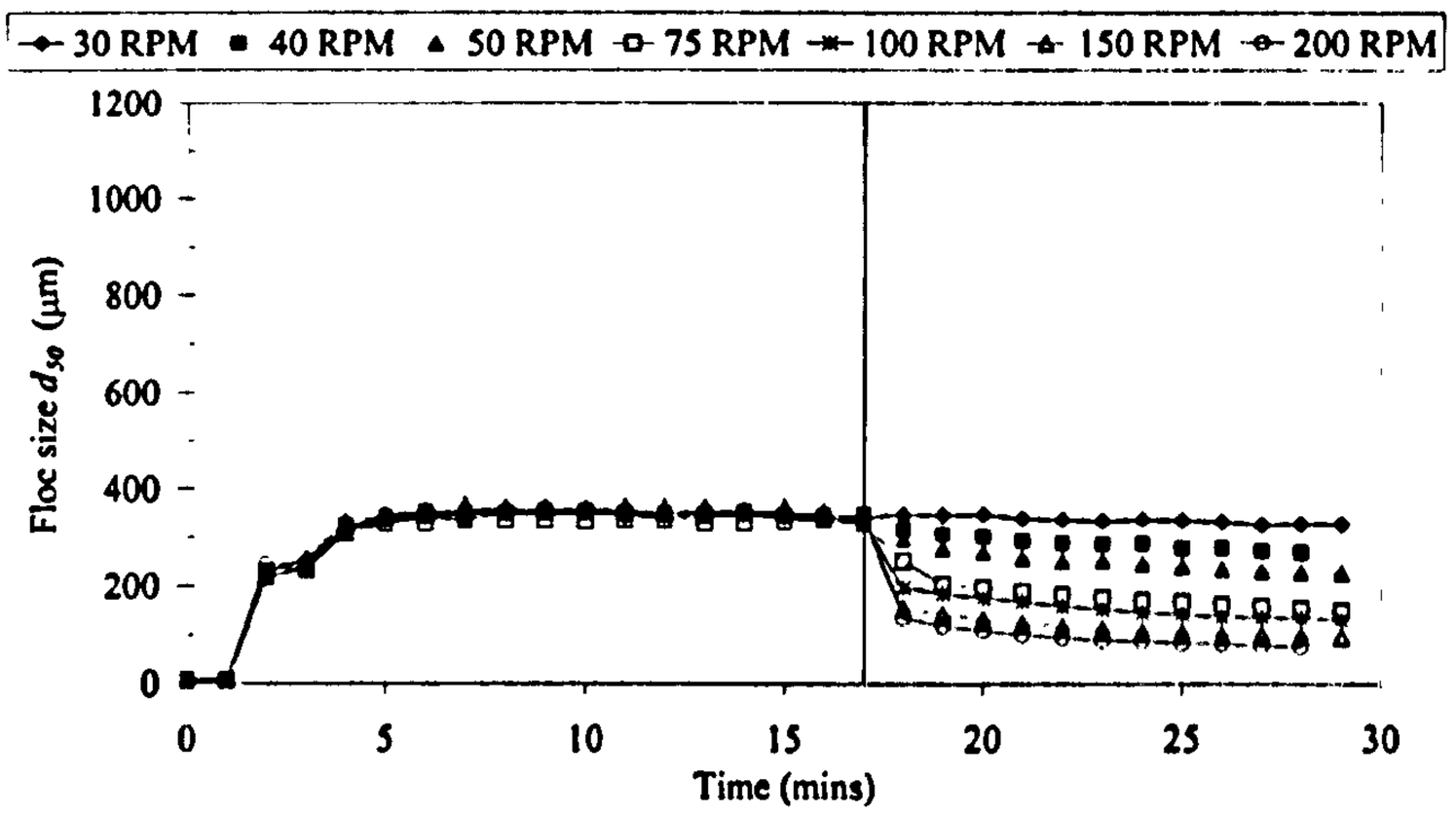

b) Kaolin

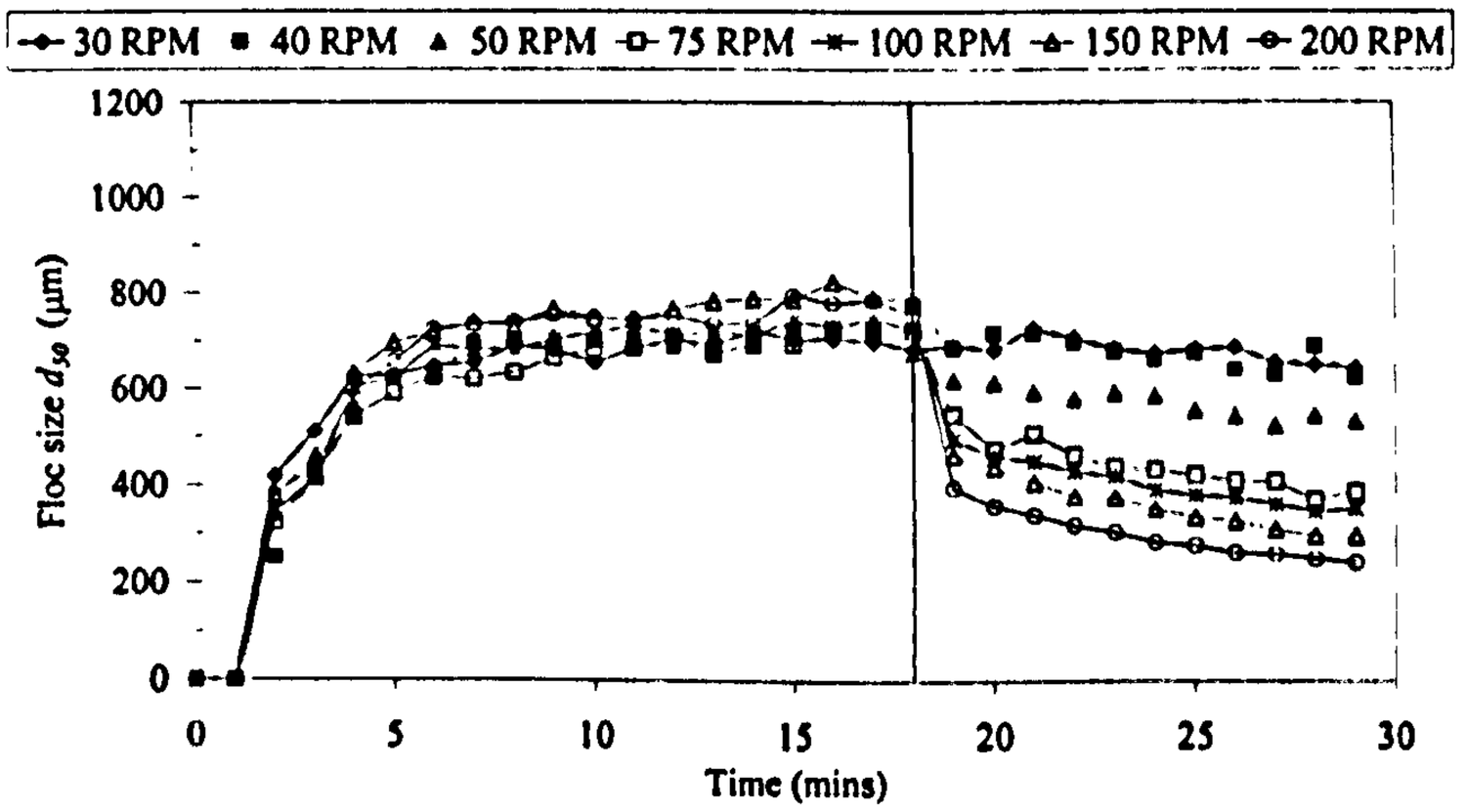

c) Raw reservoir water

Figure 3(B).1 Floc size profiles during coagulation and after exposure to increasing levels of rpm on a jar tester for the three suspensions a) iron hydroxide precipitate, b) kaolin and c) raw reservoir water. The d_{50} is the median floc size. The line indicates point at which increased shear was introduced.

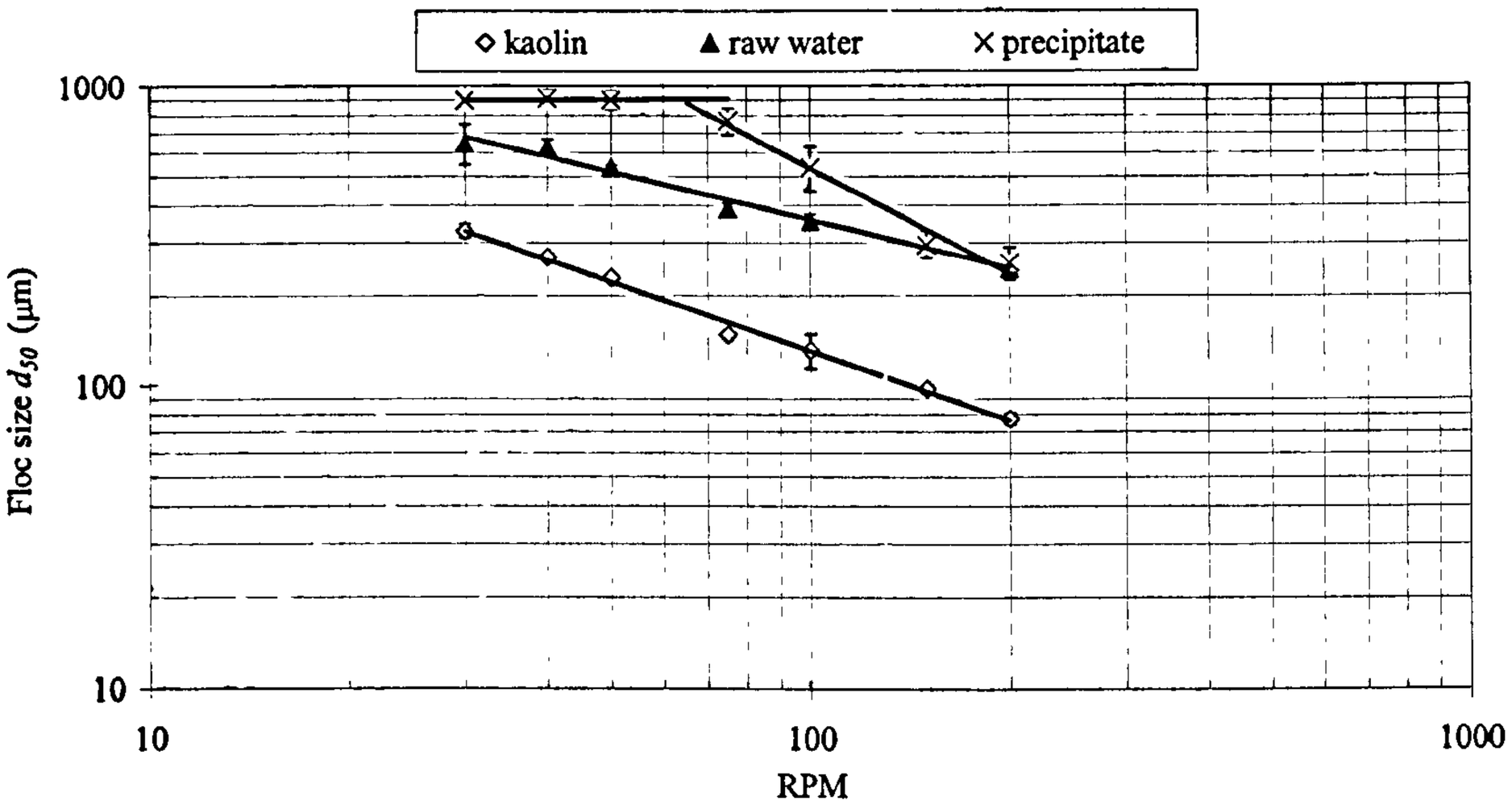

Figure 3(B).2 The steady state floc size after exposure to increased levels of shear for the three suspensions.

Two distinct zones can be identified for the floc d_{50} steady state size of the coagulant precipitate. At 50 rpm and below, the steady state floc size does not change greatly, implying resistance to these shear levels and thus high floc strength. At shear of 75 rpm and above, the degradation rate increased, with floc size rapidly falling from 900 μm to 250 μm. These two zones were not seen for the other two suspensions. Both the kaolin and the raw water flocs have a more constant rate of degradation with increasing rpm. There is a generally accepted view that organic flocs formed from NOM rich waters are weaker than turbidity flocs (Bache *et al.*, 1999). In terms of the proportional size change of flocs with increasing shear this study does not agree with this view. At low rpm (≤50 rpm), kaolin and organic matter flocs were more prone to breakage when compared to the precipitate flocs. At the low rpm range (30-50 rpm), the floc strength was of the following hierarchy: iron hydroxide> organic matter> turbidity. Across the whole shear range under investigation, this study has shown that kaolin flocs decayed to 23 % of their previous size at the highest rpm, whilst the organic flocs decreased to 38 %. The precipitate flocs decrease to 28 % of their previous size. In other words, organic flocs were shown to be the strongest across the whole rpm range followed by the precipitate flocs followed by the kaolin flocs.

The shapes of the breakage profiles in Figure 3(B).1 suggest two types of degradation occurring – a large scale change in floc size at high rpm and a more gradual change at

low rpm. Looking at the floc particle size distributions (PSD) generated by the Mastersizer it is possible to see how the aggregates are changing. Figure 3(B).3 shows the PSD of the iron hydroxide precipitate after 15 minutes slow stir, the minute after increased shear and after 15 minutes exposure to shear of 40 rpm and 200 rpm. Before shear was applied a large peak was seen around 1000 μm with a smaller one at 150 μm. With an increase in shear to 40 rpm there was a small increase in the proportion of 200-400 μm size flocs and a slight reduction in the large aggregates. A small portion of the large flocs (> 800 μm) must therefore be unstable and prone to breakage into two or three similar sized parts of between 200-400 μm giving a gradual reduction in floc size.

More significant changes in floc size were seen at 200 rpm shear. Initially after the shear was applied the large floc size peak shifts from 1000 μm to 500 μm commensurate with an increase in the flocs of size <200 μm. After 15 minutes of shear there were still remnants of the 500 μm peak but the greatest proportion of flocs were around half this size. In addition, the proportion of flocs of <200 μm increased further indicating the 500 μm were broken into smaller fragments. Similar PSD patterns were seen for the other two floc aggregates. The Mastersizer bases its measurements on particle volume rather than a particle number count, this results in a tendency to increase the importance of large particles over smaller ones. With erosion type degradation mechanisms, it would be expected that the frequency of very small particles would dramatically increase whilst the size of the larger particles would slightly decrease but stay at a similar frequency. For large scale fragmentation events it would be expected that the PSD would undergo a significant shift to the left. However, due to the volume weighted measurement of the light scattering technique, these behaviours were not as clear cut as expected. In addition, fragmentation and erosion are thought to occur simultaneously. For example, Biggs and Lant (2000) have suggested in their investigation of activated sludge aggregates, that the largest flocs undergo fracture whilst the median sized particles undergo erosion, This is combined with a view that floc collisions with each other will also lead to significant breakage (Francois, 1987). Therefore, in this case, it may be more convenient to refer to these changes as large and small scale rather than specifically ascribe a particular degradation mechanism. At 40 rpm, the small reduction in the large flocs and the

increase in small particles would suggest small scale degradation. Large scale reduction was identified by a shift in the peak of the largest flocs to smaller flocs.

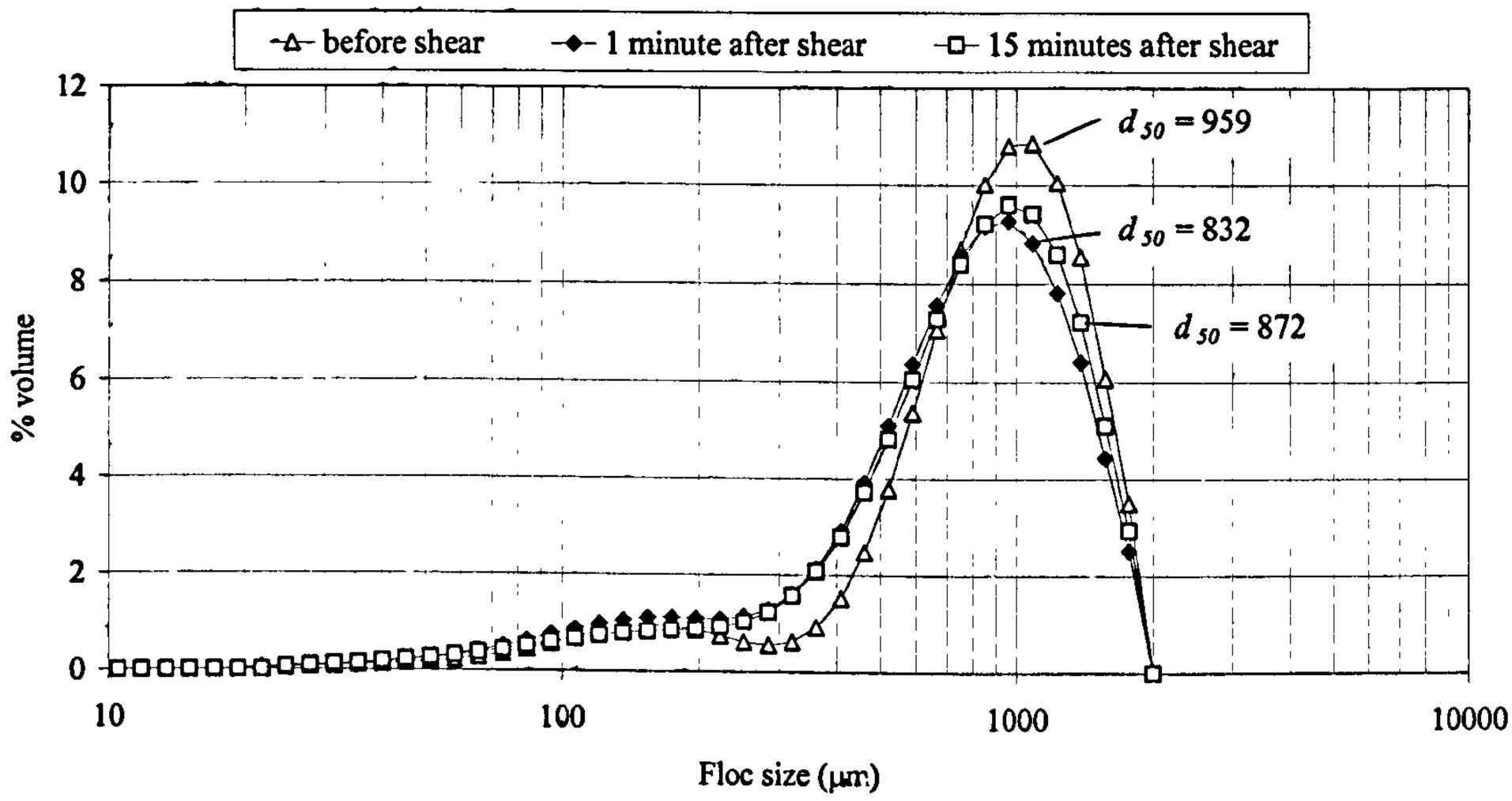

a) shear at 40 rpm

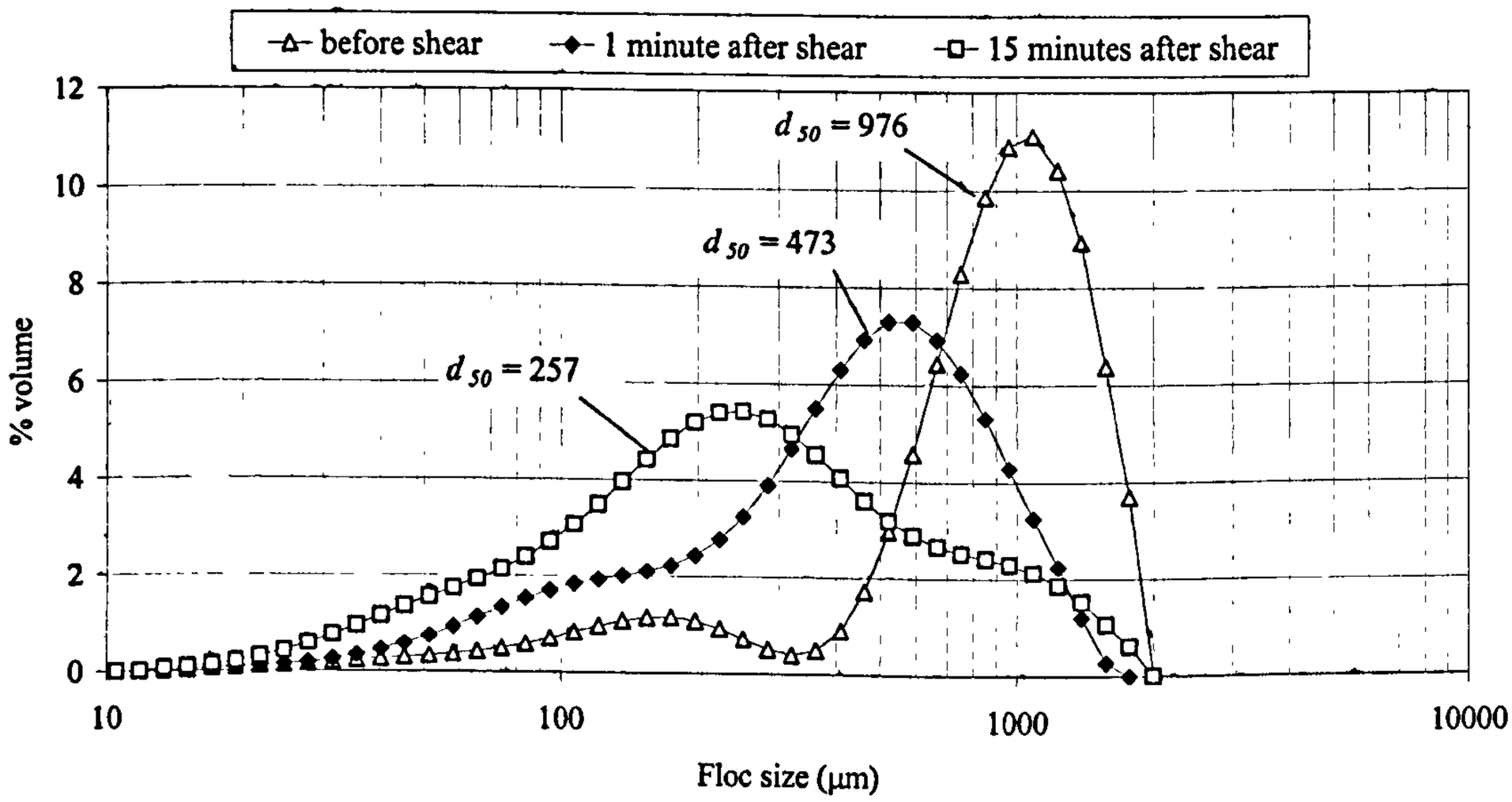

b) shear at 200 rpm

Figure 3(B).3 Iron hydroxide precipitate floc particle size distributions before and after exposure to shear of a) 40 rpm and b) 200 rpm.

Understanding floc strength and degradation mechanism cannot be confined to looking at a single indicative number such as the floc d_{50}, particularly when considering the volume based measurement of the laser instrument. The PSD must also be looked at to determine whether degradation is a small or large scale change.

3(B).3.2 Floc re-growth

The capacity for flocs to re-grow is an important operational parameter during flocculation. If a floc breaks in a flocculator at a point particularly high in shear, it may spend sufficient time in areas of non-breaking shear to allow for particle-particle contact and the potential for re-aggregation. Figure 3(B).4 shows that there was a limited capacity for the floc aggregates under investigation to re-form. This is in agreement with work carried out by Gregory and Dupont (2001) looking at the coagulation of kaolin using alum and polyaluminium chloride coagulants. The proportional size changes of the flocs during breakage and re-aggregation for the d_{10}, d_{50} and d_{90} are shown in Figure 3(B).5. The kaolin flocs were characterised by only being able to reform to below 40 % of their initial size across the whole range of floc sizes, this figure was 50 % for the raw water and between 30-50 % for the iron hydroxide precipitate. As a general rule, all of the floc suspensions were only able to increase in size by 20-40 % of their previous broken size. However, the smaller floc sizes (d_{10}) had much greater potential for re-aggregation. The iron hydroxide precipitate and the raw water floc d_{10} grew to over 50 % of the initial floc size whilst, this was 33 % for the kaolin flocs. In comparison to the broken floc size, this represented over a doubling in size for the raw water and the iron hydroxide precipitate, whilst it was only a 73 % increase for the kaolin.

The re-aggregation of flocs is a poorly understood phenomenon. Broken flocs may not be able to reform to their previous size due to a loss of bonding capacity. This has previously been described as bonds losing their 'stickiness' as a result of floc restructuring at high shear levels (Spicer *et al.*, 1998). Whilst this work was unable to provide further information on why this was occurring, it demonstrated that precipitate flocs and organic flocs have a slightly greater potential for re-growth in comparison to turbidity flocs.

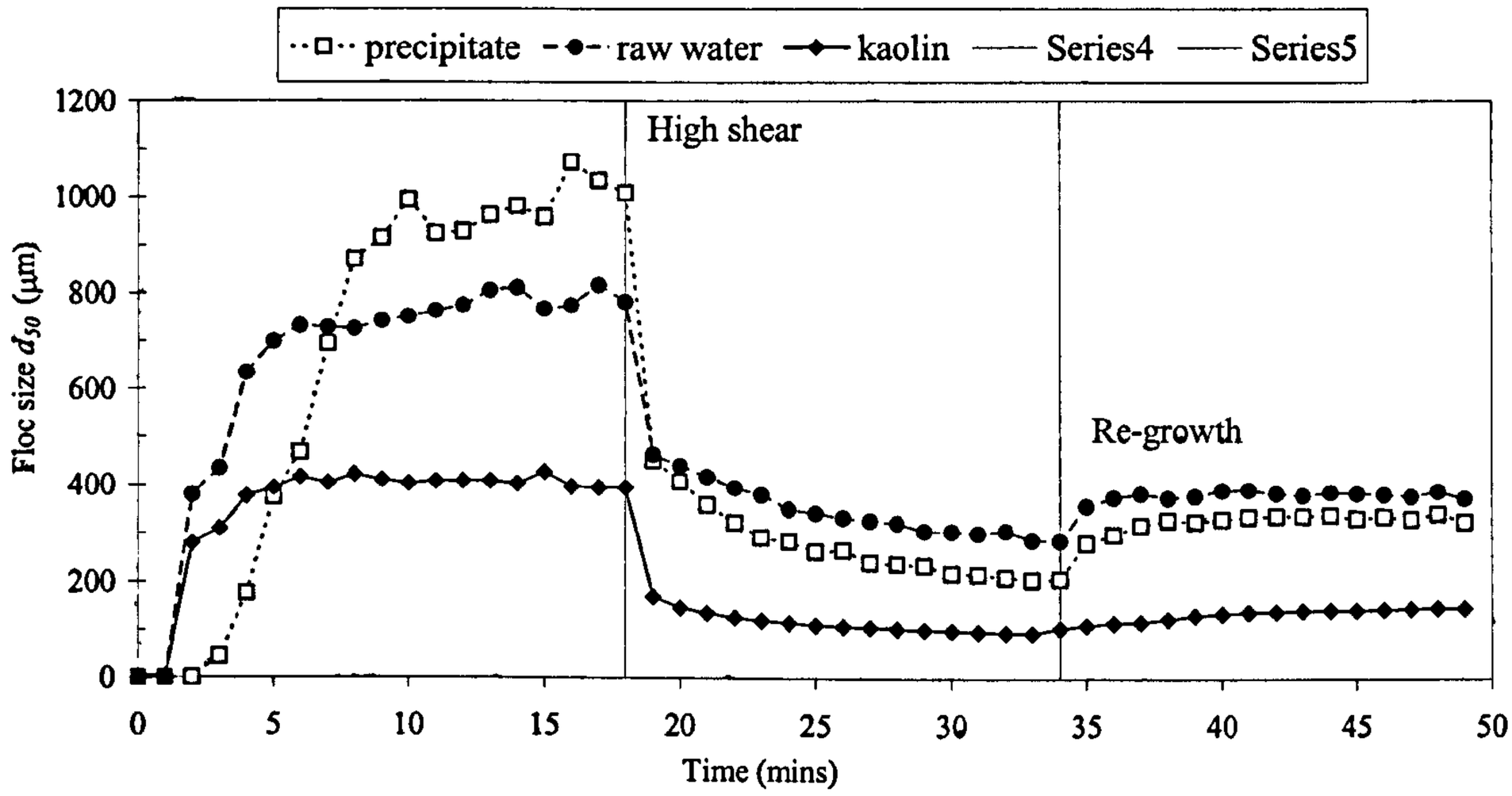

Figure 3(B).4 The potential for re-growth of flocs after breakage for the three suspensions. The first line indicates the point at which shear is applied (200 rpm), the second line indicates the point at which the slow stir is re-introduced (30 rpm).

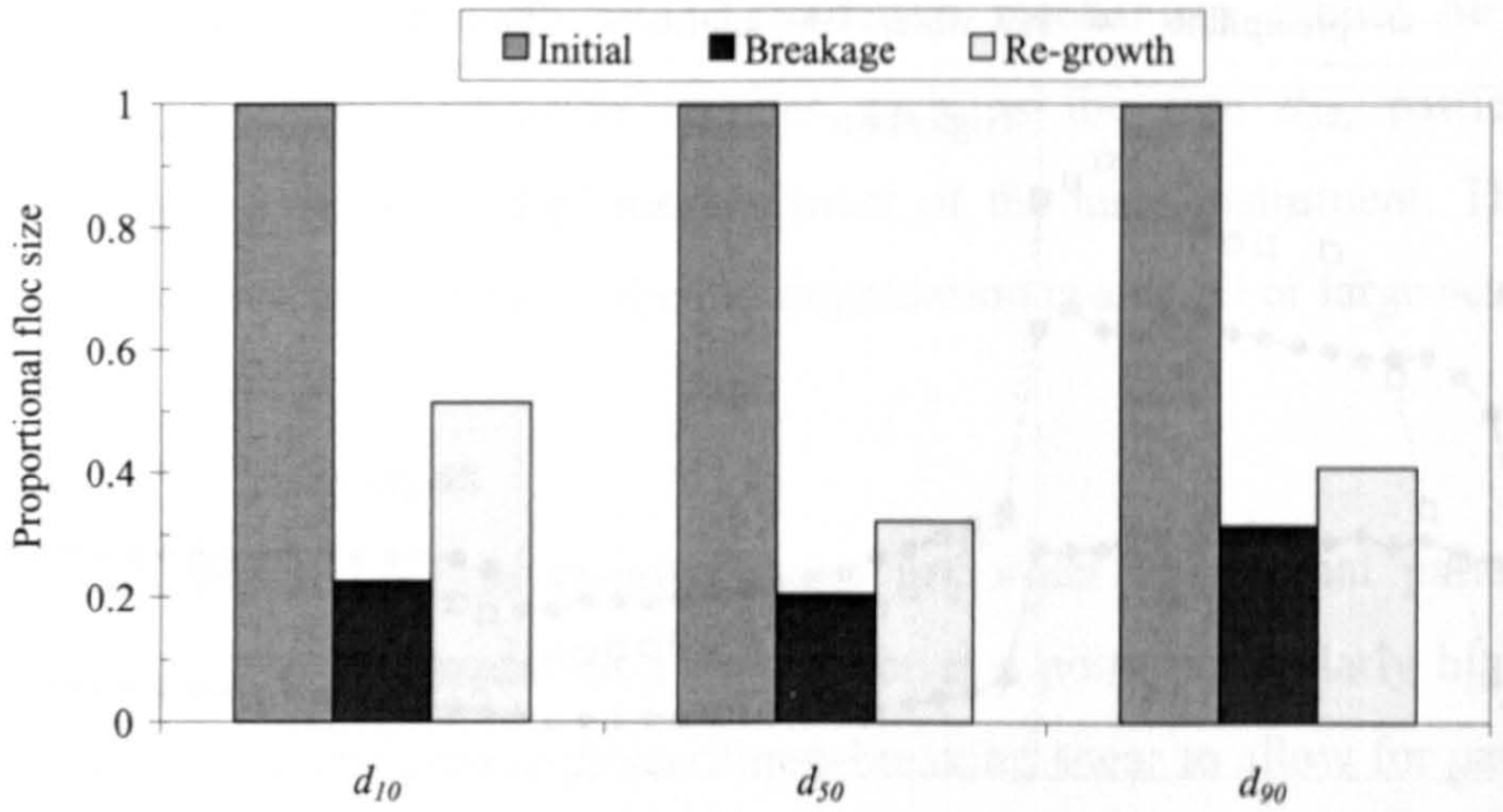

a) Iron hydroxide precipitate

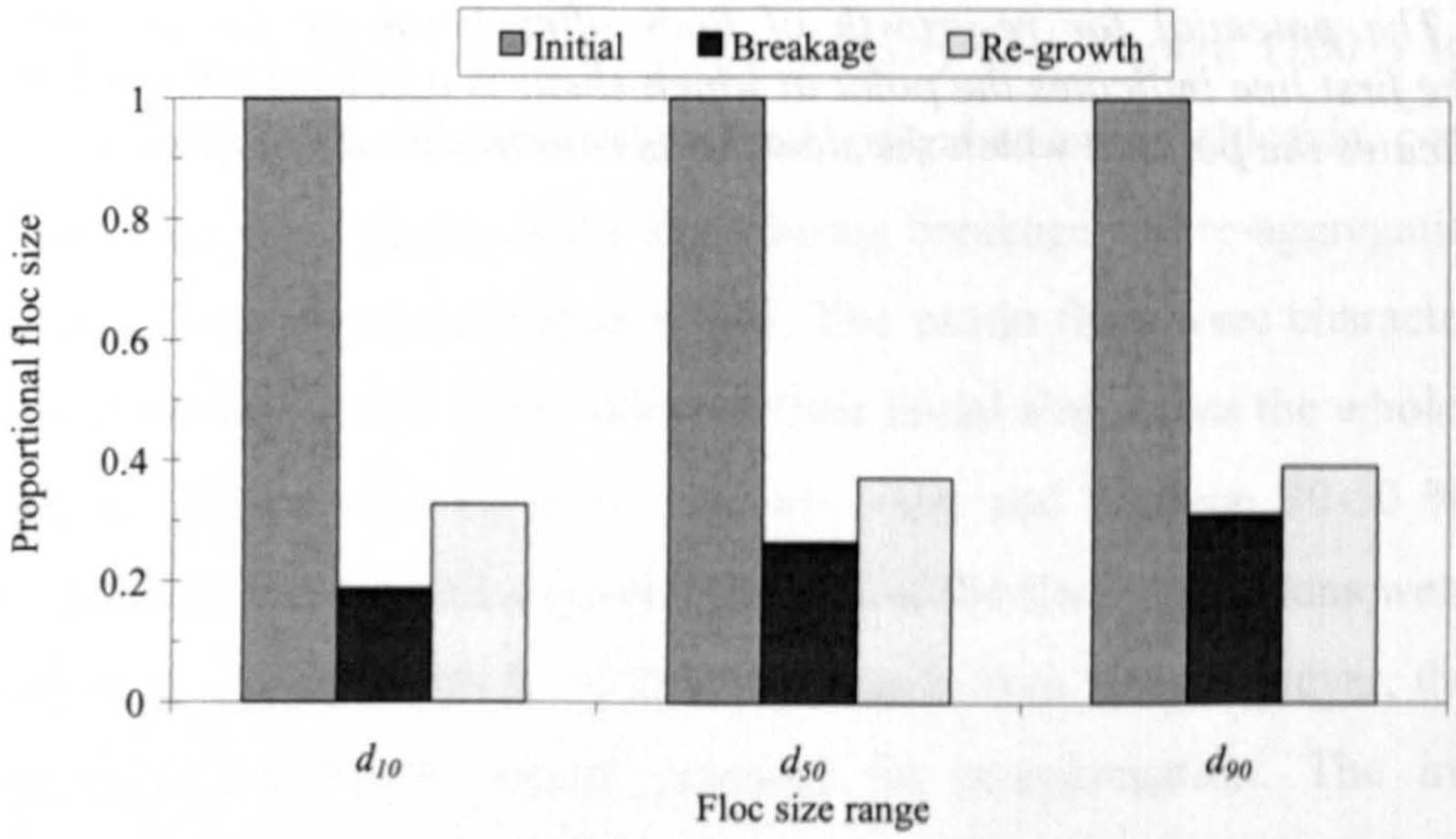

b) Kaolin

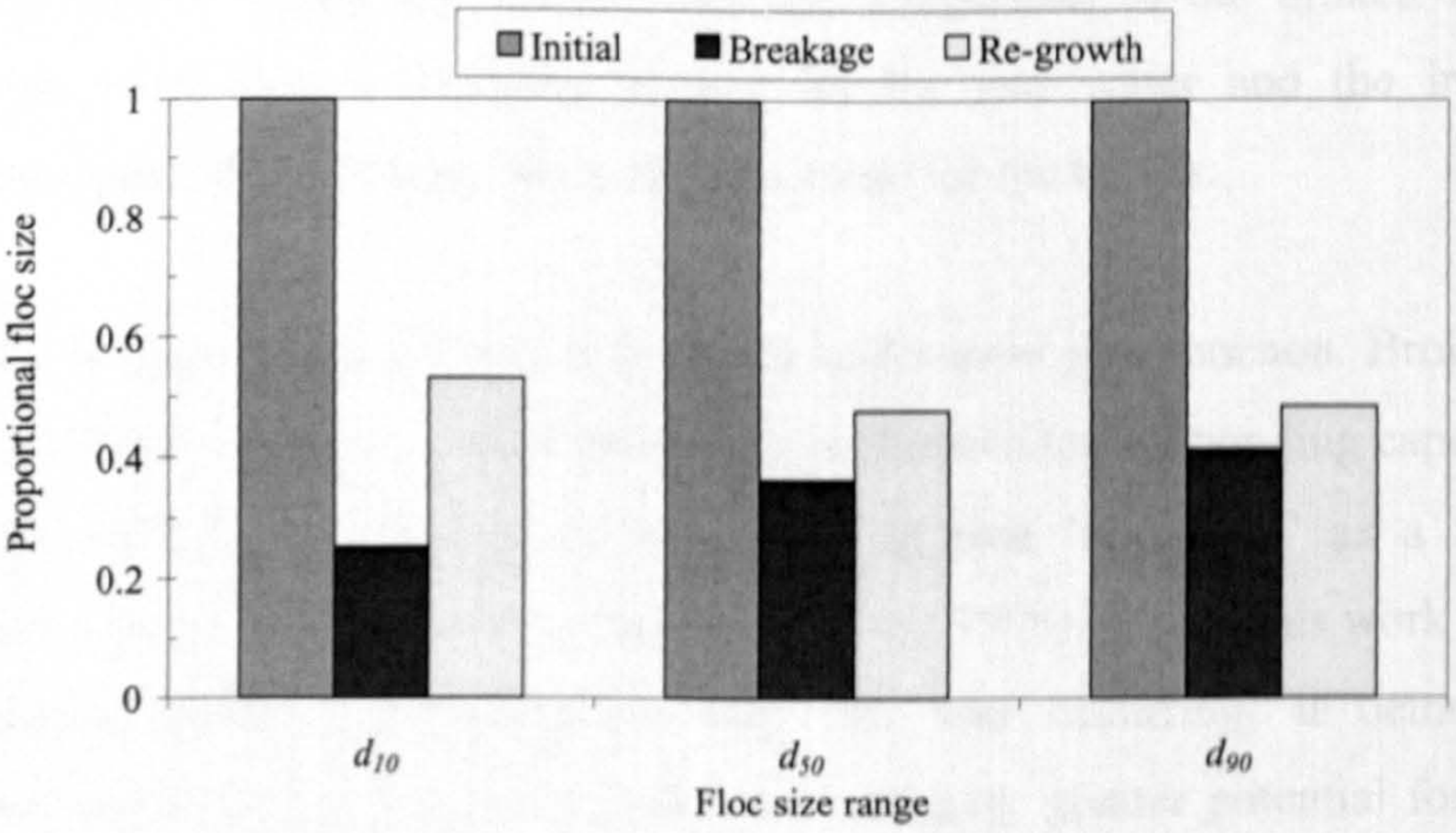

c) Raw water

Figure 3(B).5 The proportional change in floc size after breakage and re-growth for the 10, 50 and 90 percentile floc sizes for each of the three suspensions.

3(B).4 Conclusions

The results presented here show that understanding floc strength and breakage requires detailed analysis of PSD data in addition to single percentile values. At low rpm the precipitate flocs were the strongest. However at rpm of 75 and above, these flocs degraded at a very rapid rate. The organic flocs had the smallest proportional size change across the whole shear range under investigation. Kaolin had the greatest proportional size change across the shear range. Small scale and large scale floc size changes were identified. Small scale events occurred at low rpm (≤50 rpm) whilst large scale floc size changes occurred at high rpm.

The flocs under investigation were unable to re-form to their previous size after shear. The small floc size ranges showed the greatest ability to re-flocculate although the reasons for this were unclear. Precipitate flocs and organic flocs had the greatest potential to re-form.

Acknowledgements

The submitted manuscript has been made possible through funding from American Water Works Association Research Foundation and Co-funding Utilities. The information contained herein is based upon Intellectual Property which is jointly owned by Cranfield University and the Foundation. The Foundation retains its right to publish or produce the Jointly Owned Intellectual Property in part or in its entirety. The authors would also like to thank the EPSRC, Fort Collins Water, Scottish Water, Severn Trent Water, Thames Water, United Utilities and Yorkshire Water.

3(B).5 References

Bache, D. H., Johnson, C., McGilligan, J. F., and Rasool, E. (1997). A Conceptual View of Floc Structure in the Sweep Floc Domain. *Water Science and Technology* **36** (4), 49-56.

Bache, D. H., Rasool, E., Moffatt, D., and McGilligan, F. J. (1999). On the Strength and Character of Alumino-Humic Flocs. *Water Science and Technology* **40** (9), 81-88.

Biggs, C. A. and Lant, P. A. (2000). Activated Sludge Flocculation: On-Line Determination of Floc Size and the Effect of Shear. *Water Research* **34** 2542-2550.

Boller, M. and Blaser, S. (1998). Particles Under Stress. *Water Science and Technology* **37** (10), 9-29.

Bouyer, D., Line, A., Cockx, A., and Do-Quang, Z. (2001). Experimental Analysis of Floc Size Distribution and Hydrodynamics in a Jar-test. *Transactions of the Institution of Chemical Engineers* **79** (A), 1017-1024.

Essamiani, K. and de Traversay, C. (2002) Optimisation of the Flocculation Process Using Computational Fluid Dynamics. In: *Chemical Water and Wastewater Treatment VII: Proceedings of the 10^{h} Gothenburg Symposium*; International Water Association: Gothenburg, June.

Francois, R. J. (1987). Strength of Aluminium Hydroxide Flocs. *Water Research* **21** 1023-1030.

Gregory, J. and Dupont, V. (2001) Properties of Flocs Produced by Water Treatment Coagulants. *Water Science and Technology* **44** (10), 231-236.

Huang, H. (1994). Fractal Properties of Flocs Formed by Fluid shear and Differential Settling. *Physics of Fluids* **6** 3229-3234.

Kim, S. H., Moon, B. H., and Lee, H. I. (2001). Effects of pH and Dosage on Pollutant Removal and Floc Structure During Coagulation. *Microchemical Journal* **68** 197-203.

Leentvaar, J. and Rebhun, M. (1983). Strength of Feric Hydroxide Flocs. *Water Research* **17** 895-902.

Mikkelsen, L. H. and Keiding, K. (2002). The Shear Sensitivity of Activated Sludge: an Evaluation of the Possibility for a Standardised Floc Strength Test *Water Research* **36** (12), 2931-2940.

Parker, D. S., Kaufman, W. J., and Jenkins, D. (1972). Floc Breakup in Turbulent Flocculation Processes. *Journal of the Sanitary Engineering Division – ASCE* **SA 1** 79-99.

Spicer, P.T., Pratsinis, S.E., Raper, J., Amal, R., Bushell, G., and Meesters, G. (1998). Effect of Shear Schedule on Particle Size, Density and Structure During Flocculation in Stirred Tanks. *Powder Technology* **97** 26-34.

Yeung, A. K. C. and Pelton, R. (1996). Micromechanics: A New Approach to Studying the Strength and Breakup of Flocs. *Journal of Colloid and Interface Science* **184** 579-585.

CHAPTER 4

THE IMPACT ON FLOC STRUCTURE OF THE SEASONAL VARIATION IN AN ORGANIC RICH WATER SOURCE:

CHARACTERISING NATURAL ORGANIC MATTER FLOCS

Published in *Water Science and Technology: Water Supply* (2004), Vol. 4 (4), pp 79-87.

4 CHARACTERISING NATURAL ORGANIC MATTER FLOCS

PETER JARVIS, BRUCE JEFFERSON and SIMON A. PARSONS

School of Water Sciences, Cranfield University, Cranfield, Bedfordshire, MK43 0AL, United Kingdom

Abstract

Using a dynamic optical technique and settling column apparatus, natural organic matter floc structural characteristics were monitored and evaluated over a one year period to monitor the seasonal variation in floc structure at optimum coagulation dose and pH. The results show that flocs changed seasonally with different growth rates, size, response to shear and settling rate. Autumn and summer flocs were shown to be larger and less resistant to floc breakage when compared to the other seasons, suggesting reduced floc strength. Floc strength was observed to increase with larger median floc size. In summary, the autumnal flocs had significantly different floc characteristics although it was difficult to relate the floc structure with the incoming water characteristics.

Keywords

Coagulation; floc strength; natural organic matter; removal; settling velocity.

4.1 Introduction

The removal of natural organic matter (NOM) using coagulation, flocculation and solid-liquid separation techniques is now well established at water treatment works (WTW). The efficient removal of NOM is dependent upon a number of factors including pH, coagulant type and dose and the particular dosing strategy (Chow *et al.*, 1999; Billica and Gertig, 2000; Fearing *et al.*, 2004). In addition to this, floc structural quality plays a significant role in the removal process. There is a general conception that NOM flocs are weak and of low density when compared to turbidity flocs (Bache *et al.*, 1999). Furthermore, the particular nature of the NOM and the coagulant being used can have a significant impact on floc structure (Collins *et al.*, 1986). However, there is little evidence to clarify this as there has generally been no consideration and quantification given to the resulting floc physical properties. NOM is recognised as a complex mixture of organic compounds originating from one of the four main types of biopolymer; polysaccharides, peptidic material, N-acetylamine sugars and polyphenolic material (Christy and Egeberg, 2000; Nissinen *et al.*, 2001). However, there is further evidence showing that there is considerable temporal variation in NOM (Wilkinson *et al.*, 1997). An ongoing study by Goslan *et al.* (2002) has identified a change in the composition of NOM through fractionation studies. These were thought to be as a result of changes in climate, different seasonal land use and other unidentified reasons. During coagulation, NOM is removed through a combination of charge neutralisation, entrapment, adsorption and complexation with coagulant metal ions into insoluble particulate aggregates as shown in Figure 4.1 (Dempsey *et al.*, 1984; Dennett *et al.*, 1996; Vilge-Ritter *et al.*, 1999). Further agglomeration of these micro-particles leads to the formation of flocs. The way in which these interactions occur and the efficient incorporation of these molecules into the floc aggregate is dependent upon the particular nature of the NOM components with regard to molecular size, functionality, charge and hydrophobicity. Because of the variable composition of NOM, the nature of removal will invariably be different for specific types of molecule within a NOM sample.

An accurate assessment of floc structure can be a crucial tool for predicting WTW performance under certain coagulation conditions and may be used in combination with removal data to find optimum coagulation pH and dose.

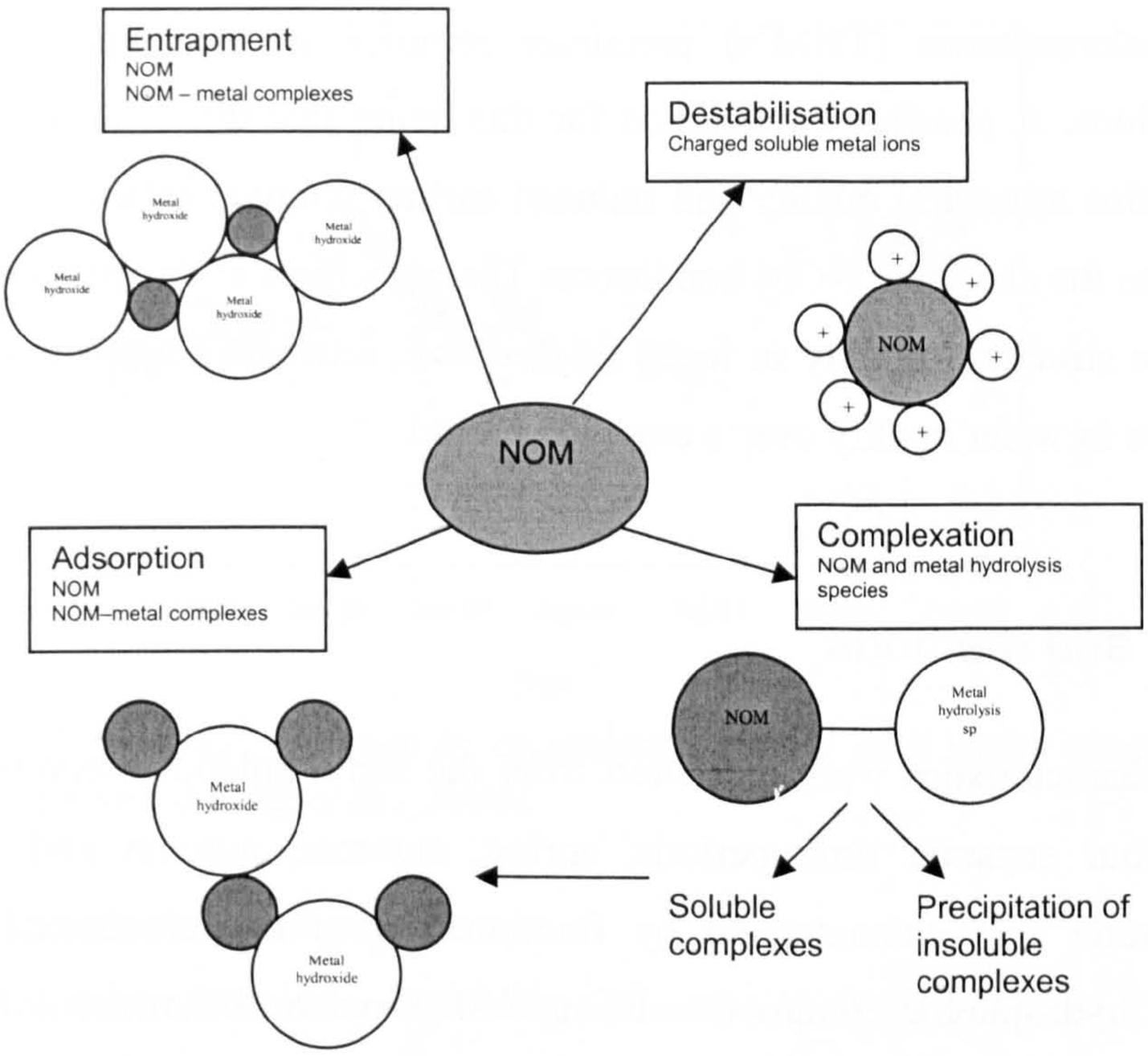

Figure 4.1 The possible removal mechanisms of NOM during coagulation.

4.2 Background and objectives

Waterworks that are principally geared towards the treatment of water of a high organic content, low alkalinity and low turbidity are periodically faced with challenging conditions that occur as a result of either a seasonal increase in the organic concentration of the raw water or a seasonal change in the nature of the organic substances in the water. In the mountainous regions of America this coincides with the spring snow melt whilst in the uplands of Europe this usually corresponds to the first heavy rainfalls of autumn. A typical example of this occurs in Yorkshire, England. Figure 4.2 shows the seasonal change in coagulant demand at a WTW in Yorkshire over a two year period (Fearing *et al.*, 2004). The coagulant dose remained around 12 mg L^{-1} as Fe during spring and summer months, whilst this was shown to increase to 17-20 mg L^{-1} Fe in some autumn and winter periods. The increase in coagulant demand between October and January coincides with water that is challenging to treat. Observed affects at the WTW include very short filter run times and early breakthrough. In addition, a decline in dissolved organic carbon (DOC),

colour and trihalomethanes (THM's) precursor removal is seen under normal operating conditions. A possible explanation for this being that this is as a result of deterioration in floc structural quality and reduced carbon removal efficiency during coagulation due to the changing NOM conditions. The objectives of this paper were to assess NOM floc structural quality in terms of floc size, settlement and strength for seasonal variation in water quality over a one year period.

4.3 Materials and methods

Floc structural characteristics were measured from the same upland reservoir water source during four separate time periods: spring, summer, autumn and winter. Seasonal raw water was characterised by fractionation of organic material into hydrophillic and hydrophobic components using XAD4 and XAD8 resins following the method of Goslan *et al.* (2002). Flocs were formed by performing a series of jar tests. A PB-900 variable speed jar tester (Phipps and Bird, Virginia, USA) was used with 76 x 25 mm flat paddle impellers with 1 L cylindrical jars containing 1 L samples of water. Two speeds were used with a rapid mix at 200 rpm for 1.5 minutes followed by a slow stir phase at 30 rpm for 15 minutes followed by a 10 minute settling time. The coagulant was a pre-polymerised ferric sulphate based coagulant as used by the WTW (Ferripol XL, Huntsman Tioxide Europe Ltd, Billingham, UK). The coagulant was added at optimised doses based upon maximum achievable NOM removal, similar to those as used by the WTW at the time of abstraction. Adjustment of pH was achieved using 1M NaOH (Fisher Scientific UK, Loughborough). In all cases the coagulation pH was around 4.5 as this corresponds to the pH as used by WTW for optimum NOM removal using this iron based coagulant. All experiments were carried out at a temperature of 21-22° C.

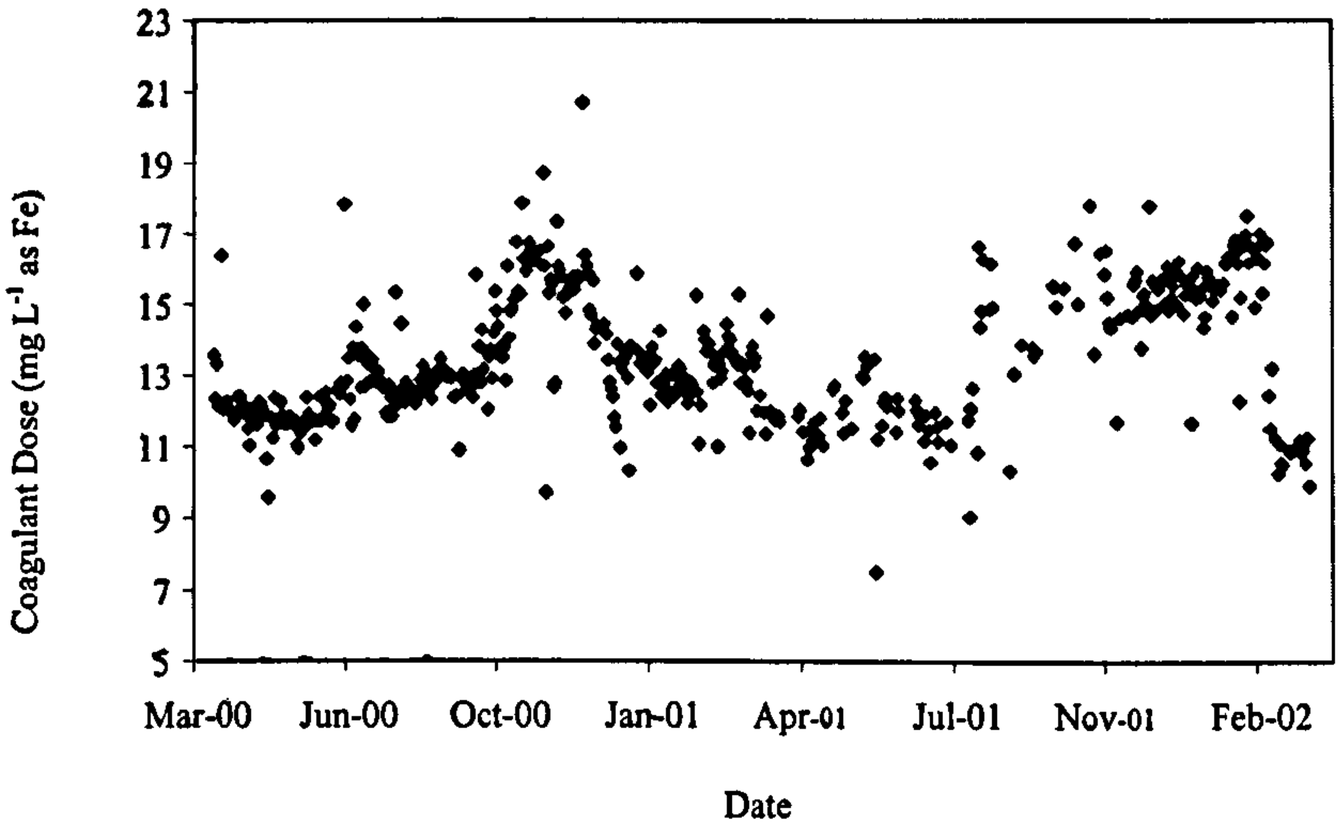

Figure 4.2 Seasonal changes in coagulant demand at a water source in Yorkshire, England (from Fearing et al., 2004).

4.3.1 Floc size and strength

A laser diffraction instrument (Malvern Mastersizer 2000, Malvern, UK) was coupled with the jar tester to measure dynamic floc size as the coagulation and flocculation process proceeded. A 1 litre cylindrical jar was used with holding ports for the inflow/outflow tubing secured onto the sides of the jar. This type of arrangement has previously been successfully applied in the analysis of other floc systems (Spicer *et al.*, 1998; Biggs and Lant, 2000). However, due to the delicate nature of the organic flocs in these experiments it was necessary to have a comparatively reduced flow rate through the tubing to prevent floc breakage. The suspension was monitored by drawing water through the optical unit of the Mastersizer and back into the jar by a peristaltic pump on the return tube using 5 mm internal diameter peristaltic pump tubing at a flow rate of 1.5 L hr^{-1}. The inflow and outflow tubes were positioned opposite to one another at a depth just above the paddle in the holding ports. Coagulant and pH adjustment chemicals were added at the start of the rapid mix. Size measurements were taken every minute for the duration of the jar test and logged onto a PC. Each size experiment was repeated 3 times for each set of conditions. For the determination of floc response to shear, the jar tester was programmed as before, however after the slow stir phase the suspension was exposed to increased shear for a further 15 minutes. Separate experiments were carried out and replicated 3 times at increased shear of 30, 40, 50, 75, 100, 150 and 200 rpm. Particle size was monitored before and after exposure to each level of shear.

4.3.2 Floc settling velocity

The measurement of floc settling velocity followed a similar protocol to numerous studies that have used photography and image analysis to observe falling flocs (Johnson *et al.*, 1996; Adachi and Tanaka, 1997; Tang *et al.*, 2002). Briefly, the system involved floc aggregates falling into a central settling column that was enclosed by a water bath. The water bath was connected to a ThermoHaake K10 heat-refrigerated circulator (Hakke, Germany) to ensure a constant temperature was maintained in the column at 21-22° C and a period of 2 hours was left for quiescent conditions to be reached. The settling column was filled with de-ionised water and left to reach the required temperature. Flocs were introduced into the settling column after flocculation on a jar tester jar using a wide mouthed pipette. Visual observation showed that little change in floc macrostructure occurred using the pipettes, however if flocs were observed to break during the transfer procedure then they were discarded. Falling floc images were captured using a CV M90 colour close-coupled device (CCD) camera (JAI UK Ltd, England). As a focused floc passed in front of the camera, the image grabber was manually triggered to take a series of 10 images with a gap of 1 second between each frame. Image analysis software (Image Pro Plus from Media Cybernetics, Maryland, USA) was used to determine floc size and distance travelled. The projected area of the floc presented in front of the camera was determined using the image analysis software and converted to an equivalent diameter. This standardised diameter was recorded along with its settling velocity for 100 aggregates for each set of coagulation conditions.

4.4 Results and discussion

4.4.1 Raw water characterisation

The water under investigation was characteristic of a moorland catchment being of high colour and NOM concentration, low turbidity (<3 NTU) and low alkalinity (<10 mg L^{-1} as $CaCO_3$). Some of the raw water characteristics are shown in Table 4.1. It can be seen that the general water characteristics do not significantly change across the periods of measurement. The specific UV_{254} absorbance (SUVA) was seen to increase by 24-30 % in the summer and autumn months. DOC removal was seen to increase with increasing coagulant dose other than in summer when high removal was

seen for a low dose. There was a drop in organic removal rates in autumn and winter at optimum doses suggesting these waters were more recalcitrant to treatment. As can be seen in Figure 4.3, fractionation of these waters shows there to be only small changes in the character of the water throughout most of the year. The hydrophobic fractions (the humic and fulvic acids) were the dominating components throughout the year, accounting for between 60-70 % of the total DOC. The largest change in the fractional composition was seen in winter when the fulvic acid fraction (FAF) was seen to increase by 20 % when compared to the other seasons. This was commensurate with a similar decrease in the humic acid fraction.

Table 4.1 The seasonal change in raw water characteristics over a one year period and the coagulant dose used and DOC removals achieved.

Seasonal water	DOC (mg L^{-1} as C)	UV Absorbance at 254 nm (m^{-1})	SUVA, (L.mg m^{-1})	Coagulant dose applied (mg L^{-1} Fe)	% DOC removal
Spring	11.4	52.6	4.6	14.4	81
Summer	8.9	50.8	5.7	8.0	88
Autumn	10.2	60.2	5.9	12.1	75
Winter	9.2	40.1	4.4	10.0	63

4.4.2 Floc size and strength

The size profiles of flocs upon exposure to increasing levels of shear on a jar tester are shown in Figure 4.4 for the seasonal waters. The data shows the 50 percentile floc size expressed as an equivalent volumetric diameter (d_{50}). The d_{50} was chosen as the representative floc size, although the same general trends were seen for other percentile floc sizes. The floc size after 15 minutes of slow stir was of the following general trend: autumn (median floc size 764 μm ± 34) > summer (724 μm ± 65) > spring (649 μm ± 38) > winter (594 μm ± 45). However, the overlap of adjacent error bands suggest this size order was indicative only. The rate of floc formation was quicker for the spring, autumn and winter waters than for the summer water which had the lowest coagulant dose, suggesting low dose significantly slows the rate of floc formation. In comparison to other studies using similar floc sizing techniques, these flocs were 6-7 times larger than activated sludge flocs (Biggs and Lant, 2000) and 5-6

times larger than kaolin coagulated with polyaluminium chloride (Lin *et al.*, 2002). There has been no previous work using a similar laser based diffraction technique to observe the size of Fe-NOM flocs, however the range of floc sizes found were of a similar size to metal-NOM flocs observed using CCD with image analysis (Bache and Rasool, 2001).

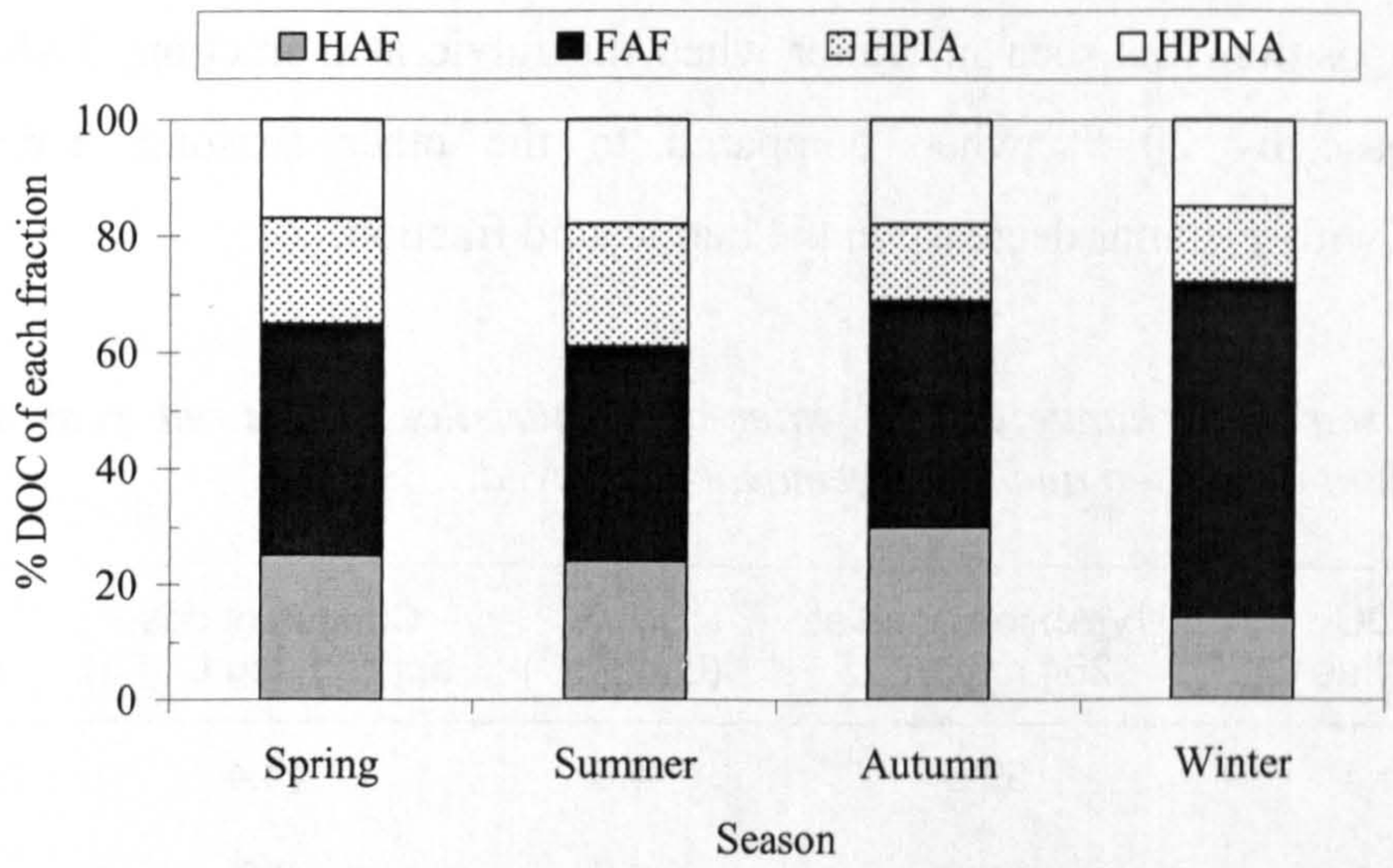

Figure 4.3 A demonstration of the change in composition of NOM with season for the Albert Reservoir, Yorkshire.

With increasing rpm on a jar tester the steady-state floc size was shown to decrease. At high rpm there was an initial large-scale decrease in floc size followed by a more gradual decline. At low rpm there was a more gradual decline in floc size until a steady state size was approached after 15 minutes exposure to shear. The size after 15 minutes at increased rpm are shown in Figure 4.5. The rate at which a floc suspension degrades with increasing rpm gives an indication of floc strength. A steeper slope suggests a floc suspension will undergo a larger proportional reduction in floc size when compared to a degradation curve with a shallower slope. The summer and autumn floc suspensions had similar degradation slopes (0.47 and 0.49 respectively) whilst the initially smaller spring and winter flocs degraded with a significantly lower slope (0.34 and 0.31 respectively). However, it should be noted that the autumn flocs remained larger than the other seasons until very high shear (>100 rpm) when flocs converged on a similar microfloc size.

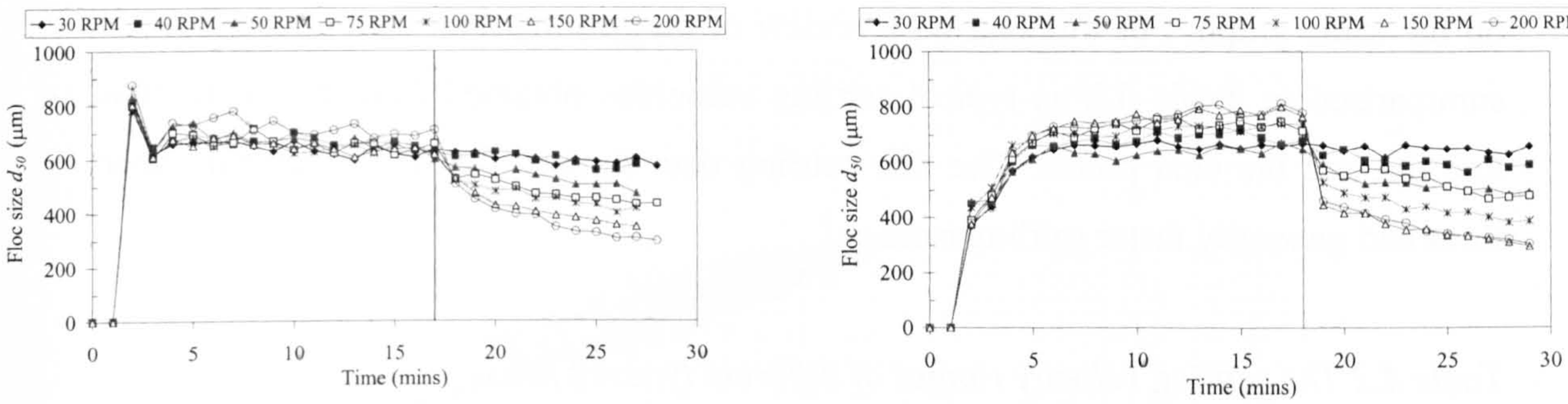

Figure 4.4 The growth and breakage behaviour of flocs with increasing shear from three seasonal periods in 2003. The line indicates the point at which increased shear was introduced.

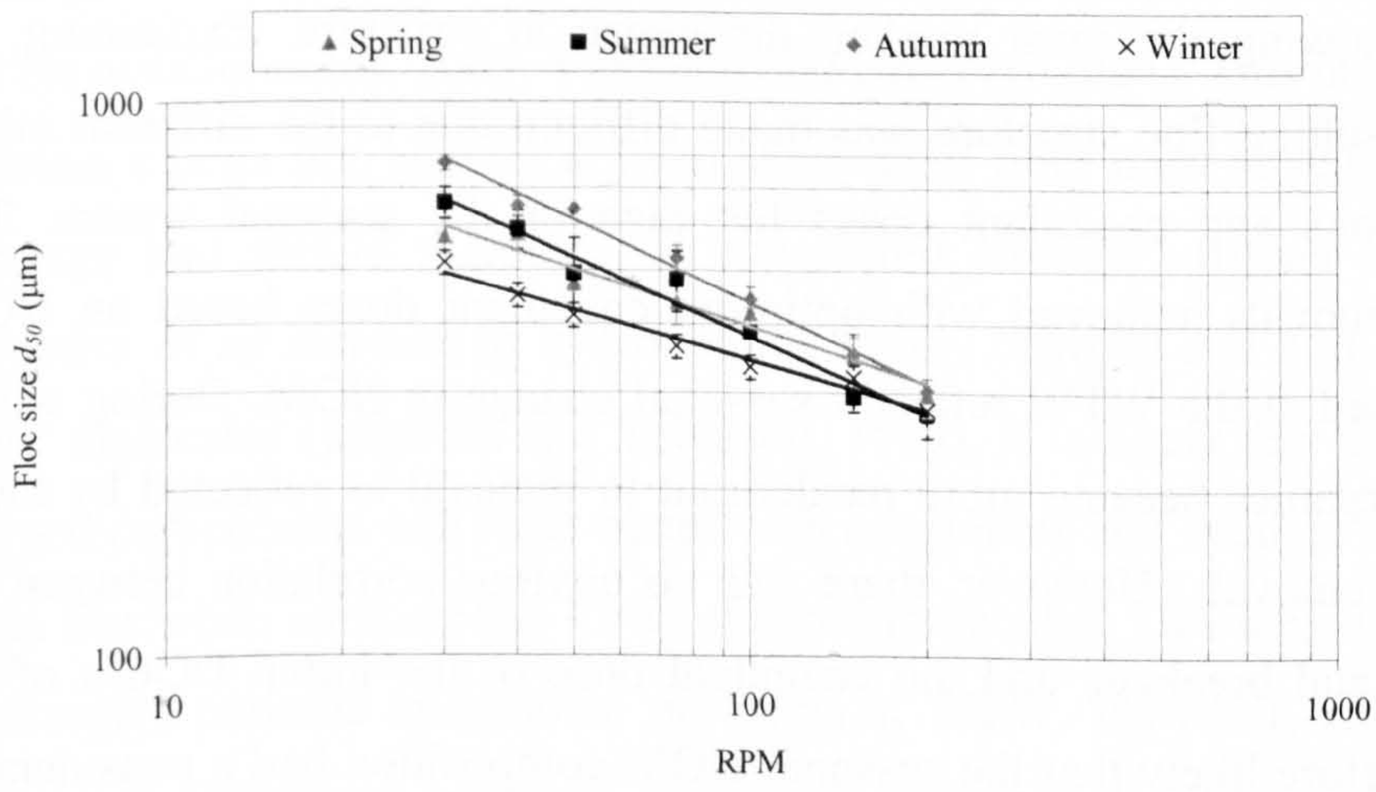

Figure 4.5 The rate of degradation of NOM flocs with increasing shear for the seasonal waters.

4.4.3 Floc settling velocity

An example of settling behaviour of Fe-NOM flocs is shown in Figure 4.6 for flocs formed from the summer and autumn water. Due to the relative scatter and crossover of the data, it was not possible to present all of the data for all of the seasonal waters

on the same graph. For this reason, a review of the settling data for organic flocs is summarised in Table 4.2 as typical settling velocities obtained from the regression line through the data points. The floc settling data showed that the autumnal water flocs had generally faster settling rates.

Table 4.2 The settling velocity ranges of different types of flocs.

Type of floc	Settling velocity range ($\mu m\ s^{-1}$)	
	Small floc (400 μm diameter)	Large floc (1000 μm diameter)
Spring	290	728
Summer	267	680
Autumn	423	891
Winter	315	763

4.4.4 Floc structure and NOM composition

These experiments have established a seasonal change in floc characteristics with the autumnal flocs showing the most marked difference in structure. Explaining the reasons for the resulting floc structure was made difficult due to the different initial NOM concentrations and coagulant doses for each of the seasonal waters. The different DOC removals achieved with optimum coagulant doses based on NOM removal and as used at the WTW reflect a seasonal change in NOM. During winter and autumn the organics became more recalcitrant to removal as reflected by lower percentage DOC removals. However, there was no obvious correlation between the floc growth, size and breakage and the coagulant dose or the initial DOC's of the water. It was therefore likely that the seasonal NOM composition had a considerable impact on the floc structure. The increase in the FAF seen during winter may be a factor that influenced the reduced floc size seen during this season when smaller flocs formed. However, significant changes in floc structure were seen during the other seasons which could not be explained by the small scale changes in NOM fractions observed during these times. It was therefore difficult to interpret how the specific fractions impacted on floc structure.

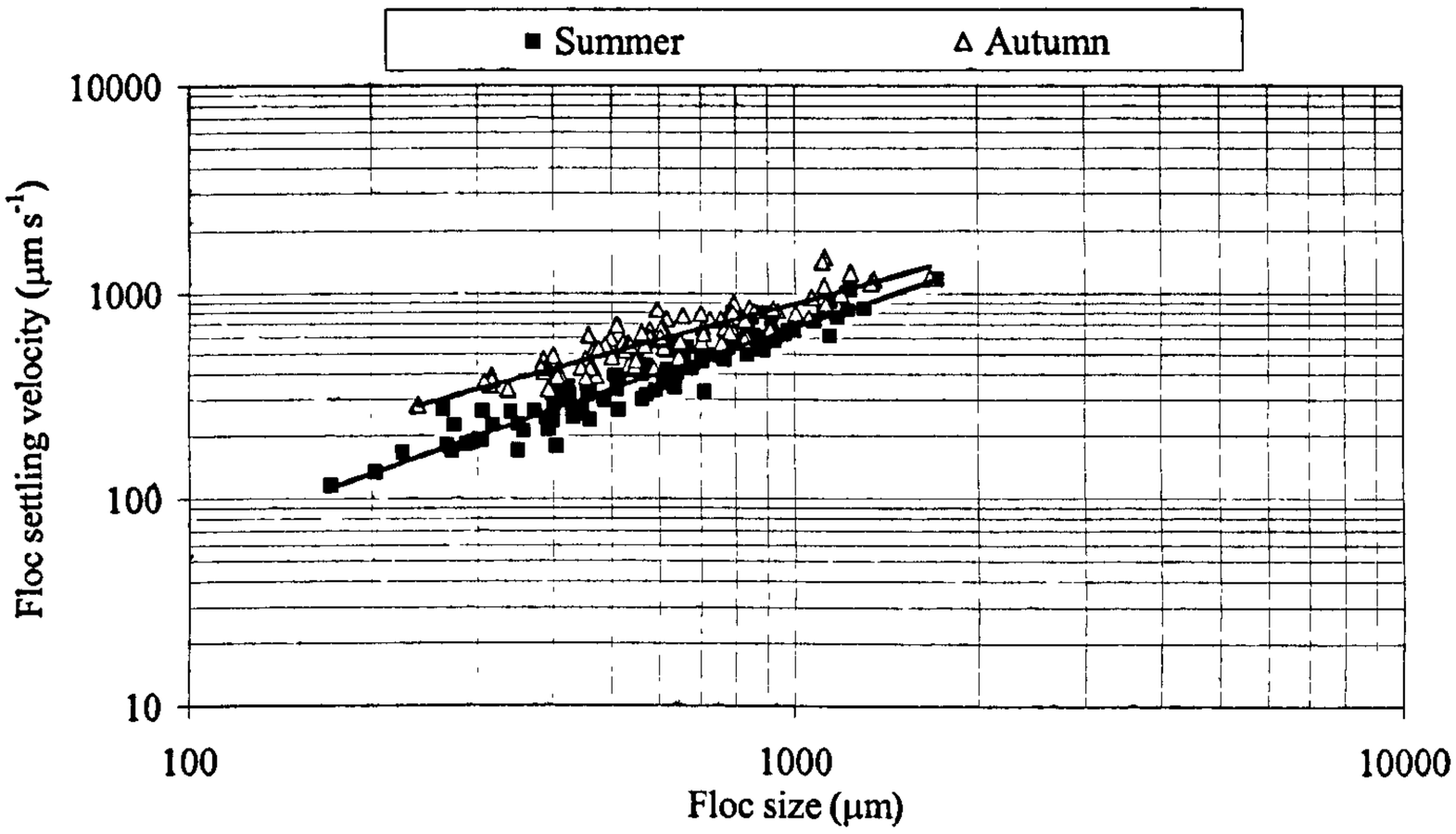

Figure 4.6 An example of the settling behaviour of NOM flocs in relation to their size.

While the specific reactions of NOM fractions with coagulant chemicals has not been fully understood, a possible explanation for the observed floc characteristics was SUVA. The autumn and summer waters had the highest SUVA and this was concurrent with flocs that were initially large whilst the low SUVA, high FAF winter water gave rise to small weak flocs. Large flocs are indicative of strong flocs (Bache and Papavasilopoulos, 2003; Yukselen and Gregory, 2004). This is because in order to maintain a large floc size for a given shear these flocs must have higher resistance to breakage and should therefore be considered stronger. Higher SUVA values are indicative of an increase in hydrophobic, highly charged and high molecular weight NOM molecules (Edzwald and Tobiason, 1999). It is likely that an increase in these charged components will react better with coagulants and become better incorporated in the floc when compared to lower charged molecules. This may help to explain why waters give periodic operational problems at WTW. However, given the previously mentioned differences in initial DOC and coagulant dose this impact needs further investigation.

An understanding of the impact of NOM on floc structure provides important information at WTW with regard to the likely removal efficiency of NOM flocs during solid-liquid separation processes. In addition, being able to quantify floc structure will allow the development of improved dosing strategies in terms of

combining improved floc quality with optimum NOM removal. However, more work is required to understand further the specific impact of NOM components and concentration and coagulant dose on floc structure. Furthermore an investigation of a wider range of NOM rich waters is required in order to assess the wider ranging impacts of NOM on floc structure.

4.5 Conclusions

(1) A seasonal change in floc structure was observed a result of the combined effects of variation in NOM composition, NOM concentration and coagulant dose, although the specific effects of each of these factors could not be quantified.

(2) The most marked difference in structure was observed for autumnal water flocs. These flocs were larger and settled faster.

(3) Smaller floc structures showed reduced proportional breakage with increased shear.

Acknowledgements

The submitted manuscript has been made possible through funding from American Water Works Association Research Foundation and Co-funding Utilities. The information contained herein is based upon Intellectual Property which is jointly owned by Cranfield University and the Foundation. The Foundation retains its right to publish or produce the Jointly Owned Intellectual Property in part or in its entirety. The authors would also like to thank the EPSRC, Fort Collins Water, Scottish Water, Severn Trent Water, Thames Water, United Utilities and Yorkshire Water.

4.6 References

Adachi, Y. and Tanaka, Y. (1997). Settling Velocity of an Aluminium-Kaolinite Floc. *Water Research* **31** 449-454.

Bache, D. H. and Papavasilopoulos, E. N. (2003). Dewatering of Alumino-Humic Sludge: Impacts of Hydroxide. *Water Research* **37** 3289-3298.

Bache, D. H. and Rasool, E. (2001). Characteristics of Alumino-Humic Flocs in Relation to DAF Performance. *Water Science and Technology* **43** (8), 203-208.

Bache, D. H., Rasool, E., Moffatt, D., and McGilligan, F.J. (1999). On the Strength and Character of Alumino-Humic Flocs. *Water Science and Technology* **40** (9), 81-88.

Biggs, C. A. and Lant, P. A. (2000). Activated Sludge Flocculation: On-Line Determination of Floc Size and the Effect of Shear. *Water Research* **34** 2542-2550.

Billica, J. A. and Gertig, K. R. (2000) Optimisation of a Coagulation Process to Treat High TOC, Low Alkalinity Water and its Impact on Filtration Performance. In: *Proceedings of the Water Quality and Technology Conference*; American Water Works Association: November.

Bratby, J. (1980) Coagulation and Flocculation. Uplands Press Ltd, Croydon, UK.

Chow, C. W. K., van Leeuwen, J. A., Drikas, M., Fabris, R., Spark, K. M. and Page, D. W. (1999). The Impact of the Character of Natural Organic Matter in Conventional Treatment with Alum. *Water Science and Technology* **40** (9), 97-104.

Christy, A. A. and Egeberg, P. K. (2000). Characterisation of Natural Organic Matter from the Nordic Typing Project Water Samples by Chemometric Analysis of their near Infrared Spectral Profiles. *Chemometrics and Intelligent Laboratory Systems* **50** 225-234.

Collins, M. R., Amy, G. L. and Steelink, C. (1986). Molecular Weight Distribution, Carboxylic Acidity and Humic Substances Content of Aquatic Organic Matter: Implications for Removal During Water Treatment. *Environmental Science and Technology* **1986** 1028-1032.

Dempsey, B. A., Ganho, R. M., and O'Melia, C. R. (1984). The Coagulation of Humic Substances by Means of Aluminium Salts. *Journal of the American Water Works Association* **76** (4), 141-150.

Dennett, K. E., Amirtharajah, A., Moran, T. F. and Gould, J. P. (1996). *Journal of the American Water Works Association* **April** 129-142.

Edzwald, J. K. and Tobiason, J. E. (1999). Enhanced Coagulation and a Broader View. *Water Science and Technology* **40** (9), 63-70.

Fearing, D., Goslan, E., Banks, J., Wilson, D., Hillis, P. H. , Campbell, A. T. and Parsons, S. A. (2004). Staged coagulation for the treatment of refractory organics. *Environmental Engineering* **130** 975-982.

Goslan, E. H., Fearing, D. A., Banks, J., Wilson, D., Hillis, P., Campbell, A.T. and Parsons, S.A. (2002). Seasonal Variations in the Disinfection By-product Precursor Profile of a Reservoir Water. *Aqua Journal of Water Supply: Research and Technology* **51** 475-482.

Johnson, C. P., Li, X. and Logan, B. E. (1996). Settling Velocities of Fractal Aggregates. *Environmental Science and Technology* **30** 1911-1918.

Lin, W. W., Sung, S. S., Lee, D. J., Chen, Y. P., Chen, D. S. and Lee, S. F. (2002). Coagulation of Humic-Kaolin-PACl aggregates. *Water Science and Technology* **47** (1), 145-152.

Nissinen, T. K., Miettinen, I. T., Martikainen, P. J. and Vartiainen, T. (2001). Molecular Size Distribution of Natural Organic Matter in Raw and Drinking Waters. *Chemosphere* **45** 865-873.

Spicer, P. T., Pratsinis, S. E., Raper, J., Amal, R., Bushell, G., and Meesters, G. (1998). Effect of Shear Schedule on Particle Size, Density and Structure During Flocculation in Stirred Tanks. *Powder Technology* **97** 26-34.

Vilge-Ritter, A., Rose, J., Masion, A., Bottero, J. Y. and Laine, J. M. (1999). Chemistry and Structure of Aggregates Formed with Fe-Salts and Natural Organic Matter. *Colloids and Surfaces A: Physicochemical and Engineering Aspects* **147** 297-308.

Wilkinson, K. J., Negre, J. C. and Buffle, J. (1997). Coagulation of Colloidal Material in Surface Waters: the Role of Natural Organic Matter. *Journal of Contaminant Hydrology* **26** 229-243.

Yeung, A. K. C. and Pelton, R. (1996). Micromechanics: A New Approach to Studying the Strength and Break-up of Flocs. *Journal of Colloid and Interface Science* **184** 579-585.

Yukselen, M. A. and Gregory, J. (2004) The Reversibility of Floc Breakage. *International Journal of Mineral Processing* **73** 251-259.

CHAPTER 5

HOW THE NATURAL ORGANIC MATTER TO COAGULANT RATIO IMPACTS ON FLOC OPERATIONAL PROPERTIES

Submitted to the *Journal of Colloid and Interface Science.*

5 HOW THE NATURAL ORGANIC MATTER TO COAGULANT RATIO IMPACTS ON FLOC OPERATIONAL PROPERTIES

PETER JARVIS, BRUCE JEFFERSON and SIMON A. PARSONS

School of Water Sciences, Building 39, Cranfield University, Cranfield, Bedford, MK40 0AL, United Kingdom.

Abstract

Periods of elevated natural organic matter (NOM) loadings at water treatment works (WTW) can lead to operational problems as a result of a deterioration in floc structural quality. This study used a range of diagnostic tools to evaluate floc structure with increasing organic fraction in the floc. It was observed that when the organic fraction in the floc went significantly over a mass ratio of 1 mg of DOC to 1 mg of Fe (coagulant) the floc size, settling velocity, fractal dimension and strength were seen to decrease even when the NOM removed during coagulation remained high. A model was proposed to explain these changes that was dependent upon the adsorption of NOM on primary particle surfaces. The operational significance of these results suggest that for the coagulant under investigation the correct coagulant dose must be applied in order to give good floc structure.

Keywords

NOM; floc strength; fractal dimension; settling velocity; structure

5.1 Introduction

The removal of natural organic matter (NOM) has become increasingly important in light of the potential for carcinogenic disinfection-by-products (DBP) to form if organic carbon is insufficiently removed and recent legislation around the world calls for the strict control of DBP's (EC drinking water directive, 1998; Gibbons, 1999). Under normal conditions, NOM can be adequately removed at water treatment works (WTW) using conventional treatment processes such as coagulation, sedimentation and filtration. However, WTW are periodically faced with challenging water conditions whereby NOM removal can be compromised. These conditions usually coincide with an increase in the organic concentration of the raw water that can arise from a number of potential causes dependent upon geographical location. In temperate regions, the first rainfalls after dry periods flush accumulated carbon from soils into water bodies (Kaiser *et al.*, 2002; Goslan *et al.*, 2002; Hurst *et al.*, 2004). In mountainous areas, snow melts in spring can increase carbon concentrations in raw water as snow is a significant sink of organic material from adsorption of atmospheric organics (Ying *et al.*, 2004). In addition, top soils freeze during winter locking carbon in the soil over winter (Niskavaara *et al.*, 1997). Both of which are then subsequently released during spring thaws.

During periods of increased carbon load, not only is NOM removal compromised but circumstantial evidence suggests that floc properties are adversely affected by the increased carbon load (Wilson, 2004). Problems reported by WTW operatives include pronounced floc breakage during solid-liquid separation, notably on filters which leads to significantly reduced filter run times as smaller particles have a lower rate of capture during filtration mechanisms (Cleasby, 1999). A review of previous work shows that for iron based coagulants, optimum NOM removals are seen around or slightly below an iron (Fe) to organic carbon mass ratio of one to one (Eikkibrook, 1999; Vilge-Ritter *et al.*, 1999; Cheng *et al.*, 2002; Fearing *et al.*, 2004). It is believed, but so far unproven, that an increase in the carbon fraction within a floc leads to a significant change in floc structure. Therefore an assessment of floc structures formed from across a range of coagulant:DOC ratios may provide a more thorough explanation for the operational observations seen at WTW during periods of high organic load. Previous experimental work in this area has been limited but flocs in

sludges have been seen to decrease in size when humic acid was added to a synthetic water with a commensurate decrease in density and a reduction in sludge dewaterability (Dulin and Knocke, 1989). NOM leads to the formation of smaller flocs when added to latex and iron oxide suspensions flocculated with ionic salts (Amal *et al.*, 1992; Walker and Bob, 2001), however there is a need for clearer elucidation of the impact of carbon on floc properties for NOM coagulated with metal salts with an additional emphasis on structural characteristics during the solid-liquid separation phase.

The measurement of floc structural properties is now well established for all types of floc formed from activated sludge; kaolin, latex and other turbidity suspensions; and organic rich water sources (Gorczyca and Ganczarczyk, 1999; Lee and Liu, 2001; Wu *et al.*, 2002; Aguillar *et al.*, 2003). Using a range of techniques, the measurement of floc size, shape, settling velocity and strength can be made to provide quantification of floc properties as they change with different variables. The degree of floc compaction can also be measured through fractal dimension analysis. Since Mandlebrot introduced the concept of fractal theory in the 1970's, the application of fractal geometry is now a well established means of describing flocs (Gregory, 1997; Gorczyca and Ganczarczyk, 1999; Thomas *et al.*, 1999; Bushell *et al.*, 2002). Flocs are known as mass fractal objects given that the internal structure and surface of the floc exhibit fractal properties. Mass fractals show a relationship between their mass M, a characteristic measure of size L and the mass fractal dimension D_f:

$$M \propto L^{D_f} \qquad \text{Equation 5.1}$$

For Euclidean space filling objects, the one-dimensional value of D_f is 1 for a linear line, 2 for a two dimensional planar shape and 3 for a compact 3 dimensional shape (Waite, 1999). Fractal objects have non-integer values of D_f and therefore show non-Euclidean dimensionality. In addition to providing useful information of differences in floc settling rates, sedimentation is a well established means of determining floc fractal dimension (Li and Ganczarczyk, 1986; Lee *et al.*, 1996; Chu *et al.*, 2004). For the purposes of determining floc fractal dimension from settling data, the fractal value (D_f) is related to floc diameter (d) and the terminal settling velocity (v_s) by:

$$v_t \propto d^{D_f - 1} \qquad \text{Equation 5.2}$$

A log-log plot of settling velocity against floc diameter yields a straight line with a slope of $D_f - 1$.

The overall objectives of this paper were to investigate how floc structural properties such as size, strength, settling rate and fractal dimension changed with increasing coagulant:NOM ratio to provide a possible explanation for the operational problems seen at WTW during periods of elevated carbon loading.

5.2 Materials and Methods

5.2.1 Coagulation tests

All experiments were carried out on raw water collected from a reservoir source in Yorkshire in the north of England with general water characteristics as shown in Table 5.1 along with the method of measurement. Coagulation experiments were carried out on a PB-900 variable speed jar tester (Phipps and Bird, Virginia, USA) with 76 x 25 mm flat paddle impellers using cylindrical jars containing 1 L samples of water. Two speeds were used with a rapid mix at 200 revolutions per minute (rpm) for 1.5 minutes followed by a slow stir phase at 30 rpm for 15 minutes followed by a 10 minute settling time. A ferric sulphate based coagulant (Ferripol XL – Huntsman Tioxide Europe Ltd, Billingham, UK) was used for all coagulation experiments from a 10 % w/v stock solution as ferric sulphate.

Table 5.1 Raw water characteristics and methods of measurement.

Characteristic	Value	How measured
Dissolved organic carbon (DOC)	7.6 mg L^{-1}	Pre-filtered sample measured on a Shimadzu TOC-5000A analyser
Ultra violet light absorption at 254 nm (UV_{254})	0.361 cm^{-1}	Pre-filtered sample measured on a Jenway 6505 UV/Vis spectrophotometer at 254 nm
Turbidity	2.6 NTU	Hach 2100N turbidimeter
Alkalinity	~ 10 mg L^{-1} as $CaCO_3$	Acid titration with bromocresol green/methyl red indicator
Conductivity	60 μS cm^{-1}	Jenway 4010 conductivity meter

Initially, coagulation optimisation tests were performed to ascertain the optimum pH range for organic removal and turbidity residual. Laboratory grade 1 M NaOH and 1 M HCl (Fisher Scientific UK, Loughborough) were used for pH adjustment. During this stage UV_{254} removal was used as an indicator of NOM removal due to the large number of samples generated during optimisation tests. This was justified given that UV_{254} has previously been shown to be a good indicator of the amount of NOM in a sample (Bolto *et al.*, 2002). After the initial optimisation tests, NOM concentration was additionally determined by measuring dissolved organic carbon (DOC).

Once the optimum pH conditions had been found floc diagnostic tests were carried out at six different DOC:Fe ratios (mg:mg). Throughout the remainder of the article the ratios are referred to as the amount of DOC in solution per mg of Fe added as a coagulant, for example a DOC:Fe ratio of 0.33 refers to 0.33 mg of DOC to 1 mg of Fe. DOC:Fe ratios of between 0 and 4 were investigated (the DOC:Fe ratio of 0 refers to a control experiment carried out on a de-ionised (DI) water solution). To achieve a near one to one ratio, 8 mg L^{-1} as Fe was added to the raw water and flocs were formed at the pH found in the optimisation study. In order to achieve the other DOC:Fe ratios two approaches were taken. Firstly, for low DOC:Fe ratios, raw water was diluted and a fixed coagulant concentration of 8 mg L^{-1} was dosed whilst maintaining a constant coagulation pH. Dilution was achieved by the addition of de-ionised water to raw water. Two dilutions were prepared at 6.0 mg L^{-1} and 2.5 mg L^{-1} DOC. The alkalinity of the diluted waters was raised to the original raw water value of approximately 10 mg L^{-1} as $CaCO_3$ by the addition of $NaHCO_3$ and similarly the conductivity was then raised to near the original value by addition of NaCl. The turbidity of the diluted waters was found to remain close to the original value of 2.6. The second approach was to reduce the coagulant dose in order to achieve high DOC:Fe ratios. Fe concentrations of 2 and 4 mg L^{-1} were dosed at constant pH. For the control solution, de-ionised water of a similar alkalinity and conductivity was prepared. 8 mg L^{-1} of Fe was added in order to form ferric hydroxide precipitate flocs in the absence of organic material. Charge of the raw water and coagulated suspensions was measured using a Zetasizer 2000 HAS (Malvern Instruments, Malvern, UK). The residual UV_{254} and DOC and settled turbidity were measured as before for each of the DOC:Fe ratios. In addition, the dry floc mass was measured by passing 1 L of coagulated sample through a pre-dried and weighed 0.45 mm fibre-

glass filter papers. This was then dried in an oven for 24 hours prior to subsequent weighing.

5.2.2 Floc size and breakage

Floc size and breakage experiments were performed using a similar experimental set-up to Spicer *et al.* (1998) and Biggs and Lant (2000). Briefly, coagulation tests were carried out on a jar tester as before however after the slow stir phase the effect of increased shear was investigated by increasing the rpm on the jar tester for a further 15 minutes. Separate experiments were carried out and repeated 3 times for rpm of 30, 40, 50, 75, 100, 150 and 200. Dynamic floc size was measured during growth and breakage of the flocs using a laser diffraction instrument (Malvern Mastersizer 2000, Malvern, UK). The suspension was monitored by drawing water through the optical unit of the Mastersizer and back into the jar by a peristaltic pump on the return tube using 5 mm internal diameter peristaltic pump tubing at a flow rate of 1.5 L hr^{-1}. Size measurements were taken every minute for the duration of the jar test and logged onto a PC.

5.2.3 Floc settling rate, fractal dimension and microscopy

The settling column apparatus consisted of a central settling column enclosed by a water bath to avoid thermal currents disrupting floc settlement. The water bath was connected to a ThermoHaake K10 heat-refrigerated circulator (Hakke, Germany) to maintain a temperature of 21 – 22 °C. The settling column was filled with de-ionised water and left to reach the required temperature. A period of 2 hours was left for quiescent conditions to be reached and the temperature to stabilise. Floc aggregates were introduced into the settling column via a tapered entry port to ensure the flocs settled into the centre of the column using a wide mouthed pipette. Floc images were captured using a CV M90 colour close-coupled device (CCD) camera (JAI UK Ltd, England). Image analysis software (Image Pro Plus from Media Cybernetics, Maryland, USA) was used to determine floc settling velocity.

Flocs were aggregated on a jar tester under the required conditions at room temperature (21-22° C). Flocs were then carefully removed from the jar using a wide mouthed pipette and re-suspended in de-ionised water held in a water bath at 21-22° C for dilution and temperature control of the flocs. Flocs were then introduced into the

settling column. Visual observation showed that little change in floc macrostructure occurred using the pipettes, however if flocs were observed to break during the transfer procedure then they were discarded. Using the described protocol ensured that flocs were able to settle in relative isolation of one another to prevent hindered settling effects.

As a focused floc passed in front of the camera, the image grabber was manually triggered to take a series of 5 images. The image analysis software was previously calibrated using a microscope graticule. The time between each frame was set at 1 second. This meant that the distance travelled by the floc could be calculated per frame and therefore per time period, thus giving a settling velocity. The projected area of the floc presented in front of the camera was determined using the image analysis software and converted to an equivalent diameter. This standardised diameter was recorded along with its settling velocity for approximately 100 aggregates for each set of coagulation conditions.

Floc structural characteristics were further investigated using an Olympus BHB light microscope (Olympus European, Hamburg, Germany) and the previously described image-analysis software (calibrated using a microscope graticule). Flocs were placed in an adapted microscope slide consisting of glass slide base with a raised rubber border with a depth of 3 mm to provide a well to contain whole flocs.

5.3 Results

5.3.1 Coagulation tests

Preliminary optimisation tests across a range of pH for a coagulant dose of 8 mg L^{-1} showed that for the iron based coagulant used in this study a pH of between 4 and 4.75 gave a combined optimum for NOM removal and residual turbidity after settlement (Figure 5.1). It was therefore decided to control the pH around 4.5 for all subsequent floc experiments. This pH also corresponds to the operational pH as used by the WTW from where the water was abstracted. As the DOC:Fe ratio changed a number of significant changes in the coagulated suspensions were observed (Table 5.2). The residual DOC remained around 1 mg L^{-1} for all of the treated waters whilst the UV_{254} was seen to increase from 0.01 to 0.06 cm^{-1} from DOC:Fe ratios of 0.33 to

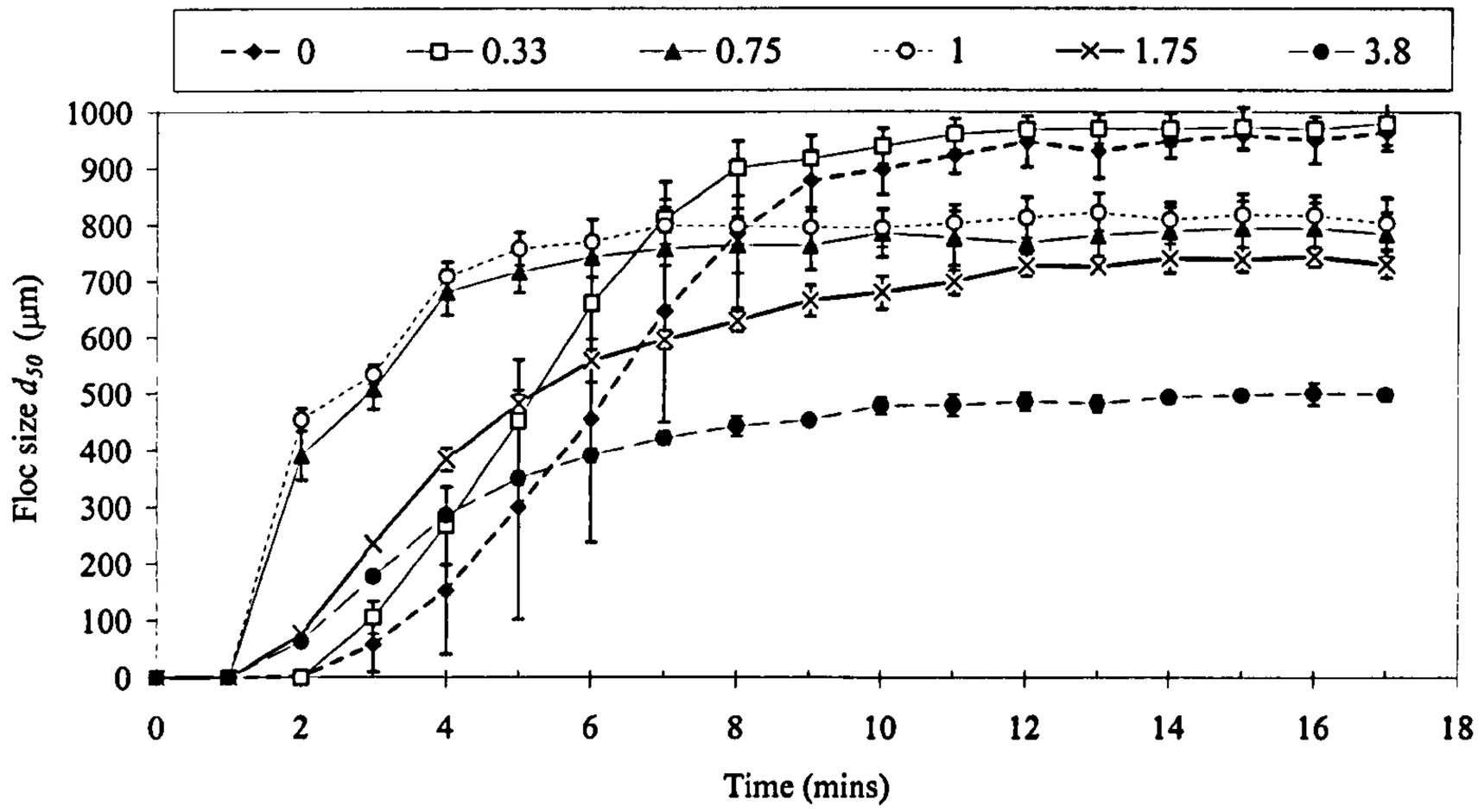

Figure 5.3 The growth rates of flocs for each of the different DOC:Fe ratios.

5.3.3 Settling and fractals

The settling rates for each of the DOC:Fe ratios are shown in Figure 5.4. The first point of note is a general decrease in the settling rate of similar sized flocs as the DOC fraction increases. For example, the settling rate of a floc of 1000 μm in equivalent diameter was around 1000 μm s^{-1} for the 0 and 0.33 ratio flocs whilst at higher DOC ratios of 1.75 and 3.8 the settling rate was around 600 μm s^{-1}. The improved settling rate of flocs with lower DOC content was further supported by a decrease in the settled turbidity at lower DOC:Fe ratios (Table 5.2). Secondly, there was a general reduction in the slopes of the data with increasing DOC proportion. This was confirmed by calculation of the floc fractal dimension. Model two reduced major axis regression was used to calculate the slopes of the lines through the data. There was good linear correlation for all of the data sets with R^2 values between 0.73-0.93. From these slopes D_f was calculated which confirmed a general tendency for D_f to decrease with increasing DOC fraction with the fractal dimension decreasing from 2.20 ± 0.04 to 1.78 ± 0.04 from the lowest to highest DOC:Fe ratio (Figure 5.5). A statistical comparison of the values of the slopes showed that there were statistical differences (two-tailed t-test, 190 df, P = 0.01) between the slope of 0 (Fe precipitate) and all of the slopes at and above ratios of 1. Further significant differences were seen between ratios of 0.33 and 3.8; 0.33 and 1.75; 0.75 and 3.8; 0.75 and 1.75.

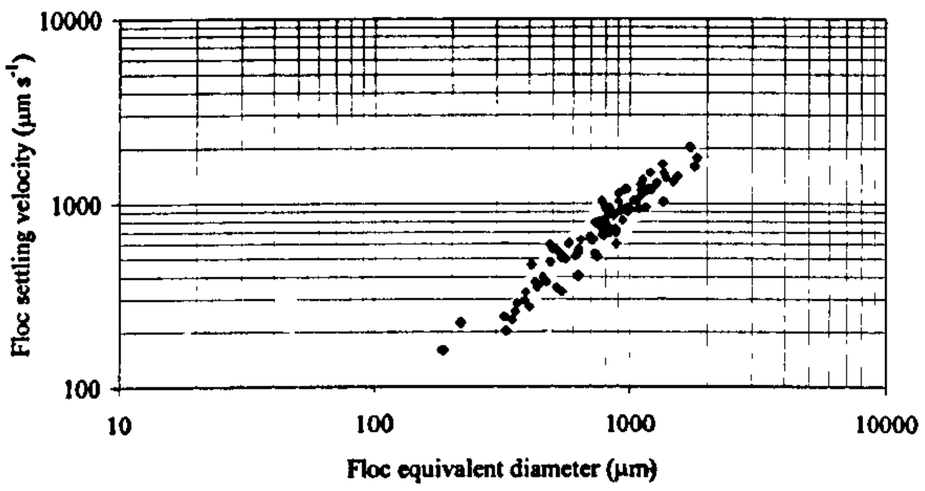

Ratio: 0 (Precipitate)

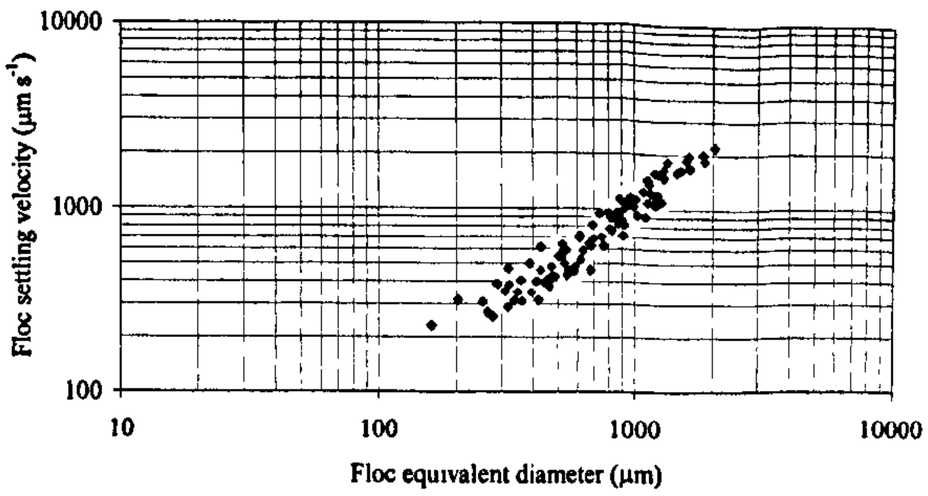

Ratio: 0.33

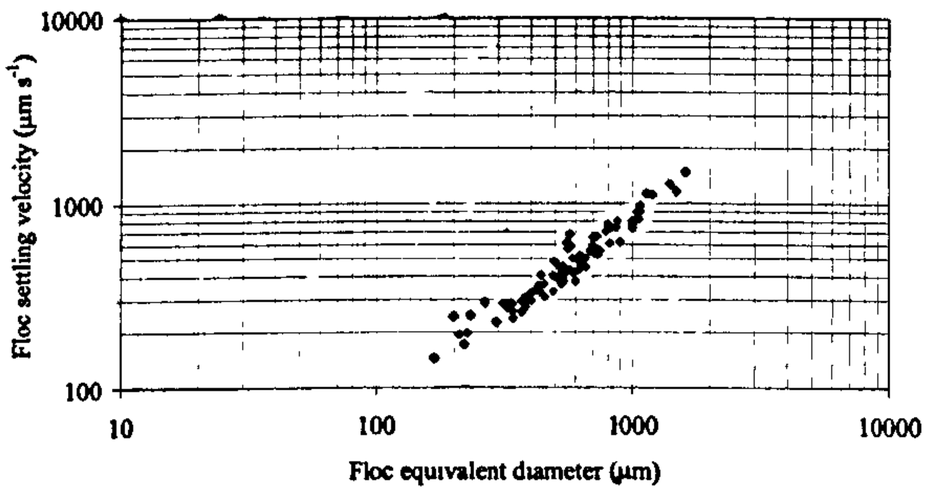

Ratio: 0.75

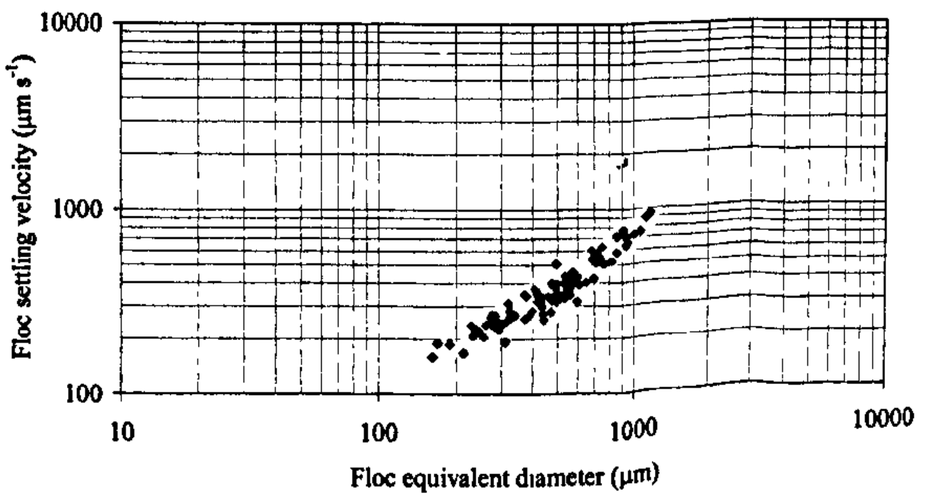

Ratio: 1

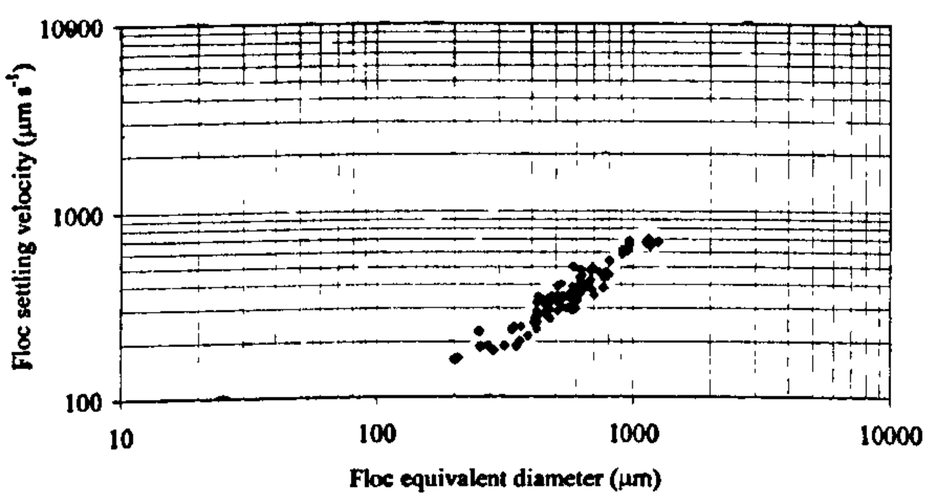

Ratio: 1.75

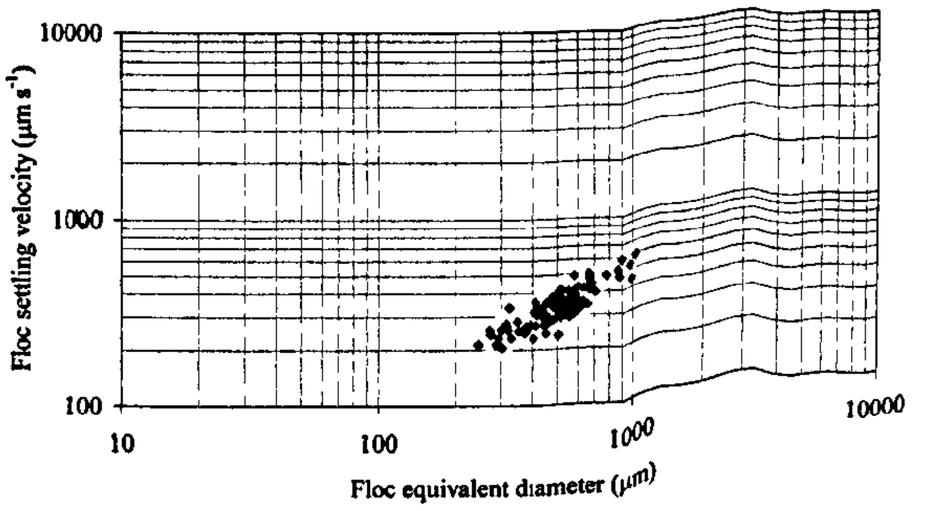

Ratio: 3.8

Figure 5.4 The settling rates of flocs for each of the different DOC:Fe ratios.

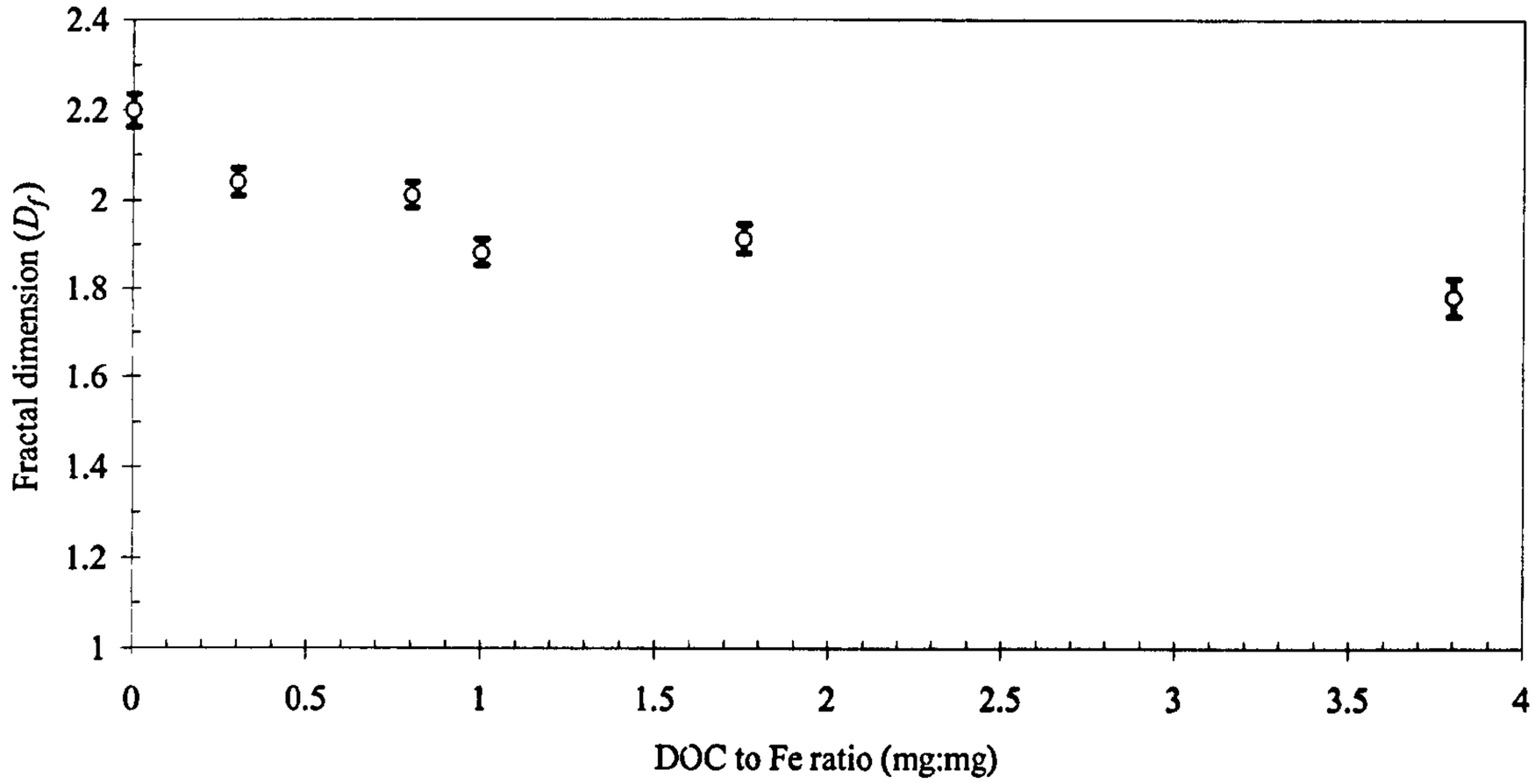

Figure 5.5 The change in fractal dimension (D_f) with increasing DOC:Fe ratio (with standard error bars).

5.3.4 Floc breakage

After the flocs had reached their steady state size during the slow stir period, they were exposed to increased shear. A comparison of the type of breakage profiles seen for flocs of an initial large size (low DOC:Fe ratio) and an initial small size (high DOC:Fe ratio) are shown in Figure 5.6. At rpm of 75 and above, there was a characteristic large scale drop in floc size immediately after the introduction of increased shear followed by a more gradual decline as the flocs approach a steady state. At lower rpm, the change in floc size follows a steadier decline in floc size. The extent of floc breakage was greater for the flocs of a low DOC:Fe ratio. For example, at 200 rpm the change in floc size after 15 minutes exposure to high shear was around 800 μm for the larger flocs whilst it was only 300 μm for the initially smaller flocs.

The response of the different DOC:Fe ratios to increases in shear were quite different (Figure 5.7). When the floc size after 15 minutes exposure to shear was plotted against rpm a straight line could be drawn through the data on a log-log scale (Figure 5.7a). It was apparent that in the absence of NOM the flocs did not change size at 50 rpm and below, however as the rpm was subsequently increased the linear relationship was then seen and subsequently changed size rapidly with increasing rpm dropping from 1000 μm to 250 μm. This was reflected by the value of the slope (-1.17). The next largest flocs (at a ratio of 0.33) decreased in size at a similarly high

rate as indicated by the slope value of -0.90. For the flocs at higher DOC:Fe ratios (and smaller floc size) the slopes were less steep and varied between -0.53 and -0.65.

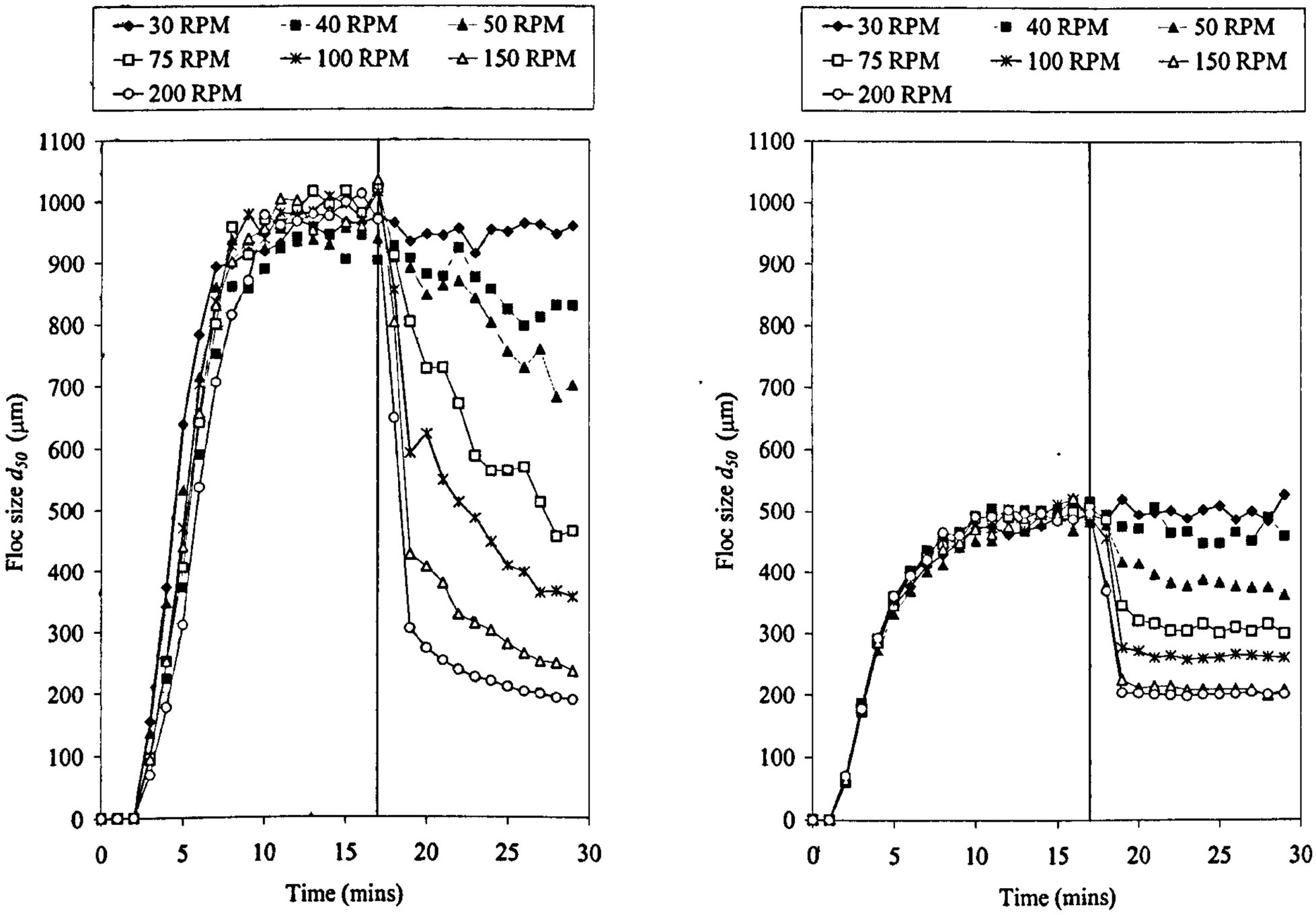

a) Low DOC:Fe ratio (0.33) b) High DOC:Fe ratio (3.8)

Figure 5.6 Typical breakage profiles for a low and high DOC:Fe ratio with increasing rpm. The line indicates the point at which high shear was introduced.

The floc systems that showed a significant difference in fractal dimension from one another also showed differences in their breakage behaviour (Figure 5.7b). It was apparent that the broken size of the flocs with a higher fractal dimension were larger than flocs with a significantly lower fractal dimension at increased shear between 30-100 rpm. For example between 30-150 rpm the 0 ratio flocs (high fractal dimension) were over 200 µm larger than the 1, 1.75 and 3.8 ratio flocs (low fractal dimension). The exception to this being when the flocs approached common values at very high shear between 150 and 200 rpm.

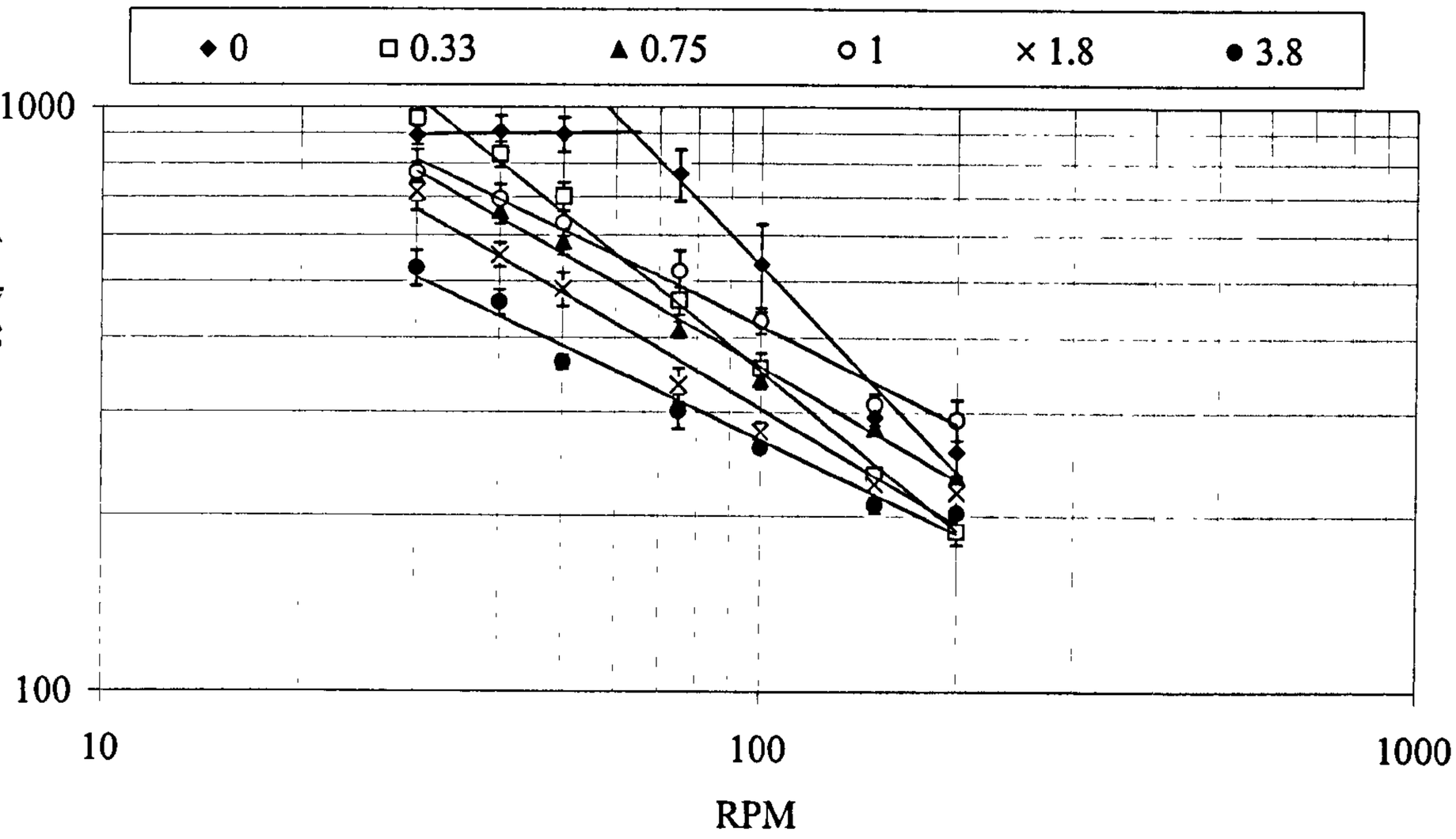

a) Floc breakage rates with increasing rpm for all the DOC:Fe ratios

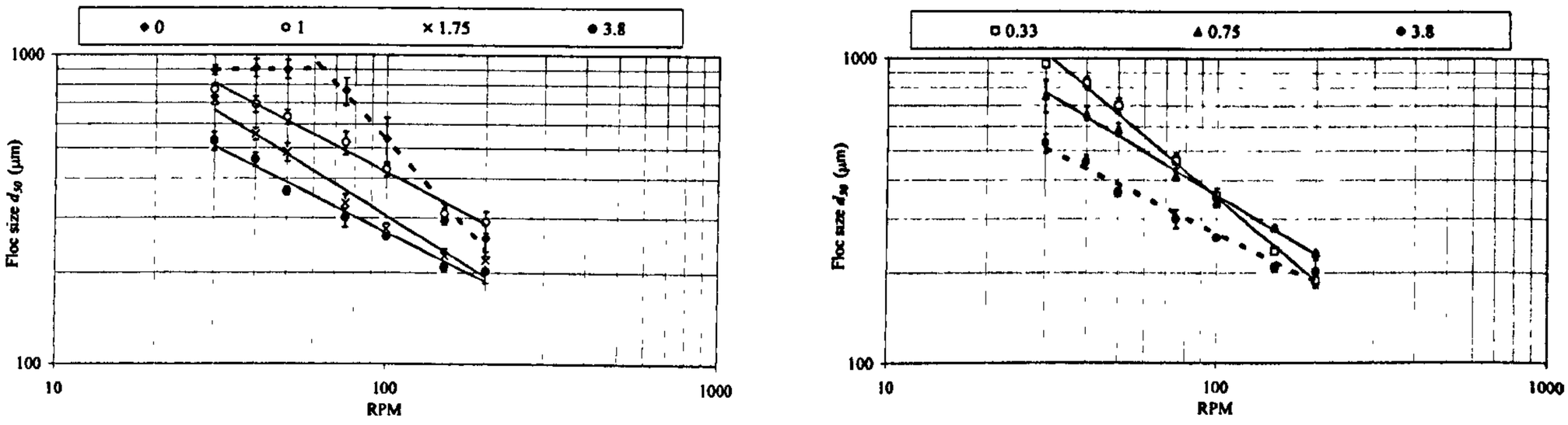

b) floc breakage rates for flocs with significantly different fractal dimensions. The heavy dashed line shows the data which has a significantly different fractal dimension from the other data.

Figure 5.7 The steady state breakage size with increasing rpm for different DOC:Fe ratios.

5.3.5 Microscopy

Typical floc images for each of the coagulant to organic ratios are shown in Figure 5.8. From a qualitative analysis of these images it can be seen that in the absence of NOM and at a DOC:Fe ratio of 0.33 the flocs appeared more solidly composed with fewer internal pores and softer edges. As the DOC fraction increases the flocs have more variation in density.

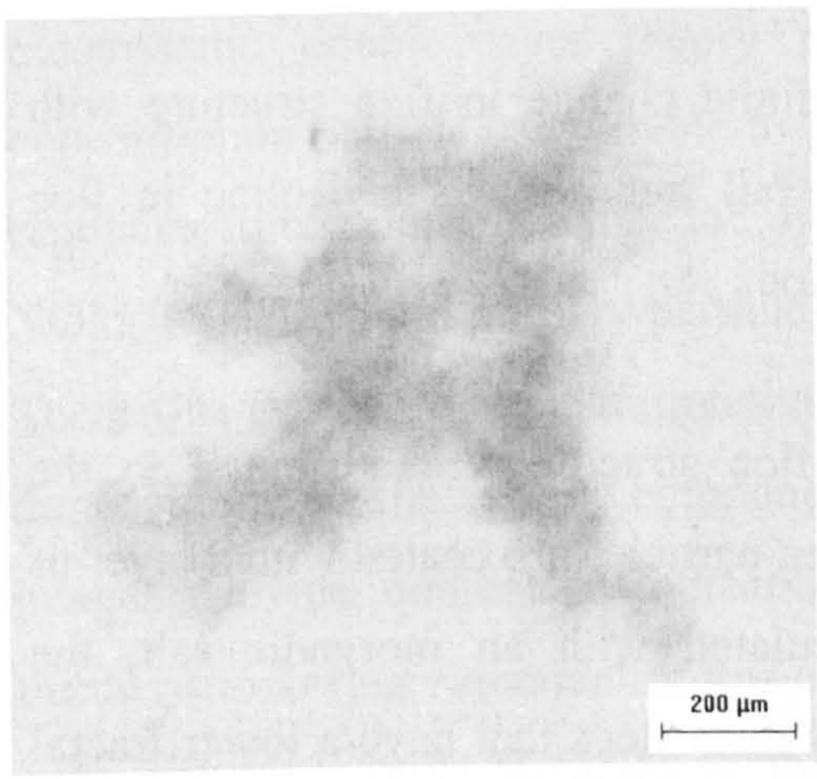

Ratio: 0 (Fe Precipitate)

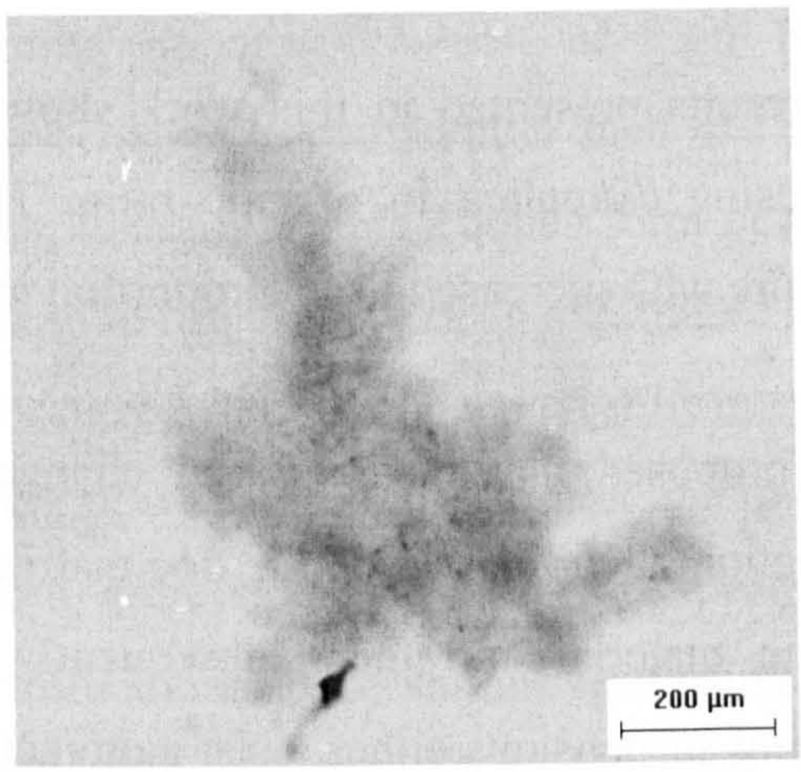

Ratio: 0.33

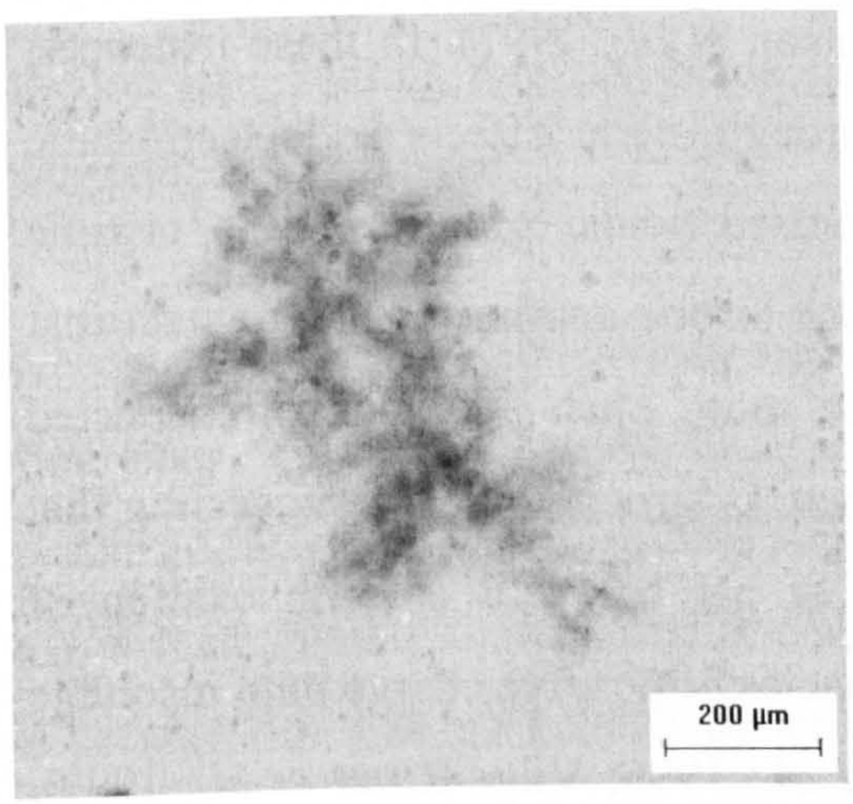

Ratio: 0.75

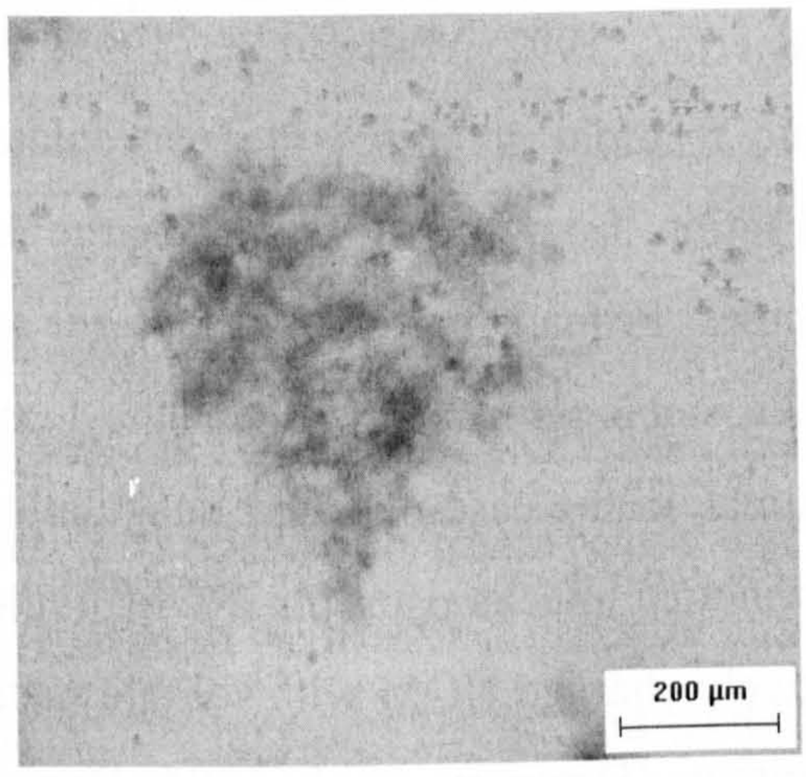

Ratio: 1

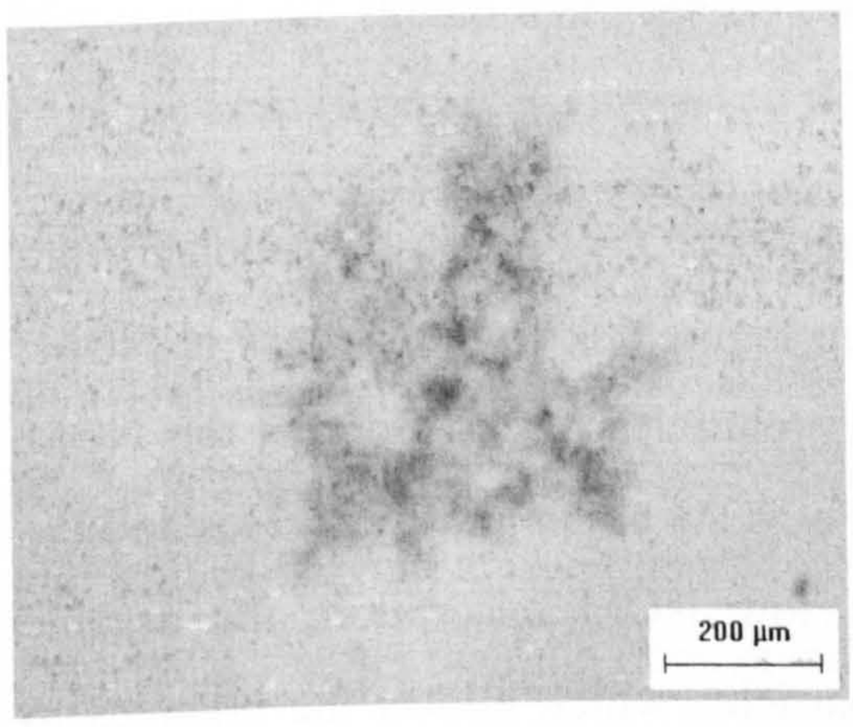

Ratio: 1.75

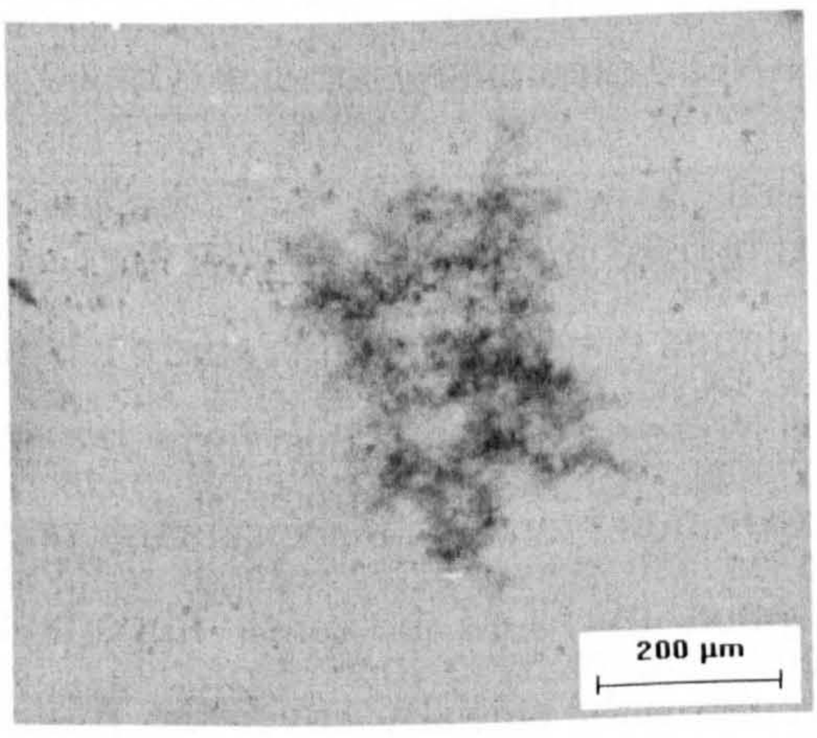

Ratio: 3.8

Figure 5.8 Microscope images of typical flocs from each of the different DOC:Fe ratios.

5.4 Discussion

The results presented in this work show a definite change in floc structure with decreasing coagulant to organic ratio. The overall trend shows a decline in floc structure with increased DOC proportion in the floc.

It is proposed that the observed changes in floc structure are attributed to the interaction of carbon within the floc matrix. When particles are coated with a layer of organic material and then subsequently flocculated with an inorganic salt, the resulting suspensions either resist aggregation or form flocs that have a lower fractal dimension than particle suspensions flocculated in the absence of organic matter (Amal *et al.*, 1992; Waite *et al.*, 1993; Wilkinson *et al.*, 1997). In these instances, organic material stabilises the particulates through steric effects and electrostatic stabilisation from the negative charge on ionised acidic groups on the organic molecules. Primary particles cannot get as close to one another as before such that they do not aggregate at all or they produce more open and loosely connected structures. In the case of NOM coagulation, there is strong evidence suggesting that the principal mechanism for NOM removal at pH below 6 is complexation of negatively charged NOM with soluble metal species of positive charge onto insoluble precipitates (Dempsey *et al.*, 1984; Dennett *et al.*, 1996; Vilge-Ritter *et al.*, 1999). The further removal of NOM in solution subsequently occurs by adsorption onto metal-NOM precipitate particles (Gregor *et al.*, 1997).

The proposed mechanistic model for the impact of NOM on floc formation for the coagulation conditions of this study is shown in Figure 5.9. In the absence of NOM, ferric hydroxide precipitates form the primary particles of the floc, as the NOM concentration increases the formation rate of Fe-NOM precipitates increases and the adsorption of NOM becomes important. At low NOM adsorption, the organic molecules only partially cover the primary particles which allows the organics to attach to individual particles at numerous sites. At higher NOM concentration increased adsorption of organics prevents this and lateral interactions between organics results in large portions of the molecules sticking out into the solution forming micelle type structures (Amal *et al.*, 1992). During further agglomeration, primary particles at low NOM concentration are able to get close enough to each

other for strong attractive bonds in the primary energy zone of classical DLVO electrostatic double layer theory to become important, whilst at high NOM concentration particles are unable to get close enough to one another such that steric repulsive forces dominate the floc properties. Instead, bridging bonds form between NOM molecules and primary particles which give rise to more open and fragile flocs. There was a strong demonstration that this occurred from the observed shift in fractal dimension when the organic component in the floc was high. In addition, microscope images provide qualitative indication that a more open structure was produced. Further supporting evidence for this comes from similar observations seen using solid latex and iron oxide particles in the presence of humic acid (Amal *et al.*, 1992; Walker and Bob, 2001). This mechanistic model provides an explanation for changes in floc size, settling rate and breakage behaviour of Fe-NOM flocs, which will be subsequently discussed.

Across the range of ratios investigated a reduction of 500 μm was seen in the median floc sizes. This initial steady state size is a good indicator of floc strength. Both Bache and Papavasilopoulos (2003) and Yukselen and Gregory (2004) show that for a given shear condition, increased floc size is as a result of increased floc strength. This is because floc size is a balance between growth and breakage (Biggs and Lant, 2000). Larger flocs must therefore have higher resistance to breakage in order to reach a bigger size and should therefore be considered stronger. This gives flocs with a low DOC:Fe ratio (0 and 0.33) increased floc strength over the 0.75, 1 and 1.75 ratio flocs, which in turn were stronger than the 3.8 ratio flocs. The decrease in floc size with increasing organic content in the floc agrees with work carried out on sludge characterization by Dulin and Knocke (1989). The average diameter of flocs in the sludge increased from 10 to 15μm when comparing flocs formed from raw water with and without humic acid. It should be noted that the floc sizes were one order of magnitude smaller than the flocs investigated in this study. however, in this example, it was the microfloc (small clusters of primary particles) size that was being measured from the sludge samples. It therefore seems that the bridging bonds formed when the organic fraction in the floc is high gives rise to weak flocs, whereas when the particles are able to get close to one another at low carbon fraction strong and large flocs form.

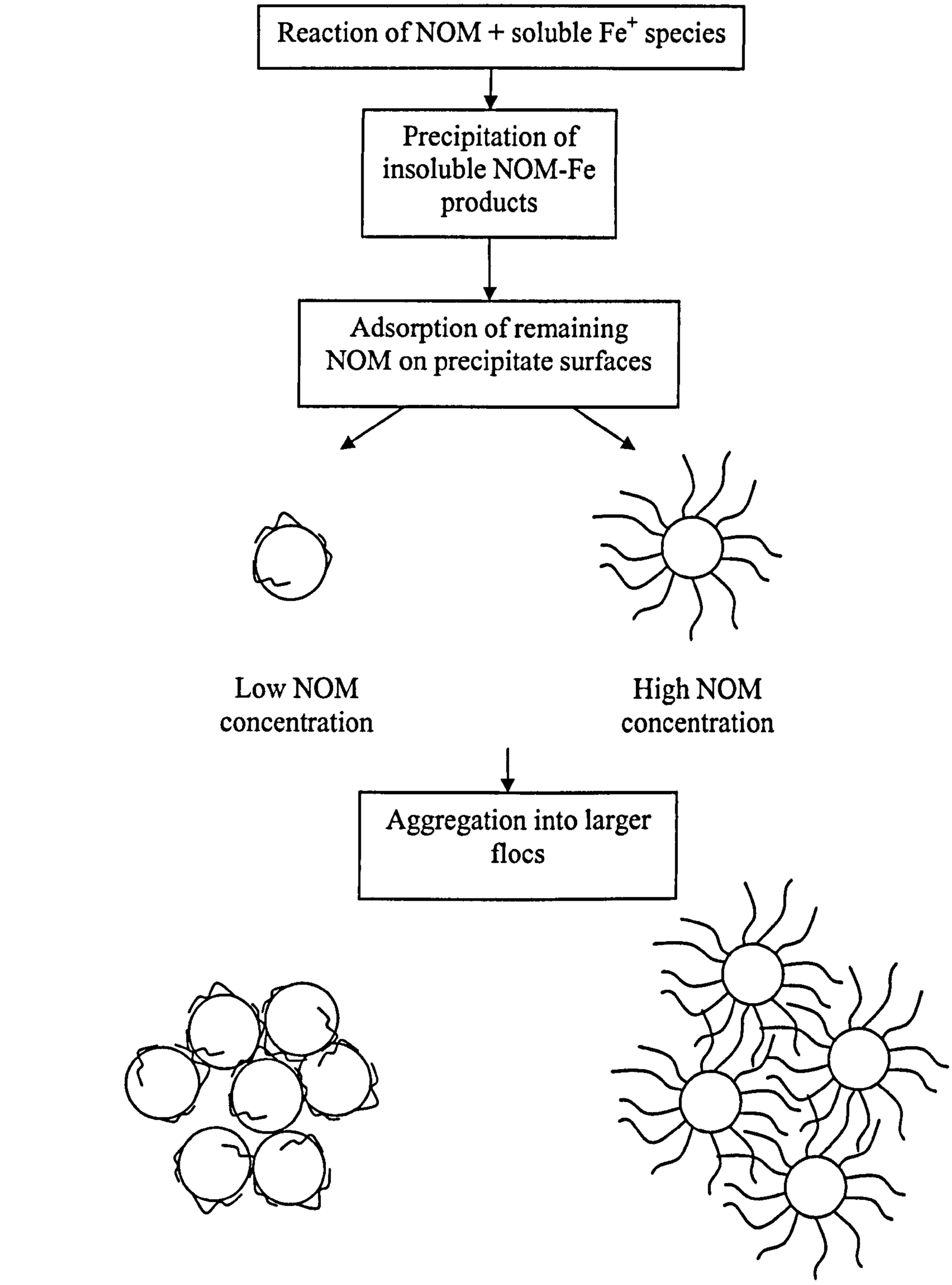

Figure 5.9 The proposed model for the formation of flocs at low and high DOC:Fe ratios.

An interesting point of note was that there was no clear relationship between zeta potential and the floc properties and it therefore seemed that the increased separation distance given by the previously described steric impact of adsorbed NOM seemed to dominate the resulting floc structure.

The impact of NOM on floc settling appeared to have two effects. Firstly there was the described change in fractal dimension and secondly there was a change in settling rate. The range of settling rates for the flocs under investigation show comparatively lower settling rates to turbidity dominated flocs but similar values to activated sludge flocs. The settling range of the flocs in this study and activated sludge flocs is 100-2000 μm s^{-1} (Li and Ganczarczyk, 1986; Wu and Lee, 1998) whilst similar sized kaolin flocs have a range up to 10,000 μm s^{-1} (Wu *et al.*, 2002). This is obviously as a result of turbidity particles in the floc giving increased floc density (kaolin dry solid density = 2600 kg m^{-3}), whilst both activated sludge flocs and NOM flocs have a high organic content which is of a lower density (humic acid dry solid density = 1750 kg m^{-3} (Hossain and Bache, 1991). The density of the Fe-organic material in the flocs is difficult to accurately establish, particularly the organic component which consists of a heterogeneous mix of molecules. However, an indication of the reduction in density with increasing organic fraction for the Fe-NOM flocs can be found from floc effective density. The effective density of flocs can be estimated from:

$$v_s = \frac{(\rho_f)gd^2}{18\mu} \qquad \text{Equation 5.3}$$

v_s is the terminal settling velocity (m s^{-1}), ρ_f is the floc effective density (kg m^{-3}), d is the floc diameter (m), μ is the dynamic viscosity of the suspending medium (m s^{-1}) and g is acceleration due to gravity (m s^{-1}).

The assumption that Stokes law can apply to irregularly shaped and porous flocs is open to some debate, but the application to flocs is widespread (Bache *et al.*, 1991; Gregory, 1997; Tang *et al.*, 2002) and provides a useful relative comparison. The effective density in the absence of NOM (0 ratio) for a floc of 1000 μm in diameter was ~1.8 kg m^{-3}, whilst this decreased to ~1.0 kg m^{-3} as the DOC fraction increased to a ratio of 3.8. Complex analysis of the dry solids in alum-humic flocs confirms this density reduction in other metal-organic floc systems where an approximation of 2000 kg m^{-3} has been cited as the density of the solid in alum-humic flocs (Hossain

and Bache, 1991), with the density of aluminium hydroxide being around 2500 kg m^{-3} (Bache, 2004).

The floc breakage behaviour was more difficult to interpret given the spread and cross over of the data. However, when the breakage profiles were separated into those flocs that showed significant differences in fractal dimension from one another some more clear trends were seen. Smaller flocs generally do not break to the same extent as larger flocs given that larger flocs become more affected by the microscale eddies that are attributed to floc breakage. At small sizes, flocs are more likely to become entrained within eddies rather than be broken by them (Parker *et al.*, 1972). This explains why large flocs break more extensively and shows how the breakage with increasing shear gives a confusing indication of how strong flocs are. However, the underlying broken floc size of the high fractal flocs were not as small as the low fractal and high organic content flocs. Given the previous definition of floc strength being related to increased floc size for a given shear, it therefore appears that the lower fractal flocs have reduced strength, confirming that increased organic carbon in the floc reduces floc strength. The exception to this being at high shear of 150 and 200 rpm when the broken floc sizes tend to converge on a common median value of between 200-300 μm as the high applied energy is greater than the internal bonding of even the strongest flocs. This is likely to be a convergence on a similar sized broken floc particle size.

The operational significance of the results suggests that the ratio of DOC:Fe is very important for the resulting floc structure. In the past, the main focus of attention has been getting the coagulant dose correct for NOM removal. However, the present study has identified that adding coagulant at a low dose can still give rise to good NOM removals, but give comparatively poor floc structure in terms of reduced floc size, settling rate, fractal dimension and strength. The broken floc size is of particular importance during solid-liquid separation because if small increases in shear during WTW unit processes give rise to floc breakage then downstream systems will be challenged by smaller particles. Reduced floc sizes give rise to lower sedimentation rates (Aguillar *et al.*, 2003) and reduces particle transport mechanisms during removal in filtration because particle capture is compromised by smaller particles (Cleasby,

1999). This can be seen by inspection of the single collector model for interception during filtration (from Cleasby, 1999):

$$\eta_I = \frac{3}{2}\left(\frac{d_p}{d_c}\right)^2 \qquad \text{Equation 5.4}$$

η_I is the filtration interception transport, d_c is the collector diameter (m) and d_p is the diameter of the particle being filtered (m).

An increase in d_p for a constant d_c will give rise to increased interception during filtration (η_I) (the only exception to this being when diffusive transport mechanisms dominate for particles < 1 μm). It is the low fractal and high DOC:Fe ratio flocs that results in small and weak aggregates that settle slower and will be filtered less efficiently. For the Fe based coagulant used in this study, it appears that coagulant doses at and above a 1:1 ratio gives rise to improved floc structure.

5.5 Conclusions

Using a range of diagnostic techniques, the impact of NOM was seen to significantly impact on floc structure. As the fraction of organic carbon in the floc matrix increased there was a significant decrease in floc size, settling rate, strength and degree of compaction. A model has been proposed to explain the results where the adsorption of NOM onto coagulant-NOM precipitates is responsible for the changes in floc character. At high NOM concentrations, bridging between primary particles gave rise to loose, open and weak floc structures, whereas at low NOM concentrations and in the absence of NOM, primary particles are able to get close enough to form strong interparticle bonds and large strong structures.

Acknowledgements

The submitted manuscript has been made possible through funding from American Water Works Association Research Foundation and Co-funding Utilities. The information contained herein is based upon Intellectual Property which is jointly owned by Cranfield University and the Foundation. The Foundation retains its right to publish or produce the Jointly Owned Intellectual Property in part or in its entirety. The authors would also like to thank the EPSRC, Fort Collins Water, Scottish Water, Severn Trent Water, Thames Water, United Utilities and Yorkshire Water.

5.6 References

Aguilar, M. I., Saez, J., Llorens, M., Soler, A. and Ortuno, J. F. (2003) Microscopic Observation of Particle Reduction in Slaughterhouse Wastewater by Coagulation-Flocculation Using Ferric Sulphate as Coagulant and Different Coagulant Aids. *Water Research* **37** 2233-2241.

Amal, R., Raper, J. A., and Waite, T. D. (1992) Effect of Fulvic Acid Adsorption on the Aggregation Kinetics and Structure of Hematite Particles. *Journal of Colloid and Interface Science* **151** (1), 244-257.

Bache, D. H. (2004). Floc Rupture and Turbulence: a Framework for Analysis. *Chemical Engineering Science* **59** 2521-2534.

Bache, D. H. and Papavasilopoulos, E. N. (2003) Dewatering of Alumino-Humic Sludge: Impacts of Hydroxide. *Water Research* **37** 3289-3298.

Bache, D. H., Hossain, M. D., Al-Ani, S. H., and Jackson, P. J. (1991) Optimum Coagulation Conditions for a Coloured Water in Terms of Floc Size, Density and Strength. *Aqua Journal of Water Supply: Research Technology* **9** 93-102.

Biggs, C. A. and Lant, P. A. (2000) Activated Sludge Flocculation: On-Line Determination of Floc Size and the Effect of Shear. *Water Research* **34** 2542-2550.

Bolto, B., Dixon, D., Eldridge, R. and King, S. (2002) Removal of THM precursors by coagulation or ion exchange. *Water Research* **36** 5066-5073.

Bushell, G. C., Yan, Y. D., Woodfield, D., Raper, J., and Amal, R. (2002) On Techniques for the Measurement of the Mass Fractal Dimension of Aggregates. *Advances in Colloid and Interface Science* **95** 1-50.

Cheng, W. P. and Chi, F. H. (2002) A Study of Coagulation Mechanisms of Polyferric Sulfate Reacting with Humic Acid Using a Fluorescence-quenching Method. *Water Research* **36** 4433-4666.

Chu, C. P., Lee D. J. and Peng, X. F. (2004) Structure of Conditioned Sludge Flocs. *Water Research* **38** 2125-2134.

Cleasby, J. L. (1999) Filtration. In: *American Water Works Association Water Quality and Treatment: a Handbook of Community Suppliers*. McGraw-Hill, New York.

Dempsey, B. A., Ganho, R. M., and O'Melia, C. R. (1984) The Coagulation of Humic Substances by Means of Aluminium Salts. *Journal of the American Water Works Association* **76** (4), 141-150.

Dennett, K. E., Amirtarajah, A., Moran, T. F., and Gould, J. P. (1996) Coagulation: its Effect on Organic Matter. *Journal of the American Water Works Association* **88** 129-142.

Dulin, B. E. and Knocke, W. R. (1989) The Impact of Incorporated Organic Matter on the Dewatering Characteristics of Aluminium Hydroxide Sludges. *Journal of the American Water Works Association* **81** (5), 74-79.

EC Drinking Water Directive (1998) – 98/83/EC.

Eikkibrook, B. (1999) Coagulation-Direct Filtration of Soft, Low Alkalinity Humic Waters. *Water Science and Technology* **40** (9), 55-62.

Fearing, D. A., Banks, J., Guyetand, S., Eroles, C. M., Jefferson, B., Wilson, D., Hillis, P., Campbell, A. T. and Parsons, S. A. (2004) Combination of Ferric and MIEX® for the treatment of humic rich waters. *Water Research* **38** 2551-2558.

Gibbons, J. and Laha, S. (1999) Water Purification Systems: a Comparative Analysis Based on the Occurrence of Disinfection By-Products. *Environmental Pollution* **106** (3), 425-428.

Gorczyca, B. and Ganczarczyk, J. (1999) Structure and Porosity of Alum Coagulation Flocs. *Water Quality Research Journal of Canada* **34** 653-666.

Goslan, E. H., Fearing, D. A., Banks, J., Wilson. D., Hillis, P., Campbell, A. T. and Parsons, S. A. (2002) Seasonal Variations in the Disinfection By-Product Precursor Profile of a Reservoir Water. *Aqua Journal of Water Supply: Research Technology* **51** 475-482.

Gregor, J. E., Nokes, C. J., and Fenton, E. (1997) Optimising Natural Organic Matter Removal from Low Turbidity Waters by Controlled pH Adjustment of Aluminium Coagulation. *Water Research* **31** 2949-2958.

Gregory, J. (1997) The Density of Particle Aggregates. *Water Science and Technology* **36** (4), 1-13.

Hossain, M. D. and Bache, D. H. (1991) Composition of Alum Flocs Derived from a Coloured, Low-Turbidity Water. *Aqua Journal of Water Supply: Research Technology* **40** (5), 298-303.

Hurst, A. M., Edwards, M. J., Chipps, M., Jefferson, B. and Parsons, S. A. (2004) The Impact of Rainstorm Events on Coagulation and Clarifier Performance in Potable Water Treatment. *Science of the Total Environment* **321** (1-3), 219-230.

Kaiser, K., Guggenberger, M., Kaupenjohann, M. and Zech, W. (2002) Refractory Organic Substances in Aggregated Forest Soils – Retention Verses Translocation. In: *Refractory Organic Substances in the Environment.* Wiley-VCH, Weinheim.

Lee, C. H. and Liu, J. C. (2001) Sludge Dewaterability and Floc Structure in Dual Polymer Conditioning. *Advances in Environmental Research* **5** 129-136.

Lee, D. J., Chen, G. W., Liao, Y. C. and Hsieh, C. C. (1996) On the Free-Settling Test for Estimating Activated Sludge Floc Density. *Water Research* **30** 541-550.

Li, D. H. and Ganczarczyk, J. J. (1986) Physical Characteristics of Activated Sludge Flocs. *CRC Critical Reviews in Environmental Control* **17** (1), 53-87.

Niskavaara, H., Reimann, C., Chekushin V. and Kashulina, G. (1997) Seasonal Variability of Total and Easily Leachable Element Contents in Topsoils (0–5 cm) from Eight Catchments in the European Arctic (Finland, Norway and Russia). *Environmental Pollution* **96** (2), 261-274.

Parker, D. S., Kaufman, W. J., and Jenkins, D (1972) Floc Breakup in Turbulent Flocculation Processes. *Journal of the Sanitary Engineering Division: Proceedings of the American Society of Civil Engineers* **SA 1** 79-99.

Spicer, P. T., Pratsinis, S. E., Raper, J., Amal, R., Bushell, G., and Meesters, G. (1998) Effect of Shear Schedule on Particle Size, Density and Structure During Flocculation in Stirred Tanks. *Powder Technology* **97** 26-34.

Tang, P., Greenwood, J. and Raper, J. A. (2002) A Model to Describe the Settling Behaviour of Fractal Aggregates. *Journal of Colloid and Interface Science* **247** 210-219.

Thomas, D. N., Judd, S. J., and Fawcett, N. (1999) Flocculation Modelling: A Review. *Water Research* **33** 1579-1592.

Vilgé-Ritter, A., Rose, J., Masion, A., Bottero J. -Y. and Lainé, J. -M. (1999) Chemistry and Structure of Aggregates Formed with Fe-salts and Natural Organic Matter. *Colloids and Surfaces A: Physicochemical and Engineering Aspects* **147** 297-308.

Waite, T. D. (1999) Measurement and Implications of Floc Structure in Water and Wastewater Treatment. *Colloids and Surfaces A: Physicochemical and Engineering Aspects* **151** 27-41.

Waite, T.D., Amal, R., Ngo, H., and Vigneswaran, S. (1993) Effects of Adsorbed Organic Matter on Size, Structure and Filterability of Iron Oxyhydroxide Flocs. *Water Science and Technology* **27** (11), 133-142.

Walker, H. W. and Bob, M. M. (2001) Stability of Particle Flocs Upon Addition of Natural Organic Matter Under Quiescent Conditions. *Water Research* **35** 875-882.

Wilkinson, K. J., Negre, J. C., and Buffle, J. (1997) Coagulation of Colloidal Material in Surface Waters: the Role of Natural Organic Matter. *Journal of Contaminant Hydrology* **26** 229-243.

Wilson, D. (2004), Personal Communication.

Wu, R. M. and Lee, D. J. (1998) Hydrodynamic Drag Force Exerted on a Moving Floc and its Implication to Free-Settling Tests. *Water Research* **32** 760-768.

Wu, R. M., Lee, D. J. Waite, T. D. and Guan, J. (2002) Multilevel Structure of Sludge Flocs. *Journal of Colloid and Interface Science* **252** 383-392.

Ying Y. D., Lei, D. and Wania F. (2004) Is Rain or Snow a more Efficient Scavenger of Organic Chemicals? *Atmospheric Environment* **38** 3557-3571.

Yukselen, M. A. and Gregory, J. (2004) The Reversibility of Floc Breakage. *International Journal of Mineral Processing* **73** 251-259.

CHAPTER 6

THE IMPACT ON FLOC STRUCTURE OF DIFFERENT TREATMENT OPTIONS:

6(A) FLOC STRUCTURAL CHARACTERISTICS USING CONVENTIONAL COAGULATION FOR A HIGH DOC, LOW ALKALINITY SURFACE WATER SOURCE

Submitted to *Water Research.*

6(B) THE IMPACT ON NOM FLOC SRUCTURE USING DIFFERENT TREATMENT OPTIONS

Submitted to the *Journal of the American Water Works Association.*

6(A) FLOC STRUCTURAL CHARACTERISTICS USING CONVENTIONAL COAGULATION FOR A HIGH DOC, LOW ALKALINITY SURFACE WATER SOURCE

PETER JARVIS, BRUCE JEFFERSON and SIMON A. PARSONS

School of Water Sciences, Building 39, Cranfield University, Cranfield, Bedford, MK40 0AL, United Kingdom.

Abstract

Removal of natural organic matter (NOM) is well established using metal salt coagulants. In addition, flocculant aids are also commonly used to improve solid removal. The objectives of this paper were to describe the impacts of both NOM and polymer on floc structure. The study offered a comparison of floc physical characteristics for coagulant precipitate flocs, organic-coagulant flocs and organic-coagulant-polymer flocs for optimum coagulant and polymer doses. A ferric sulphate based coagulant was used as the primary coagulant and the polymer selected was a high molecular weight (MW) cationic polydiallyldimethylammonium chloride (polyDADMAC). Floc size, breakage, re-growth and settling characteristics were measured. Precipitate flocs were larger than organic flocs and had better settling characteristics when compared to NOM-coagulant flocs. When polymer was added, floc size and compaction was seen to further reduce. An explanation was offered in terms of the mode of flocculation involved. Floc breakage behaviour showed that polymer reduced the rate of floc degradation but did not greatly improve floc re-growth potential after breakage, which was generally poor for all of the suspensions.

Key words

Floc breakage; fractal dimension; re-growth; settling velocity; strength

6(A).1 Introduction

The aggregation of fine particles and colloids into larger particles is a well established means of removing turbidity, colour and other organic and inorganic pollutants at water treatment works (WTW). These larger aggregates are known as flocs. Flocs may be defined as highly porous, irregularly shaped and loosely connected aggregates composed of smaller primary particles (Huang, 1994; Kim *et al.*, 2001). The size and structure of flocs are considered fundamental to the operation of industrial unit processes. The removal of natural organic material (NOM) at water treatment works is now well established using conventional coagulation and filtration techniques (Fearing *et al.*, 2004) the impact of organic matter on floc structure is less well understood.

Synthetic polymers have long been used as both primary coagulants and flocculant aids. When polymer is used in combination with a conventional coagulant the aim is to achieve better floc characteristics in terms of size, strength, settleability and filterability (Bratby, 1980; Lee *et al.*, 1998). In addition, considerable savings on coagulant dose can be made when used in combination with organic polymer for the same removal performance (Bolto *et al.*, 2001). The most common practice is to add polymer some time after the primary coagulant to allow destabilization to occur from the metal ions of the initial coagulant. This is then followed by adsorption when the polymer is added, allowing particle-polymer-particle bridging to occur (Aguilar *et al.*, 2003).

Measuring floc physical characteristics can be achieved by using a number of different techniques such as microscopy (Li and Ganczarczyk, 1986), laser diffraction techniques (Biggs and Lant, 2000; Waite *et al.*, 2001), Coulter counters (Selomulya *et al.*, 2001) and settling rates (Huang, 1994). Floc strength, breakage and re-growth has been examined using a range of macroscopic and microscopic techniques, however most evolve around the use of applying a shear and observing the effect this has on floc size (Boller and Blaser, 1998). Previous research on the impact of polymer on floc structure has shown that slaughterhouse wastewater flocs settle better with the presence of additional polymer through an increase in particle size (Aguilar *et al.*, 2003). Wu *et al.* (2002) reported a reduction in floc compaction as determined by the

fractal dimension from floc settling data for activated sludge flocs when polymer was added as a floc aid.

In the case of NOM rich water, previous research has shown that better removal performance can be achieved when polymer is used in combination with a conventional coagulant (Bolto *et al.*, 2001; Walker and Kim, 2001). However, for the specific purpose of examining the effect of different types of coagulant and polymer on NOM floc structure, there has been little published as most work has concentrated on flocs from turbidity dominated water and wastewater (Gregory and Nelson, 1986; Wu *et al.*, 2002; Gregory, 2003). Organic flocs formed during the treatment of water for drinking are generally considered to be fragile, open structures that have a low settling velocity (Bache *et al.*, 1999). The addition of polymer should therefore act to improve NOM-floc structural character. Bache and Rasool (2001) compared the strength and size of a range of metal-humic flocs formed from seven different WTW in the UK. All of the WTW were using alum or ferric as primary coagulants with two of the seven works dosing unspecified polymer as a coagulant aid at a dose of 0.1 mg L^{-1}. However, no direct structural comparison could be made of organic flocs formed with and without polymer as the water samples had been taken from different sources, and coagulant doses were not consistent across the range of water works.

In this work, water was taken from a reservoir containing moorland source water characteristically of high colour and dissolved organic carbon (DOC) concentration, low turbidity and alkalinity. The water treatment works treating this water traditionally uses a ferric sulphate based coagulant. During periods of elevated DOC, small doses of polymer are often added with the aim of improving floc structure. This work aims to firstly determine the effect of organic matter on floc structure and secondly investigate the impact on floc structure of adding a polymer for the same initial primary coagulant dose for this specific NOM rich water source. Floc structural characteristics will be measured in terms of aggregate size and shape, settleability and response to increasing shear levels through breakage and subsequent re-growth potential.

6(A).2 Materials and methods

6(A).2.1 Coagulation optimisation

Experiments were carried out on raw water obtained in June 2003 from a reservoir source in the moorlands of Yorkshire, England. This source is typical of a moorland catchment being of high colour and DOC, low turbidity and low alkalinity. Some of the general water parameters are shown in Table 6(A).1.

Table 6(A).1 Raw water characteristics from the reservoir source abstracted in June 2003.

Characteristic	Value
Dissolved organic carbon	6.9 mg L^{-1} DOC
Turbidity	5.0 NTU
pH	6.0
Alkalinity	< 10 mg L^{-1} as $CaCO_3$
Conductivity	75 µs cm^{-1}
UV absorbance at 254 nm	50.8 m^{-1}

Coagulation experiments were carried out by performing a series of jar tests. A PB-900 variable speed jar tester (Phipps and Bird, Virginia, USA) was used with 76 x 25 mm flat paddle impellers with cylindrical jars containing 1 L samples of water. Two speeds were used with a rapid mix at 200 rpm for 1.5 minutes followed by a slow stir phase at 30 rpm for 15 minutes followed by a 10 minute settling time. A ferric sulphate based coagulant (Ferripol XL – Huntsman Tioxide Europe Ltd, Billingham, UK) was used for all coagulation experiments from a 10 % w/v stock solution as ferric sulphate. A 100 mL sample was then withdrawn using a syringe filter and passed through a 0.45 µm glass fibre filter paper for analysis. In all cases the coagulation pH was 4.5. This corresponds to the pH as used by WTW and the optimum for NOM removal using this iron based coagulant.

Optimum coagulation conditions were determined by carrying out a series of jar tests with incremental increases in the coagulant dose (between 2-20 mg L^{-1} as Fe). Due to

the acidity of the ferric sulphate, preliminary experiments were performed to find the volume of 1M NaOH required in order to reach the coagulation pH for each coagulant dose. Treatment performance was assessed by measuring NOM removal from UV_{254} absorption removal for each sample in a 1 cm cell using a Jenway 6505 UV/Vis spectrophotometer and DOC removal using a Shimadzu TOC-5000A analyser.

The flocculant aid tested was a cationic high molecular weight polydiallyldimethylammonium chloride (polyDADMAC) with a charge density of 100% supplied by SNF UK Ltd. This was selected as it is the floc aid used at the WTW from where the water was abstracted. Polymer was prepared by diluting a 40 % w/v stock solution to a working solution of 10 g L^{-1}. When used as a polymer aid, best results are seen when the polymer is added some time after the addition of the primary coagulant for rapid dispersion and adsorption (Bratby, 1980). For this reason, for coagulant-flocculant aid experiments, the polymer was added after 85 seconds of the rapid mix to allow 10 seconds of rapid dispersion of the polymer after the formation of microflocs. The optimum polymer dose was found by incrementally increasing the polymer dose at the optimum coagulation dose as found above and assessed for UV and DOC removal as before. In order to assess the effect of both NOM and polymer on floc structure, a control experiment was performed producing coagulant precipitate flocs. This was achieved by adding the optimum coagulant dose to de-ionised water containing a small amount of alkalinity (20 mg L^{-1} of $NaHCO_3$) and performing the jar test procedure as before. Once the optimum coagulant and coagulant/floc aid conditions had been found, comparative floc structural experiments could be carried out for the three floc suspensions.

6(A).2.2 Floc size, shape, breakage and re-growth

A laser diffraction instrument (Malvern Mastersizer 2000, Malvern, UK) was used to measure dynamic floc size as the coagulation and flocculation process proceeded. Experiments were carried out as before on a jar tester. A 1 L cylindrical jar was used with holding ports for the inflow/outflow tubing secured on to the sides of the jar. The suspension was monitored by drawing water through the optical unit of the Mastersizer and back into the jar by a peristaltic pump on the return tube using 5 mm internal diameter peristaltic pump tubing at a flow rate of 1.5 L hr^{-1}. The inflow and outflow tubes were positioned opposite to one another at a depth just above the paddle

in the holding ports. This type of arrangement has previously been successfully applied in the analysis of activated sludge flocs (Biggs and Lant, 2000) and alum-polystyrene flocs (Spicer *et al.*, 1998). However, due to the delicate nature of the organic flocs in these experiments it was necessary to have a comparatively reduced flow rate through the tubing to prevent floc breakage. Water samples were placed on the jar tester under the following conditions: 200 rpm for 1.5 minutes, followed by a slow stir phase at 30 rpm for 15 minutes. Coagulant and pH adjustment chemicals were added at the start of the rapid mix. Size measurements were taken every minute for the duration of the jar test and logged onto a PC. Each size experiment was repeated 3 times for each set of conditions.

For floc breakage experiments, the jar tester was programmed as before, however after the slow stir phase the suspension was exposed to increased shear for a further 15 minutes. Separate experiments were carried out and replicated 3 times at increased shear of 30, 40, 50, 75, 100, 150 and 200 rpm. Particle size was monitored before and after exposure to each level of shear. For floc re-growth tests, flocs were exposed to short periods (30 seconds) and long periods (15 minutes) of high shear (200 rpm) followed by a return to the original slow stir (30 rpm) for 15 minutes. Particle size was monitored as before.

6(A).2.3 Floc settling

Floc aggregates were introduced into a settling column via a tapered entry port to ensure the flocs settled into the centre of the column using a wide mouthed pipette. In order to avoid thermal currents disrupting floc settlement, the central settling column was enclosed by a water bath. The water bath was connected to a ThermoHaake K10 heat-refrigerated circulator (Hakke, Germany) to ensure a constant temperature was maintained in the column at 21 – 22 °C. The settling column was filled with de-ionised water and left to reach the required temperature. A period of 2 hours was left for quiescent conditions to be reached. Floc images were captured using a CV M90 colour close-coupled device (CCD) camera (JAI UK Ltd, England). Image analysis software (Image Pro Plus from Media Cybernetics, Maryland, USA) was used to determine floc settling velocity.

Flocs were aggregated on a jar tester under the required conditions at room temperature (21-22° C). Flocs were then carefully removed from the jar using a wide mouthed pipette and re-suspended in de-ionised water held in a water bath at 21-22° C for dilution and temperature control of the flocs. Individual flocs could then be removed and placed in the settling column in isolation of one another to prevent hindered settlement from particle/particle interactions. Visual observation showed that little change in floc macrostructure occurred using the pipettes, however if flocs were observed to break during the transfer procedure then they were discarded.

As a focused floc passed in front of the camera, the image grabber was manually triggered to take a series of 10 images. The time between each frame was set at 1 second. This meant that the distance travelled by the floc could be calculated per frame and therefore per time period, thus giving a settling velocity. The projected area of the floc presented in front of the camera was determined using the image analysis software and converted to an equivalent diameter. This standardized diameter was recorded along with its settling velocity for 100 aggregates for each set of coagulation conditions. For all floc suspensions settled turbidity was also measured.

6(A).3 Results

6(A).3.1 Coagulation optimisation

UV_{254} removal plateaued at between 85-95 % for coagulant doses of 8 mg L^{-1} Fe and above. DOC removal reached a plateau of between 80-90 % for coagulant doses of 6 mg L^{-1} Fe and above. The optimum coagulant dose was chosen as 8 mg L^{-1} Fe as this showed a similar level of removal when compared to higher doses and was representative of the coagulant dose as used by the WTW at the time of abstraction.

It was found that most of the floc polymer doses investigated (0.1-5 mg L^{-1} polymer) showed no improvement in DOC or UV_{254} removal when compared to the coagulant dose alone. However, the 1 and 2 mg L^{-1} polymer concentration slightly improved DOC removal from 85 % to 87 %. It was also observed that at polymer doses at and above 2 mg L^{-1}, the maximum floc size was much reduced than for lower doses. For these reasons, a dose of 1 mg L^{-1} was chosen and can be considered a typical floc aid dose for NOM rich waters (Bolto *et al.*, 2001).

6(A).3.2 Floc size, shape, breakage and re-growth

Some of the physical characteristics of the flocs under investigation are shown in Table 6(A).2. The size data from the Malvern Mastersizer 2000 size is expressed as an equivalent volumetric diameter (d). From this data it can be seen that the precipitate flocs were larger than the two other floc suspensions for the 50 and 90 percentile floc size (d_{50} and d_{90}) whilst the d_{10} percentile flocs were the smallest. The presence of polymer reduced floc size further. The lower settled turbidity of the larger precipitate flocs suggests that these flocs have better settling characteristics than organic flocs, whilst the polymer flocs had the worst settleability.

Table 6(A).2 The physical characteristics of the flocs formed during this study.

Floc conditions	Floc equivalent volumetric diameter (μm)			Settled turbidity (NTU)
	d_{10}	d_{50}	d_{90}	
Fe Precipitate	221 ± 21	901 ± 90	1513 ± 76	0.55
Organic + 8 mg L^{-1} as Fe	292 ± 21	670 ± 55	1330 ± 75	1.80
Organic + 8 mg L^{-1} as Fe + 1 mg L^{-1} PolyDADMAC	252 ± 6	577 ± 9	1193 ± 77	2.32

The floc growth and breakage profiles for the three floc suspensions are shown in Figure 6(A).1. The d_{50} was chosen as the representative floc size, although the same general trends were seen for d_{10} and d_{90} floc sizes. From these profiles it is evident that the different coagulation conditions gave rise to different floc sizes and growth rates. The growth stage shows that the precipitate flocs were much slower to form when compared to the other flocs. The peak floc size was reached after 10 minutes, whilst this was 5 minutes for the organic flocs. This implies that the coagulant-NOM interactions and consequent precipitation and floc formation occur much quicker than when compared to the ferric hydroxide precipitation in the absence of NOM at this pH.

The response of the flocs to increased levels of shear after 15 minute of slow stir show that the floc d_{50} decreases with increasing shear rate. The profiles show that there is an immediate large scale decline in floc size during the two minutes after the introduction of shear at high rpm (>70), followed by a more gradual reduction in floc

size. For low rpm (between 30-50) there is no characteristic jump in floc size, only a gradual decline. After 10 minutes exposure to the shear, the floc aggregates approach a steady state floc size after which no further significant degradation in floc size is seen. The extent of the response to increasing shear is slightly different between the three floc types. Between 30-50 rpm, the precipitate flocs do not show any decline in floc size, whilst the organic flocs show a gradual decline at these low shear levels. The precipitate flocs showed a much larger proportional size change for rpm of 100 and above.

The rate at which a floc suspension decays on exposure to shear is indicative of the strength of the flocs within the system as the steady state floc size is governed by the prevailing shear/stress conditions within the containing vessel. A large body of floc strength work has investigated the empirical relationship between floc size and the applied shear as shown in Equation 6(A).1 (Parker *et al.*, 1972; Leentvaar and Rebhun, 1983; Francois, 1987; Bache *et al.*, 1999).

$$d = CG_{av}^{-\gamma} \qquad \text{Equation 6(A).1}$$

d is the floc diameter (m); C is the floc strength co-efficient; G_{av} is the average velocity gradient (s^{-1}) and γ is the stable floc size exponent.

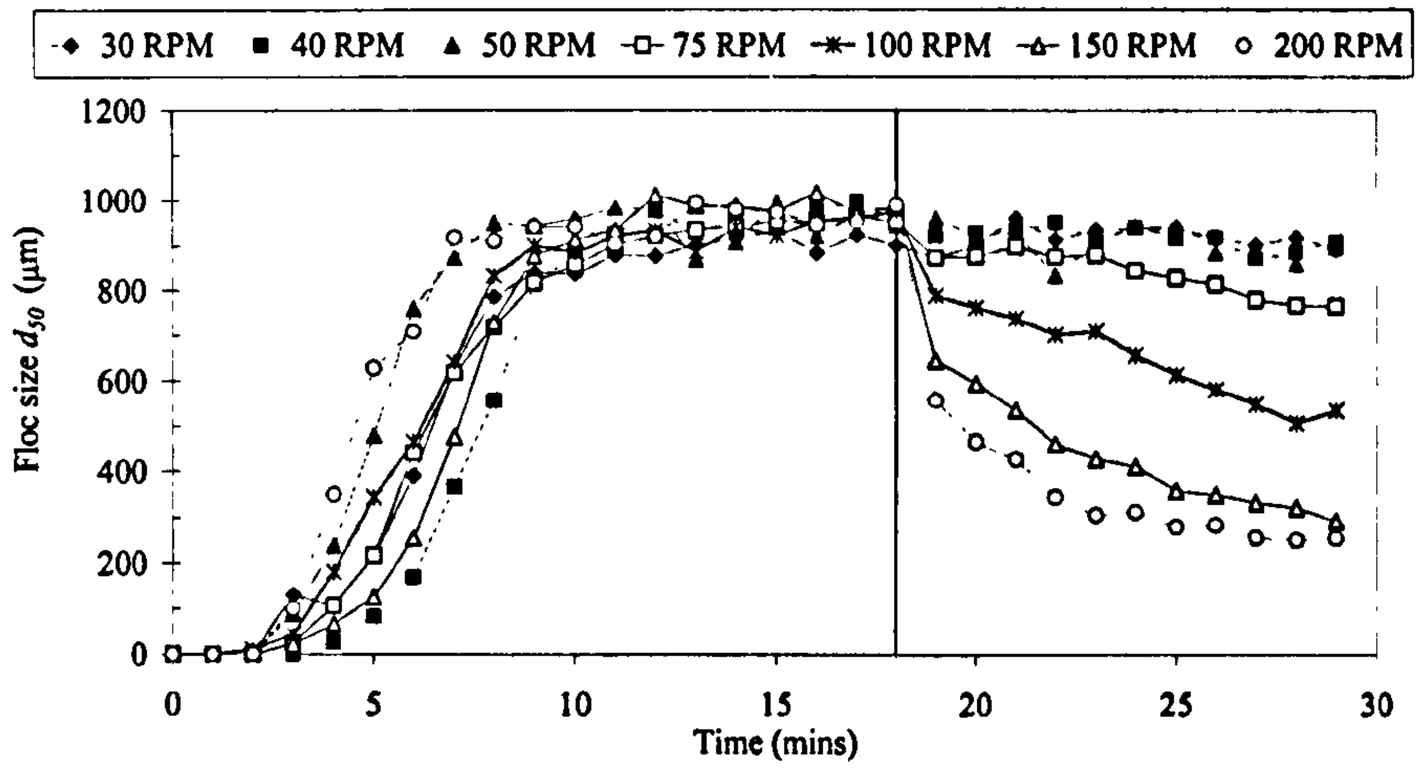

a) Fe precipitate

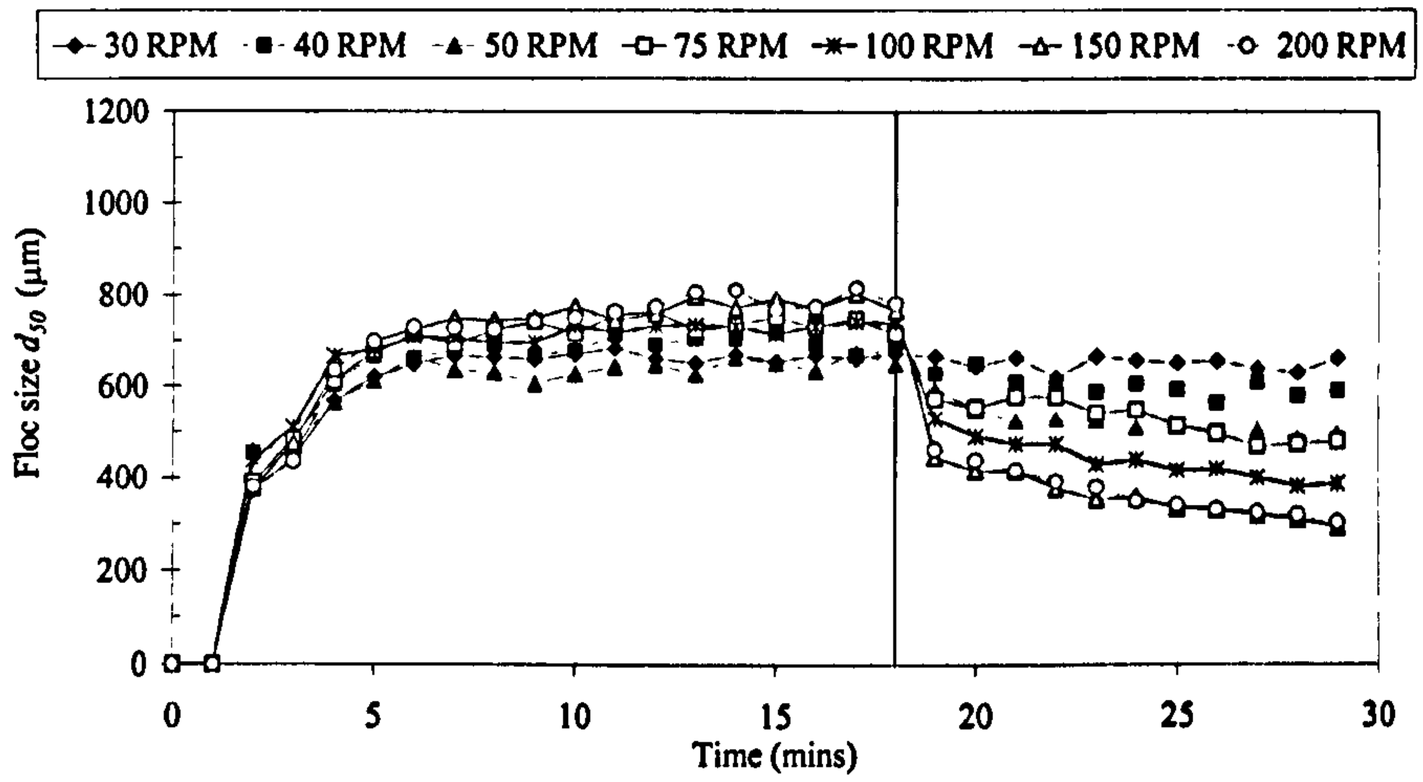

b) Organic + Fe flocs

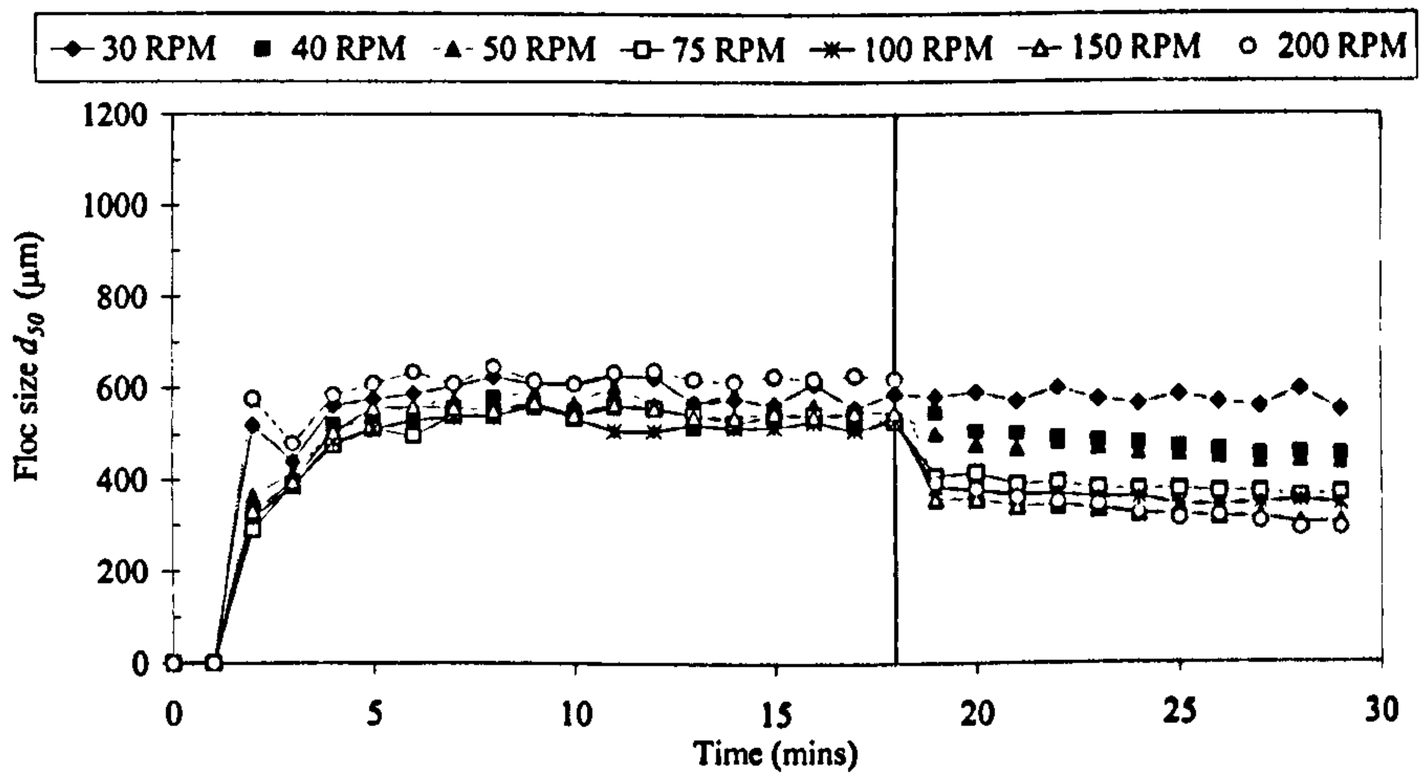

c) Organic + Fe + polymer flocs

Figure 6(A).1 The growth and breakage profile of the 50 percentile floc size for the floc suspensions for increasing rpm on a jar tester. The line indicates point at which increased shear was introduced.

In this instance the floc size after 15 minutes shear was plotted against the rpm on the jar tester on a log-log scale. The rpm was used instead of the average velocity gradient (G_{av}) due to the confusion surrounding its use. Whilst G_{av} has widespread use in the water industry, Boller and Blaser (1998) have concluded that G_{av} was not sufficient to describe shear as experienced by a particle in a stirred vessel. There is a large body of evidence suggesting that local G values are more important than G_{av} in a stirred vessel for determining floc size distributions (Francois, 1987; Essamiani and de Traversay, 2002). In addition, different impeller geometries can supposedly have the same G_{av} value but give different floc size distributions (Bouyer *et al.*, 2001; Griffith, 2003). Due to this confusion and the lack of consistency between technique geometries and impeller type between studies, a simpler indicator of shear for this impeller system – the rpm on the jar tester – was used in this work. As Figure 6(A).2 shows there was a similar empirical relationship between floc size and rpm for the suspensions under investigation. Therefore an adapted version of Equation 6(A).1 was used as shown below (Equation 6(A).2):

$$d = C' rpm^{-\gamma'} \qquad \text{Equation 6(A).2}$$

d is the floc diameter (m); C' is the modified floc strength co-efficient; rpm is the revolutions per minute on the jar tester (rpm) and γ' is an adapted floc size fitting exponent.

Two distinct zones can be identified for the floc d_{50} steady state size of the coagulant precipitate. At 50 rpm and below, the steady state floc size does not change greatly, implying resistance to these shear levels and thus high floc strength. At a shear of 75 rpm and above, the degradation rate increased, with floc size rapidly falling from 900 μm to 250 μm. These two zones were not seen for the organic floc suspensions. Organic flocs, with and without polymer, showed a more constant reduction in size across the shear range. The slope of this line gives an indication of the rate of degradation. During the breakage phase for the precipitate, the degradation rate (μm rpm^{-1}) was 1.17, for the organic flocs this was 0.44 whilst for the organic flocs with polymer the degradation rate was 0.32. This compares to values of between 0.29-0.81 observed for other investigations of floc breakage (Leentvaar and Rhebhun, 1983; Bache and Rasool, 2001) types of floc. The floc strength coefficient log C' was greatest for the Fe precipitate (5.06) followed by the NOM-Fe flocs (3.46) with the polymer-NOM-Fe flocs having the lowest value (3.19).

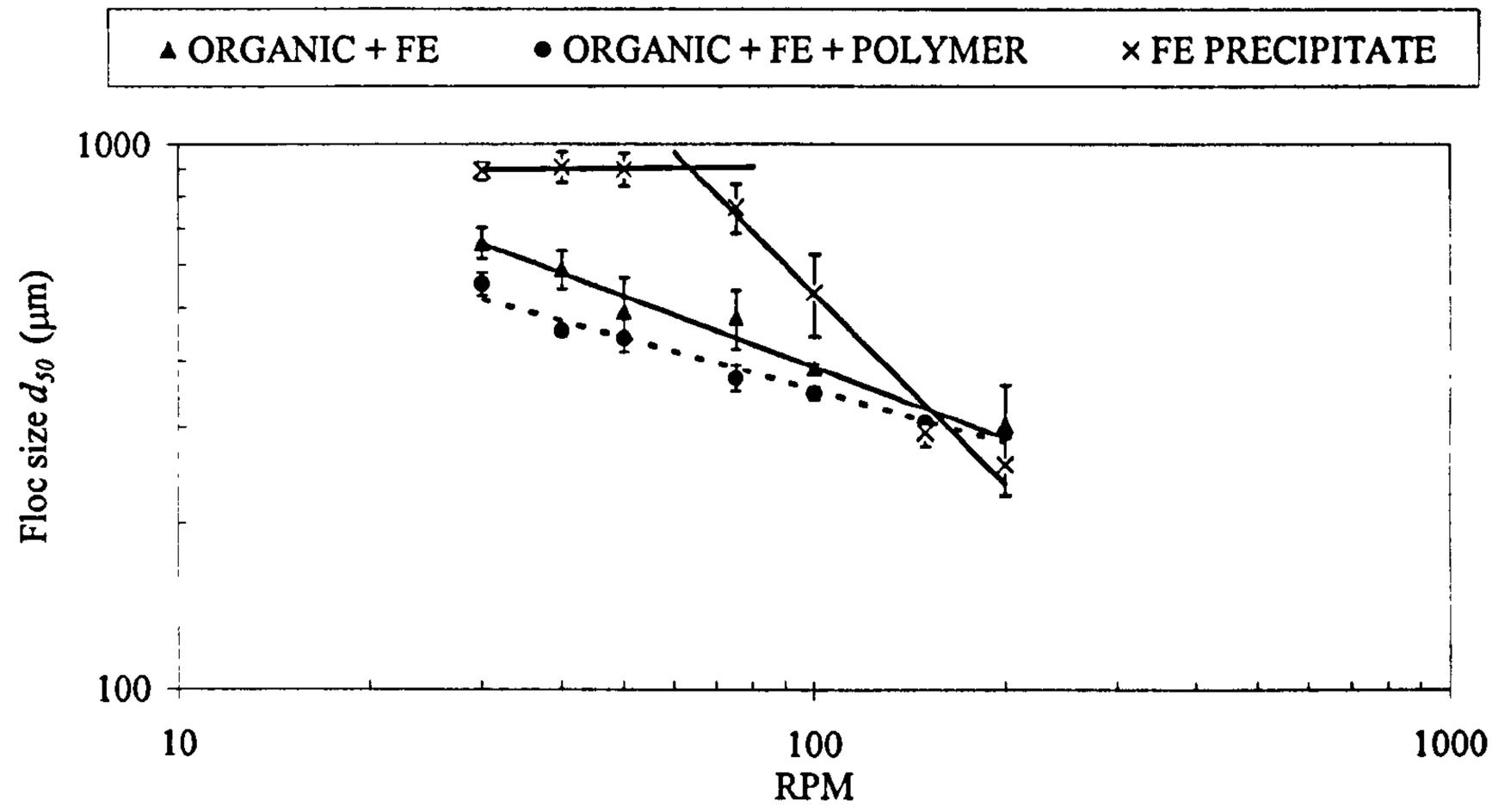

Figure 6(A).2 The change in steady state floc size at different rpm for the three floc suspensions

When flocs were exposed to high shear for a sustained period of 15 minutes there was only a limited capacity for floc re-growth and flocs were never able to reach their previous size (Figure 6(A).3). The organic flocs (with and without polymer) re-grew to a larger size (d_{50} = 375 µm) than the precipitate flocs (d_{50} = 300 µm), although it is important to note that the precipitate flocs were initially broken to a smaller size. The proportional size change for each of the floc suspensions is shown in Table 6(A).3 for the d_{10}, d_{50} and d_{90}. This shows that the flocs have essentially the same capacity to re-grow when exposed to this level of shear regardless of the initial coagulation conditions. It was evident that the smallest flocs had a better capacity for re-aggregation because the d_{10} was approximately doubled during re-aggregation for all the floc types whilst the d_{50} and d_{90} showed only a slight increase. The presence of polymer showed no significant improvement in re-growth potential.

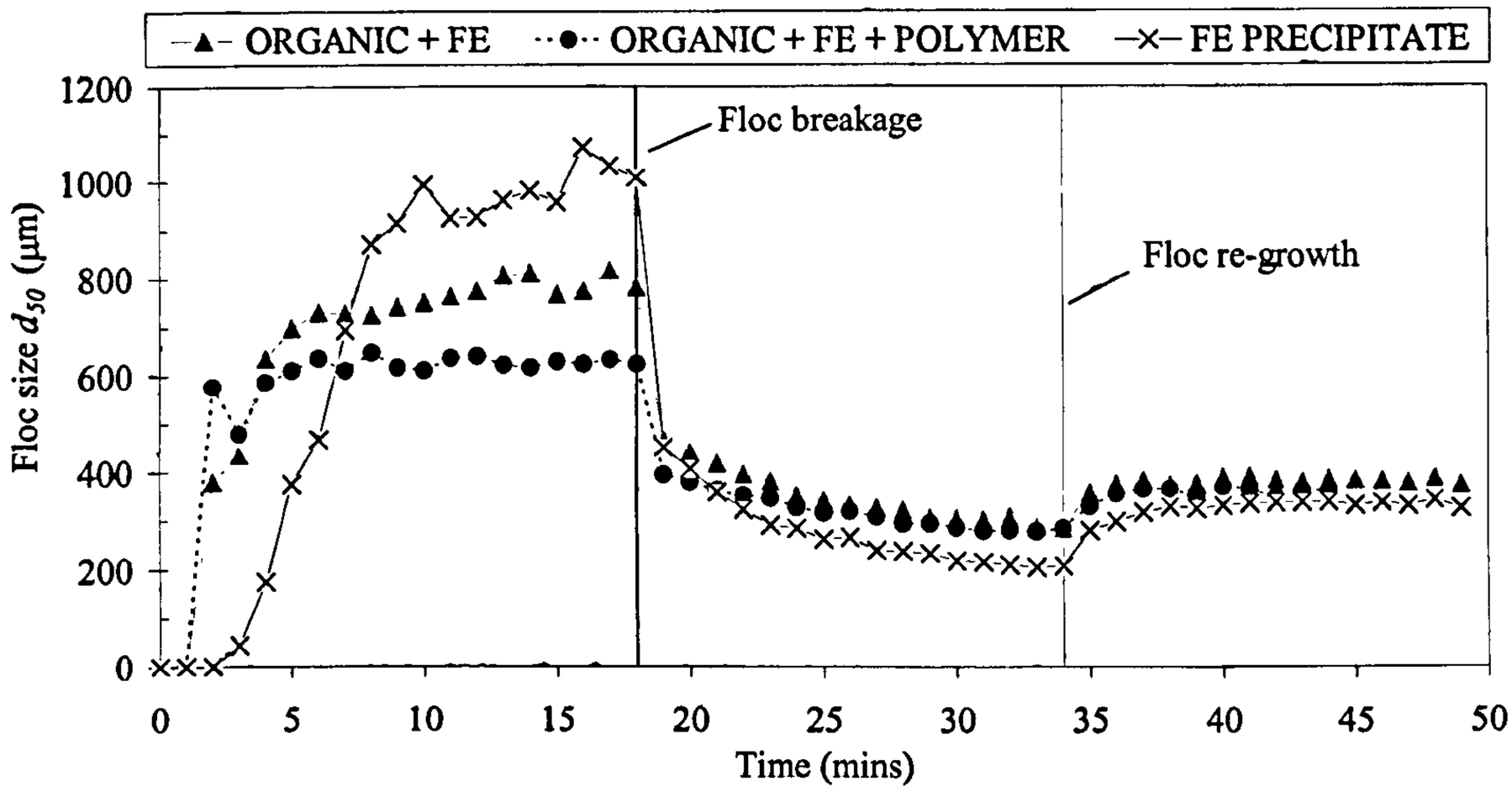

Figure 6(A).3 The re-growth capacity of flocs after exposure to increased shear (200 rpm) for 15 minutes. During the growth phases flocs were exposed to shear of 30 rpm on the jar tester.

Table 6(A).3 The proportional change in floc size after exposure to 15 minutes of high shear (breakage) followed by a return to the slow stir rate for 15 minutes (re-growth). The floc size was normalised to the size prior to breakage.

	Fe Precipitate flocs			Organic + Fe flocs			Organic + Fe + polymer flocs		
	d_{10}	d_{50}	d_{90}	d_{10}	d_{50}	d_{90}	d_{10}	d_{50}	d_{90}
Breakage	0.22	0.20	0.32	0.25	0.36	0.41	0.32	0.45	0.48
Re-growth	0.51	0.32	0.41	0.53	0.48	0.49	0.63	0.58	0.55

When flocs were exposed to a much shorter period of high shear (30 seconds) the extent of floc breakage was much less and the flocs were able to re-grow to a size close to their previous size (Figure 6(A).4). As shown in Table 6(A).4, the precipitate floc d_{50} and d_{90} reached 0.95 of their initial size, whilst the d_{10} increased above the previous size. For the organic flocs, the addition of polymer slightly improved the re-growth potential of the aggregates for similar proportional breakages.

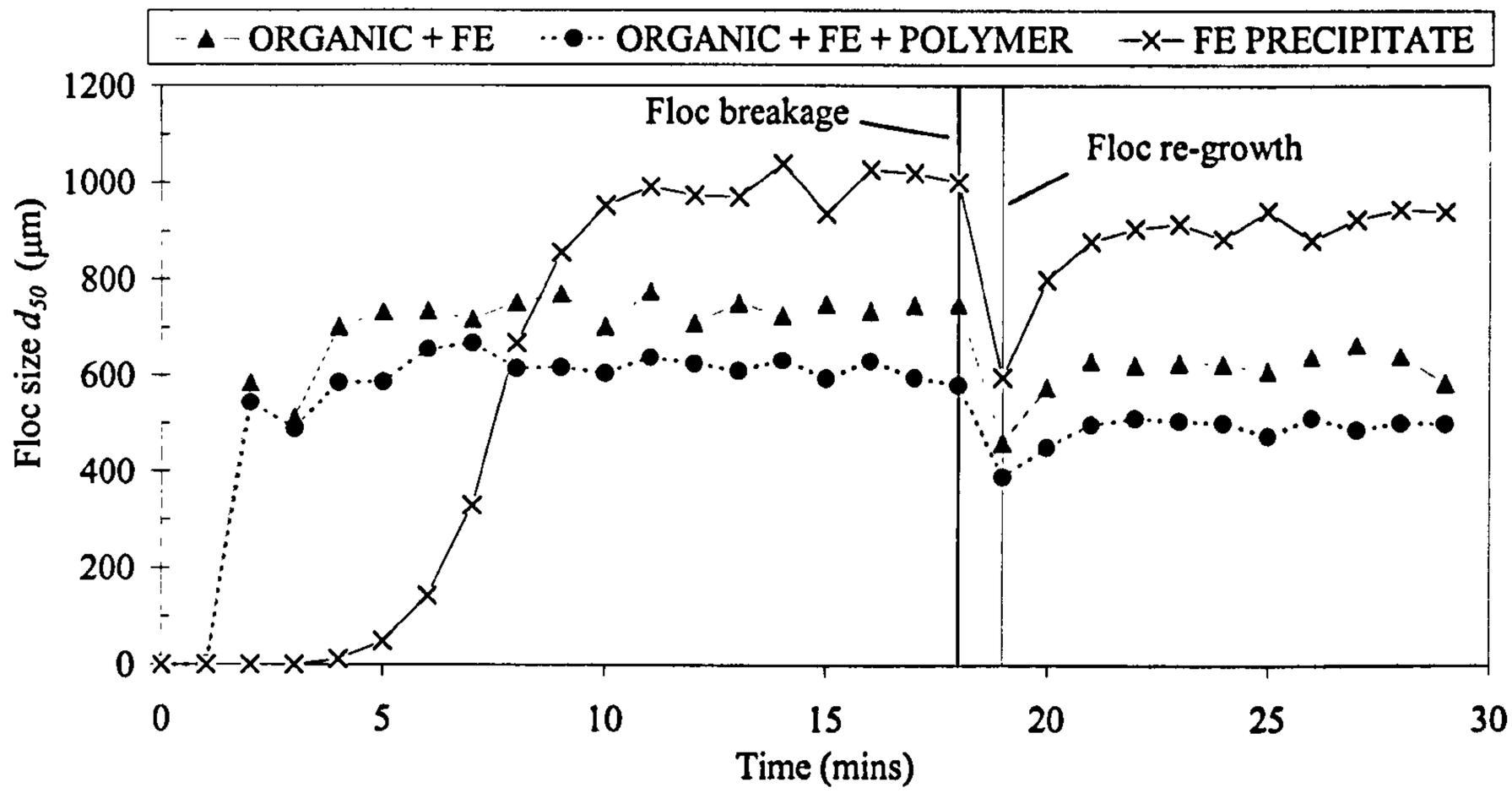

Figure 6(A).4 The re-growth capacity of flocs after exposure to increased shear (200 rpm) for 30 seconds. During the growth phases flocs were exposed to shear of 30 rpm on the jar tester.

Table 6(A).4 The proportional change in floc size after exposure to 15 minutes of high shear (breakage) followed by a return to the slow stir rate for 15 minutes (re-growth). The floc size was normalised to the size prior to breakage.

	Fe Precipitate flocs			Organic + Fe flocs			Organic + Fe + polymer flocs		
	d_{10}	d_{50}	d_{90}	d_{10}	d_{50}	d_{90}	d_{10}	d_{50}	d_{90}
Breakage	0.67	0.59	0.81	0.45	0.62	0.72	0.48	0.67	0.72
Re-growth	1.62	0.94	0.97	0.83	0.78	0.83	0.87	0.86	0.94

6(A).3.3 Floc settling

The terminal settling velocities of floc aggregates are shown in Figure 6(A).5. The precipitate flocs had higher settling velocities when compared to the organic flocs for similar sized particles. The relationship between floc size and terminal settling velocity gives an indication of the degree of compaction for aggregated particles as found from Equation 6(A).3.

$$v_s = \frac{d_f^{D_f-1} 4kg}{3A(\beta)\mu}$$ Equation 6(A).3

v_s is the terminal settling velocity (m s^{-1}), k is a proportionality constant (kg m^{-D}), ρ_l is the density of the liquid (kg m^{-3}), $A(\beta)$ is a correction factor for advection through the floc, μ is the viscosity of the suspending medium (m s^{-1}) and g is acceleration due to gravity (m s^{-1}).

It is generally valid that the correction factor $A(\beta)$ is constant over the range of Reynolds numbers under investigation for settlement of flocs (Wu *et al.*, 2002). Therefore, a log-log plot of terminal settling velocity against floc size will have a line with a slop of D_f-1. Figure 6(A).5 shows that the fractal dimension of organic flocs (D_f = 2.00) was lower when compared to precipitate flocs (D_f = 2.14). When polymer was added the fractal dimension was further reduced to 1.86. Although these are not large changes the slopes of the line are statisticaliy significant at the 95 % level (t-test with 198 df).

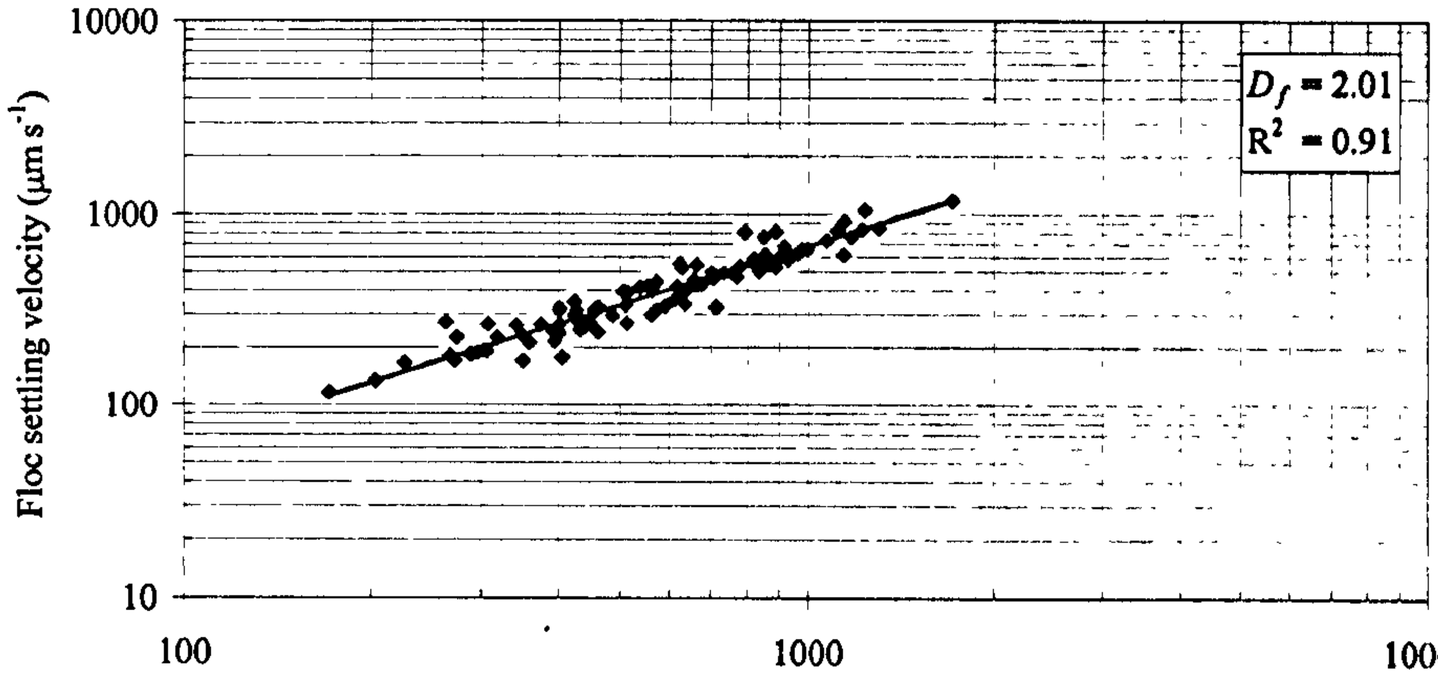

a) Organic + Fe

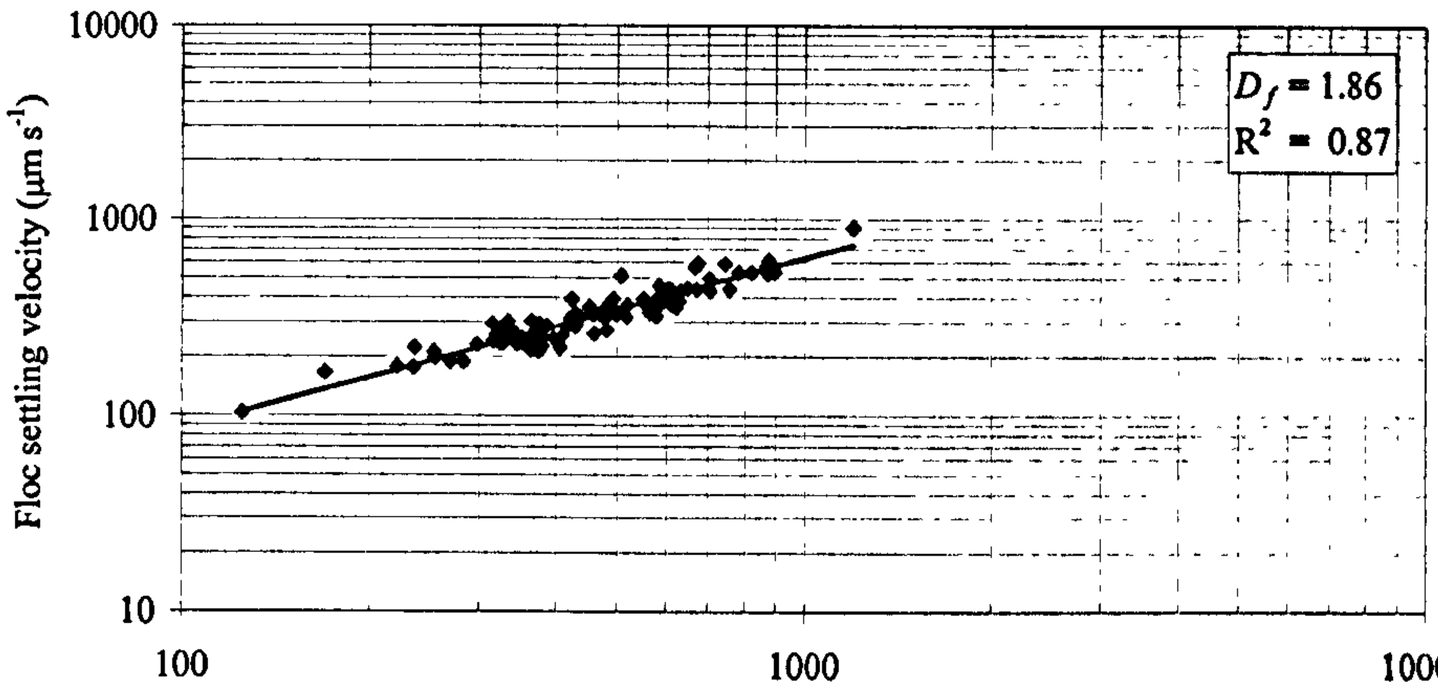

b) Organic + Fe + polymer

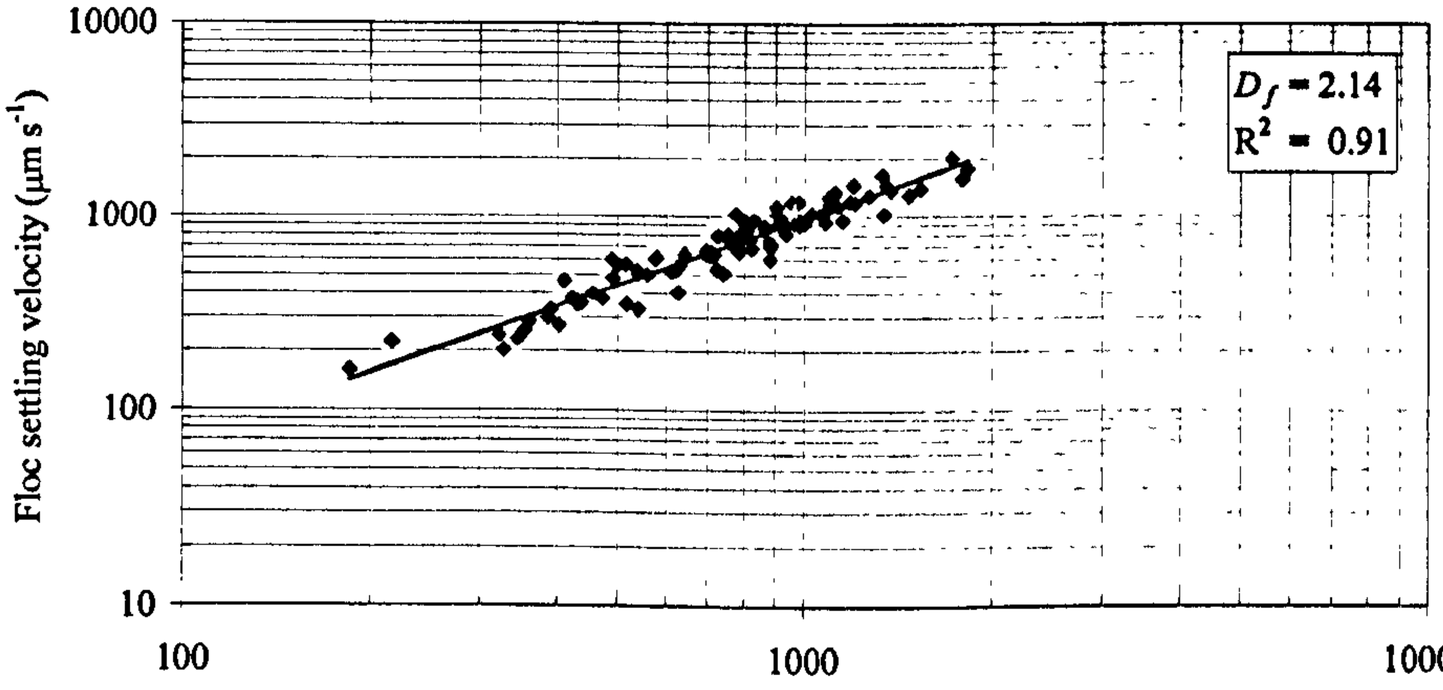

c) Fe precipitate

Figure 6(A).5 The settling velocity of floc aggregates with increasing size on a log-log scale with the fractal dimension (D_f) for a) Fe precipitate flocs, b) organic + Fe flocs and c) organic + Fe + polymer flocs.

6(A).4 Discussion

The approach adopted by this investigation of floc structure has provided detailed information on the effect of both organic and polymer on floc structure for flocs formed from a high DOC and low alkalinity water. An overview of the results can be seen in Table 6(A).5.

Table 6(A).5 An overview of the structural characteristics for the floc suspensions under investigation.

Floc type	Size	Rate of degradation – low rpm	Rate of degradation – high rpm	Re-growth capacity – extended shear	Re-growth capacity – short shear	Settleability	Compaction
Precipitate	Largest	No degradation	Rapid decline	Poor	Good	Good	Most compact
Organic + Fe	Small	Steady decline	Steady decline	Poor	Poor	Poor	Medium compaction
Organic + Fe + polymer	Smallest	Steady decline	Steady decline	Poor	Average	Poor	Least compaction

The current understanding of floc formation is for destabilized primary particles to come together to form small flocculi which further aggregate to microflocs soon after the addition of coagulant (Gorczyca and Ganczarczyk, 1999). For this specific water, floc size was seen to decrease when flocs were formed in the presence of NOM, however the rate of formation was faster than for the coagulant Fe precipitate, suggesting that the mechanisms involved for NOM floc formation are different from those for the coagulant precipitate flocs. NOM-coagulant precipitation reactions were shown to occur faster than the precipitation of ferric hydroxide at the pH investigated.

The removal of NOM using metal coagulants is complex and pH dependent. Charge neutralization by metal ions and enmeshment and adsorption of NOM onto metal hydroxide precipitates (sweep flocculation) are the most generally thought of removal routes for organics in water (Shen and Dempsey, 1998; Bache *et al.*, 1999). However, this is confused by the chemical reactions that occur between soluble NOM and metal species to form both soluble and insoluble NOM-metal complexes (Gregor *et al.*,

1997). At pH >6 the removal of NOM is believed to be dominated by adsorption onto precipitated metal hydroxides, whilst at pH <6 the complexation of NOM with soluble metal species into insoluble precipitates is the main removal route (Dempsey *et al.*, 1984; Dennett *et al.*, 1996). Recent molecular analysis has confirmed the presence of Fe-O-C bonds as evidence for complexation of NOM at pH 5 (Vilge-Ritter *et al.*, 1999). In this investigation coagulation dose and pH were chosen that mirrored conditions used at an operational WTW for this type of water. At a coagulation pH of between 4-5 complexation should therefore be important. In addition, Kim *et al.* (2001) have shown that charge neutralization flocs are smaller and less compact than when compared to 'sweep' flocs for the coagulation of a river water of high DOC. This may imply that the smaller and less compact organic flocs seen in this study were more dominated by charge neutralization mechanisms than for sweep flocculation of the coagulant precipitate. Furthermore, the slower formation of Fe precipitate flocs over the organic-Fe flocs could prevent any sweep flocs forming as a result of enmeshment in metal hydroxide precipitate. This suggests that charge neutralization and NOM-Fe complexation initially dominate for organic flocs. Sweep flocculation could then occur as soluble NOM-Fe complexes and other colloidal species are enmeshed into precipitated NOM-Fe complexes.

When polymer is added as a flocculant aid, its aim is to bind already formed microflocs into larger aggregates by supplementing orthokinetic flocculation (Bratby, 1980). It can be seen from the results obtained that adding polymer generally reduced floc structural quality by reducing floc size, settleability and compaction. In part agreement with this observation, Wu *et al.* (2002) have seen the fractal dimension of activated sludge flocs decrease with increasing polymer dose. High MW cationic polymer such as the one used in this study have previously been shown to improve NOM removal and reduce coagulant dose (Waite *et al.*, 2001). In this study, no improvement in removal rates were observed. The zeta potential of the NOM suspension was slightly negative under the optimum removal conditions (ζ = 0 to -5mV), whilst the polymer was positively charged. It is generally accepted that electrostatic patch mechanisms occur when cationic polymers are applied to particles of opposite charge (Gregory, 1989). In this instance, mosaics of alternately charged areas exist when polymer has adsorbed onto the particles allowing other particles to align together at areas of opposite charge much like charge neutralization mechanisms.

A possible hypothesis for the observed floc characteristics is that following the initial addition of coagulant, NOM-Fe complexes form and/or direct charge neutralization of NOM colloids occurs by metal coagulant ions. In the absence of polymer, enmeshment of soluble metal complexes and NOM may occur by insoluble NOM-Fe precipitates during orthokinetic flocculation. Therefore a combination of charge neutralization and sweep flocculation occurs as reflected by the intermediate floc size and fractal dimension. When polymer was added, dispersion and adsorption onto particles should occur very rapidly (Bratby, 1989). This implies that all microflocs and colloid particles are quickly covered by polymer patches therefore promoting charge neutralization mechanisms. This was reflected by the lower floc size and fractal dimension for the NOM-Fe-polymer flocs.

The breakage and re-growth behaviour of the flocs was difficult to interpret. Only the precipitate flocs showed some resistance to increased shear at low rpm, however at higher rpm there was a rapid rate of floc degradation. Leentvaar and Rhebun (1983) have shown that a higher value of log *C* indicates greater floc strength. If this is applied to the floc suspensions under investigation, the order of floc strength would be the following: precipitate>organic-Fe>organic-Fe-polymer. However, the rate of degradation as determined from the slope of a log-log plot of floc size against rpm indicates the relative floc proportional size change with increasing shear. A steeper slope is indicative of flocs that are less able to withstand changes in hydrodynamic shear (Bache and Rasool, 2001). From this interpretation, the organic-polymer flocs were better able to withstand high shearing and the order of floc strength was reversed.

The operational implications of these results are that a WTW should aim to initially produce large flocs due to their improved settling rates and flotation rates (Fukishi *et al.*, 1995). In addition the flocs should have a low degradation rate on exposure to shear to prevent flocs breaking into very small particles. For this reason the value of the slope is a more useful number to analyse in combination with the initial floc size than the floc strength co-efficient. From the results of this study, the addition of polymer acts to reduce the degradation rate when compared to the organic-Fe flocs. However, because of the larger size of the organic flocs in the absence of polymer across the whole range of rpm, there was little benefit in adding the cationic polymer.

The results have shown that sustained exposure to high shear will break flocs with little re-growth capacity even after the addition of polymer. This is in agreement with previous research that has shown re-growth is limited for most coagulants (Leentvaar and Rebhun, 1983; Gregory, 2003). No sufficient model has been shown to adequately explain why flocs are unable to re-grow. A possible reason could be re-structuring of primary flocs during exposure to shear, such that flocs are broken into smaller aggregates and the primary particles re-arrange themselves into stable, smaller and more compact floc structures (Spicer *et al.*, 1998). Prolonged shear has a more detrimental impact on floc re-growth. Floc suspensions have a much better capability to reach their previous size when only exposed to short periods of high shear. This may in part be due to a much reduced level of breakage but also due to there being less time for flocs to re-structure into stable and smaller structures. In flocculators at WTW areas of high shear exist, such as in small localized regions close to the stirring impellers (Griffith, 2003). Because these regions occupy only a small volume of a flocculating vessel, flocs are only likely to experience regions of high shear for short periods. As shown in this study, this gives rise to much reduced floc breakage and better floc re-growth. Floc breakage was more limited because the probability of flocs entering high shear breakage zones close to the impeller was much less. Improved re-growth may have occurred because flocs had less time to re-structure, therefore there was a higher chance of bonding between broken flocs.

It must also be considered that high NOM removals of over 80 % were seen in this study. In comparison to most operational requirements this is considered to be high, for example the United States Environmental Protection Agency requires a maximum of 50 % DOC removal for enhanced coagulation (Edzwald *et al.*, 1999). Therefore, the impact of NOM on floc structure will probably be more evident for this type of water when compared to systems where lower NOM removal is seen. The high organic removals seen using the coagulant alone may also explain why the addition of polymer did not give any increase in removal.

Whilst optimum NOM removal is an essential requirement at WTW, the resulting floc structure should also be considered as an important parameter for efficient and improved overall process optimisation. Organic matter has a significant impact on floc structural characteristics. Most applications of organic polymer as a flocculant aid

for the removal of NOM have used cationic polymer. As has been discussed, the polymer is likely to work by promoting charge neutralization type mechanisms at the pH under investigation. However, as this polymer offered no real benefit in terms of improving NOM floc structural quality, the use of anionic polymers as a floc aid may be of more use. This is because the primary particle complexes formed from metal hydroxide species as a result of metal coagulant addition tend to be positively charged under most conditions (Bratby, 1980). Polymer bridging is therefore more likely to occur between the negative polymer and the positive primary particles. This in turn may act to increase floc strength and size. Further investigations along these lines are required before a more satisfactory understanding of polymer action is achieved.

6(A).5 Conclusions

(1) A series of experimental procedures were developed in order to assess floc structural parameters. Flocs formed at a low pH from a low alkalinity and high DOC water source showed significant differences in structure when compared to flocs formed in DI water with a significant decrease in floc size and a reduction in floc compaction.

(2) For the given water and coagulation conditions, the addition of polyDADMAC as a floc aid did not improve NOM floc structure.

(3) All of the flocs under investigation showed a limited capacity to re-form when they had been previously broken at a higher shear.

Acknowledgements

The submitted manuscript has been made possible through funding from American Water Works Association Research Foundation and Co-funding Utilities. The information contained herein is based upon Intellectual Property which is jointly owned by Cranfield University and the Foundation. The Foundation retains its right to publish or produce the Jointly Owned Intellectual Property in part or in its entirety. The authors would also like to thank the EPSRC, Fort Collins Water, Scottish Water, Severn Trent Water, Thames Water, United Utilities and Yorkshire Water.

6(A).6 References

Aguilar, M. I., Saez, J.; Llorens, M.; Soler, A. and Ortuno, J. F. (2003) Microscopic Observation of Particle Reduction in Slaughterhouse Wastewater by Coagulation-Flocculation Using Ferric Sulphate as Coagulant and Different Coagulant Aids. *Water Research* **37** 2233-2241.

Bache, D. H. and Rasool, E. R. (2001) Characteristics of Alumino-Humic Flocs in Relation to DAF Performance. *Water Science and Technology* **43** (8), 203-208.

Bache, D. H., Rasool, E., Moffatt, D., and McGilligan, F. J. (1999) On the Strength and Character of Alumino-Humic Flocs. *Water Science and Technology* **40** (9), 81-88.

Biggs, C. A. and Lant, P. A. (2000) Activated Sludge Flocculation: On-Line Determination of Floc Size and the Effect of Shear. *Water Research* **34** 2542-2550.

Boller, M. and Blaser, S. (1998) Particles Under Stress. *Water Science and Technology* **37** (10), 9-29.

Bolto, B., Dixon, D., Eldridge, R., and King, S. (2001) Cationic Polymer and Clay or Metal Oxide Combinations for Natural Organic Matter Removal. *Water Research* **35** 2669-2676.

Bouyer, D., Line, A., Cockx, A., and Do-Quang, Z. (2001) Experimental Analysis of Floc Size Distribution and Hydrodynamics in a Jar-test. *Transactions of the Institute of Chemical Engineers* **79** (A), 1017-1024.

Bratby, J. (1980) *Coagulation and Flocculation*. Uplands Press Ltd, Croydon UK.

Dempsey, B. A., Ganho, R. M., and O'Melia, C. R. (1984). The Coagulation of Humic Substances by Means of Aluminium Salts. *Journal of the American Water Works Association* **76** (4), 141-150.

Dennett, K. E., Amirtharajah, A., Moran, T .F. and Gould, J. P. (1996). Coagulation: Its Effect on Organic Matter. *Journal of the American Water Works Association* **84** (4), 129-142.

Essamiani, K. and de Traversay, C. (2002) Optimisation of the Flocculation Process Using Computational Fluid Dynamics. In: *Chemical Water and Wastewater Treatment VII: Proceedings of the 10th Gothenburg Symposium*; International Water Association: Gothenburg, June.

Fearing, D. A., Goslan, E. H., Banks, J., Wilson, D., Hillis, P., Campbell, A. T. and Parsons, S. A. (2004). Staged Coagulation for the Treatment of Refractory Organics. *Journal of Environmental Engineering ASCE* **130** 975-982.

Francois, R. J. (1987) Strength of Aluminium Hydroxide Flocs. *Water Research* **21** 1023-1030.

Fukishi, K.; Tambo, N. and Matsui, Y. (1995) A kinetic Model for Dissolved Air Flotation in Water and Wastewater Treatment. *Water Science and Technology* **31** (3-4), 37-47.

Gorczyca, B. and Ganczarczyk, J. (1999) Structure and Porosity of Alum Coagulation Flocs. *Water Quality Research Journal of Canada* **34** (4), 653-666.

Gregor, J. E., Nokes, C. J., and Fenton, E. (1997) Optimising Natural Organic Matter Removal from Low Turbidity Waters by Controlled pH Adjustment of Aluminium Coagulation. *Water Research* **31** 2949-2958.

Gregory, J. (1989) Fundamentals of Flocculation. *Critical Reviews in Environmental Control* **19** (3), 185-230.

Gregory, J. (2003) Monitoring Floc Formation and Breakage. In: *Proceedings of the Nano and Micro Particles in Water and Wastewater Treatment Conference*; International Water Association: Zurich, September

Gregory, J. and Nelson, D. W. (1986) Monitoring of Aggregates in Flowing Suspension. *Colloids and Surfaces* **18** 175-188.

Griffith, S. (2003) Flocculation: a New Design Procedure. *Journal of the Australian Water Association* **30** (6), 44-54.

Huang, H. (1994) Fractal Properties of Flocs Formed by Fluid shear and Differential Settling. *Physical Fluids* **6** (10), 3229-3234.

Kim, S. H., Moon, B. H., and Lee, H. I. (2001). Effects of pH and Dosage on Pollutant Removal and Floc Structure During Coagulation. *Microchemical Journal* **68** 197-203.

Lee, J. F., Liao, P. M., Tseng, D. H., and Wen, P. T. (1998) Behaviour of Organic Polymers in Drinking Water Purification. *Chemosphere* **37**, 1045-1061.

Leentvaar, J. and Rebhun, M. (1983) Strength of Feric Hydroxide Flocs. *Water Research* **17** 895-902.

Li, D. H. and Ganczarczyk, J. J. (1986) Physical Characteristics of Activated Sludge Flocs. *CRC Critical Reviews in Environmental Control* **17** (1), 53-87.

Parker, D. S., Kaufman, W. J., and Jenkins, D (1972) Floc Breakup in Turbulent Flocculation Processes. *Journal of the Sanitary Engineering Division: Proceedings of the American Society of Civil Engineers* **SA 1** 79-99.

Selomulya, C., Amal, R., Bushell, G., and Waite, T.D. (2001) Evidence of Shear Rate Dependence on Restructuring and Break-up of Latex Aggregates. *Journal of Colloid and Interface Science* **236** 67-77.

Shen, Y. H. and Dempsey, B. A. (1998) Fractions of Aluminium Coagulants as a Function of pH. *Environmental Technology* **19** 845-850.

Spicer, P. T., Pratsinis, S. E., Raper, J., Amal, R., Bushell, G., and Meesters, G. (1998) Effect of Shear Schedule on Particle Size, Density and Structure During Flocculation in Stirred Tanks. *Powder Technology* **97** 26-34.

Vilge-Ritter, A., Rose, J., Masion, A., Bottero, J. Y. and Laine, J. M. (1999). Chemistry and Structure of Aggregates Formed with Fe-Salts and Natural Organic Matter. *Colloids and Surfaces A: Physicochemical and Engineering Aspects* **147** 297-308.

Waite, T. D., Cleaver, J. K., and Beattie, J. K. (2001) Aggregation Kinetics and Fractal Structure of y-Alumina Assemblages. *Journal of Colloid and Interface Science* **241** 333-339.

Walker, H. W. and Kim, E. K. (2001) Influence of Flocculant Aids and NOM Characteristics on the on the Removal of DPB Precursors During Enhanced Coagulation. In: *Proceedings of the Water Quality Technology Conference*; American Water Works Association: Nashville, Novemver.

Wu, R. M.; Lee, D. J., Waite, T. D. and Guan, J. (2002) Multilevel Structure of Sludge Flocs. *Journal of Colloid and Interface Science* **252** 383-392.

6(B) THE IMPACT ON NOM FLOC SRUCTURE USING DIFFERENT TREATMENT OPTIONS

PETER JARVIS[1], BRUCE JEFFERSON[1], DAVID DIXON[2] and SIMON A. PARSONS[1]

[1]*School of Water Sciences, Building 39, Cranfield University, Cranfield, Bedford, MK40 0AL, United Kingdom.*

[2]*Department of Chemical and Biomolecular Engineering, University of Melbourne, 3010, Australia.*

Abstract

A range of treatment options were compared for their impact on natural organic matter (NOM) floc structure at optimum coagulant doses. The treatment options were ferric, ferric + polymer, alum, polymer and magnetic ion exchange (MIEX®) pre-treatment followed by ferric coagulation. Using a range of diagnostic techniques, the size, strength, breakage and settling rate of the treatment options were compared. Ion exchange pre-treatment gave rise to significantly improved floc structure in terms of increased size, settling rate and strength. Comparison of conventional ferric and alum coagulants suggested that ferric gave rise to improved floc structure combined with better NOM removals. The cationic polymer investigated did not give rise to improved floc structure. The reasons for the observed changes were thought to be related to the type of organic material incorporated into the floc matrix.

Keywords

Floc; natural organic matter; settling velocity; size; treatment options.

6(B).1 Introduction

The removal of natural organic matter (NOM) using coagulation, flocculation and solid-liquid separation techniques remains the principle treatment pathway for control of organics and trihalomethanes (THMs) in potable water production. The efficient removal of NOM is dependent on a number of factors including pH, coagulant type, dose and dosing strategy (Fearing *et al.*, 2004). NOM is removed through a combination of charge neutralization, entrapment, adsorption and complexation with coagulant metal ions into insoluble particulate aggregates (Dempsey *et al.*, 1984; Dennett *et al.*, 1996; Vilgé-Ritter, 1999). Further agglomeration of these micro-particles leads to the formation of flocs. The way in which these interactions occur and the efficient incorporation of these molecules into the floc aggregate is dependent upon the particular nature of the NOM components with regard to molecular size, functionality, charge and hydrophobicity. In addition, the use of different coagulants may have significant impact on NOM floc structure. There is currently a paucity of information on the comparison of floc properties as a function of coagulant choice and dosing strategy, particularly for NOM flocs as most previous research emphasis has investigated floc structure for turbidity flocs (Bottero *et al.*, 1990; Gregory and Dupont, 2001).

Floc structural quality plays a significant role in the removal process. There is a general conception that NOM flocs are weak and of low density when compared with turbidity flocs (Bache *et al.*, 1999) although further explanation is still required as structural properties are not normally investigated during coagulation trials. However, an accurate assessment of floc structure can be a crucial tool for predicting WTW performance under certain coagulation conditions and may be used in combination with removal data to find optimum coagulation pH and dose. Floc properties that should be considered operationally important include:

Floc strength - strength is a particularly important operational parameter in solid liquids separation for efficient and robust removal of aggregated pollutants. The strength of the floc comes from the number and intensity of the individual connection points within the floc matrix (Bache *et al.*, 1997). The understanding of strength is severely hampered in NOM systems as the material is extremely heterogeneous with

no consistent primary particle size. Consequently a myriad of different bond strengths are possible. Indications of floc strength can be found from:

a) Floc size – increased floc size is a good indicator of increased floc strength for a similar level of shear (Bache and Papavasilopoulos, 2003; Yukselen and Gregory, 2004). This is given that on average large flocs must have higher resistance to breakage during the floc growth phase in order to reach a bigger size and should therefore be considered stronger. For weaker flocs a higher degree of breakage occurs restricting the final floc size formed (Duan and Gregory, 2002).

b) Floc response to shear – flocs are subjected to a range of shear after they have grown to their steady state size in a flocculator. This includes floc transfer across weirs, 'hot-spot' high shear regions in unit processes that are designed to minimize floc breakage or in high energy processes such as dissolved air flotation. By exposing fully grown flocs to an increased shear, an indication of floc degradation can be found. An empirical relationship between the steady state floc size and the applied shear has frequently been observed (Parker *et al.*, 1972; Francois, 1987; Biggs and Lant, 2000; Bache, 2004; Jarvis *et al.*, 2004). Plotted on a log-log graph the line is described by:

$$d = CG^{-\gamma} \qquad \text{Equation 6(B).1}$$

where d is the floc diameter (m), C is the floc strength co-efficient, G is the average velocity gradient (s^{-1} or rpm) and γ is the stable floc size exponent.

The floc strength coefficient can be further interpreted as an indicator of the mechanism of breakage such that gradients of around 0.5 indicate fragmentation and values between 1 and 2 indicate surface erosion. However, qualitative comparisons suggest that the most significant trend is between floc size and shear, with smaller initial flocs having lower values of γ (Bache *et al*, 1997). The precise interpretation of this is not clear, but the general view is that the floc size relative to a critical breakage eddy size is important (Parker *et al.*, 1972).

Floc settling rate – improved floc settling rate can give rise to improved removal efficiency. Floc size and shape is an important factor in floc sedimentation (Aguilar *et al.*, 2003). In addition to this, floc effective density and porosity both impact on the settling rate (Gregory, 1997).

The paper presents structural data obtained during the coagulation of a NOM rich water source under optimum conditions for a range of coagulant systems. This evaluation of floc structure includes traditional coagulants such as ferric sulfate and alum. In addition, given the recent emphasis on improving NOM removal, consideration of the flocs formed from more novel treatment options such as polymers and ion exchange resin pre-treatment have been investigated. A high molecular weight cationic polydiallyldimethylammonium chloride polymer with a charge density of 100% (SNF UK Ltd, Castleford, UK) was investigated.

For the ion exchange pre-treatment an anionic magnetic ion exchange resin was used (MIEX®). The background as to the effectiveness of using this particular resin for NOM adsorption has previously been described in Fearing *et al.* (2004) and shows very good potential for NOM removal. MIEX® is a strong base anionic exchange resin of a macroporous structure with active ammonium sites attached around a magnetic centre with a mean particle size of 150 μm. During ion exchange for NOM removal, DOC adsorbs onto the MIEX® in a stirred vessel. After contact time of between 10-30 minutes, rapid separation of solid and liquid may be achieved due to the magnetic properties of the resin resulting in agglomeration into flocs. In addition, the material is of high density which increases sedimentation rates. Downstream coagulation is required in order to remove any suspended material and residual DOC. However, water pre-treated by MIEX® significantly reduces the coagulant demand needed when compared to conventional coagulation.

The overall objective of this paper was to offer a rigorous comparison of NOM flocs formed from different coagulants by measuring the previously described structural parameters.

6(B).2 Materials and methods

6(B).2.1 Treatment options

All experiments were carried out on raw water obtained from a reservoir source in the uplands of Yorkshire, England. The source is typical of a moorland catchment with high colour and dissolved organic carbon (DOC), low turbidity and alkalinity. Flocs were formed using bench scale jar tests. For the traditional ferric and alum coagulants

the raw water was pH adjusted with 1M NaOH (Fisher scientific, Loughborough, UK) and coagulated with either a pre polymerized ferric sulfate (Ferripol, Huntsman Tioxide Europe Ltd, Billingham, UK) or alum (Fisher scientific, Loughborough, UK).

In all coagulation systems the optimum conditions were determined through a series of jar tests to obtain dose and pH for NOM removal and settled turbidity for each system for the subsequent floc diagnostics. During initial removal trials, NOM removal was measured by using UV_{254} as it is an established indicator of the amount of NOM in a sample (Bolto *et al.*, 2002). DOC levels were then found at the optimum doses. The methods of Fearing *et al.* (2004) were followed for MIEX® pre-treatment (Orica, Melbourne, Australia). This involved preparing 200 mL of settled resin volume in measuring cylinders. Resin was left to settle for two hours before adjustment to the required resin volume using a plastic pipette. The resin was then added to the water to be tested in a 10 L stirred vessel to give a concentration of 20 mL L^{-1}. At the end of the allotted time, the treated water was immediately filtered to 0.45 μm using glass fibre filter papers. The water was then coagulated using Ferripol as described above at an optimum dose. The structural characteristics of NOM flocs were compared to turbidity flocs formed from a kaolin suspension at a concentration of 80 mg L^{-1} using Ferripol coagulant.

6(B).2.2 Analytical techniques

Coagulated waters were tested for ultra-violet absorbance at 254 nm (UV_{254}), DOC, settled turbidity and high performance size exclusion chromatography (HPSEC). UV_{254} was measured using a Jenway 6505 UV-Vis spectrophotometer. DOC was measured with a Shimadzu TOC-5000A analyzer. Turbidity was measured using a Hach 2100N turbidimeter. HPSEC analysis was carried out using a Shimadzu VP series high performance liquid chromatogram (HPLC) using UV_{254} detection. The mobile phase was 0.1 M sodium acetate flowing at 1 mL min^{-1}. A TSK-gel G3000SW 7.5 mm (internal diameter (ID)) by 30 cm column was used with a TSK gel 7.5 (ID) mm by 30 mm guard column (Tosoh Biosep GmbH, Stuttgart, Germany). The system was calibrated with source water filtered through ultra filtration membranes at different molecular weight cut-offs.

6(B).2.3 Floc size and breakage

Floc size was measured during the coagulation and flocculation process by coupling a variable speed jar tester (PB-900, Phipps and Bird, Virginia, USA) with a dynamic laser diffraction instrument (Malvern Mastersizer 2000, Malvern, UK). The jar test sequence involved a 200 rpm rapid mix for 90 seconds followed by a slow stir phase at 30 rpm for 15 minutes. For floc breakage experiments, the jar tester was programmed as before, however after the slow stir phase the suspension was exposed to increased shear for a further 15 minutes. Separate experiments were carried out and replicated 3 times at increased shear of 30, 40, 50, 75, 100, 150 and 200 rpm. Particle size was monitored before and after exposure to each level of shear.

6(B).2.4 Floc settling

The settling velocity of falling flocs was measured by direct image capture of individual flocs settling in a constant temperature settling column. Floc aggregates were introduced into the settling column via a tapered entry port to ensure the flocs settled into the centre of the column. In order to avoid thermal currents disrupting floc settlement, the central settling column was enclosed by a water bath. Floc images were captured using a CV M90 colour close-coupled device (CCD) camera (JAI UK Ltd, England). Image analysis software (Image Pro Plus from Media Cybernetics, Maryland USA) was used to determine floc settling velocity. Falling flocs were captured as image sequences. As a focused floc passed in front of the camera, the image grabber was manually triggered to take a series of 10 images. The time between each frame was set at 1 second. This meant that the distance travelled by the floc could be calculated per frame and therefore per time period, thus giving a settling velocity. The projected area of the floc presented in front of the camera was determined using the image analysis software and converted to an equivalent diameter. This standardized diameter was recorded along with its settling velocity for 100 aggregates for each set of coagulation conditions.

6(B).2.5 Microscopy

Qualitative floc structural characteristics were investigated using an Olympus BHB light microscope (Olympus European, Hamburg Germany) and the previously described image-analysis software (calibrated using a microscope graticule). Flocs were placed in an adapted microscope slide consisting of glass slide base with a raised

rubber border with a depth of 3 mm to provide a well to contain whole flocs. The suspension was then secured by placing another microscope slide on top.

6(B).3 Results

6(B).3.1 Treatment options

Optimisation of the coagulant conditions through preliminary jar testing revealed that the highest removals were obtained at different water pH depending on the choice of coagulant. Typical profiles of how the residual turbidity and UV_{254} change with pH at the dose that achieved maximum removals are shown in Figure 6(B).1 and the selected optimum conditions are shown in Table 6(B).1. The initial DOC of the raw water was 8.5 (± 2.5) mg L^{-1} and the UV_{254} was 50.6 (± 2.5) m^{-1}. In the case of the ferric based systems optimum DOC removals of 83, 87 and 87 % were achieved at pH 4.5 for the ferric only, ferric + polyDADMAC and MIEX® + ferric systems respectively. MIEX® pre-treatment showed good DOC removal of 75 % and the subsequent ferric dose could be reduced to 4 mg L^{-1} to achieve similar removals to the higher ferric dose. In comparison, an optimised DOC removal of 72 % was observed when coagulating alum at pH 6.5 and 50% when coagulating with polyDADMAC at pH 6.2. Settled turbidities for all of the optimised systems were between 1-2 NTU.

Comparison of the different treatments using HPSEC showed that the different options removed different MW portions of the NOM (Figure 6(B).2). High MW molecules pass through the HPSEC column at a faster rate than low MW species, therefore the lower peak numbers of the raw water profile are indicative of higher MW relative to the higher peak numbers (Figure 6(B).2a). Through calibration of the column, each of the peaks can be roughly equated to a specific MW range with peaks 1-2 being >5000 Daltons (Da), peaks 3-4 between 2000-5000 Da and peaks 5-6 <2000 Da (Fearing *et al.*, 2004). For each of the treatment options shown in Figure 6(B).2a preferential removal of the high MW organics was seen with poor removal of the low MW compounds. This was especially observed for MW of <2000 Da. The Fe and Fe + polymer had better removals of the 2000-5000 Da organics when compared to Al, whilst the polmer showed poor removal at MW <5000 Da. Comparison of the Ferric and MIEX® systems revealed a significant change in the MW removals (Figure

6(B).2b). The coagulant and ion exchange resin preferentially remove different portions of the NOM with the ion exchange resin removing the medium to low MW's whilst barely impacting on the high MW material (peak 1). When the Fe coagulant was added after MIEX®, the high MW compounds were then subsequently removed. The combined system giving rise to improved NOM removal across all MW's.

Table 6(B).1 Summary of optimum coagulation conditions and removal characteristics.

System	Optimised coagulant dose ($mg.L^{-1}$)	Optimised pH	DOC removal (%)	UV_{254} removal (%)
NOM + Fe	8 (as Fe)	4.5	83	93
NOM + Al	10 (as Al)	6.5	72	81
NOM + poly	10 (as poly)	6.2	50	71
NOM + Fe + poly	8 (as Fe) + 1 as (poly)	4.5	87	90
NOM + MIEX®	20*	5.5	76	77
NOM + MIEX® + Fe	20* + 4 (as Fe)	4.5	87	98
Kaolin + Fe	8 (as Fe)	6	N/A	N/A

*($mL.L^{-1}$)

6(B).3.2 Floc structure

A qualitative visual comparison of typical flocs formed from each of the systems is shown in Figure 6(B).3. It can be seen that the flocs formed using Fe based coagulants were darker in appearance than Al flocs. For the NOM flocs, the MIEX® pre-treated flocs had a more rounded and compact appearance than the other treatment options which appeared to show a more dendritic structure.

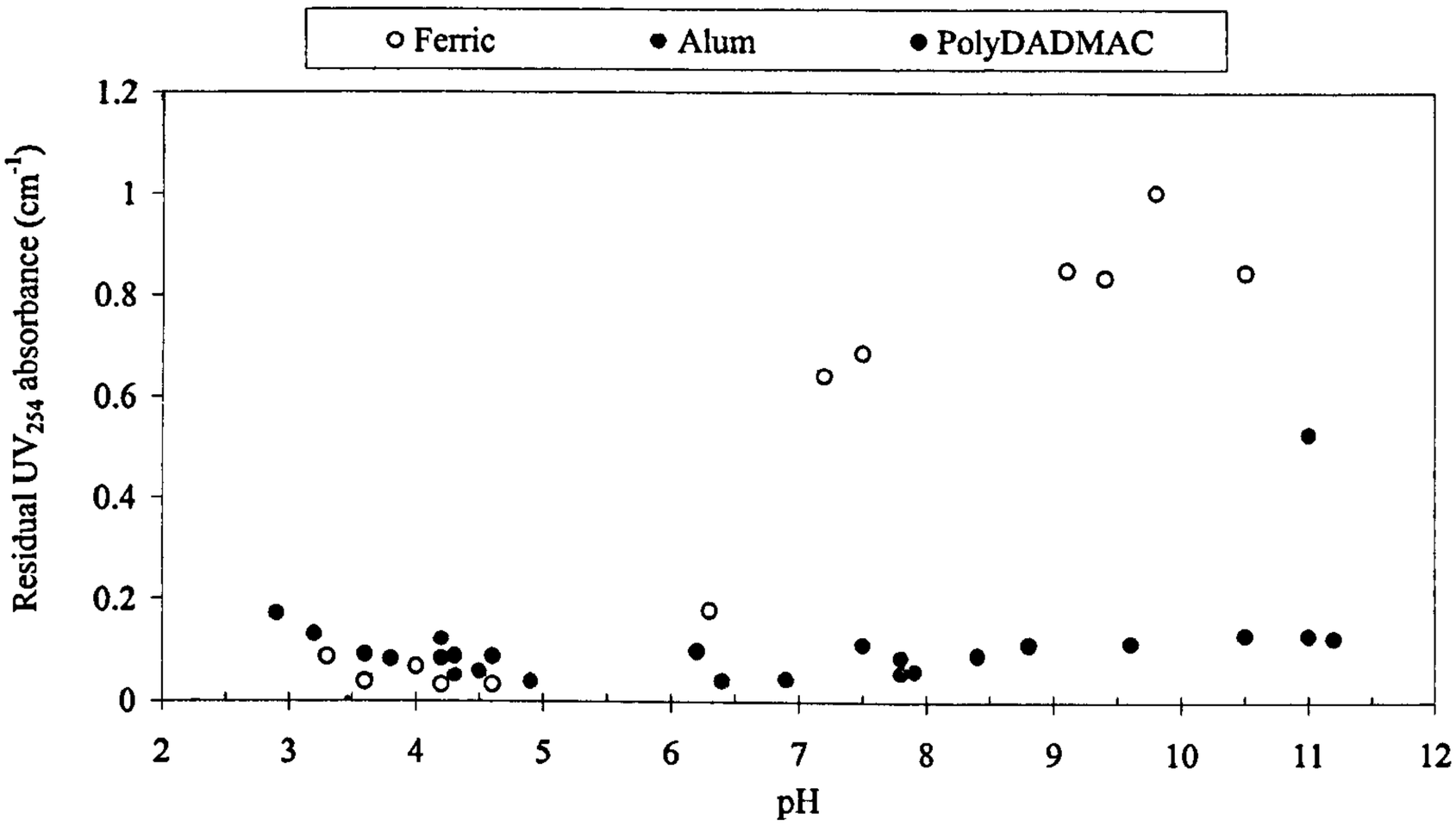

a. UV_{254} residual for the treatment options.

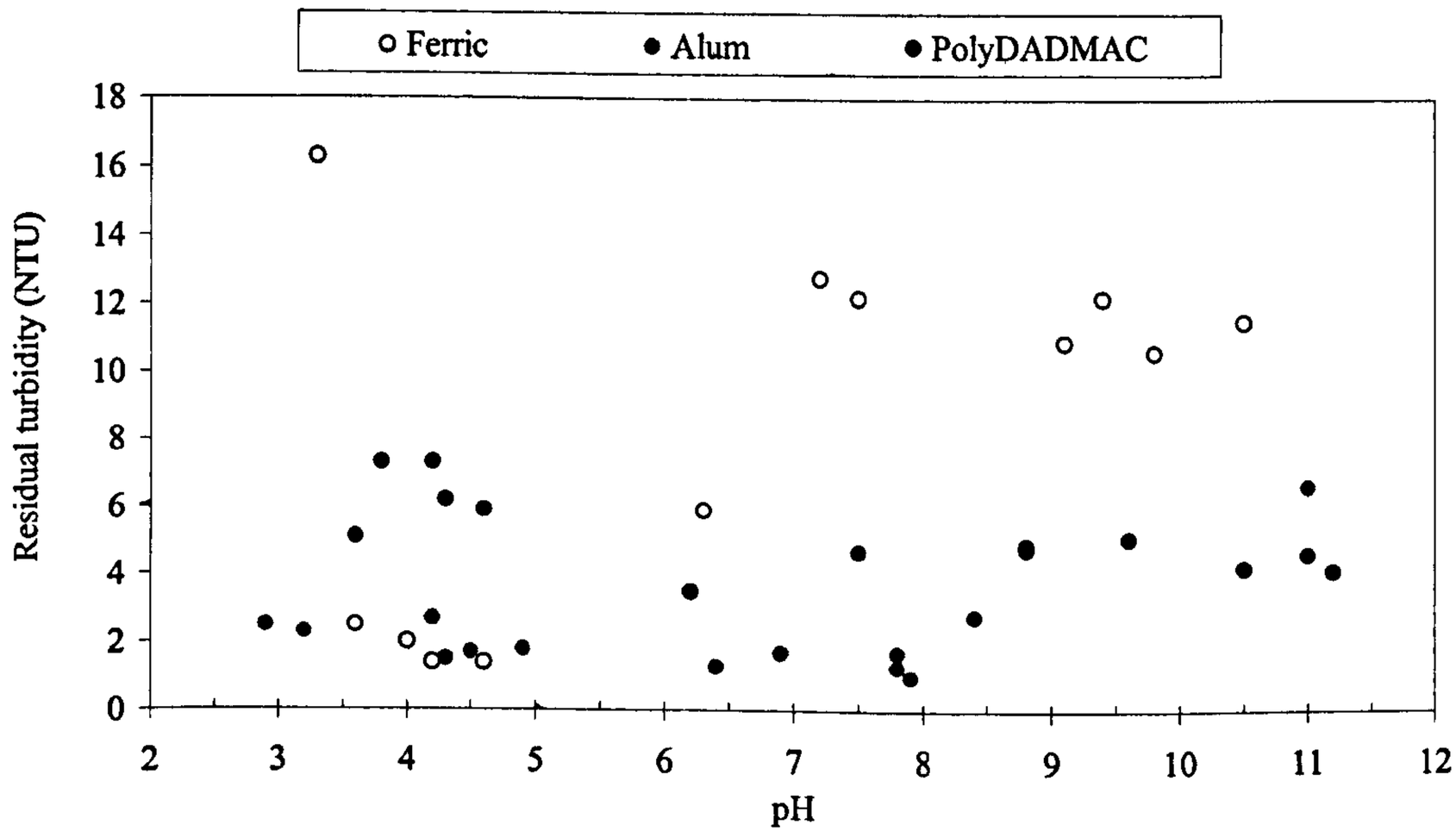

b. Residual turbidity for the treatment options.

Figure 6(B).1 The coagulant optimisation experiments for the different treatment options.

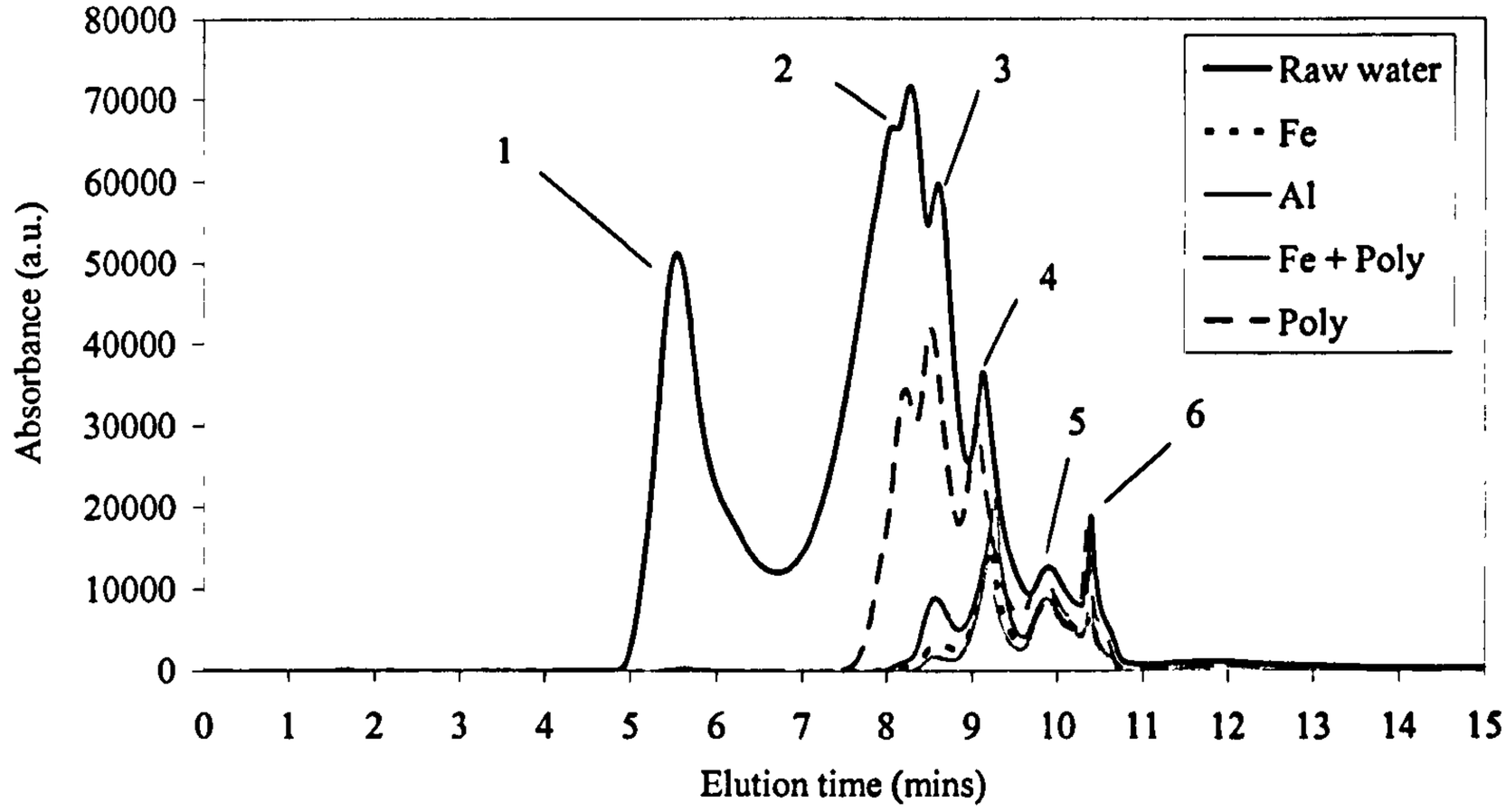

a. HPSEC chromatogram of the raw reservoir water and the treated water using different coagulants.

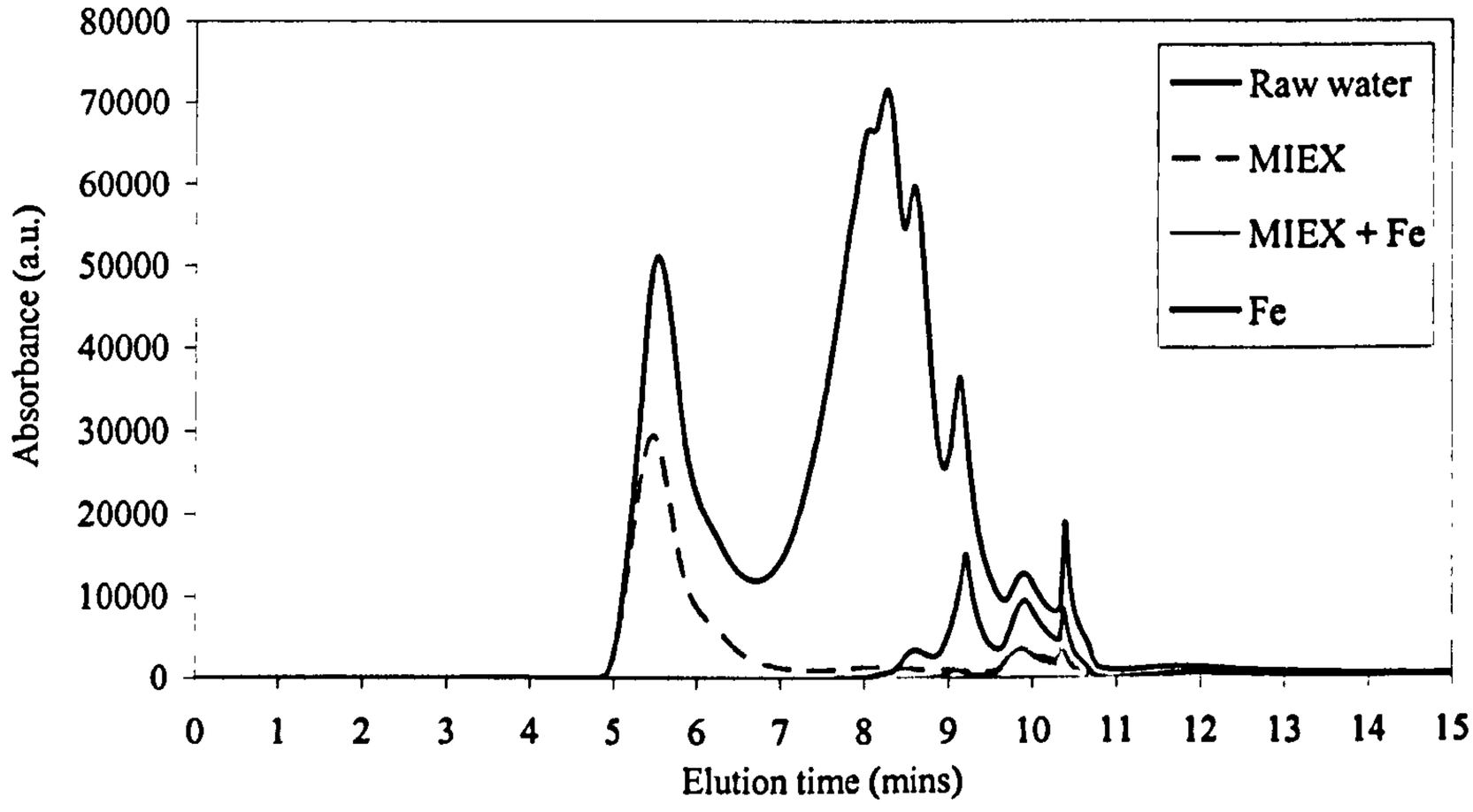

b. HPSEC chromatogram of the MIEX® treated waters compared with the raw water and iron treatments.

Figure 6(B).2 HPSEC chromatogram profiles of the different treatment options.

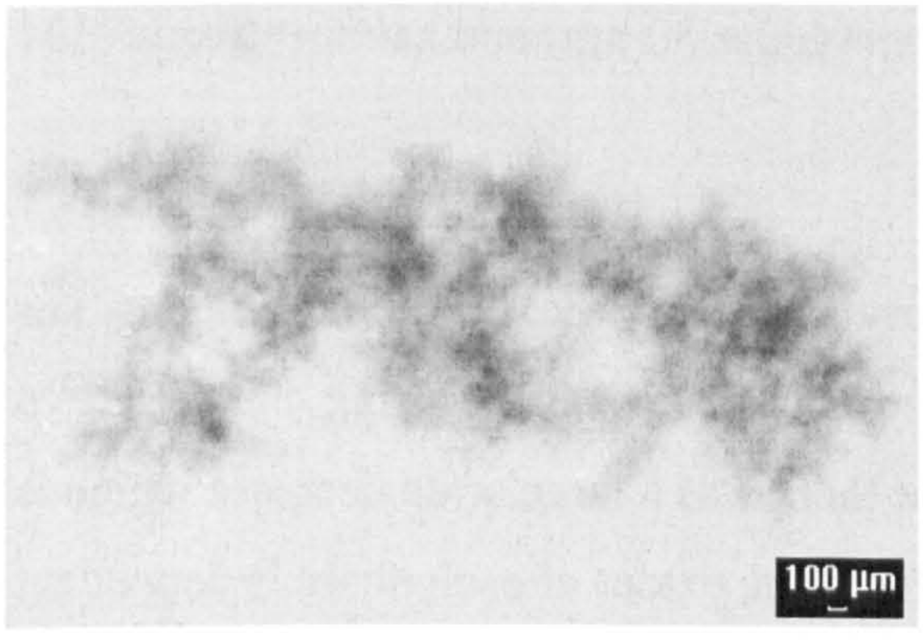

NOM + Fe

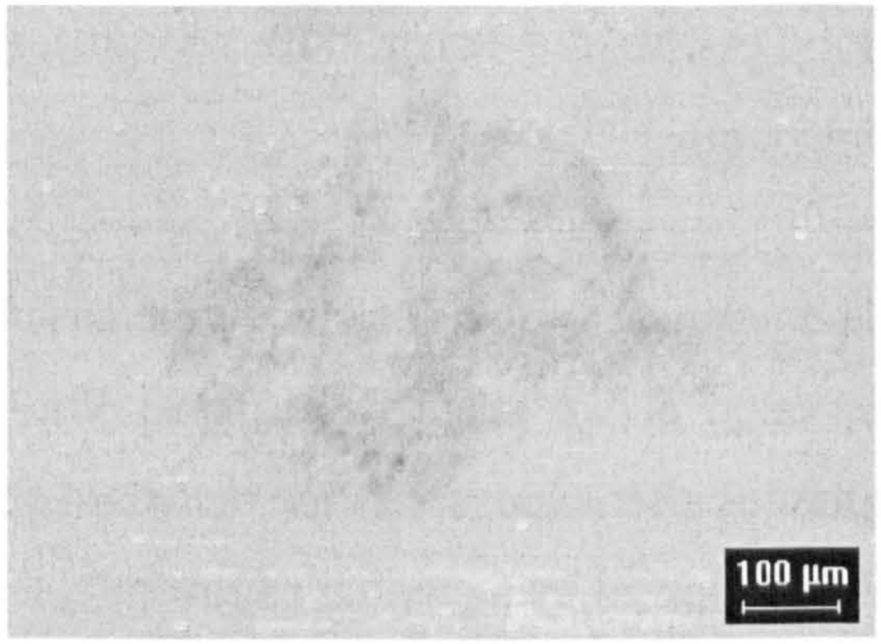

NOM + Alum

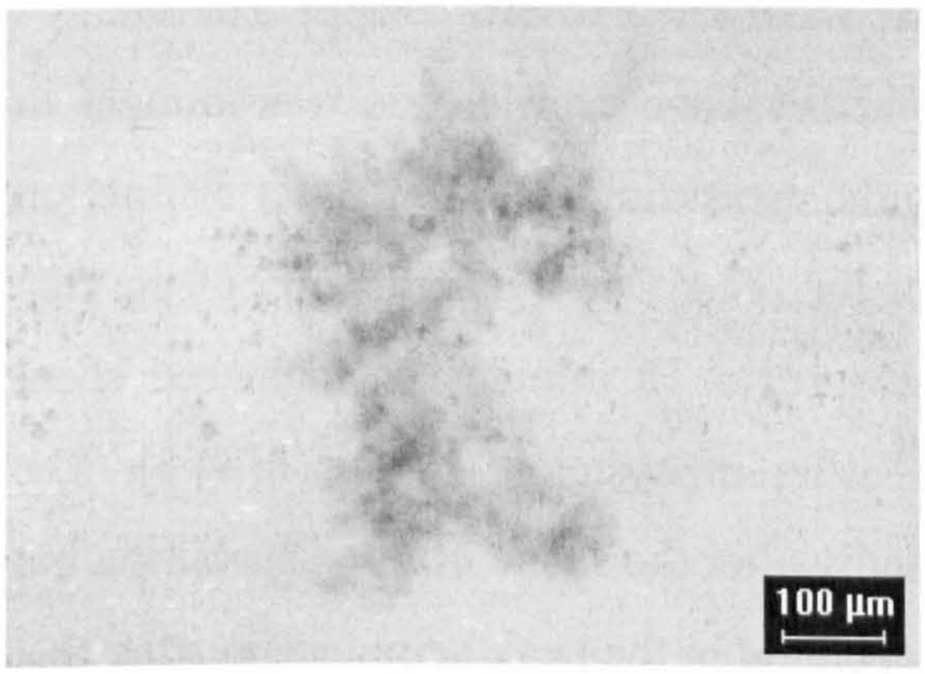

NOM + Fe + Poly

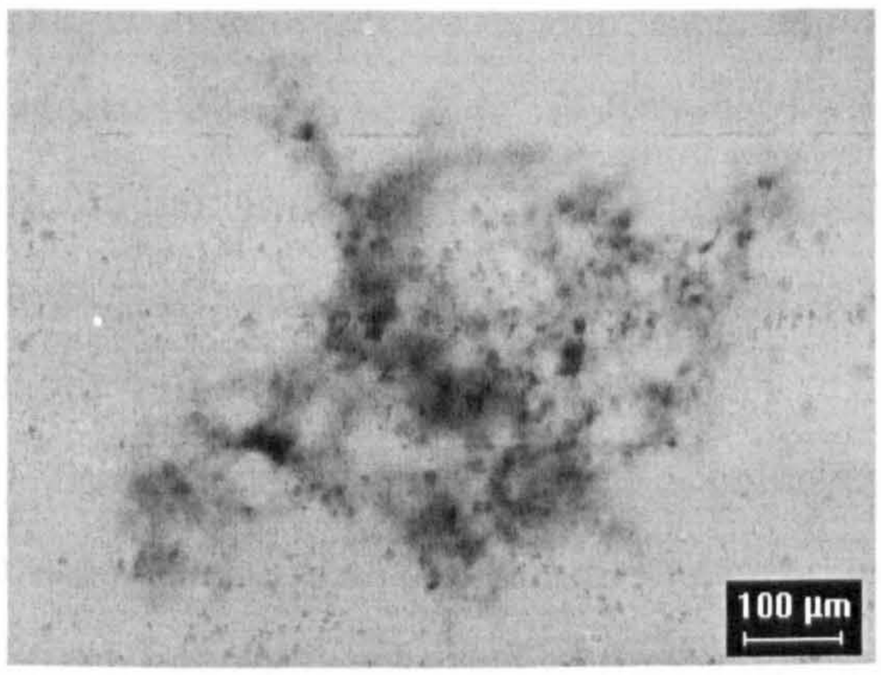

NOM + Poly

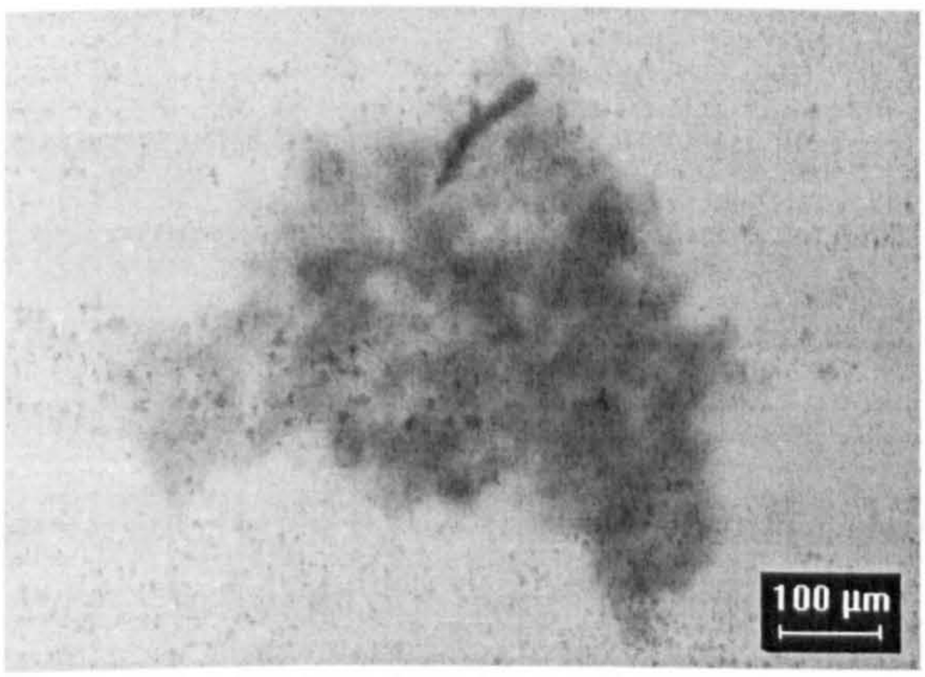

NOM + MIEX® + Fe

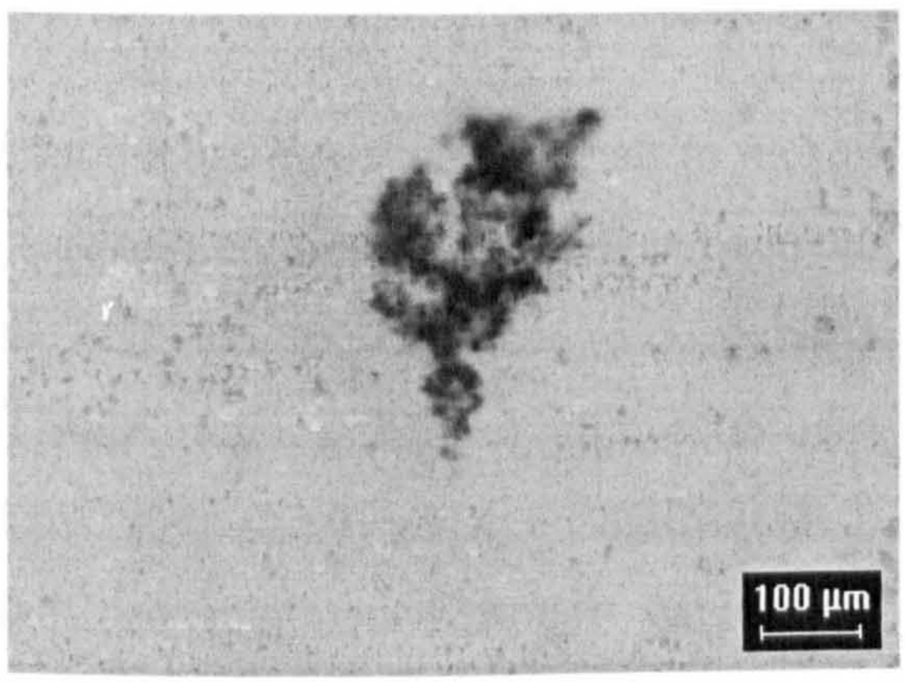

Fe + Kaolin (no NOM)

Figure 6(B).3 Microscope images of typical examples of each type of floc.

6(B).3.3 Floc growth and breakage

Comparison of the floc growth profiles demonstrates that, as expected, the floc size was highly dependent on chemical choice (Figure 6(B).4). The d_{50} floc size after 15 minutes decreased according to the following coagulant system: MIEX® + Ferric (1000 ± 200 µm), polyDADMAC (840 ± 74 µm), Ferric (720 ± 84 µm),

polyDADMAC + Ferric (573 ± 65 μm), Alum (463 ± 30 μm) and kaolin + Ferric (334 ± 15 μm).

The response of the floc size to increased levels of shear after 15 minutes of slow stir revealed a two stage decrease in floc size (Figure 6(B).4). During the first two minutes after exposure to the increased shear there was a large scale decrease which is then followed by a gradual exponential decline. The extent of each phase is dependent on coagulant choice, initial floc size and the imposed shear. For instance in most systems no rapid decline is observed until the shear rate exceeds 50 rpm. The MIEX® pre-treated flocs showed a more inconsistent breakage profile, this was thought to result from these flocs sticking and blocking the measuring cell of the laser diffraction instrument; properties that were not seen for the other flocs. Examination of the floc size distributions before and after the exposure to 15 minutes of increased shear revealed a basic pattern between all the different systems (Figure 6(B).5). The exposure to increased shear did not substantially alter the shape of the distribution but caused a shift in particles sizes and a slight decrease in the peak height suggesting that the effect of shear was consistent across all size classes.

For all of the flocs under investigation, a straight line relationship was seen between the applied shear (rpm) and the floc size on a log-log scale with an R^2 correlation co-efficient between 0.93-0.99 (Figure 6(B).6). The slopes of the lines increased according to the following order: Alum (0.29), polyDADMAC + Ferric (0.32), Ferric (0.47), MIEX® + ferric (0.54), polyDADMAC (0.74) and Kaolin + ferric (0.77). The coefficients reported here suggest that degradation of most of the flocs were dominated by fragmentation mechanisms whilst the kaolin and polyDADMAC flocs were more balanced between fragmentation and erosion mechanisms. For the NOM flocs it was observed that the flocs that were initially larger remained larger until shear of above 100 rpm when floc sizes tended to converge on a common floc size of between 200-300 μm. The exception to this being the MIEX® pre-treated flocs which remained larger at all shear levels.

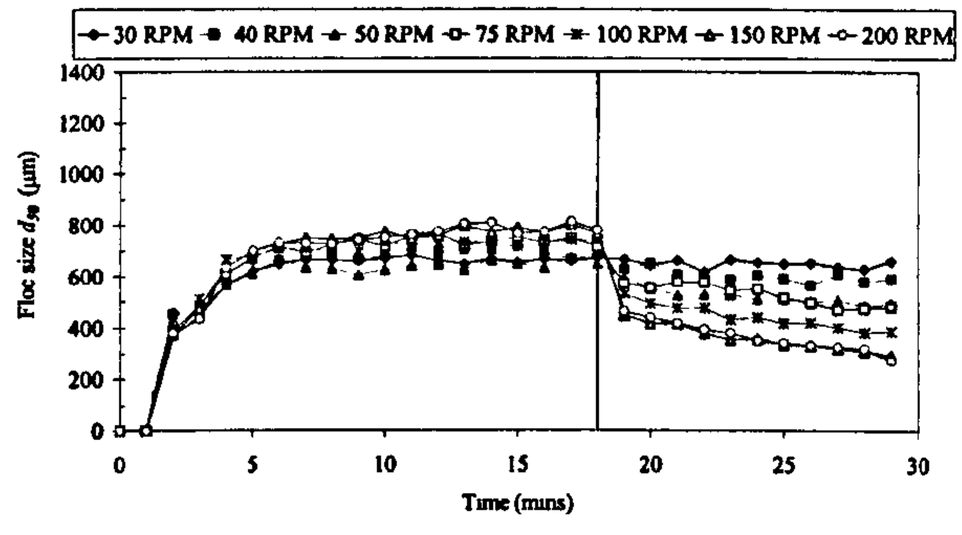

NOM + Fe

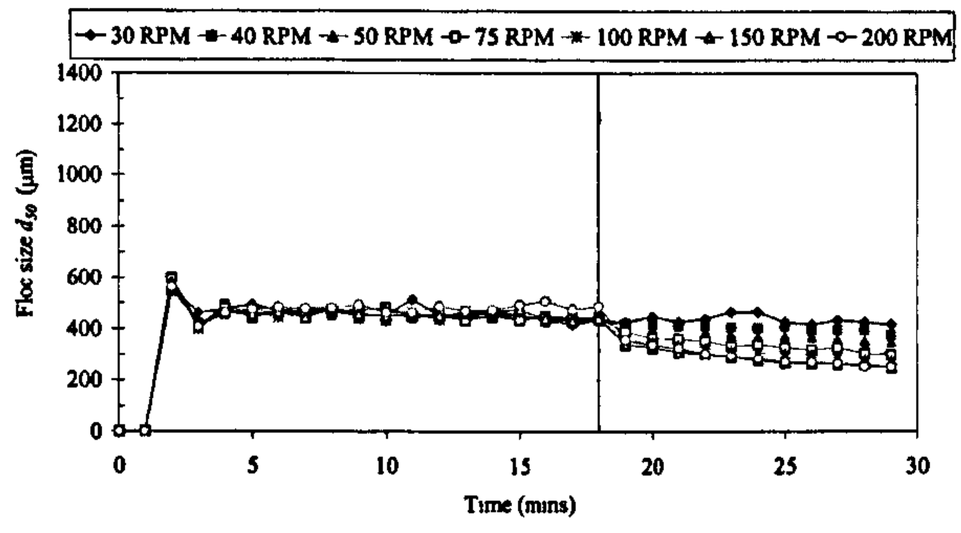

NOM + Al

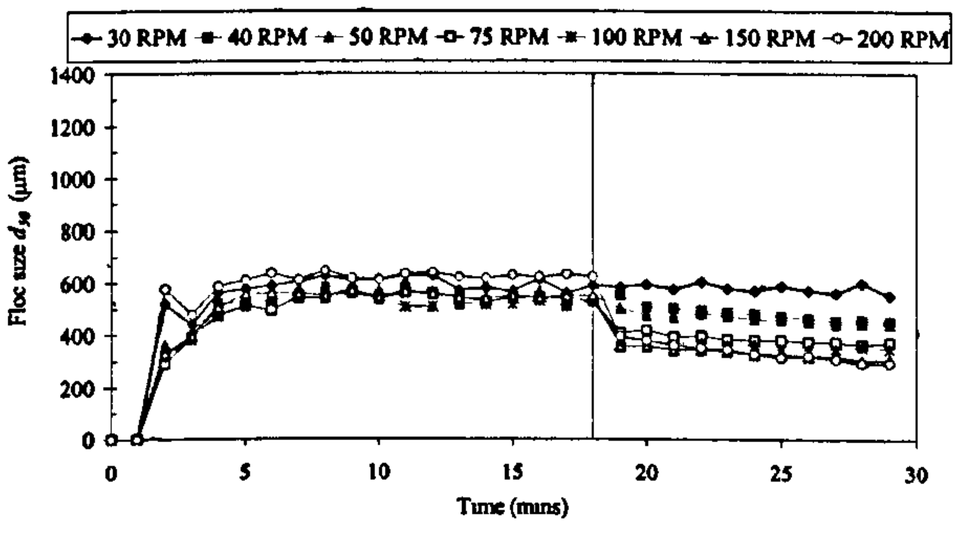

NOM + Fe + Poly

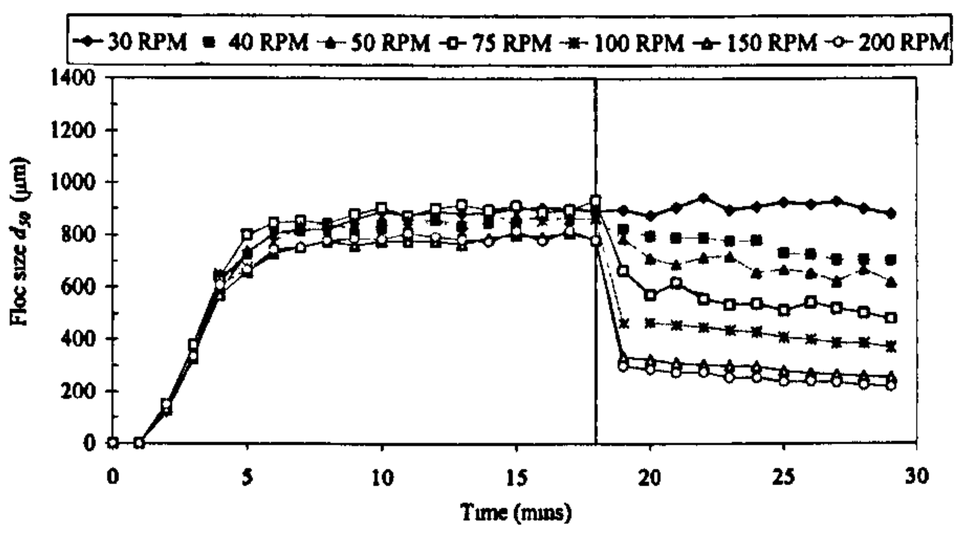

NOM + Poly

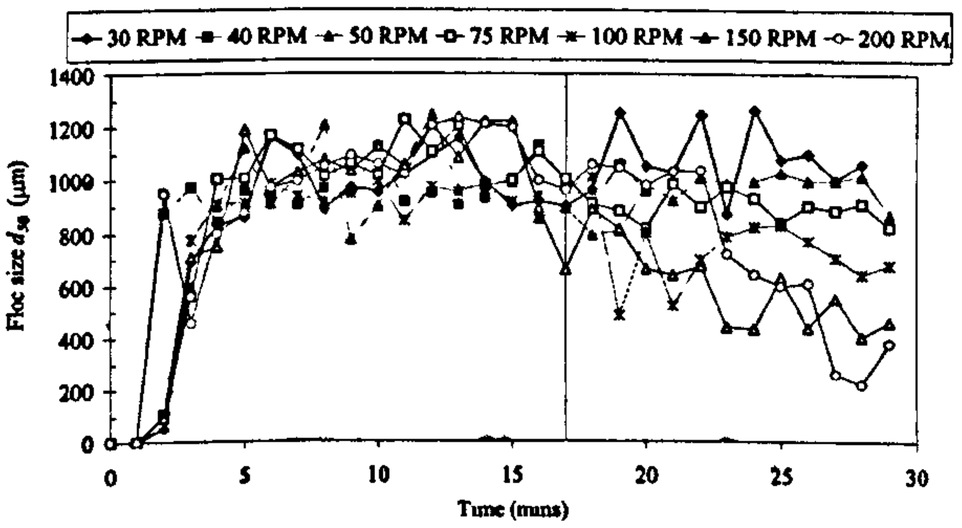

NOM + MIEX® + Fe

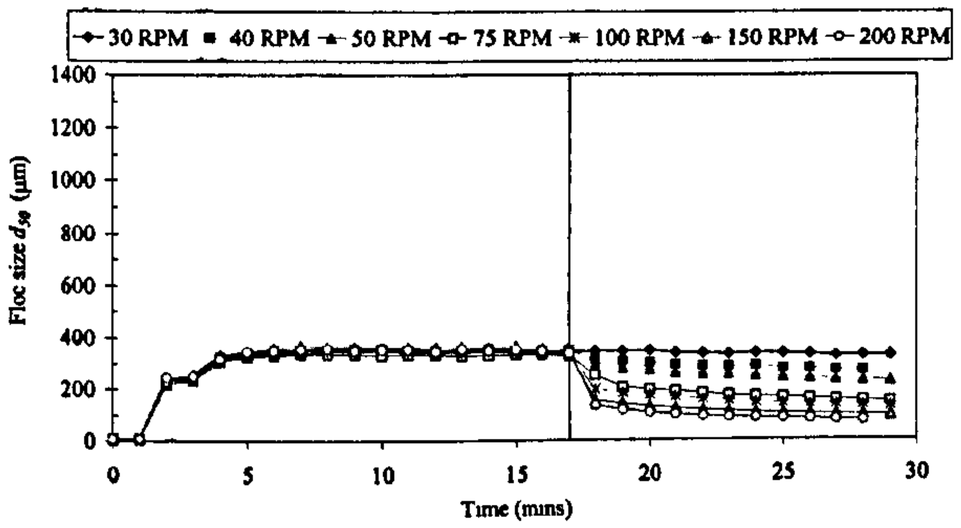

Fe + Kaolin (no NOM)

Figure 6(B).4 Floc growth and breakage patterns for the different coagulated systems. The line indicates the point at which high shear was introduced.

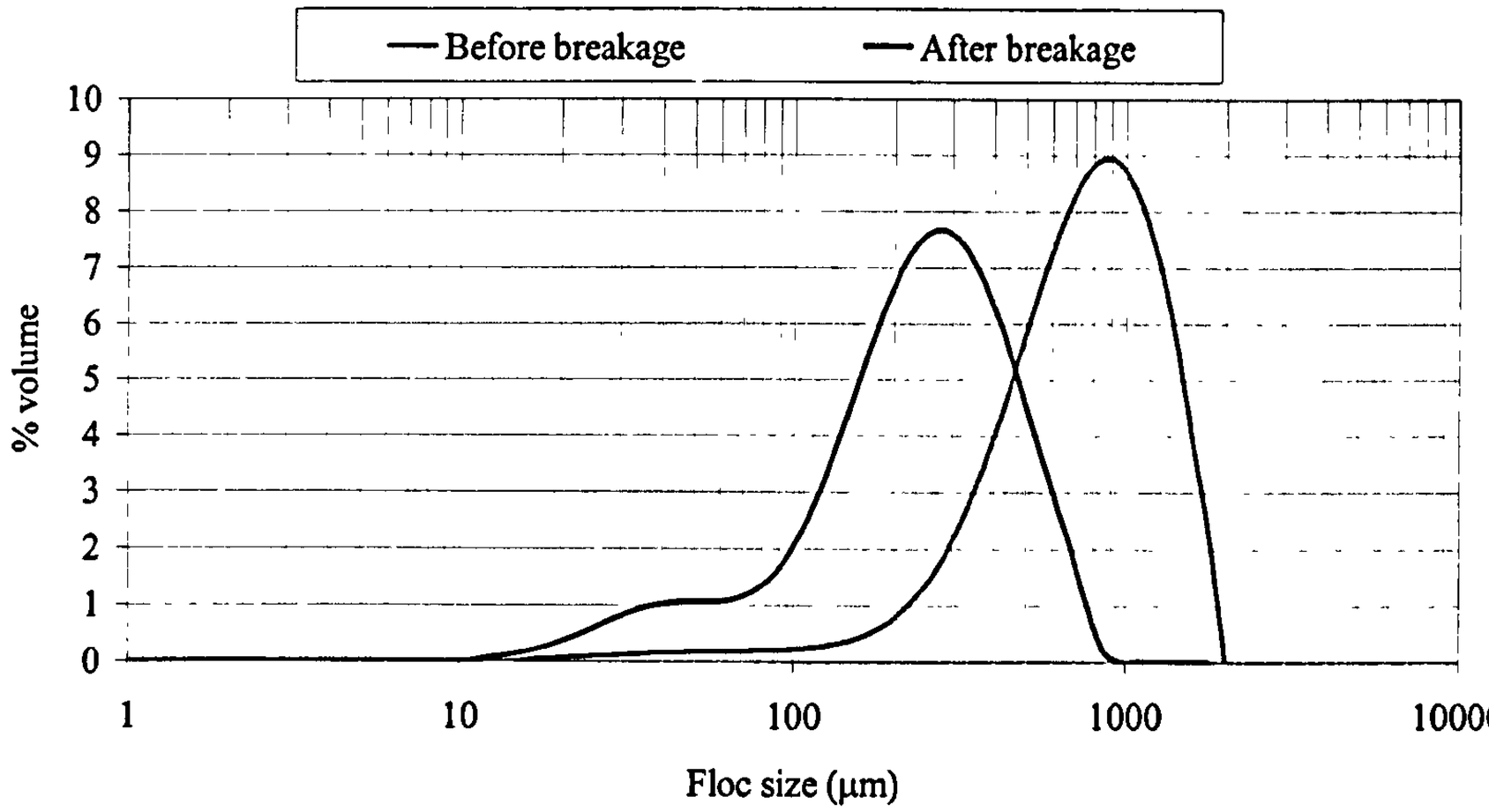

Figure 6(B).5 Typical size distributions before and after breakage at 200 rpm for Fe + NOM system.

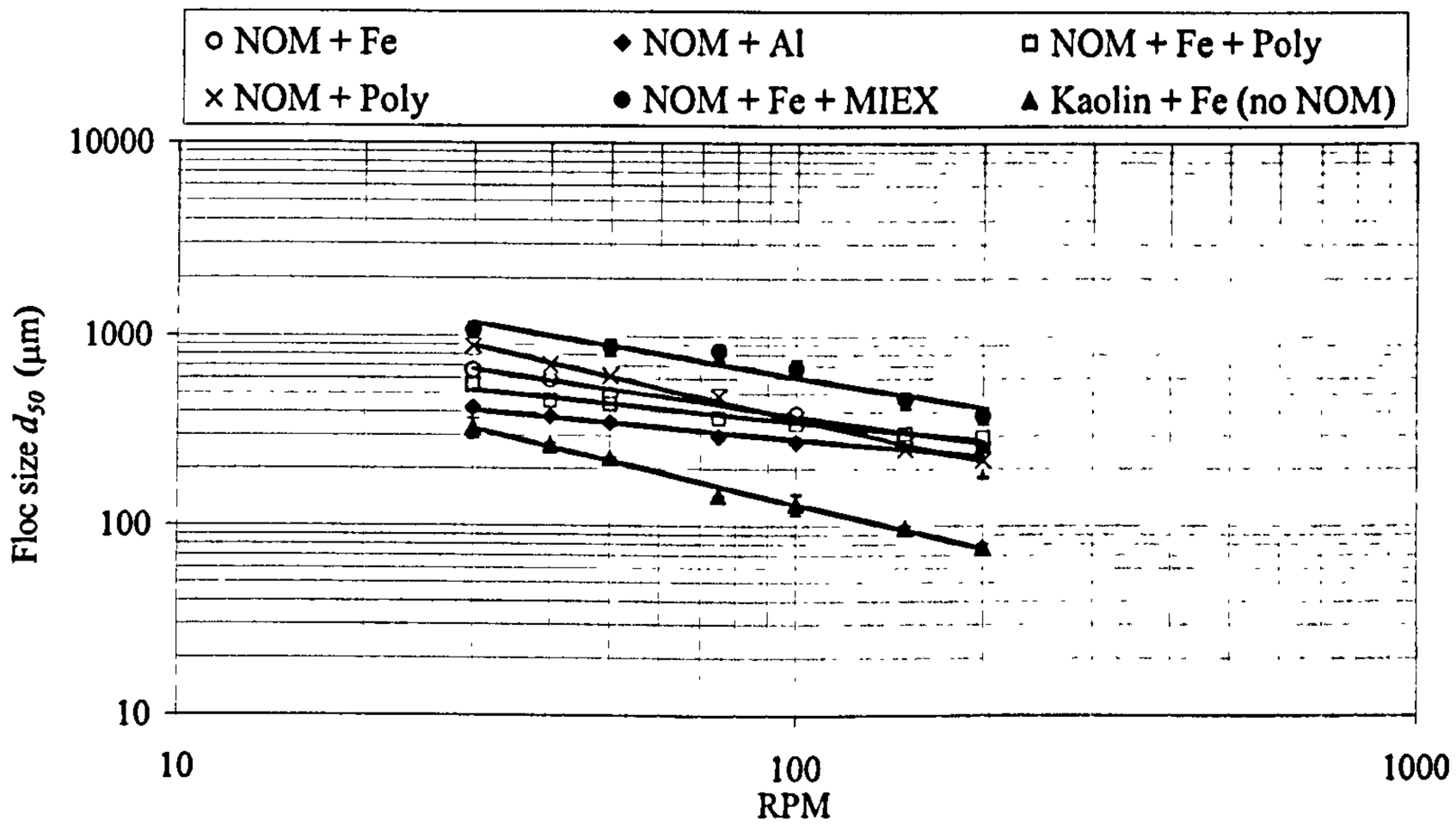

Figure 6(B).6 Strength profiles for the different systems.

6(B).3.4 Settling and structural characteristics

The settling characteristics of the floc systems demonstrated a characteristic log-log relationship between floc size and settling velocity (Figure 6(B).7). One data set missing was for the alum flocs. The contrast difference between the pale, translucent

flocs and the background could not be precisely defined which did not allow the image analysis software to accurately size the floc which prevented the alum data being included in the study. This was despite image analysis enhancements and changes in background lighting conditions. Visual observation of the other data revealed two distinct groups of settling rates. The higher settling rate group included the kaolin + ferric (no NOM) and MIEX® + ferric flocs whilst the slower settling group included the ferric, ferric + polyDADMAC and polyDADMAC flocs. For instance, the settling rate of a typical 500 μm floc generated from the MIEX® + ferric system was 977 μm s^{-1} and 1079 μm s^{-1} for the kaolin compared to 382 μm s^{-1} for the ferric system, 323 μm s^{-1} for polymer and 348 μm s^{-1} for the ferric + polymer (Table 6(B).2). Closer inspection of the data showed that 95 % confidence limits on individual value estimates as predicted by the regression line gave wide intervals. However, the confidence limits of the two identified groups did not cross over for the range of floc sizes investigated, showing that there was a statistical difference between these two sets.

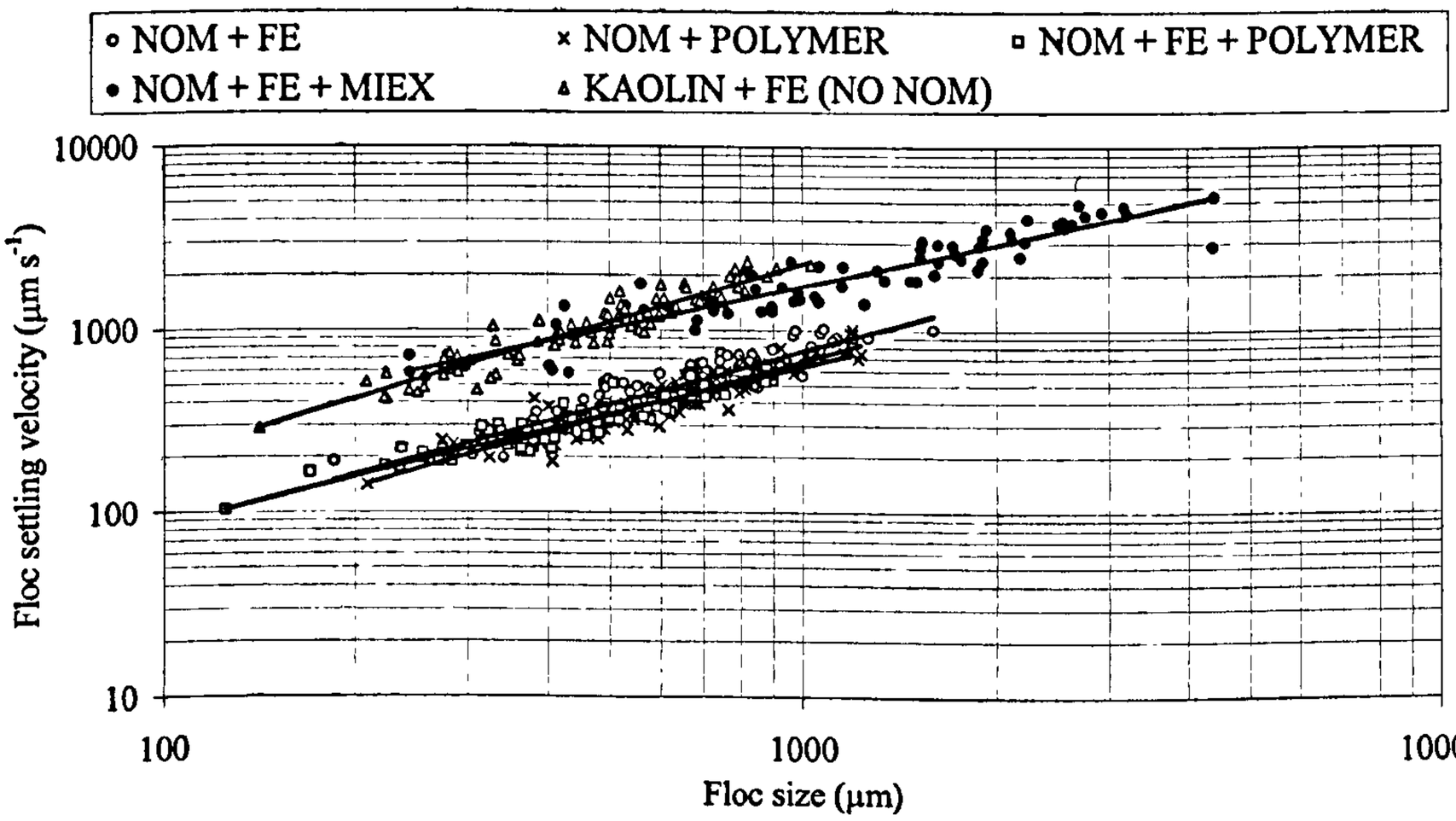

Figure 6(B).7 Settling rates of the different systems under investigation.

Table 6(B).2 Settling velocity ranges for the different floc systems.

System	Settling velocity range (μm s^{-1})	
	500 μm floc (95 % confidence limits)	1000 μm floc (95 % confidence limits)
NOM + Fe	382 (276-531)	793 (570-1101)
NOM + Al	N/A	N/A
NOM + poly	323 (241-458)	682 (509-973)
NOM + poly + Fe	348 (270-447)	659 (509-851)
NOM + MIEX® + Fe	977 (641-1489)	1698 (1135-2616)
Kaolin + Fe	1079 (807-1445)	2333 (1734-3140)

6(B).4 Discussion

A ranking of the floc properties from the different coagulated systems at optimised coagulant doses revealed that the different treatment options gave rise to some very different floc properties (Table 6(B).3). Both the increased size of the initial and broken flocs of the MIEX® + Fe treatment suggested that these flocs were the strongest and the NOM floc strength was of the following order: MIEX® + Fe > Polymer > Fe > Fe + Poly > Al. The MIEX® + Fe flocs also showed improved floc settling characteristics over the systems. The marked difference in the properties of MIEX® pre-treated flocs over the other treatment systems was surprising. For example, after ion exchange pre-treatment the flocs had a settling rate close to that of kaolin flocs despite the density of the kaolin used in this study being 2600 kg m^{-3} whilst humic material is estimated to have a density of 1750 kg m^{-3} (Hossain and Bache, 1991). The use of ion exchange for the removal of NOM has been previously been shown as a good alternative to coagulation for NOM removal (Bolto *et al.*, 2002). However, it has also been shown that combining ion exchange with conventional coagulation has been shown to give rise to improved NOM removal, particularly of recalcitrant organics (Fearing *et al.*, 2004). This is of current importance given the evermore strict control of disinfection by-products in North America, Australasia and Europe. This study has presented evidence showing that ion-exchange pre-treatment

combined with conventional coagulation can give rise to improved NOM floc structure, the knowledge of which may be of potential operational consequence.

Table 6(B).3 Ranking of different NOM floc properties from the different treatment options.

Parameter	Highest				Lowest
DOC Removal	Fe	≈Fe + Poly	≈MIEX® + Fe	Al	Poly
Size	MIEX® + Fe	Poly	Fe	Fe + Poly	Al
Strength	MIEX® + Fe	Poly	Fe	Fe + Poly	Al
Re-growth	MIEX® + Fe	Al	Fe	≈Fe + Poly	≈Poly
Settling rate	MIEX® + Fe	Fe	≈Poly		≈Fe + Poly

≈means values were similar to previous system

Previous trials have indicated that as the organic fraction in a NOM-Fe floc decreases the floc size and settling rate are seen to increase to a maximum at 0 NOM concentration (Jarvis *et al.*, 2004). Given that the organic concentration was reduced by 70 % after ion exchange this effect was thought to explain this phenomenon at least in part. However the increase in size and settling rate of the MIEX® + Fe flocs in this study was considerably above that seen in Jarvis *et al.*, 2004 suggesting that other factors were also important.

Analysis of the HPSEC chromatograms showed that the ferric coagulant preferentially removed the high and medium MW compounds whilst the ion exchange preferentially removed the medium to low MW compounds. This meant that after MIEX® pre-treatment only the high MW organics were incorporated into the floc matrix. Without ion exchange pre-treatment the full range of MW compounds were contained within the floc matrix and it is this difference that provides an explanation for the change in properties when compared to the other treatment options. The Fe, Fe + poly and Al treatments showed good all round removals for all organics other than the small MW compounds, whilst the polymer used alone also showed poor removal of the medium MW organics. The polymer flocs were the next biggest flocs to the MIEX® + Fe flocs. Polymer bridging may in part explain the increased floc size and strength seen for the polymer flocs (Gregory and Dupont, 2001). However, the absence of the medium to

low MW compounds in the floc matrix was also likely to be a contributory factor given the differences in floc structure seen for the MIEX® + Fe floc. The specific nature of these medium and low MW compounds was not identified in this study, but the nature of organics has been shown to have a significant impact on floc structure (Vilge-Ritter *et al.*, 1999). However, further investigation of medium and low MW NOM compounds is necessary in order to see whether this was a site specific effect or is applicable to all NOM rich waters.

The use of ferric and alum based coagulants have traditionally been favoured as the principal chemicals of choice at WTW throughout the world (Johnson and Amirtharajah, 1983). It is therefore useful to compare the properties of the NOM flocs formed from these coagulants. The results of this work have shown that the ferric based coagulant gave better floc structural characteristics than alum in terms of floc size and resistance to shear. The main coagulation mechanisms for the removal of NOM using traditional metal salts is the precipitation of metal-NOM complexes by charge neutralization and the adsorption of NOM onto precipitates of either metal hydroxide or the complexation products (Dempsey *et al.*, 1984; Dennett *et al.*, 1996; Gregor, 1997; Vilgé-Ritter *et al.*, 1999). There is little evidence in the literature to explain the difference in floc properties of the alum and ferric systems. The situation is complicated as a myriad different molecules exist which can form different initial micro flocs with each coagulant. Previous comparisons of ferric and alum coagulants suggest that they operate in a similar manner and are of a similar coagulant efficacy (Johnson and Amirtharajah, 1983). In addition the precipitates of the metal hydroxides have similar surface areas and particle size (Bache, 2004). Speciation products for Al and Fe consist of similar hydrated monomers, dimers, trimers and larger polymers which operate in a similar way (Cheng and Chi, 2002). In this study the alum and ferric operated at optimum removals at pH 6.5 and pH 4.5 respectively, typical values seen previously for NOM removal using alum and ferric coagulants (Dennett *et al*, 1996; Edzwald and Tobiason, 1999; Armitharajah and O'Melia, 1999). Coagulation pH may therefore play a significant role in the floc structure as it has been seen to give rise to more loosely connected NOM aggregates with increasing pH (Vilge-Ritter, 1999). Increased deprotonation of organic molecules at high pH give rise to increased electrostatic repulsion within Fe-NOM flocs leading to a more open and a weaker floc as a result. However, this effect has not been previously seen for Al-NOM flocs when

lowering the coagulation pH from the optimum conditions led to slow forming small flocs with poor settling characteristics (Gregory and Carlson, 2003). It is therefore at present unclear why the two coagulants give rise to different floc characteristics, however the results of this study lead to the recommendation of the use of ferric coagulants over alum for NOM coagulation due to the improved removals and floc structure seen.

Polymers are traditionally used in combination with conventional coagulants as an aid to improve floc structure by increasing floc size, strength and settleability (Lee *et al.*, 1999; Bolto *et al.*, 2001). In the current study the Fe-NOM flocs coagulated with and without polyDADMAC showed that the polymer reduced the strength of the floc with a corresponding decrease in size and settleability. Added after the primary coagulant polymers work by bridging together primary particles (Bratby, 1980). However, quaternary ammonium polymers such as polyDADMAC that are of high MW and charge density operate better as a primary coagulant operating like conventional coagulants rather than a floc aid (Bolto *et al.*, 2001). In terms of floc structure, the use of polymer as a primary coagulant did improve floc strength and size but offered no improvement in floc settling rate and crucially showed much reduced organic removal than for the other treatment options. Therefore it was established that the high MW cationic polymer used in this study offered no overall benefit as a floc aid or as a primary coagulant.

The response of flocs to increases in shear is of particular operational significance. After they have been formed, flocs are exposed to a range of shear stresses such as high shear regions around impellers of flocculators or transfer over ledges and weirs (McCurdy *et al.*, 2004). Flocs must resist these stresses in order to prevent breakage. It was observed that the initially larger NOM flocs tended to break proportionally greater than the smaller NOM flocs (as reflected by a higher value of the degradation curve) but still maintained larger broken floc sizes until the flocs approached a common value at very high shear. This is in agreement with data presented by Bache and Rasool (2001) for a range of Al-NOM flocs formed from low alkalinity, low turbidity and highly coloured waters at different water treatment works. The implications of this being that coagulation regimes can be tailored to potentially meet criteria for downstream processes as well as the primary coagulation and flocculation

stage. For example in unit processes which are likely to expose NOM flocs to very high shear (i.e. an equivalent to >150 rpm) such as dissolved air flotation the control of floc size is not important as larger flocs will be broken to the same size regardless of any increase in the relative strength of smaller flocs. This is because the average velocity gradient in a jar tester at 150 rpm is less than 100 s^{-1} (Bouyer *et al.*, 2001), whilst in a DAF unit estimates are around 1000 s^{-1} (Bache and Rasool, 2003). This high shear will break even the strongest flocs to similar sizes. Whereas for low shear settling processes coagulation regimes that generate large flocs should be preferred due to the operational benefits during solid-liquid separation as increased floc size gives rise to increased sedimentation rates (Aguilar *et al.*, 2003) and improves particle transport mechanisms during removal in filtration (Cleasby, 1999).

6(B).5 Conclusions

A range of treatment options were evaluated in terms of the floc structural properties resulting from optimum coagulant doses based upon NOM removal and settled turbidities. Coagulation with ferric after ion exchange pre-treatment gave rise to a significant improvement in floc size, strength and settling rate when compared to single stage ferric coagulation and the other treatment options investigated. It was believed that the removal of specific MW compounds prior to ferric coagulation gave rise to the change in floc properties. Comparison of conventional alum and ferric coagulants showed that ferric flocs were on average larger and stronger than the alum flocs. This combined with the improved NOM removals seen with ferric suggests that the ferric based coagulant should be used for NOM removal at WTW. The use of the polyDADMAC polymer as a floc aid did not improve floc structure and when used as a primary coagulant gave good floc structure but the poor comparative NOM removals would likely preclude its operational use.

6(B). 6 References

Aguilar, M. I., Saez, J., Llorens, M., Soler, A. and Ortuno, J. F. (2003) Microscopic Observation of Particle Reduction in Slaughterhouse Wastewater by Coagulation-Flocculation Using Ferric Sulphate as Coagulant and Different Coagulant Aids. *Water Research* **37** 2233-2241.

Amirtharajah, A. and O'Melia, C. R. (1999) Coagulation Processes: Destabilisation, Mixing and Flocculation. In: *American Water Works Association Water Quality and Treatment: a Handbook of Community Suppliers*. McGraw-Hill, New York.

Bache, D. H. (2004). Floc Rupture and Turbulence: a Framework for Analysis. *Chemical Engineering Science* **59** 2521-2534.

Bache, D. H. and Papavasilopoulos, E. N. (2003) Dewatering of Alumino-Humic Sludge: Impacts of Hydroxide. *Water Research* **37** 3289-3298.

Bache, D. H., Johnson, C., McGilligan, J. F., and Rasool, E. (1997) A Conceptual View of Floc Structure in the Sweep Floc Domain. *Water Science and Technology* **36** (4), 49-56.

Bache, D. H. and Rasool, E.R. (2001) Characteristics of Alumino-Humic Flocs in Relation to DAF Performance. *Water Science and Technology* **43** (8), 203-208.

Bache, D. H., Rasool, E., Moffatt, D., and McGilligan, F. J. (1999) On the Strength and Character of Alumino-Humic Flocs. *Water Science and Technology* **40** (9), 81-88.

Biggs, C. A. and Lant, P. A. (2000) Activated Sludge Flocculation: On-Line Determination of Floc Size and the Effect of Shear. *Water Research* **34** 2542-2550.

Bolto, B., Dixon, D., Eldridge, R. and King, S. (2001) Cationic Polymer and Clay or Metal Oxide Combinations for Natural Organic Matter Removal. *Water Research* **35** 2669-2676.

Bolto, B., Dixon, D., Eldridge, R, King, S. and Linge, K. (2002) Removal of Natural Organic Matter by Ion Exchange. *Water Research* **36** 5057-5065.

Bottero, J. Y., Tchoubar, D., Axelos, M. A., Quienne, P and Fiessinger, F. (1990) Flocculation of Silica Colloids with Hydroxy Aluminium Polycations. Relation Between Floc Structure and Aggregation Mechanisms. *Langmuir* **6** 596-602.

Bouyer, D., Line, A., Cockx, A. and Do-Quang, Z. (2001) Experimental Analysis of Floc size Distribution and Hydrodynamics in a Jar Tester. *Transactions of the Institute of Chemical Engineers* **79** (A), 1017-1024.

Bratby, J. (1980) *Coagulation and Flocculation*. Uplands Press Ltd, Croydon, UK.

Cheng, W. P. and Chi, F. H. (2002). A Study of Coagulation Mechanisms of Polyferric Sulfate Reacting with Humic Acid using a Fluorescence-Quenching Method. *Water Research* **36** 4583-4591.

Cleasby, J. L. (1999) Filtration, In: AWWA Water Quality and Treatment: a Handbook of Community Suppliers; McGraw-Hill, New York, 269-365.

Dempsey, B. A., Ganho, R. M., and O'Melia, C. R. (1984) The Coagulation of Humic Substances by Means of Aluminium Salts. *Journal of the American Water Works Association* **76** (4), 141-150.

Dennett, K. E., Amirtharajah, A., Moran, T. F., and Gould, J. P. (1996) Coagulation: Its Effect on Organic Matter. *Journal of the American Water Works Association* **88** 129-142.

Duan, J. and Gregory, J. (2002) Coagulation by Hydrolysing Metal salts. *Advances in colloid and interface science* **100-102** 475-502.

Fearing, D. A., Banks, J., Guyetand, S., Eroles, C. M., Jefferson, B., Wilson, D., Hillis, P., Campbell, A. T. and Parsons, S. A. (2004) Combination of Ferric and MIEX® for the treatment of humic rich waters. *Water Research* **38** 2551-2558.

Francois, R. J. (1987) Strength of Aluminium Hydroxide Flocs. *Water Research* **21** 1023-1030.

Gregory, D. and Carlson, K. (2003) Relationship of pH and Floc Formation Kinetics to Granular Media Filtration Performance. *Environmental Science and Technology* **37** 1398-1403.

Gregory, J. (1997) The Density of Particle Aggregates. *Water Science and Technology* **36** (4), 1-13.

Gregory, J. and Dupont, V. (2001) Properties of Flocs Produced by Water Treatment Coagulants. *Water Science and Technology* **44** 231-236.

Hossain, M. D. and Bache, D. H. (1991) Composition of Alum Flocs Derived from a Coloured, Low Turbidity Water. *Journal of Water Supply: Research and Technology - AQUA* **40** (5), 298-303.

Jarvis, P., Jefferson, B. and Parsons, S. A. (SUBMITTED) How the Natural Organic Matter to Coagulant Ratio Impacts on Floc Operational Properties. Submitted to *Water Research* 2004.

Johnson, P. N. and Amirtharajah, A. (1983) Ferric Chloride and Alum as Single and Dual Coagulants. *Journal of the American Water Works Association* **May** 232-239.

Lee, J. F., Liao, P. M., Tseng, D. H., and Wen, P. T. (1998) Behaviour of Organic Polymers in Drinking Water Purification. *Chemosphere* **37** 1045-1061.

McCurdy, K., Carlson, K. and Gregory, D. (2004) Floc Morphology and Cyclic Shearing Recovery: Comparison of Alum and Polyaluminium Chloride Coagulants. *Water Research* **38** 486-494.

Parker, D. S., Kaufman, W. J., and Jenkins, D. (1972) Floc Breakup in Turbulent Flocculation Processes. *Journal of the Sanitary Engineering Division: Proceedings of the American Society of Civil Engineers* **SA 1** 79-99.

Vilgé-Ritter, A., Rose, J., Masion, A., Bottero J.-Y. and Lainé, J.-M. (1999) Chemistry and Structure of Aggregates Formed with Fe-salts and Natural Organic Matter. *Colloids and Surfaces A: Physicochemical and Engineering Aspects* **147** 297-308.

Yukselen, M. A. and Gregory, J. (2004) The Reversibility of Floc Breakage. *International Journal of Mineral Processing* **73** 251-259.

CHAPTER 7

THE BREAKAGE, RE-GROWTH AND FRACTAL NATURE OF NOM FLOCS

Submitted to *Environmental Science and Technology.*

7 THE BREAKAGE, RE-GROWTH AND FRACTAL NATURE OF NOM FLOCS

PETER JARVIS, BRUCE JEFFERSON and SIMON A. PARSONS

School of Water Sciences, Building 39, Cranfield University, Cranfield, Bedford, MK40 0AL, United Kingdom

Abstract

The growth, breakage, re-growth and fractal nature of flocs was investigated using a laser diffraction particle sizing device. A range of coagulants were investigated for the coagulation of natural organic matter (NOM) and compared to other coagulated systems. The results showed NOM floc structural characteristics varied in steady state size depending upon which coagulant was used. When compared to other systems, the order of floc size was Fe precipitate > Fe-NOM > latex (in NaCl solution). Floc re-growth after exposure to high shear was limited for all of the flocs under investigation other than for latex in an inert electrolyte. This highlighted differences in the internal bonding structure of flocs, with the results suggesting that physical bonds have a capacity to re-form after breakage. Fractal dimension analysis using small angle laser light scattering (SALLS) had limited applicability to large flocs that dominated all of the systems under investigation, but the degree of compaction increased as flocs were broken in high shear. This provided a possible mechanistic reason for the irreversible breakage seen.

Keywords

Coagulation; floc breakage; floc re-growth; fractal dimension; natural organic matter.

7.1 Introduction

Coagulation and flocculation remains the most common process used for the removal of turbidity particles and natural organic matter (NOM) at water treatment works (WTW). Whilst the major removal mechanisms of these pollutants during coagulation and flocculation has been well studied, little thought is generally given to the fundamental floc operational parameters. These include physical properties such as floc size, compaction and strength. One property that may have a significant impact at a WTW is the potential for flocs to re-grow after being broken. Unit processes at WTW are generally designed to minimize floc breakage, however often in practice this is not the case, with regions of high shear being prevalent (McCurdy *et al.*, 2004). This may include areas around the impeller zone of flocculating tanks or transfer over weirs and ledges. A capacity to re-grow may improve subsequent floc removal process efficiency if broken flocs are subsequently allowed to re-form during further particle-particle contact. The relative breakage and re-growth of different flocculated systems have previously been compared using floc strength and breakage factors (Francois, 1987; Fitzpatrick *et al.*, 2003; Yukselen and Gregory, 2004) which may be calculated from (Equation 7.1 and 7.2):

$$Strength\ factor = \frac{d(2)}{d(1)} \times 100 \qquad \text{Equation 7.1}$$

$$Recovery\ factor = \frac{d(3) - d(2)}{d(1) - d(2)} \times 100 \qquad \text{Equation 7.2}$$

where $d(1)$ is the average floc size (m) of the plateau before breakage, $d(2)$ is the floc size after the floc breakage period (m) and $d(3)$ is the floc size after re-growth to the new plateau (m).

An increased value of strength factor indicates flocs that are better able to withstand shear and thus should be considered stronger than a suspension with a lower factor. Likewise, an increase in the recovery factor shows flocs that have better re-growth after high shear.

Using model spherical particles, such as latex beads, it has been previously shown that aggregates formed at a low velocity gradient in salt solutions that are then broken into smaller aggregates on exposure to an increased shear field will re-form to their initial size if the original velocity gradient is subsequently re-applied (Spicer *et al.*, 1998). This behaviour is known as reversible breakage and is also observed during cyclical

breakage and re-growth of activated sludge flocs (Chaignon *et al.*, 2002). However, in most instances where conventional metal coagulants and polymers are used for the aggregation of small particle suspensions (such as kaolin and latex beads), irreversible breakage is usually seen, such that the initial floc size is never subsequently achieved after breakage. Differing degrees of recoverability have been seen depending upon the coagulant under investigation. Mono-disperse polystyrene beads coagulated with aluminium sulphate have been shown to have variable re-growth depending on the intensity of the breakage shear (Spicer *et al.*, 1998). For the coagulation of kaolin particles, alum and polyaluminium chloride have been shown to have the poorest re-growth reaching only one third of their previous size after shear, poly(diallyldimethylammonium) chloride (polyDADMAC) showed near complete re-growth, whilst a copolymer of acrylamide and cationic monomer showed total re-growth (Yukselen and Gregory, 2004). From these studies there is a suggestion that the particular coagulant used and therefore the coagulation mechanism involved has a considerable impact of floc re-growth potential. There has been no previous work showing the re-growth potential of NOM flocs with different coagulants so an understanding of these properties may provide an important addition to the well studied field of NOM coagulation and removal.

Since Mandlebrot introduced the concept of fractal theory in the 1970's, the application of fractal geometry is now a well established means of describing the complicated structure of floc aggregates (Gregory, 1998; Tang, 1999; Waite *et al.*, 2001; Wu *et al.*, 2002; Bushell *et al.*, 2002). Flocs are examples of mass fractal objects as both the internal and surface structure of the aggregate exhibit fractal properties as opposed to surface fractals where the fractal relationship is only evident on the outside of the particle. Mass fractals may be summarized by the relationship between their mass M, a characteristic measure of size L and the mass fractal dimension D_f (Equation 7.3).

$$M \propto L^{D_f} \qquad \text{Equation 7.3}$$

For Euclidean objects, the one-dimensional value of D_f will be 1 for a line, 2 for a two dimensional planar shape and 3 for a compact three dimensional shape (Waite, 1999). Fractal objects take non-integer values of D_f and are therefore said to show non-

Euclidean dimensionality. Recent work has successfully used small angle laser light scattering (SALLS) for the determination of fractal dimension for the aggregation of model primary particles such as latex (Tang, 1999) and aluminium oxide (Waite *et al.*, 2001). Application of SALLS to more complex natural systems such as activated sludge have been more difficult to interpret due to the fact that these flocs are thought to have two or more characteristic fractal dimensions as a result of a multilevel structure (Wu *et al.*, 2002). Furthermore, in the past relatively little work has investigated the fractal properties of NOM flocs and the application of SALLS to large NOM flocs has yet to have been fully explored. Understanding the changes in aggregate compaction during floc growth, breakage and re-growth may help to explain floc structural changes seen during these periods.

The overall objectives of this paper were to compare the structural properties of NOM flocs coagulated with ferric sulphate, alum or high molecular weight cationic polymer using an on-line laser diffraction particle sizing instrument. NOM flocs were then compared to model floc systems composed of mono-disperse latex and coagulant precipitate. Floc aggregates were characterized in terms of their size, fractal dimension, breakage and re-growth potential. This work also investigated the effect of shear exposure time on the recoverability of flocs.

7.2 Materials and methods

7.2.1 Suspension preparation and coagulation optimisation.

The NOM rich water source was taken from a reservoir in the north of the UK. The water was of high colour and DOC (10 mg L^{-1} as C), low turbidity (0.5 NTU) and low alkalinity (<10 mg L^{-1} as $CaCO_3$). For the coagulation of NOM, the coagulants under investigation were ferric sulphate (Ferripol XL, Huntsman Tioxide Europe Ltd, Billingham, UK), alum (Fisher Scientific UK, Loughborough, UK) and high molecular weight (MW) cationic polydiallyldimethylammonium chloride (polyDADMAC) (SNF UK Ltd, Castleford, UK). Coagulants were added at doses that corresponded to optimum dissolved organic carbon (DOC) removal (measured using a Shimadzu TOC-5000A analyser), UV_{254} removal (Jenway 6505 UV/Vis spectrophotometer at 254 nm) and settled turbidity (Hach 2100N turbidimeter) found during preliminary studies and as such represented doses that may be typically found

at water treatment works and therefore the operational significance of the results could be discussed. For the comparison of Fe-NOM flocs with coagulant precipitate flocs, ferric sulphate was added into de-ionized water at the same coagulant dose and pH as for the Fe-NOM flocs. For the coagulation of latex, stabilized latex particles were aggregated in 1M NaCl.

Mono-disperse latex stabilized with sulphate surface groups (Sigma-Aldrich) was used as the model spherical particulate system. The latex was nominally of a particle diameter of 300 nm. From an initial 10 % w/w solid stock suspension, a suspension of 9 mg L^{-1} was made for flocculation experiments, this equated to an approximate particle concentration of 6×10^{11} L^{-1}.

7.2.2 Floc formation, breakage and re-growth

Flocs were formed by performing a series of jar tests. A PB-900 variable speed jar tester (Phipps and Bird, Virginia, USA) was used with 76 x 25 mm flat paddle impellers with cylindrical jars containing 1 L samples of each suspension. Coagulation experiments involving chemical coagulants were carried out and repeated three times as follows: a rapid mix at 200 rpm for 1.5 minutes followed by a slow stir phase at 30 rpm for 15 minutes followed by a breakage phase at 200 rpm. Two separate breakage periods were investigated: 1) a long break period of 15 minutes and 2) a short breakage period of 30 seconds. After the breakage phase the slow stir at 30 rpm was re-introduced for a further 15 minutes. For the latex, a slightly different protocol was adopted due to the longer time taken for coagulation/flocculation to occur. Previously stable latex was rapidly dispersed in a 1M NaCl solution at 200 rpm for 1 minute, this was then followed by a slow stir phase at 30 rpm for 2 hours. Flocs were then exposed to an increased shear of 200 rpm for 15 minutes followed by a restoration of the 30 rpm slow stir phase for 2 hours.

A laser diffraction instrument (Malvern Mastersizer 2000, Malvern, UK) was used to measure dynamic floc size as the coagulation and flocculation process proceeded. The suspension was monitored by drawing water through the optical unit of the Mastersizer and back into the jar by a peristaltic pump on the return tube using 5 mm internal diameter peristaltic pump tubing. The inflow and outflow tubes were positioned opposite to one another at a depth just above the paddle in the holding

ports. Coagulant and pH adjustment chemicals were added at the start of the rapid mix. Size measurements were taken every minute for the duration of the jar test and logged onto a PC. This type of arrangement has previously been successfully applied in the analysis of activated sludge flocs (Biggs and Lant, 2000) and alum-polystyrene flocs (Spicer *et al.*, 1998). Flocs were pumped through the system at a flow rate of 1.5 L hr^{-1}. Preliminary experimentation showed that flow rates above those quoted gave rise to floc breakage, whilst below this rate flocs settled in the tubing. Experiments were temperature controlled and carried out at 22° C.

7.2.3 Floc structural analysis

During small angle light scattering, a light beam is passed through a sample. The particles in the sample scatter light proportional to their size and at a constant angle independent of which part of the particle is hit by the beam. Small particles scatter light at high angles, whilst large particles scatter at lower angles. The Malvern Mastersizer has an array of photo-sensitive detectors at different angles between 0.01 – 40.6 ° which detect the light scattered by the sample. The determination of fractal dimension using SALLS has been previously well covered (Tang, 1999; Waite *et al.*, 2001; Wu *et al.*, 2002), so only a brief overview is given below. The total scattered light intensity $I(Q)$ is a function of the wave number Q, where Q (m^{-1}) is the difference in magnitude of the incident and scattered laser beam (Spicer *et al.*, 1998), which is given by:

$$Q = \frac{4\pi n \sin(\theta/2)}{\lambda} \qquad \text{Equation 7.4}$$

n is the refractive index of the suspending medium, θ is the scattered angle, λ is the wavelength of the radiation in a vacuum (m).

For independently scattering aggregates, $I(Q)$ is related to Q and the fractal dimension by D_f:

$$I(Q) \propto Q^{-D_f} \qquad \text{Equation 7.5}$$

A confirmation of the power relationship in Equation 7.5 is to plot I against Q on a log-log scale. A power law relationship exists if this yields a straight line, the slope of which is used to give D_f. The relationship only holds when the length of investigation is much larger than the primary particles and much smaller than the floc aggregates:

$$\frac{1}{R_{agg}} << Q << \frac{1}{R_{part}} \qquad \text{Equation 7.6}$$

R_{agg} is the radius of the aggregate (m) and R_{part} is the radius of the primary particle (m).

Floc structural information was obtained from the Mastersizer for the long shear period in the form of raw output data which could then be converted to provide the angle of each detector and the intensity of light at each detector using a spreadsheet provided by Malvern Instruments (Malvern, UK).

7.3 Results

7.3.1 Suspension characterisation and coagulant optimisation

The laser diffraction instrument used in these studies reported particle size as an equivalent volumetric diameter. NOM is a heterogeneous matrix of colloidal and dissolved organic material. Because of this, the NOM primary particle size distribution (PSD) could not be determined as the particle size was below the lower detection limit (< 20 nm) of the laser diffraction instrument used for particle sizing.

Through standardized jar testing procedures it was found that for the removal of NOM the optimum ferric sulphate dose was 8 mg L^{-1} in the pH range 4-5 as Fe based on DOC removal and settled turbidity. For alum the optimum dose was 10 mg L^{-1} as Al in the pH range 5.5-6.5. These pH correspond well with reported optimums for Al and Fe coagulants (Amirtharajah and O'Melia, 1999). PolyDADMAC achieves optimum removals across a broad pH range and was dosed at an optimum of 10 mg L^{-1} at its natural pH of 6.0. The NOM removals as determined by DOC removal were 80 % for alum and ferric sulphate and 50 % for polyDADMAC.

7.3.2 Floc formation, breakage and re-growth.

7.3.2.1 NOM flocs

After the slow stir phase, Fe-NOM flocs had reached a d_{50} floc size of 700 μm and polyDADMAC-NOM had a median floc size of 800 μm (Figure 7.1a). This was approximately double the size of the Al-NOM flocs. There was very close agreement between experimental repeats with floc size values varying by less than 5 %. In all cases, floc size was immediately reduced following an increase in shear. The size of

the d_{50} flocs after 15 minutes exposure to shear was 300 μm for the ferric sulphate coagulant whilst the alum and polyDADMAC flocs were broken into smaller floc sizes of around 200 μm. As the shear was reduced again the flocs begin to re-grow, however the NOM flocs could not re-grow to anywhere near their previous size regardless of the coagulant used. The ferric sulphate and polyDADMAC flocs re-grew to a d_{50} size of 400 μm. Alum flocs increased in equivalent diameter to a value approaching 300 μm. Analysis of the floc PSD in Figure 7.1b show a shift in the major peak after breakage to under half the original value. There was also a considerable increase in the smaller peak at floc sizes between 10-100 μm. After the re-growth phase, this smaller peak was reduced with a commensurate shift to the right of the major peak.

The strength factor values in Table 7.1 show that the larger polymer flocs had a greater proportional size change after increased shear such that the associated strength factor was 25 compared to 40 for alum and ferric NOM flocs. The re-growth of ferric sulphate flocs was poor with a recovery factor of only 18, this was considerably lower than a value of 40 for alum and 32 for polyDADMAC.

The effect of reducing the period of exposure to high shear is shown in Figure 7.2. The extent of floc breakage was much less at the reduced shear period of 30 seconds for all of the coagulants with the floc strength factor increasing by an additional 15-25 from the longer shear period (Table 7.1). Ferric and alum flocs were better able to resist shear with floc strength factor values of 56 and 64 respectively. The polymer flocs had a floc strength factor of 40 when exposed to the increased shear. At the short shear time, floc re-growth was seen to improve considerably with the recoverability factor between 66-71 for all the NOM flocs. The PSD data again showed a reduction in the flocs around 10-100 μm after floc re-growth for all of the flocs (Figure 7.2b).

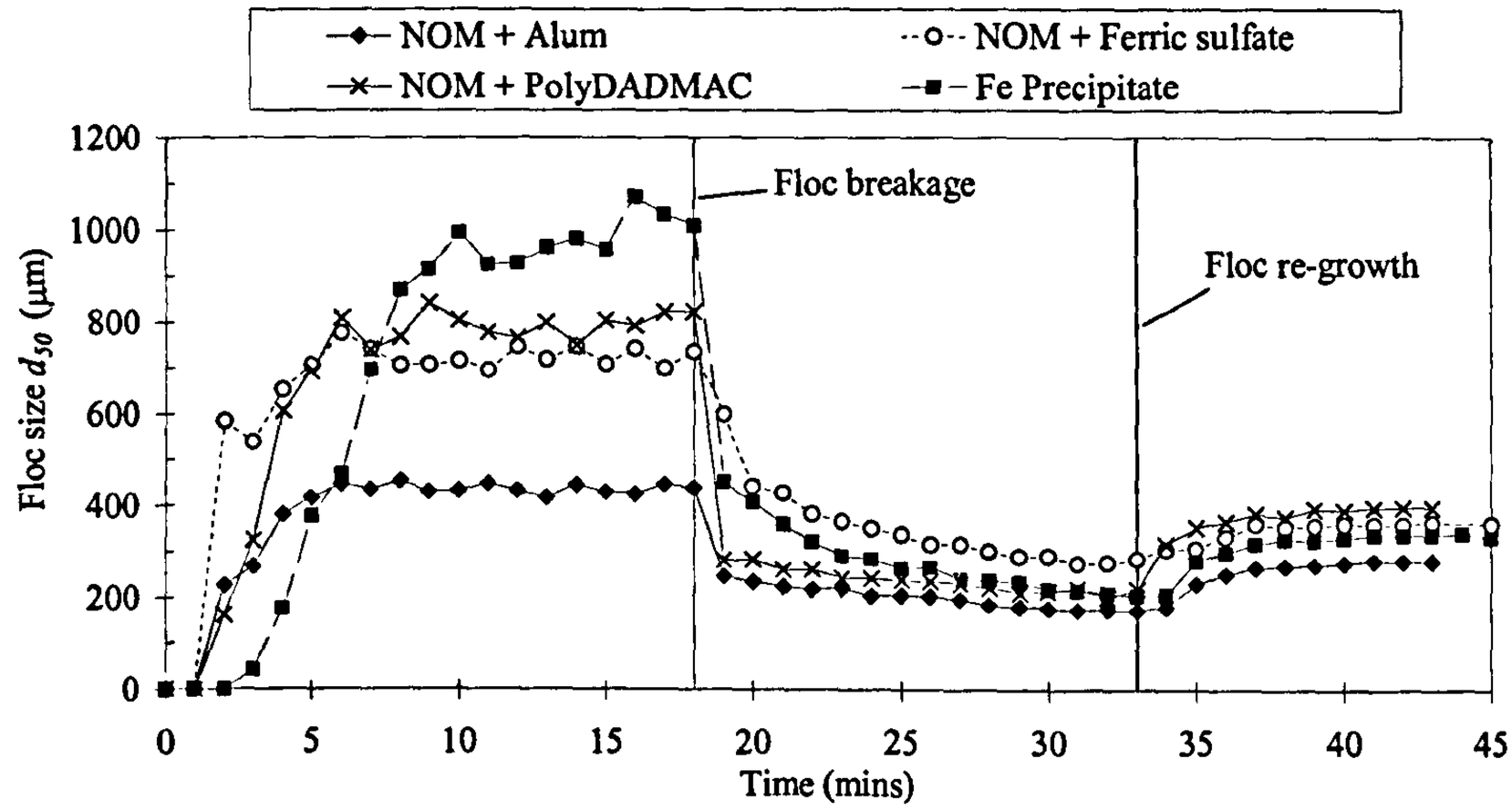

a) d_{50} floc size

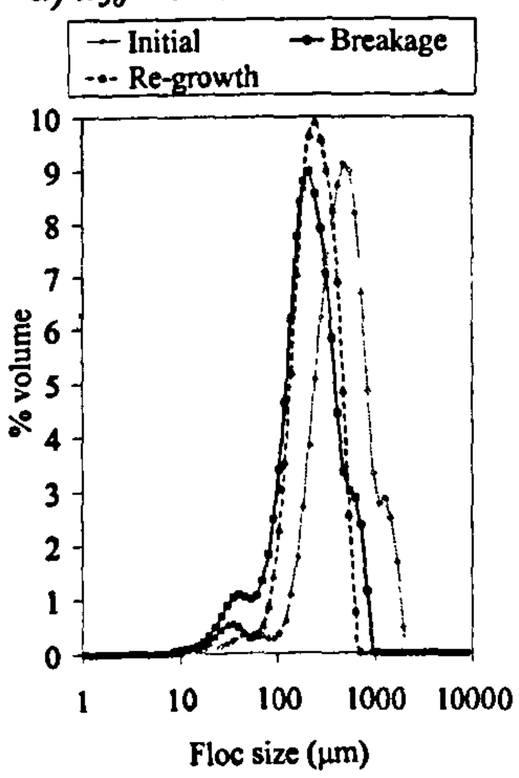

NOM + Al

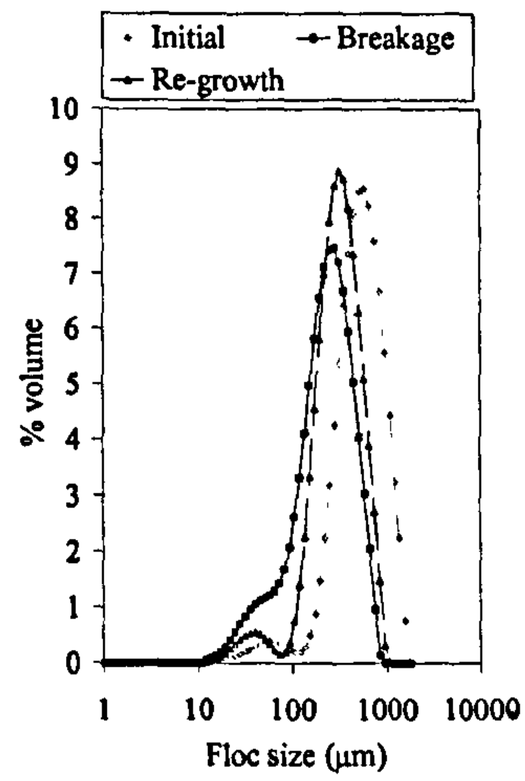

NOM + Fe

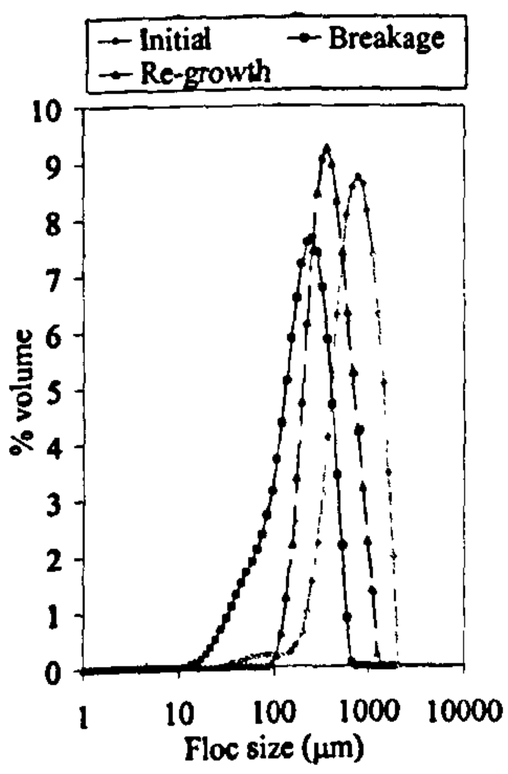

NOM + PolyDADMAC

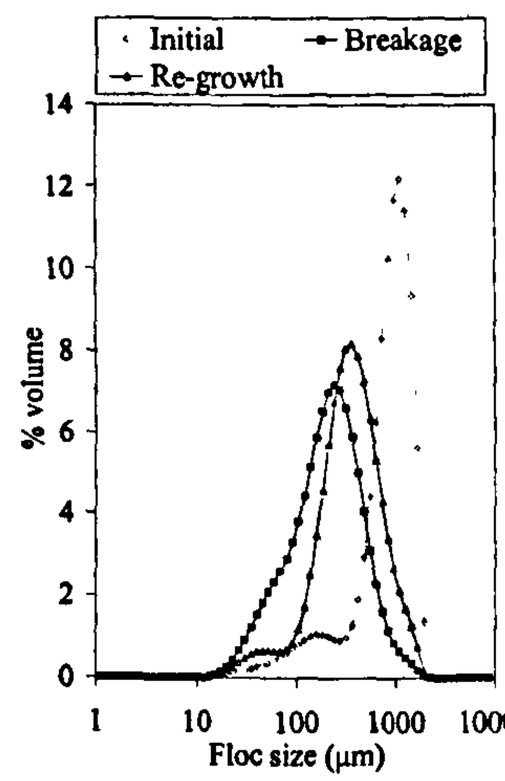

Fe precipitate

b) Particle size distributions

Figure 7.1 Long shear period – a) the breakage and re-growth profile of NOM flocs formed from three different coagulants (alum, ferric sulphate and polyDADMAC). b) the particle size distributions of the NOM flocs after growth, breakage and re-growth after 15 minutes high shear time.

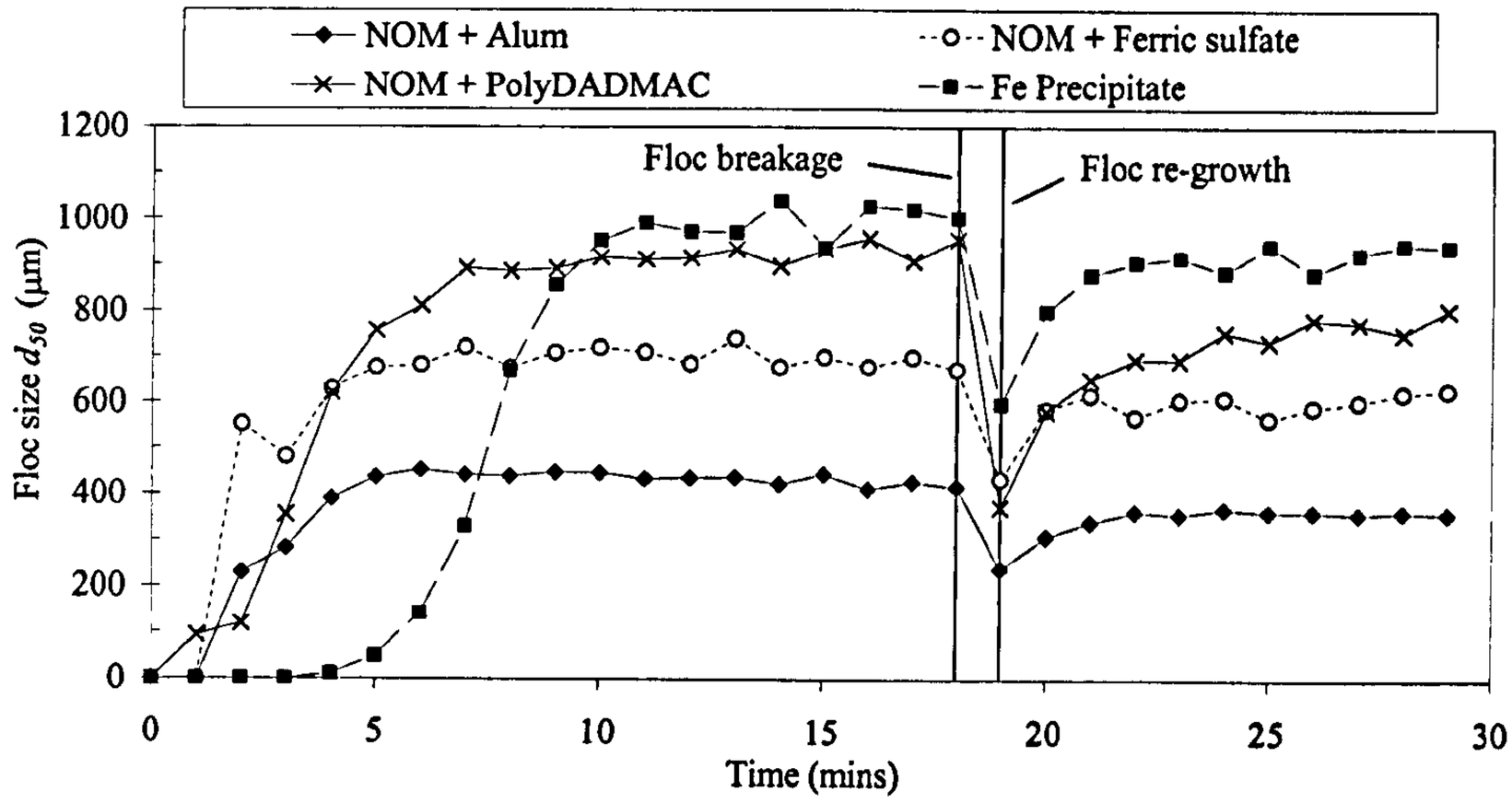

a) d_{50} floc size

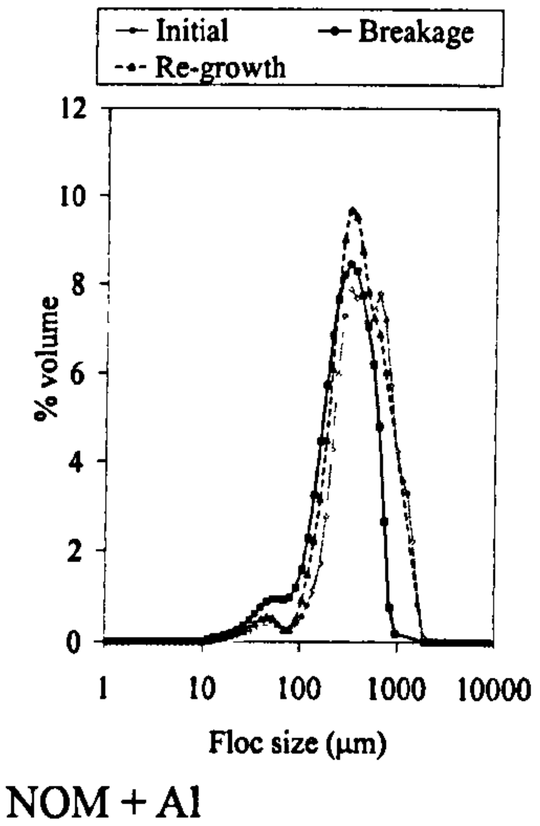

NOM + Al

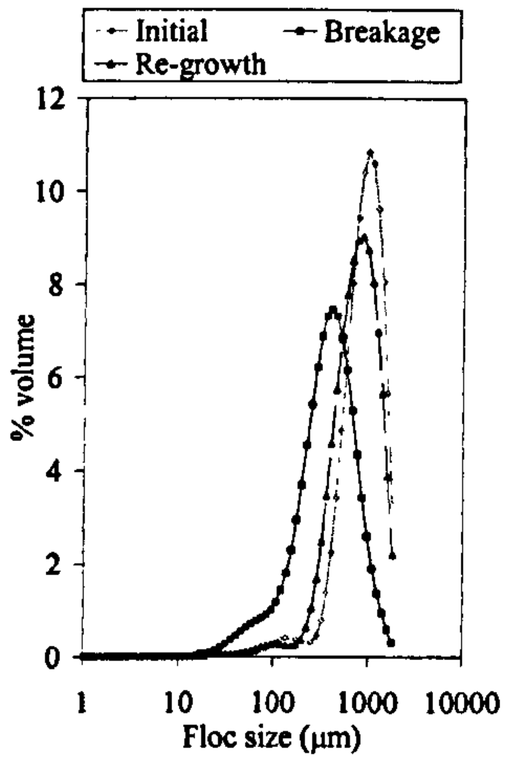

NOM + PolyDADMAC

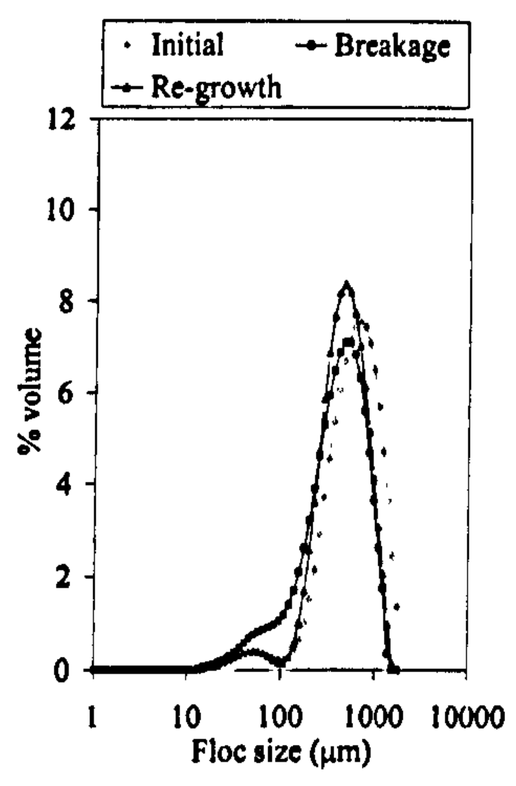

NOM + Fe

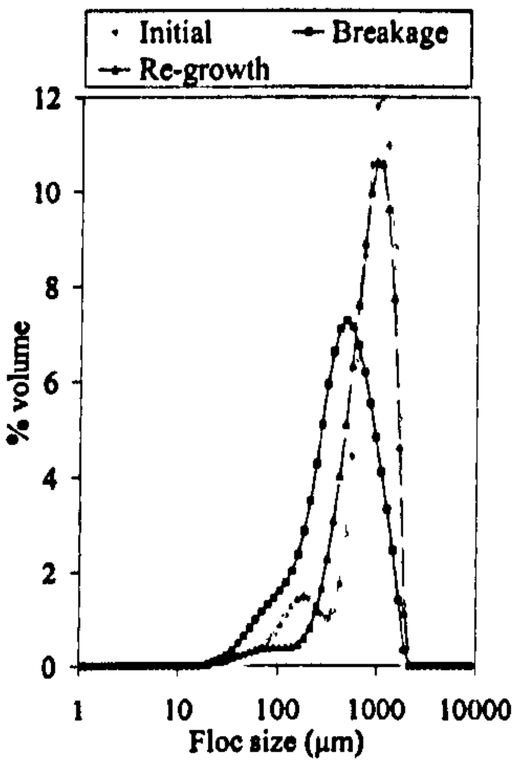

Fe precipitate

b) Particle size distributions

Figure 7.2 Short shear period – a) the breakage and re-growth profile of NOM flocs formed from three different coagulants (alum, ferric sulphate and polyDADMAC). b) the particle size distributions of the NOM flocs after growth, breakage and re-growth after 30 seconds high shear time.

Table 7.1 The strength and breakage factors of different sized NOM flocs formed from three different coagulants after a short (30 seconds and long breakage period (15 minutes).

	Strength Factor		Recovery Factor	
	Long break	Short break	Long break	Short break
Alum	40	56	40	66
Ferric sulphate	40	64	18	67
PolyDADMAC	25	40	32	71

7.3.2.2 Different starting suspensions.

The median size of the flocs formed from ferric sulphate precipitate were 1000 μm after the initial slow stir phase (Figure 7.1). This was considerably larger than the Fe-NOM flocs which reached 700 μm. The pattern of the breakage and re-growth behaviour of the flocs was similar to that seen previously. After exposure to 15 minutes of shear, the Fe-NOM flocs were broken to a median size of 300 μm. The Fe precipitate flocs were smaller with a median equivalent diameter of 200 μm. The Fe precipitate flocs had a low floc strength factor of 21, well below the value of 40 for Fe-NOM flocs (Table 7.2). Once broken, the Fe precipitate flocs had very poor recoverability with a re-growth factor of less than 20. The latex coagulated in salt solution reached a median floc size of 150 μm after the initial slow stir phase (Figure 7.3). On exposure to increased shear the flocs were broken to a d_{50} size of 25 μm with a low strength factor of 18. Once the original slow stir speed was restored, the flocs showed extensive recoverability with the flocs re-growing above their initial size to a median size of 200 μm. Two more subsequent breakage/re-growth cycles were therefore investigated which showed that there was a progressive drop-off in floc size and recoverability following these cycles (Table 7.2).

Table 7.2 The strength and breakage factors of flocs formed from different initial suspensions after a short (30 seconds) and long breakage period.

	Strength Factor				Recovery Factor			
	Long break			Short break	Long break			Short break
NOM	40			64	18			67
Precipitate	21			59	16			81
Latex	cycle 1	cycle 2	cycle 3	-	cycle 1	cycle 2	cycle 3	-
	18	20	24		139	84	64	

The short shear period did not break the suspensions to the same degree as for the longer shear with the floc strength factor remaining at around 60 for all of the suspensions. The recoverability of flocs improved relative to the longer shear period. The precipitate flocs had significantly higher recovery when compared to all of the flocs investigated at this short shear period with a re-growth factor of 81 compared to 6 for Fe-NOM flocs. The PSD data of both the long and short shear period shown in Figures 7.3 and 7.5 showed similar changes in aggregate size as seen for the NOM flocs.

7.3.3 Floc structural analysis.

The derivation of floc fractal dimension from the scattered light intensity ($I(Q)$) as a function of wave number (Q) are shown in Figure 7.6 for NOM flocs and different starting suspensions after 15 minutes slow stir when the flocs had reached their maximum steady state size. The linear portion of the curves suggests that there were mass fractal scaling relationships within the aggregates. For the NOM flocs it was evident that at values of $\log Q > -1.75$ and $\log Q < -3.5$ the data began to deviate from the linear region as the Porod and Guiner regimes were entered respectively. This gives an upper aggregate size ($1/R_{agg}$) in the region of 3 μm. This suggests that the floc fractal dimension as obtained from light scattering behaviour cannot be applied to the larger flocs that dominate NOM systems where the median size was 700 μm. For latex flocs, $\log Q$ was < -3.2 giving an upper aggregate size of 1.6 μm, over five times the value of the primary particle size but still much smaller than the median floc size of 150 μm.

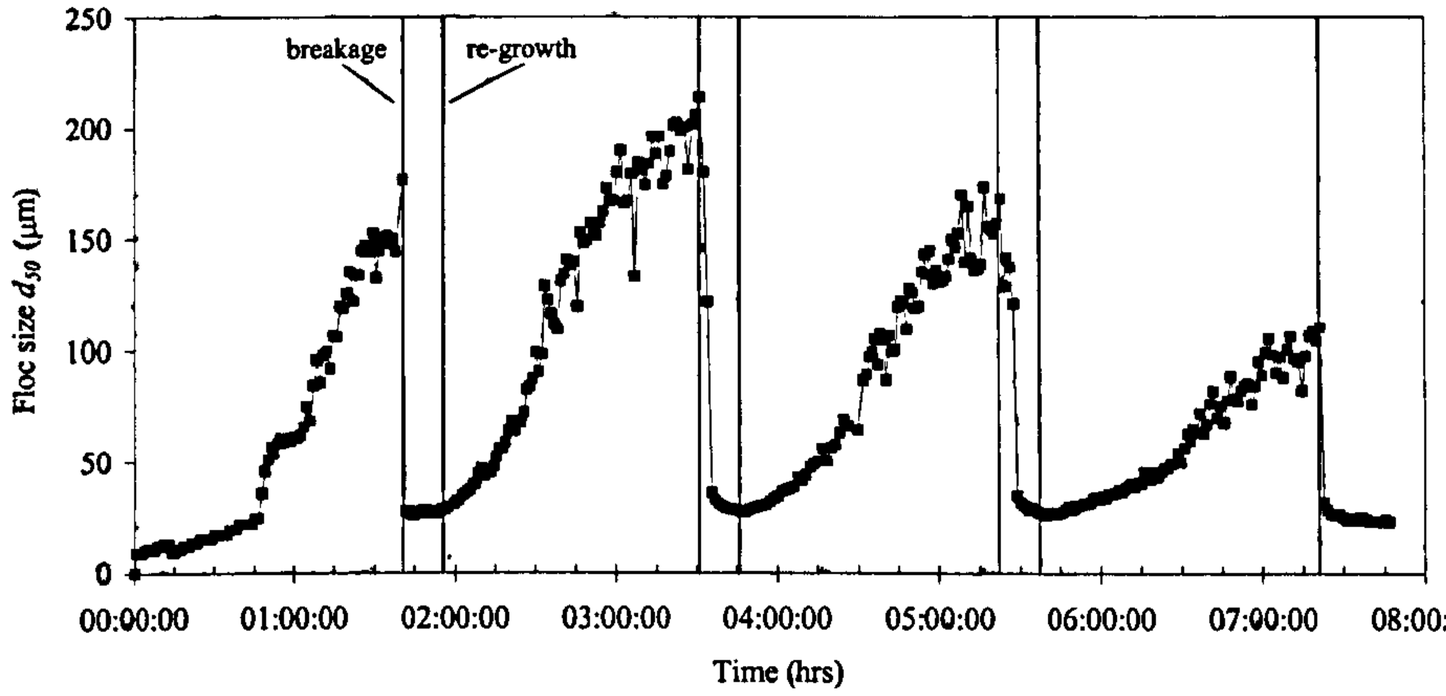

a) Latex beads (three break/re-growth cycles)

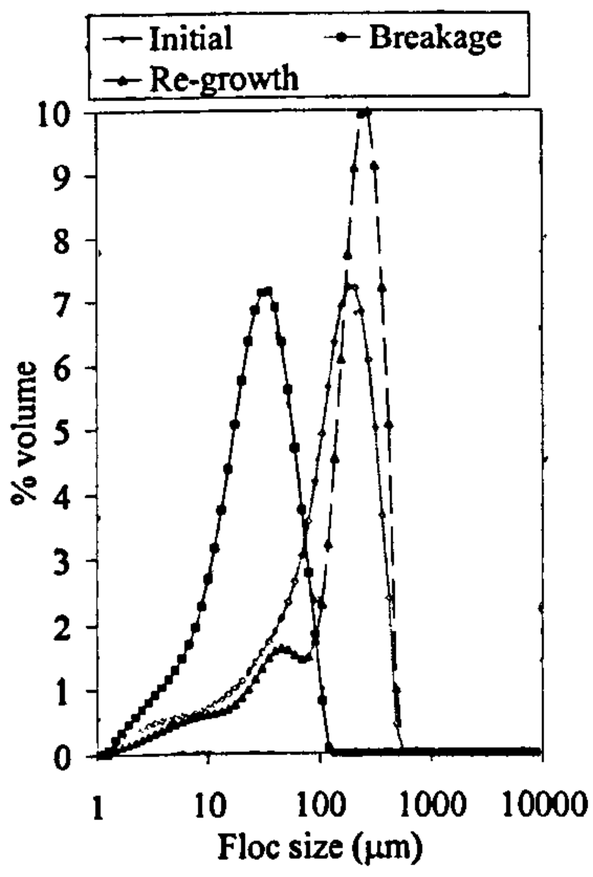

b) Latex floc size distributions

Figure 7.3 a) the growth, breakage and re-growth of latex beads coagulated in a 1M NaCl solution after 3 breakage/re-growth cycles. The shear period was 15 minutes. b) The floc size distributions of latex beads after growth, breakage and the initial re-growth cycle.

Similar curves to those shown in Figure 7.4 were formed for the coagulating suspensions as they were grown, broken and subsequently re-grown. This demonstrated how the degree of floc compaction changed with different shearing patterns for the small flocs in the system. There was a considerable difference in NOM floc fractal dimension for the different coagulants (Figure 7.5). Prior to breakage, ferric-NOM flocs had the lowest D_f of 2.25 whilst alum flocs appeared to have a higher degree of compaction with a D_f of 2.45 with the polymer flocs still more compact at a D_f of 2.55. On exposure to high shear, the D_f value of the alum and ferric

NOM flocs did not change considerably. PolyDADMAC flocs had a considerable reduction of D_f to 2.3 when broken and once the original shear had been returned to, floc compaction was seen to increase for all of the flocs.

After 15 minutes slow stir the D_f was 2.15 for the coagulant precipitate. D_f increased to 2.6 for Fe precipitate flocs after breakage and then reduced to 2.25 during re-growth. The cyclical breakage and re-growth of latex coagulated in NaCl showed that floc aggregates reached a D_f of 1.67 after the initial growth phase (Figure 7.6). The degree of compaction increased to *Df* of 2.05 following the first breakage. Once the original slow stir was returned a D_f of 1.7 was reached. Further breakage cycles increased D_f to 2.0 and then fell to a constant value of around 1.7 when the flocs re-grew.

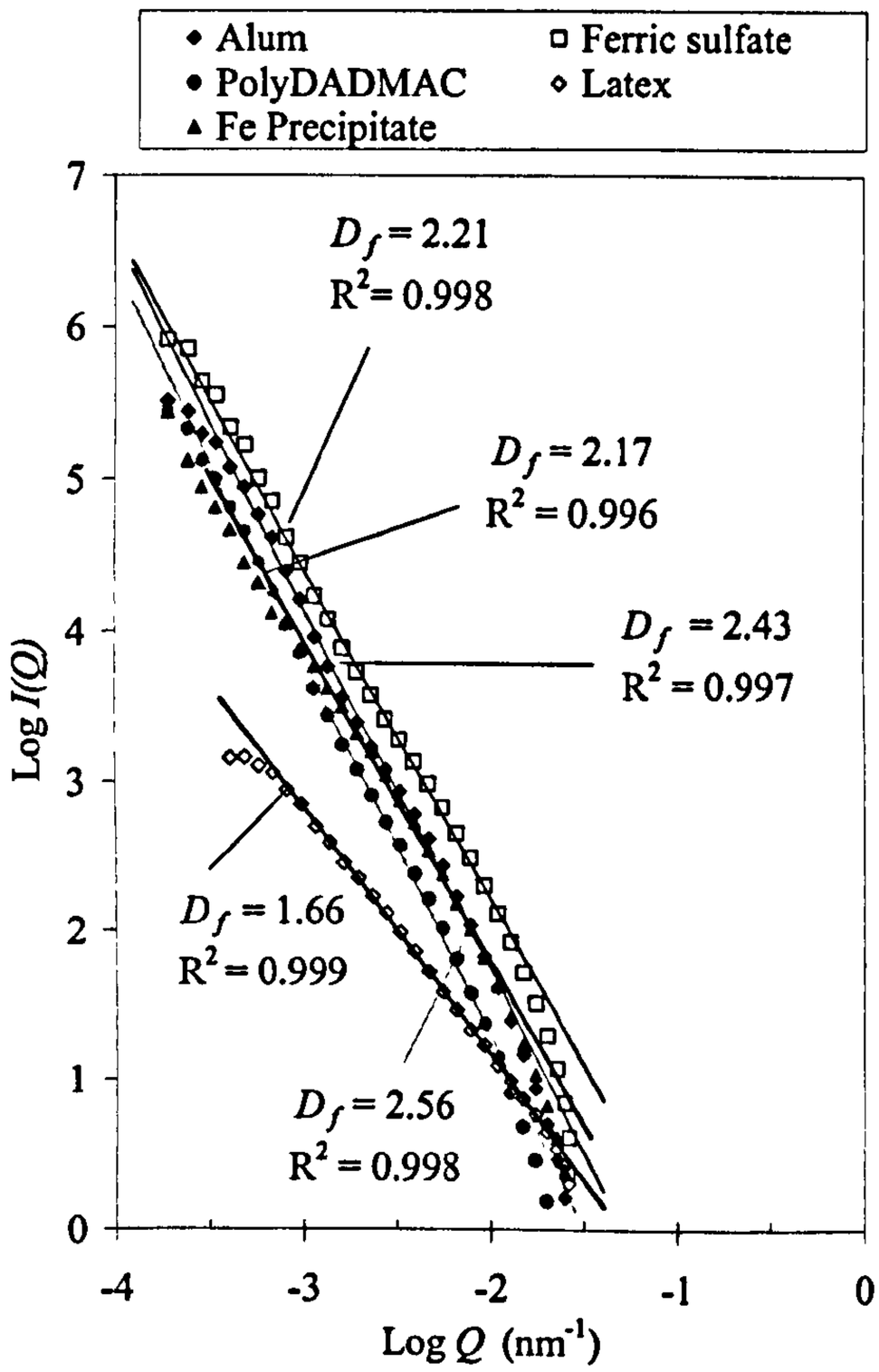

Figure 7.4 The relationship between the scattered light intensity (I(Q)) and the wave number (Q) on a log-log scale and the determination of the fractal dimension for different flocs after the initial growth phase for a) NOM flocs coagulated with different coagulants and b) different initial starting suspensions.

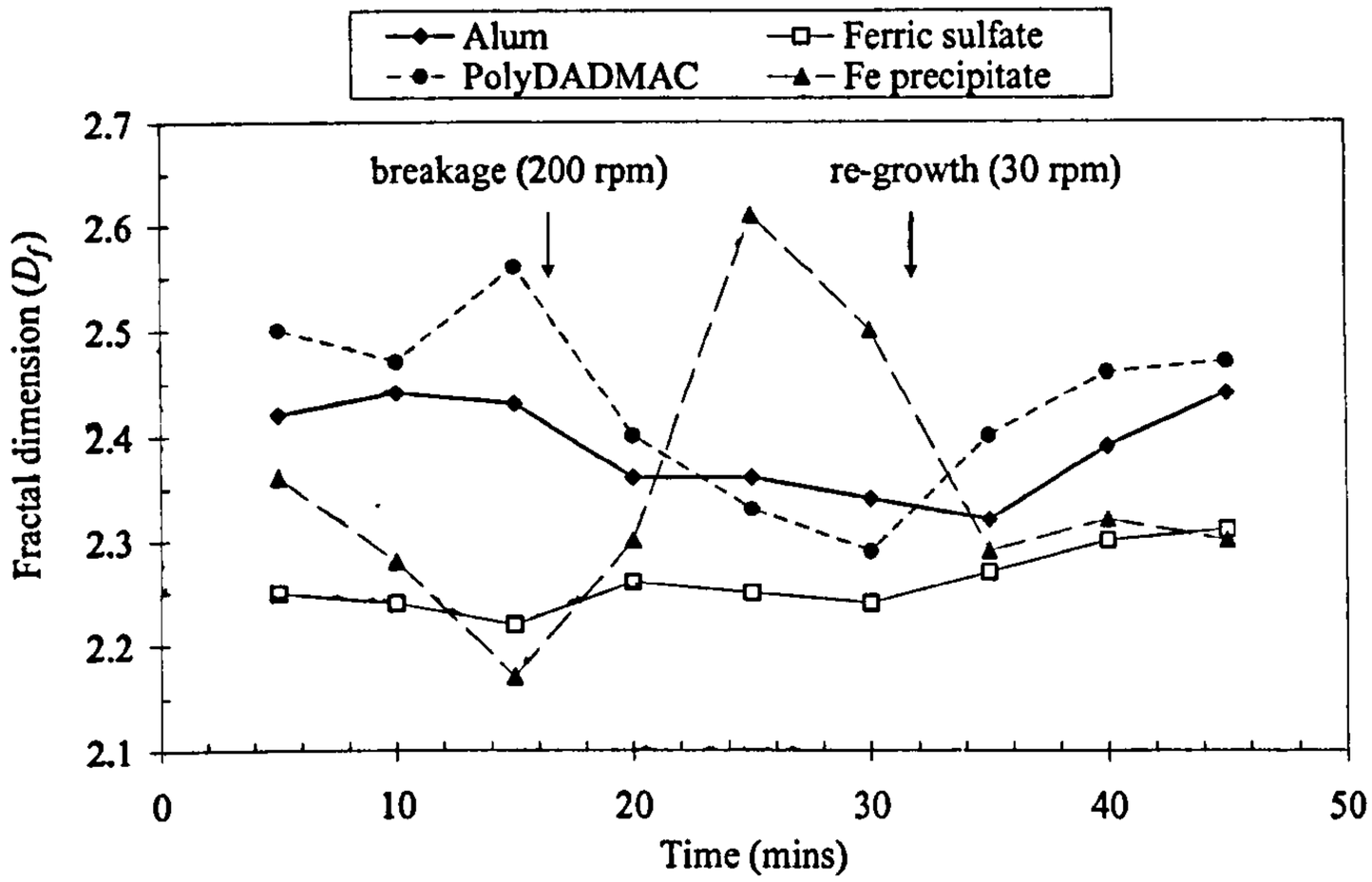

Figure 7.5 The change in fractal dimension of NOM flocs and Fe precipitate flocs with time for different coagulants after growth (30 rpm), breakage (200 rpm) followed by a return to the initial 30 rpm for re-growth.

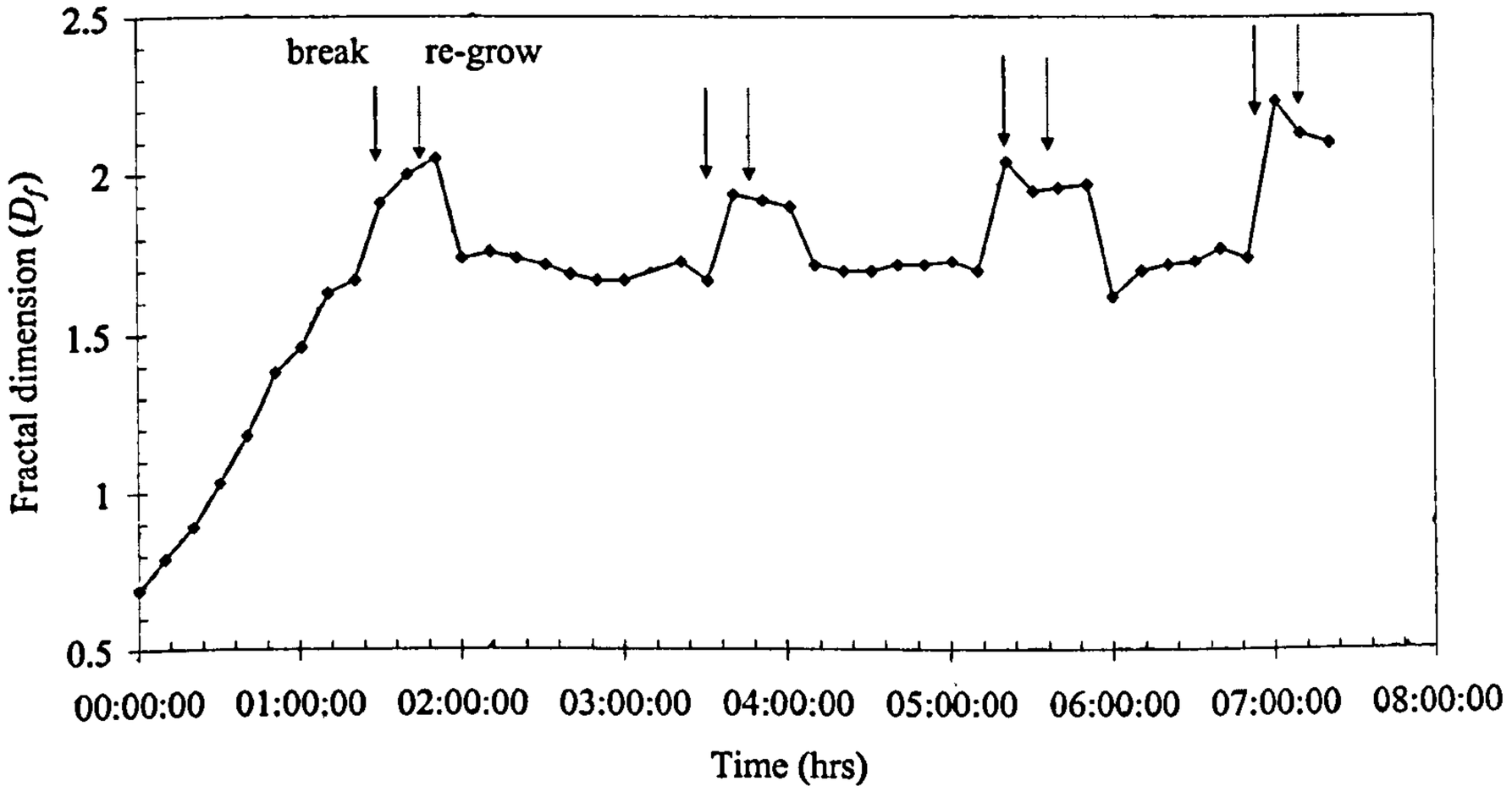

Figure 7.6 The change in fractal dimension with time of latex flocs coagulated in 1 M NaCl for cyclical breakage and re-growth regimes.

7.4 Discussion

The results presented in this work clearly show differences in floc growth, breakage and recoverability for a number of different coagulants and starting suspensions. Interpreting floc growth and breakage can give important indications of floc strength. Current understanding of the floc formation process shows it to be a balance between the rate of aggregation and the rate of breakage for a given shear condition (Biggs and Lant, 2000). Increased floc size after the suspension has reached a plateau at the end of the initial slow stir phase is one interpretation of increased floc strength (Yukselen and Gregory, 2004). This is because the larger flocs are able to reach a larger size before being checked by breakage. Using this definition, the strength of the NOM flocs is of the following order polyDADMAC > ferric sulphate >> alum. This would concur with the general conception that the use of polymer gives rise to bigger and therefore stronger flocs: a phenomenon seen for drinking water sludge (Wu *et al.*, 2002), activated sludge flocs (Leentvaar and Rebhun, 1983), NOM flocs (Bache and Rasool,, 2001) and kaolin turbidity flocs (Gregory and Dupont, 2001). The removal of organic material with high MW cationic polymer is essentially the reaction of polyelectrolyte with carboxyl and phenol groups on organic molecules. This produces insoluble precipitates which may be bridged together by 'spare' polymer forming large flocs (Bratby, 1980). For hydrolyzing coagulants such as ferric sulphate and alum, a combination of charge neutralization and entrapment/adsorption of NOM onto metal precipitates are the major floc formation routes (Gregor *et al.*, 1997). These flocs are subsequently considered weak and fragile (Bache *et al.*, 1997); probably as a result of no bridging bonds holding these flocs together. This may in part explain why alum and ferric NOM flocs formed smaller initial flocs.

Whilst the polymer flocs were able to grow to a large size at low shear, the low floc strength factor showed the break-up behaviour of these flocs on exposure to an increased shear was very high. This can be attributed to large flocs being more exposed to micro-scale energy dissipating eddies that give rise to floc breakage (Boller and Blaser, 1998; Thomas *et al.*, 1999). Smaller flocs are more likely to become entrained within these eddies rather than being broken by them. However, this does not explain the differences seen between ferric and alum NOM flocs in terms of their initial size and the floc strength factor and highlights an unidentified

difference in the way in which these coagulants operate in their interaction with NOM at their optimum DOC removal and settled turbidity doses. The poor DOC removal of only 50 % using only polymer would preclude the operational use of polyDADMAC at most water treatment works geared towards treating NOM when significantly more organic can be removed using conventional Fe and Al coagulants. Therefore, from a combined view of DOC removal and floc structural character, the use of an Fe coagulant appeared to give more benefit than alum. Interestingly, previous work has shown that the addition of polyDADMAC in combination with ferric sulphate does not improve NOM floc structure or DOC removal (Jarvis *et al.*, SUBMITTED).

As a comparison to Fe-NOM flocs, the increased size of the Fe precipitate flocs highlights the importance NOM plays during coagulation. The Fe precipitate flocs can be considered similar to sweep flocs in that they are composed of coagulant metal hydroxides. Therefore, the interaction of NOM in the floc formation process through direct chemical reaction and adsorption onto metal precipitates significantly reduced growth. However, the Fe-NOM flocs showed increased relative resistance to shear and the median size of the broken flocs were 50-100 μm in diameter larger than the Fe precipitate flocs. This can be explained by the Fe precipitate flocs being on average initially larger but also as a result of NOM within the aggregate helping to bind the floc together. The latex flocs formed in an inert electrolyte (NaCl) showed extensive floc breakage. These flocs form by charge neutralization through a suppression of the electric double layer, giving weak physical particle-particle bonds such as van der Waals forces (Yan *et al.*, 2000). Therefore, as has been shown in this study, it may be expected that these flocs do not have great floc strength both in their initial size and breakage.

The results of this work have shown that floc re-growth was limited with the exception of latex. The recoverability of flocs gives some indication of the floc internal bonding structure. Previous research has shown that flocs formed by charge neutralization should give total recoverability (Chaignon *et al.*, 2002). This work has shown that this was the case for latex beads coagulated in an ionic solution during one breakage/re-growth cycle. Subsequent cycles saw a drop off in recoverability, perhaps

as a result of impurities entering the system during the seven hours required for these experiments.

The irreversible breakage of the NOM flocs and Fe-precipitate flocs was seen as evidence that the flocs formed in these systems were not dominated by pure charge neutralization mechanisms and were therefore held together by chemical rather than physical bonds. For polymers, breakage of polymer chains at high shear rates is thought to reduce floc bridging capability during re-growth, whilst the reasons for irreversible floc breakage for hydrolyzing coagulants has yet to have been satisfactorily explained (Yukselen and Gregory, 2004). It was therefore difficult to give a chemical explanation for the reduced re-growth of Fe-NOM flocs when compared to alum given the poorly understood speciation chemistry of these coagulants during NOM coagulation. However, from a physical standpoint, the reduced breakage of the Fe-NOM flocs resulted in a lower frequency in floc number when compared to the Al-NOM and polyDADMAC-NOM flocs which may have resulted in fewer possible particle-particle contacts to allow for possible aggregation during the re-growth phase. The limited re-growth of Fe precipitate flocs suggests that sweep flocs show limited re-growth. This agrees with the findings of other research showing that sweep flocs formed from natural waters and Fe-kaolin flocs give poor re-growth after breakage (McCurdy *et al.*, 2004; Jarvis *et al.* 2004). A reduction in the time exposed to a similar shear showed both a significant reduction in floc breakage and an increase in floc re-growth, an effect also seen by Yukselen and Gregory (2004). This shows that flocs can resist a certain amount of shear. This results from a proportion of flocs remaining outside of floc breakage zones around impellers during the short breakage periods. Under longer breakage periods, the probability of flocs entering breakage zones is much higher.

In this study, the degree of floc compaction was measured using fractal dimension analysis. It was evident that the flocs under investigation exhibited scattering behavior typical of mass fractal objects. The fractal values of NOM flocs were in the region of 2.2-2.6 for the coagulants under investigation using SALLS. As a direct comparison, this agrees with the D_f of 2.2 seen for flocs formed from a raw water of high organic content (5-6 mg L^{-1}) using a similar technique (Kim *et al.*, 2001). The increased fractal dimension of polyDADMAC flocs over the other floc types indicated that

polymer bridging gives rise to the most compact structures. This does not agree with findings found for activated sludge flocs and mineral flocs which show a general decreasing of fractal dimension as polymer bridging is increased (Boller and Blaser, 1998; Wu *et al.*, 2002). In addition, there was no significant difference in the fractal value of Fe-NOM flocs and Fe precipitate flocs. This was surprising given the differences seen in the floc growth and breakage behaviour. Organic material has previously been shown to both stabilize and de-stabilize particles dependent upon the organic concentration (Walker and Bob, 2001). It therefore seems highly likely that adsorbed NOM within a floc should provide either increased attraction or repulsion leading to differing degrees of compaction.

A possible explanation for these inconsistencies being that in the current study the scale of investigation of the fractal dimension analysis was three to four orders of magnitude smaller than the average size of the flocs under investigation. This is a finding consistent with a number of other studies (Yan *et al.*, 2000; Selomulya *et al.*, 2001; Tang *et al.*, 2002). Using SALLS, the fractal scaling law breaks down at increased floc size as the light becomes scattered by the whole aggregates rather than the primary particles (Guan *et al.*,, 1998). Larger flocs may also have inconsistent fractal dimensions such that they exhibit degrees of compaction from one another. Therefore, the findings of the floc compaction work must be limited to a small proportion of the flocs in each distribution. Specifically for coagulant-NOM flocs, little is known about the exact nature and homogeneity of the primary particles in comparison to the other systems. It was therefore concluded that the adopted fractal protocol was not sensitive enough to help explain the observed differences in NOM flocs in this instance. For model systems such as small spherical beads, the technique seemed to provide more consistent results. The D_f value of 1.67 for latex aggregated in NaCl was similar to previous values found from latex aggregated in McIllvaine buffer (D_f = 1.8) (Tang, 1999) and latex aggregated in potassium nitrate (D_f = 1.7-1.8) (Selomulya *et al.*, 2001).

Current understanding suggests that flocs become more compact on exposure to increases in shear as they break at their weak points and re-arrange into more stable structures (Spicer *et al.*, 1998; Selomulya *et al.*, 2001). The NOM flocs did not follow this expected change and the reverse was seen, which was further evidence for the

limited applicability of SALLS to NOM flocs in this instance. The Fe precipitate and latex flocs followed this expected change in compaction as indicated by the change in fractal dimension such that D_f was seen to increase by 0.2-0.3 as flocs were broken into smaller and more compact structures. An increase in floc compaction provides a further explanation for the limited re-growth seen for most of the flocs. As chemical bonds are broken and flocs re-arrange into more compact structures, bonding sites that were previously available become unavailable, as they re-form within the broken aggregate. Whilst the same conclusions cannot be drawn for NOM flocs using the current experimental procedure, further research using other fractal dimension analysis tools (such as floc settling) may provide this information. For physical bonding (as seen for latex), floc compaction still occurs after breakage but the opportunities for floc re-formation are much greater because van der Waals forces can form anywhere on the latex particle surface such that further particle-particle contact between exposed regions can lead to physical bonds forming, thus producing similar sized flocs during re-growth.

The results of this work have shown that NOM flocs have different properties dependent on which chemical coagulant is used. The resulting structure seems to be determined by mechanisms of coagulation with bridging flocs forming the largest flocs. Furthermore, it appears that the bonds holding NOM flocs together are not purely physical bonds given the limited re-growth seen. The use of SALLS was not applicable to the NOM flocs in this instance even though a straight line relationship was seen between log Q and log I. On a wider scale, SALLS is recommended for model and uniform particles, but even then can only be applied to the small flocs in a system.

Acknowledgements

The submitted manuscript has been made possible through funding from American Water Works Association Research Foundation and Co-funding Utilities. The information contained herein is based upon Intellectual Property which is jointly owned by Cranfield University and the Foundation. The Foundation retains its right to publish or produce the Jointly Owned Intellectual Property in part or in its entirety. The authors would also like to thank the EPSRC, Fort Collins Water, Scottish Water, Severn Trent Water, Thames Water, United Utilities and Yorkshire Water.

7.5 References

Amirtharajah, A. and O'Melia, C. R. (1990) Coagulation Processes: Destabilisation, Mixing and Flocculation. In: *American Water Works Association Water Quality and Treatment A Handbook of Community Water Supplies*. McGraw-Hill, New York.

Bache, D. H., Johnson, C., McGilligan, J. F., and Rasool, E. (1997) A Conceptual View of Floc Structure in the Sweep Floc Domain. *Water Science and Technology* **36** (4), 49-56.

Bache, D. H. and Rasool, E. (2001). Characteristics of Alumino-Humic Flocs in Relation to DAF Performance. *Water Science and Technology* **43** (8), 203-208.

Biggs, C. A. and Lant, P. A. (2000). Activated Sludge Flocculation: On-Line Determination of Floc Size and the Effect of Shear. *Water Research* **34** 2542-2550.

Boller, M. and Blaser, S. (1998) Particles Under Stress. *Water Science and Technology* **37** (10), 9-29.

Bratby, J. (1980). Coagulation and Flocculation. Uplands Press Ltd, Croydon, UK.

Bushell, G. C., Yan, Y. D., Woodfield, D., Raper, J., and Amal, R. (2002) On Techniques for the Measurement of the Mass Fractal Dimension of Aggregates. *Advances in Colloid and Interface Science* **95** 1-50.

Chaignon, V., Lartiges, B. S., El Samrani, A. and Mustin, C. (2002) Evolution of Size Distribution and Transfer of Mineral Particles Between Flocs in Activated Sludges: an Insight into Floc Exchange Dynamics. *Water Research* **36** 676-684.

Fitzpatrick, C. S. B., Fradin, E. and Gregory, J. (2003) Temperature Effects on Flocculation Using Different Coagulants. In: *Proceedings of the Nano and Micro Particles in Water and Wastewater Treatment Conference*; International Water Association: Zurich, September.

Francois, R. J. (1987) Strength of Aluminium Hydroxide Flocs. *Water Research* **21** 1023-1030.

Gregor, J. E., Nokes, C. J., and Fenton, E. (1997) Optimising Natural Organic Matter Removal from Low Turbidity Waters by Controlled pH Adjustment of Aluminium Coagulation. *Water Research* **31** 2949-2958.

Gregory, J. (1998) The Role of Floc Density in Solid-Liquid Separation. *Filtration and Separation* **35** 367-371.

Gregory, J. and Dupont, V. (2001) Properties of Flocs Produced by Water Treatment Coagulants. *Water Science and Technology* **44** 231-236.

Guan, J., Waite, T. D. and Amal, R. (1998) Rapid Structure Characterisation of Bacterial Aggregates. *Environmental Science and Technology* **32** 3735-3742.

Jarvis, P., Jefferson, B. and Parsons, S. A. (SUBMITTED) Floc Structural Characteristics Using Conventional Coagulation for a High DOC, Low Alkalinity Surface Water Source. *Water Research.*

Jarvis, P., Jefferson, B., and Parsons, S. A. (2004) The Duplicity of Floc Strength. *Water Science and Technology* 50 (12), 63-70.

Kim, S. H., Moon, B. H., and Lee, H. I. (2001). Effects of pH and Dosage on Pollutant Removal and Floc Structure During Coagulation. *Microchemical Journal* **68** 197-203.

Leentvaar, J. and Rebhun, M. (1983) Strength of Ferric Hydroxide Flocs. *Water Research* **17** 895-902.

McCurdy, K., Carlson, K. and Gregory, D. (2004) Floc Morphology and Cyclic Shearing Recovery: Comparison of Alum and Polyaluminium Chloride Coagulants. *Water Research* **38** 486-494.

Selomulya, C., Amal, R., Bushell, G., and Waite, T. D. (2001) Evidence of Shear Rate Dependence on Restructuring and Break-up of Latex Aggregates. *Journal of Colloid and Interface Science* **236** 67-77.

Spicer, P. T., Pratsinis, S. E., Raper, J., Amal, R., Bushell, G., and Meesters, G. (1998). Effect of Shear Schedule on Particle Size, Density and Structure During Flocculation in Stirred Tanks. *Powder Technology* **97** 26-34.

Tang, P., Greenwood, J. and Raper, J. A. (2002) A Model to Describe the Settling Behavior of Fractal Aggregates. *Journal of Colloid and Interface Science* **247** 210-219.

Tang, S. (1999) Prediction of Fractal Properties of Polystyrene Aggregates. *Colloids and Surfaces A: Physicochemical and Engineering Aspects* **157** 185-192.

Thomas, D. N., Judd, S. J., and Fawcett, N. (1999) Flocculation Modelling: A Review. *Water Research* **33** 1579-1592.

Waite, T. D. (1999) Measurement and Implications of Floc Structure in Water and Wastewater Treatment. *Colloids and Surfaces A: Physicochemical and Engineering Aspects* **151** 27-41.

Waite, T. D., Cleaver, J. K. and Beattie, J. K. (2001) Aggregation Kinetics and Fractal Structure of γ-Alumina Assemblages. *Colloid and Interface Science* **241** 333-339.

Walker, H. W. and Bob, M. M. (2001) Stability of Particle Flocs Upon Addition of Natural Organic Matter Under Quiescent Conditions. *Water Research* **35**, 875-882.

Wu, R. M., Lee, D. J., Waite, T. D. and Guan, J. (2002) Multilevel Structure of Sludge Flocs. *Journal of Colloid and Interface Science* **252** 383-392.

Yan, Y., Burns, J. L., Jameson, G. J. and Biggs, S. (2000) The Structure and Strength of Depletion Force Induced Particle Aggregates. *Chemical Engineering Journal* **80** 23-30.

Yukselen, M. A. and Gregory, J. (2004) The Reversibility of Floc Breakage. *International Journal of Mineral Processing* **73** 251-259.

CHAPTER 8

OVERALL SUMMARY

8 OVERALL SUMMARY

The following discussion focuses firstly on the development and application of a range of diagnostic tools for characterising delicate NOM flocs. This included the measurement of floc size, growth, breakage, re-growth and floc settling behaviour and fractal dimension. Secondly, the practical implications of the main findings and outcomes of the experimental work presented in the preceding series of papers are discussed. These findings may be summarised as:

(1) The application of floc diagnostic tools showed a change in NOM floc character over a period of one year using the coagulation conditions of a real WTW from where the water was abstracted.

(2) Following from the above study, the impact of increasing the organic fraction within the floc matrix showed a significant deterioration in floc structural quality in terms of floc size, strength and settling rate.

(3) The comparison of a range of coagulants and pre-treatment options resulted in different floc characteristics. Of those tested, MIEX® pre-treatment gave the most improved floc structure, forming very large, strong and fast settling flocs.

8.1 Method development

The tools developed to analyse floc structure have provided a framework within which to investigate a challenging type of floc. NOM flocs are difficult to measure due to their inherent fragility but also because they can reach large sizes. For example the d_{90} floc sizes were often above an equivalent volumetric diameter of 2 mm. A similar experimental set-up was developed to measure floc size as used by Spicer *et al.* (1998) and Biggs and Lant (2000). However, the upper size ranges investigated for alum-latex flocs was around 400 μm (Spicer *et al.*, 1998), whilst for activated sludge this was 300 μm (Biggs and Lant, 2000). This required considerable adaptation of the methodology in order to analyse NOM flocs. As shown in the Appendix, pump optimisation studies showed that a much reduced comparative flow rate was required in order to prevent breakage of the NOM flocs. Repeatability trials showed the methodology was able to provide reliable particle size data for floc growth and breakage tests.

8.2 Floc size and strength

One of the principal requirements of the floc diagnostic tools was to determine floc strength through the floc response to shear. Through the series of papers presented here a number of different views related to floc strength have been presented and discussed. The first experimental paper in Chapter 3 discusses the use of theoretical values of the exponent γ. Parker *et al.* (1972) and Francois (1989) have attributed the slope of the line from a log-log plot of floc size against shear to a particular floc breakage mode of fragmentation or erosion. The values of γ' as found for the NOM flocs throughout this study were around 0.5, similar to those found by Bache *et al.*, 1999 and Bache and Rasool, 2001 for alumino-humic flocs. This suggests floc breakage was dominated by large scale fragmentation. However, the underlying reasons for these theoretical values of breakage are not clear. For this reason it was therefore decided to investigate other avenues of floc breakage

The following papers looked at the absolute change and proportional change in floc size across the range of rpm's investigated. One of the major assumptions of this study has been that floc size is intrinsically related to floc strength with a floc that is broken into smaller pieces being considered weaker than a floc broken into larger pieces when exposed to increased shear. Whilst not providing an absolute value of floc strength, this assumption seems fair given that in order for a floc to be broken into smaller sizes for the same applied shear more of the bonds that hold the floc together in the first place must be broken. This tends to concur with the view that large flocs are indicative of strong flocs because maintaining a large floc size for a given shear shows these flocs have higher resistance to breakage (Bache and Papavasilopoulos, 2003; Yukselen and Gregory, 2004).

The use of increased floc size as an indicator of increased floc strength was therefore adopted as the best indicator of floc strength. This shows that initially larger flocs tend to maintain a larger broken size with increased shear until high rpm (150-200 rpm) when there was a general convergence on a similar floc size. The larger flocs tended to have steeper degradation slopes when floc size was plotted against rpm. The likely reason for this being that at very high shear, the applied energy is strong enough to break all flocs to a similar sized microfloc size regardless of the floc strength.

Following from this three general strength trends for NOM flocs were found in this study:

(1) A seasonal evaluation of floc structure using WTW coagulation conditions showed autumnal flocs to be the strongest.

(2) NOM floc strength decreased with increasing organic fraction in the floc.

(3) Different treatment options gave the following NOM floc strength hierarchy (strongest first): MIEX® > polyDADMAC > Ferric sulphate > Ferric sulphate + floc aid > Alum.

In addition, in comparison to other floc systems initially larger NOM flocs were less affected by high shear than kaolin flocs both in their proportional and absolute change in size. The implication being that NOM flocs should be considered stronger than turbidity type flocs. These findings go against research suggesting that metal-organic flocs are comparatively weak and fragile. For example the specific bonding strength of alumino-humic flocs has been estimated as <0.5 N m^{-2} (Bache *et al.*, 1999) whilst for polymer-turbidity flocs strength estimates range up to 100-1000 N m^{-2} (Yeung and Pelton, 1996). However it should be noted that in these studies the turbidity flocs being measured had an average size of 25-50 μm compared to 100-200 μm for the humic flocs. This indicates that the turbidity flocs could not reach a large initial size and therefore the strength estimate may be a measure of the microfloc strength rather than the floc as a whole suggesting the observations seen in this study hold true.

8.3 Floc re-growth

Floc re-growth was limited for all of the flocs formed by the addition of a chemical coagulant, particularly when the floc suspension was exposed to extended high shear periods. As a comparison, flocs formed from charge neutralisation in a salt solution gave rise to complete floc re-growth after break-up. The limited re-growth after breakage of NOM, turbidity and Fe precipitate flocs formed using ferric sulphate as the coagulant was in agreement with a number of other studies for different systems. Turbidity flocs using alum and polyaluminium chloride coagulants show similar re-growth behaviour (Yukselen and Gregory, 2004) and latex beads coagulated with alum also have limited re-growth (Spicer *et al.*, 1998). However, it should be noted that some floc systems do show complete re-growth after breakage. In this study, latex

formed by charge neutralisation in a salt solution showed good recovery, whilst activated sludge exhibits complete re-growth (Chaignon *et al.*, 2002) and some polymers give rise to total recovery for turbidity flocs (Yukselen and Gregory, 2004). NOM flocs formed using a high charge density polymer (polyDADMAC) did not show any improved re-growth in this study. The mechanisms for the observed re-growth behaviour has been previously discussed suggesting that only flocs held together by physical van der Waals forces were able to show significant re-growth after breakage. The practical consequence of this observation for NOM flocs suggests that extended floc breakage should be minimised because NOM flocs do not reach their previous size after breakage.

8.4 Floc settling and fractal dimension analysis

In most cases NOM flocs showed similar settling rates regardless of the incoming water quality and treatment options chosen. However a slight but significant increase in settling velocity was seen for the autumn flocs during the seasonal evaluation of floc structure. The most marked increase was for the MIEX® pre-treated flocs. These NOM flocs had settling rates comparable to turbidity flocs even though the density of organic material in the flocs was significantly less than that for the kaolin in the turbidity flocs.

Fractal dimension of the flocs was evaluated in two separate ways using settling and scattered light intensity. Using the relationship between floc size, settling and fractal dimension it was seen that statistically significant differences were seen in NOM floc fractal dimension for:

(1) Optimum coagulant dose gave the most compact flocs compared to under dosing with a fractal dimension (D_f) value of 2.00 at an optimum dose of 14.4 mg L^{-1} as Fe whilst a lower dose of 8 mg L^{-1} as Fe gave a D_f of 1.75. (Chapter 3(A)).

(2) Floc fractal dimension decreased with increasing carbon concentration, with D_f decreasing from 2.2 to 1.75 from the highest to lowest carbon fraction in the floc. Visual observation of microscope images seemed to confirm this observation (Chapter 5). This trend also followed the order of floc size and strength.

(3) Floc fractal dimension decreased from 2.20 for Fe precipitate to 2.01 for Fe-NOM to 1.86 for Fe-polymer-NOM. This trend also followed the order of floc size and strength (Chapter 6).

Using light scattering, slightly different values of the fractal dimension for Fe-NOM flocs were found. A D_f of 2.25 was found compared to values of between 1.75 and 2.00 as found from settling data. For Fe precipitate flocs a value of 2.15 was found using light scattering, showing closer agreement with the D_f of 2.20 as found from settling. A previous comparison of the two techniques has also shown an increase in floc fractal dimension when using light scattering with activated sludge giving a D_f value of 1.31 for settling whilst D_f was 1.86 using scattering (Wu *et al.*, 2002). Whilst there is no complete understanding for these differences, it is likely that some of assumptions for light scattering are not met when using light scattering for complex flocs with non-uniform refractive index. For example, NOM is likely to have different light scattering properties when compared to the Fe precipitate and Fe-NOM complexes that are all thought to constitute the floc matrix. This is further supported by the more uniform Fe precipitate flocs showing similar fractal values between the two techniques. The conclusion from this being that light scattering is not applicable to complex NOM flocs in this instance. When light scattering was applicable to the more uniform systems (for Fe precipitate flocs and latex flocs) the technique could be very easily used to find D_f and in combination with the breakage experiments showed some interesting trends with floc fractal dimension increasing after breakage and then subsequently decreasing again upon re-growth, however limited the re-growth was. One further consideration with light scattering was that the characteristic straight line relationship between $I(Q)$ and Q on a log-log scale was only seen for small flocs, much below the mean floc size of each system. The straight line relationship between floc size and settling velocity on a log-log scale was always observed across the whole range of floc sizes investigated for all floc types.

As the Fe-NOM floc fractal dimension (as found from settling) was seen to increase the flocs were larger and more resistant to shear and were therefore considered stronger. This suggests that as the components of the NOM flocs become closer to one another the strength and/or number of the bonds holding the floc together increases

giving rise to stronger and bigger flocs. In the case of NOM flocs, significantly increasing the amount of NOM in the flocs reduces the floc fractal dimension.

8.5 Practical implications of the findings

The inference that the initial floc size is the most important indicator of floc strength suggests that the most crucial operational control of NOM flocs should occur during the first few minutes of floc growth. This is because for all of the flocs investigated, they had reached their maximum steady state size after 3-5 minutes following the rapid mix and slow stir phase. A possible consequence of this being that extended slow stir/flocculation stages beyond 5 minutes are unnecessary for NOM flocs. However, further work is required in this field in order to ascertain whether the proceeding mixing phase allows further floc re-structuring (with no net increase in floc size) that imparts increased floc strength.

The seasonal evaluation of flocs over a one year period revealed the autumnal flocs to have the best overall structural characteristics. This was surprising given that operational problems with floc quality have generally been seen in autumn. However, the period of investigation (Spring 2003-Winter 2004) can be considered an anomalous year with the organic content of the raw water remaining around 10 mg L^{-1} DOC for each of the seasonal periods of investigation. The increase in carbon load during the autumnal months was not seen whilst operational problems were also not reported at WTW during this period. The lack of rain throughout the year may explain why the NOM in the surface water source remained low as it was not flushed through from the soil. The improved floc conditions seen in autumn were believed to have resulted from a change in the specific nature of the NOM.

Given that the annual evaluation did not provide an increased carbon load a separate series of experiments evaluated different coagulant to NOM ratios. The results of which have shown the importance of dosing correctly in order to obtain good NOM floc structure. Whilst the principal concern at a WTW treating water of high NOM concentration will be the optimum removal of organics to prevent the formation of downstream THM's, consideration of floc structure should also be of importance. As an example, for the raw water used in this study excellent DOC removals were

achieved using coagulant doses of 2 and 8 mg L^{-1} as Fe, however the resulting floc properties were very different. The higher coagulant dose gave flocs that were on average 300 μm larger in diameter, did not break to the same extent in shear, settled faster and had a more compact structure. This illustrates the need to consider floc structure during conventional optimisation studies at WTW with the requirement to ensure that the organic fraction within the floc does not become too high. However, over-dosing the coagulant will give rise to an excess sludge production. For the Ferripol coagulant used in this study an empirical ratio of 1 mg Fe to 1 mg DOC gave the optimum floc structure whilst also giving good removal efficacy.

A number of different treatment options were assessed. The operational use of a coagulant for NOM removal should be evaluate in combined terms of DOC removal and the resulting floc structure. For example, polyDADMAC showed good floc structure in terms of size and strength, but performed poorly with DOC removal. Conversely, alum showed good DOC removal but the resulting flocs were small and weak. The treatment option that showed significantly improved floc structure for size, strength and settling velocity was the use of an anionic ion exchange resin pre-treatment followed by conventional coagulation. This was believed to have resulted from the previously described effect of reducing the NOM in the floc matrix but also due to the removal of specific MW components from the floc structure. The absence or presence of specific NOM components from the floc structural matrix may also help explain the differences seen in floc structure resulting from seasonal variations in the water source. Given that the ratio of coagulant to DOC only ranged from 0.8 to 1.1 during the seasonal evaluation the differences seen in floc structure were not likely to be as a result of extreme variations in DOC concentration in the floc. It therefore seems that a change in the nature of the NOM resulted in a change in the floc structure.

The significance of these findings matched to the initial objectives are that:

(1) Specific temporal variations in the raw water source can give rise to a deterioration in floc structure.

(2) Increases in DOC can result in deterioration in floc structure.

(3) Of the treatment systems evaluated the order of best to worst treatment systems were: MIEX® + Fe > Fe > Fe + polymer > Al > polyDADMAC.

(4) NOM floc re-growth was limited, although reducing the time exposed to shear improved floc re-growth.

These findings allow an understanding of how 'better' flocs may be built at a water treatment works specifically geared towards treating NOM rich water sources. From the results of this work, the use of an anionic ion exchange pre-treatment gave rise to the most improved floc structure. The pre-treatment stage gave rise to significant organic removal and the following coagulant dose was also much reduced suggesting that the combined treatment system could reduce sludge production and therefore disposal costs. Of the conventional coagulation options, better flocs were produced using ferric sulphate when compared to alum. In order to balance efficient NOM removal with improved structure an empirical ratio of 1 mg Fe to 1 mg DOC should be applied.

8.6 Mechanistic understanding of the observations seen

A mechanism was proposed for the change in floc structure resulting from an increase in the organic fraction within the floc showing how increased NOM adsorbed onto the floc precipitate could result in increased steric repulsion between primary particles within the floc. However applying this mechanism to all the observations seen does not hold. For example, MIEX® pre-treatment was seen to reduce the DOC prior to coagulation. The resulting flocs were significantly larger and faster settling than any of the flocs investigated during the DOC:Fe ratio study, suggesting that it was a combined effect of reducing the DOC and the removal of specific NOM components that gave rise to the improved structure rather than simply less organic in the floc. Significant differences in floc structure were also seen for two of the most universally used coagulants: alum and ferric. The differences seen in floc structure could not be adequately explained based upon current understanding of how these two coagulants

function, suggesting there are differences in their specific chemical operation. As yet the incomplete understanding of the specific reactions that occur during NOM coagulation (particularly for different coagulants), the differences in the nature of the organics removed and their incorporation into the floc matrix, and the seasonal variation in NOM do not allow a complete knowledge of the mechanisms involved in NOM coagulation.

However, whilst the mechanisms are not yet fully understood the presented experimental protocol has provided a diagnostic framework within which complex NOM floc structures may be accurately quantified. This will allow the development of coagulation strategies that can improve floc character and improve NOM removal to continue to meet and surpass ever more stringent water quality regulations. Furthermore, by placing more emphasis on analysis and characterisation of floc structure, it is hoped that more complex techniques may be applied to floc structure investigations in order to give a better understanding of the mechanisms involved during NOM coagulation.

8.7 References

Bache, D. H. and Papavasilopoulos, E. N. (2003) Dewatering of Alumino-Humic Sludge: Impacts of Hydroxide. *Water Research* **37** 3289-3298.

Bache, D. H. and Rasool, E. R. (2001) Characteristics of Alumino-Humic Flocs in Relation to DAF Performance. *Water Science and Technology* **43** (8), 203-208.

Bache, D. H., Rasool, E., Moffatt, D., and McGilligan, F. J. (1999) On the Strength and Character of Alumino-Humic Flocs. *Water Science and Technology* **40** (9), 81-88.

Biggs, C. A. and Lant, P. A. (2000) Activated Sludge Flocculation: On-Line Determination of Floc Size and the Effect of Shear. *Water Research* **34** 2542-2550.

Chaignon, V., Lartiges, B. S., El Samrani, A. and Mustin, C. (2002) Evolution of Size Distribution and Transfer of Mineral Particles Between Flocs in Activated Sludges: an Insight into Floc Exchange Dynamics. *Water Research* **36** 676-684.

Francois, R. J. (1987) Strength of Aluminium Hydroxide Flocs. *Water Research* **21** 1023-1030.

Parker, D. S., Kaufman, W. J., and Jenkins, D (1972) Floc Breakup in Turbulent Flocculation Processes. *Journal of the Sanitary Engineering Division: Proceedings of the American Society of Civil Engineers* **SA 1** 79-99.

Spicer, P. T., Pratsinis, S. E., Raper, J., Amal, R., Bushell, G., and Meesters, G. (1998) Effect of Shear Schedule on Particle Size, Density and Structure During Flocculation in Stirred Tanks. *Powder Technology* **97** 26-34.

Wu, R. M.; Lee, D. J., Waite, T. D. and Guan, J. (2002) Multilevel Structure of Sludge Flocs. *Journal of Colloid and Interfacial Science* **252** 383-392.

Yeung, A. K. C. and Pelton, R. (1996) Micromechanics: A New Approach to Studying the Strength and Breakup of Flocs. *Journal of Colloid and Interface Science* **184** 579-585.

Yukselen, M. A. and Gregory, J. (2004) The Reversibility of Floc Breakage. *International Journal of Mineral Processing* **73** 251-259.

CHAPTER 9
CONCLUSIONS

9 CONCLUSIONS

9.1 Method development

- A range of methodologies were developed to measure NOM floc structural characteristics. This included the measurement of floc size, growth, breakage and settling velocity.
- Analysis of floc size data identified small scale floc size changes at low rpm (< 50 rpm) and large scale changes at high rpm (> 50 rpm).
- A better understanding of floc breakage can be found by analysis of floc particle size distribution data.

9.2 The impact on floc structure of the seasonal variation in an organic rich water source

- A seasonal change in floc structure was observed a result of the combined effects of variation in NOM composition, NOM concentration and coagulant dose, although the specific effects of each of these factors could not be quantified.
- The most marked difference in structure was observed for autumnal water flocs. These flocs were larger and settled faster.
- Smaller floc structures showed reduced proportional breakage with increased shear.

9.3 How the natural organic matter to coagulant ratio impacts on floc operational properties

- An increase in the NOM fraction in the floc significantly reduced floc size, settling rate, strength, and degree of floc compaction.
- At low NOM concentrations primary particles in the floc allows strong interparticle bonds giving large and strong flocs.
- At high NOM concentrations bridging between primary particles due to the high concentration of adsorbed NOM gives rise to loose, open and weak structures.

- An empirical ratio of 1 mg Fe to 1 mg DOC gave the best combined NOM removal and floc structure.

9.4 The impact on floc structure of different treatment options

- The addition of a high MW cationic polymer (polyDADMAC) did not improve floc structure when used as a floc aid.
- Coagulation with ferric after anionic ion-exchange pre-treatment (MIEX®) gave rise to improved floc structure when compared to single stage ferric coagulation and the use of alum and polymer coagulation.
- Alum and ferric coagulants showed different floc structural characteristics at optimum coagulant doses. Ferric flocs gave rise to flocs that were larger and stronger than alum flocs.
- Of the treatment options considered the best to worst treatment options followed the order: MIEX® + Fe > Fe > Fe + polymer > Al > polyDADMAC.

9.5 The breakage, re-growth and fractal nature of NOM flocs

- Floc re-growth was seen to be limited for NOM flocs regardless of the coagulant used.
- The use of small angle light laser diffraction was not applicable to NOM flocs for the determination of floc fractal dimension.
- For model spherical systems (e.g. latex) floc fractal dimension was seen to increases after breakage followed by a decrease after re-aggregation. This was not seen for NOM flocs.
- An evaluation of floc fractal dimension techniques showed that NOM flocs were best evaluated using settling techniques. Using settling floc fractal dimension increased when 1) the optimum coagulant dose was applied and 2) as the organic fraction in a floc decreased.

CHAPTER 10

FURTHER WORK

10 Further work

The described work has presented a range of floc structural characterisation techniques that have been used to evaluate NOM flocs. By understanding NOM floc structure, WTW may be able to adapt their treatment processes in order to optimise floc removal during solid-liquid separation processes. However, more research is required in this area and should concentrate on:

(1) Floc structural characterisation from a range of NOM rich raw water sources. This work only presented data from a single organic rich raw water and therefore the findings of the work presented here cannot be universally applied to all low alkalinity and NOM rich water sources.

(2) The investigation of a further range of polymers on the impact on floc structure. This study presented data on polyDADMAC – a widely used cationic polymer of high charge density. In terms of combined performance of DOC removal and floc structure, this polymer performed poorly. However, a number of other commercial cationic and anionic polymers are available and should be evaluated as either primary coagulants or floc aids for NOM removal.

(3) A further understanding of the differences seen in floc structure between Fe and Al coagulants. This work has shown how these two coagulants give rise to different floc structure under optimum coagulation conditions, however the mechanistic explanation for these differences has not been adequately described. Work should include a fundamental analysis of the molecular attraction between NOM and the metal hydroxide for the different coagulants using tools such as atomic force microscopy.

(4) This work has shown that initial floc size indicates floc strength. The steady state floc size was reached after only 3-5 minutes for the NOM flocs investigated, with further slow stir period not giving rise to net increases in floc size. The impact of shearing flocs after just 5 minutes should be investigated to establish whether continued slow stir is necessary to subsequently improve floc structure. This could potentially reduce the operational flocculation time at WTW.

APPENDIX

METHOD DEVELOPMENT

APPENDIX
METHOD DEVELOPMENT

The following section describes the validation and reproducibility experiments carried out on firstly the settling column apparatus and secondly the floc size and breakage protocol. Initial method development experiments used kaolin suspensions due to the relative robustness of these flocculated systems when compared to organic flocs and the kaolin suspensions could be prepared relatively quickly and easily. The following section describes the settling column and floc size measurement.

A.1 Settling column

The settling column and image analysis systems were used to gather information on floc settling and size characteristics. The settling column apparatus are shown in Figure A.1. Particles were introduced into the settling column via a tapered entry port to ensure the flocs settled into the centre of the column. In order to avoid thermal currents disrupting floc settlement, the central settling column was enclosed by a water bath. The water bath was connected to a heat-refrigerated circulator to ensure a constant temperature was maintained in the column. A large column size was chosen in order to ensure wall effects had negligible effects on floc settling.

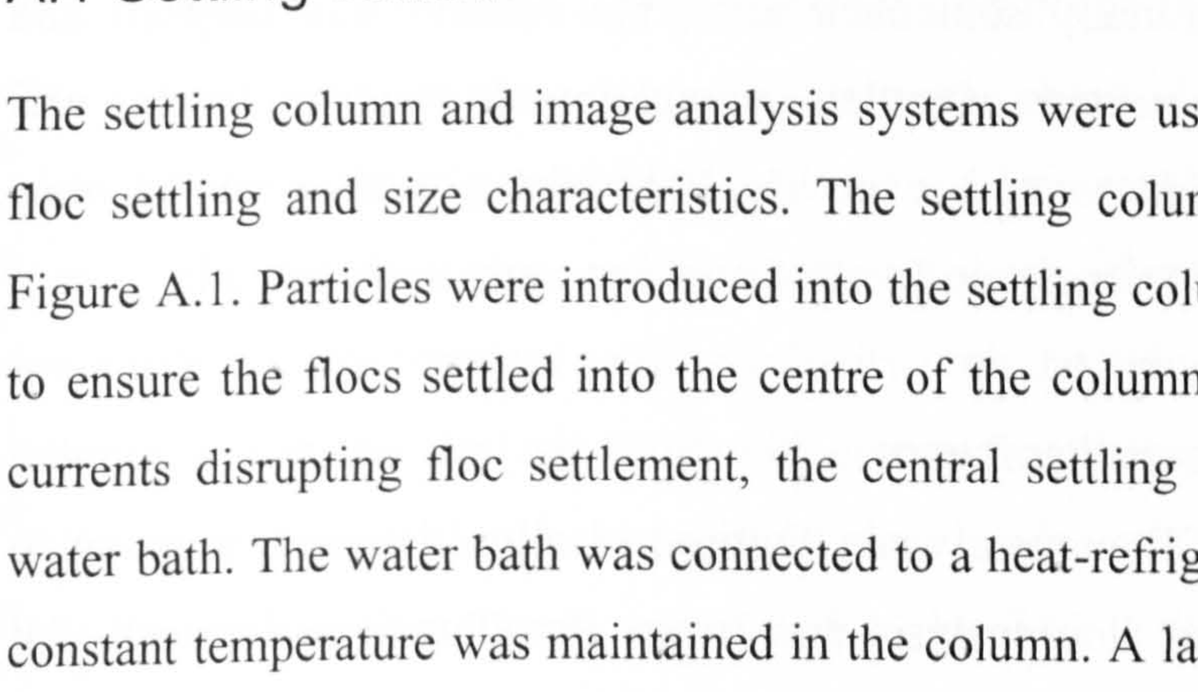

Figure A.1 Settling column apparatus. A = the CCD camera linked to PC and image analysis software; B = the central settling column contained within a sealed water bath; C = lamp for background lighting; D = temperature control unit for the water bath.

A.1.1 System set-up

On each occasion prior to settling column tests the following procedure was followed:

(1) The settling column was filled with de-ionised water and left to reach a temperature of 21.5 – 22.0 °C.

(2) A 1 cm microscope graticule with 100 graduations was suspended in the centre of the settling column to allow the CCD camera to be focused on the centre of the column and to enable the image analysis software to be calibrated.

(3) The graticule was removed and the tapered entry port placed in the column. A period of 2 hours was left for quiescent conditions to be reached.

(4) Particles were then added into the settling column (as described below).

(5) Upon completion of daily settlement tests, the column was emptied and cleaned ready for the next set of settlement experiments. Regular cleaning was found to be important to ensure no algal/bacterial growth occurred, thus maintaining a constant density and viscosity of the water in the column.

A.1.2 Image analysis tools and software

Source images from the CCD camera were digitised to allow image processing to occur. The software used for floc analysis was Image Pro Plus from Datacell. All captured images were converted into grey scale images with a bit depth of 16, providing 65,536 levels on the grey scale. Size measurements were made by comparing an aggregate image to an image containing something of a known size. In this case, a 1 cm microscope graticule with 100 graduations was used for system calibration. A focused image of the graticule was captured and digitised. Calibration was then achieved by specifying the number of units the reference graticule represents and, using the software drawing tools, by placing a defining line over the length specified. Because image analysis software bases measurements on pixel size a pixel/size unit scale is reported.

The arranged system ensures that only flocs falling in the same plane as the centrally positioned graticule will be in focus. The tapered entry port directs flocs towards the centre of the column to increase the chances of images being in focus. The accurate measurement of focused flocs is dependent upon the depth of field of the image. This is the combined distance in front and behind the central focusing point (CFP) of the

camera. Flocs may appear in focus even though they are not passing through the CFP, thus reducing the accuracy of any measurement made from flocs in front or behind the CFP. However, more accurate measurements may be made by increasing the magnification of the image because this reduces the depth of field. Ideally, the depth of field should be one floc diameter thus ensuring that flocs in focus will be passing through the CFP. In practical terms this is very difficult to achieve because the range of floc sizes may vary by up to 2 orders of magnitude. For the purposes of these experiments it was decided to use a relatively high order of magnification and accept some degree of error on measurements of small flocs. Very small flocs below 50 μm were ignored for this reason.

A.1.3 System calibration using standardised glass beads

The validity of the settling column system was checked by using standardised soda-glass spheres (Duke Scientific Ltd) of known diameter 99.1 μm ± 5.0 and density 2.45 g cm^{-3}. The beads are close to being perfect spheres, therefore a comparison of Stokes law predictions of terminal settling velocity with the value calculated from the settling column and image analysis tools will ensure that the system provides rigorous and valid results. The settling velocity of 40 glass beads were measured. The mean settling velocity of the glass beads was found to be 7.62 ± 0.54 mm s^{-1}. This compared favourably to a value of 7.7 mm s^{-1} as predicted by Stokes law using a water density of 1000 kg m^{-3} and viscosity of 0.001 Pa s^{-1}. It was therefore accepted that the system was able to accurately measure settling velocity.

A.2 Floc size measurement

The requirement to measure on-line floc size involved the evaluation of two available laboratory instruments: a photometric dispersion analyser (PDA) and a laser diffraction device (Malvern Mastersizer 2000). The two instruments can be operated in a continuous loop to allow dynamic monitoring of floc suspensions as they grow and break (Figure A.2).

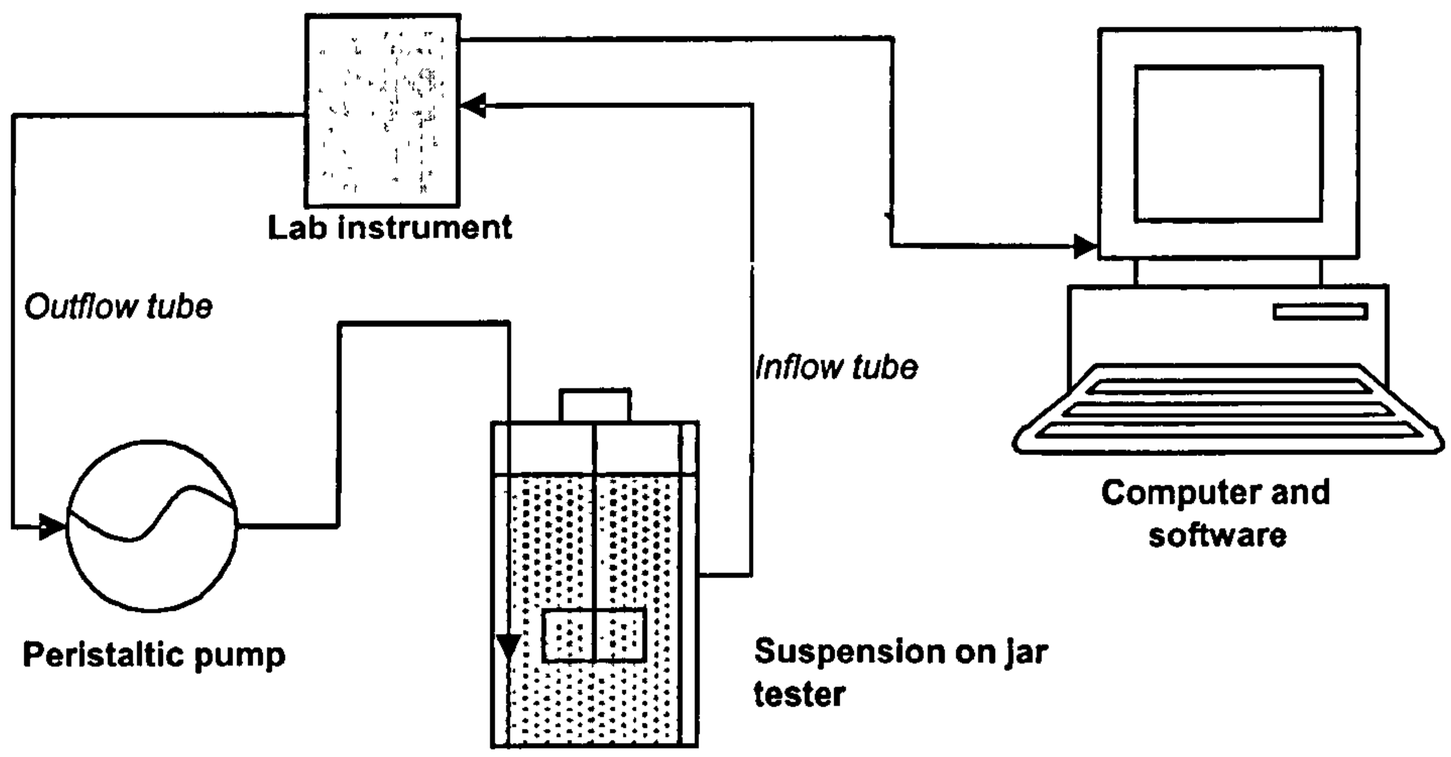

Figure A.2 System schematic showing the on-line measurement of floc size. The lab instrument refers to the either the PDA or the laser diffraction devices tested.

In order to provide the necessary shear to break the floc suspensions for both the PDA and Mastersizer instruments, a jar tester with controllable rpm was used. The calibration of the jar tester was checked by comparing the rpm displayed on the control panel with the real rpm as determined by frame by frame analysis of video film. As can be seen in Figure A.3 there was close agreement between the displayed rpm and the actual rpm, implying that the jar tester could be reliably used to provide controllable shear.

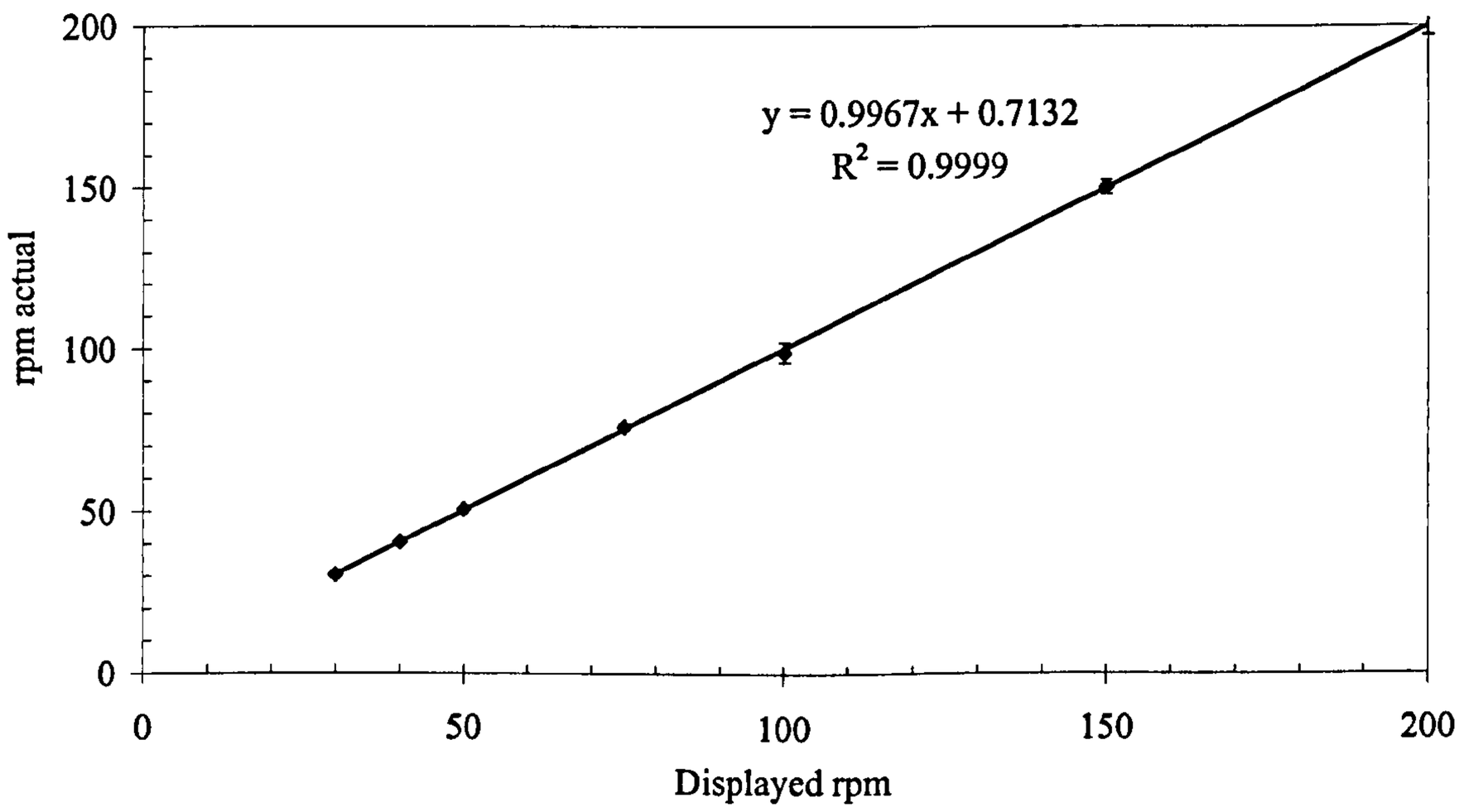

Figure A.3 The calibration of the jar tester.

An example of the growth and breakage profiles of kaolin flocs dosed with 8 mg L^{-1} using the PDA and Mastersizer devices are shown in Figures A.4 an A.5 for the following conditions: rapid mix at 200 rpm for 1.5 minutes; slow stir at 30 rpm for 15 minutes; breakage shear at 150 rpm for 15 minutes. As can be seen, the reproducibility using the PDA was not in as close agreement as the Mastersizer, this was particularly evident during the growth phase. Of more concern was the variation in shape of the growth profile as given by the PDA, whilst the Mastersizer gave a consistent growth profile. It was thought that bubbles interfered with the PDA result giving more unpredictable floc size estimation. A complete set of floc breakage experiments were therefore performed for rpm between 30 and 200 rpm using the Mastersizer (Figure A.6). As can be seen from the small standard deviation bands, there was little variation between the three repeats for all rpm under investigation.

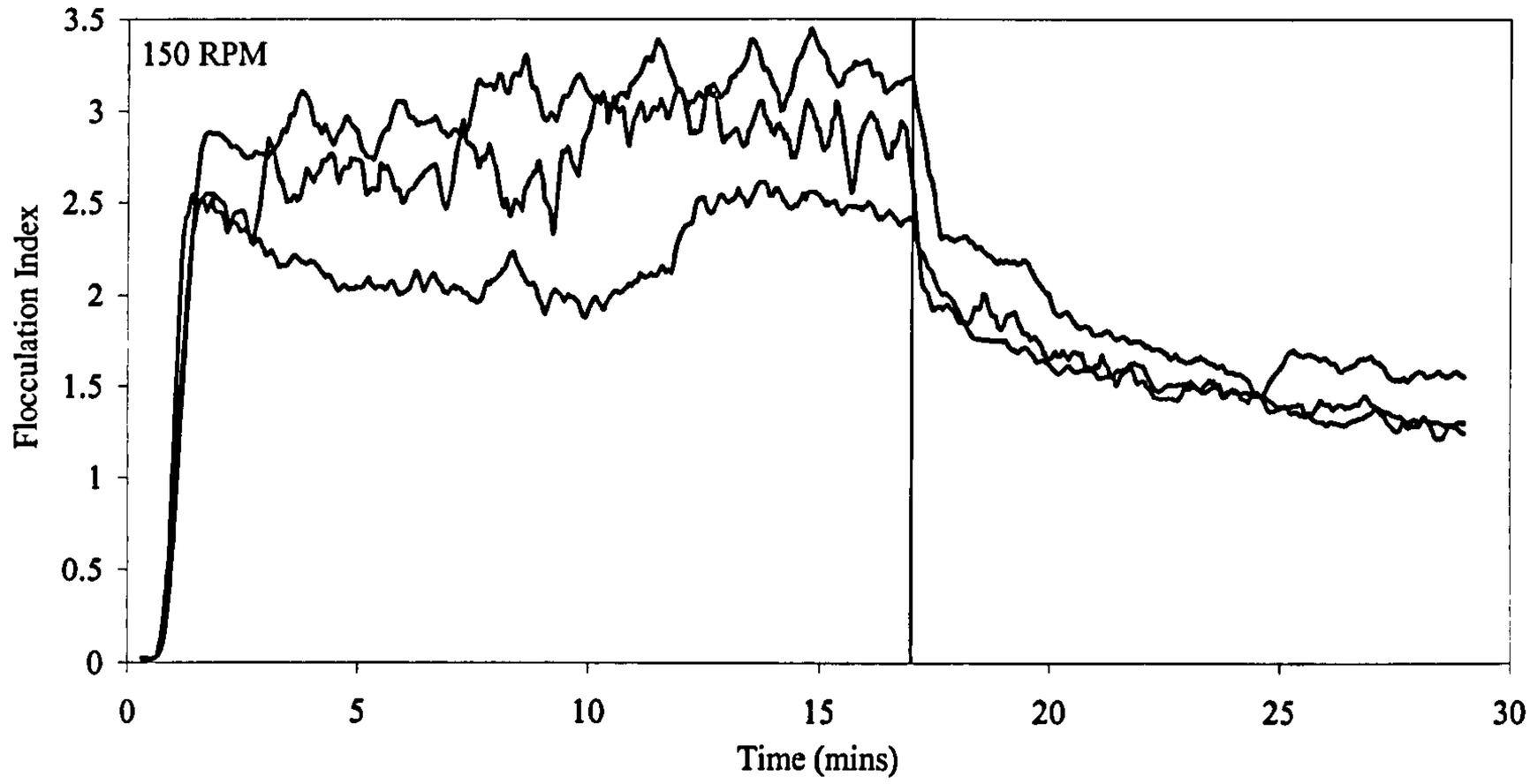

Figure A.4 The reproducibility of floc breakage experiments using the PDA device. Each line represents a single experiment performed under the same conditions with a breakage at 150 rpm (indicated by the vertical line).

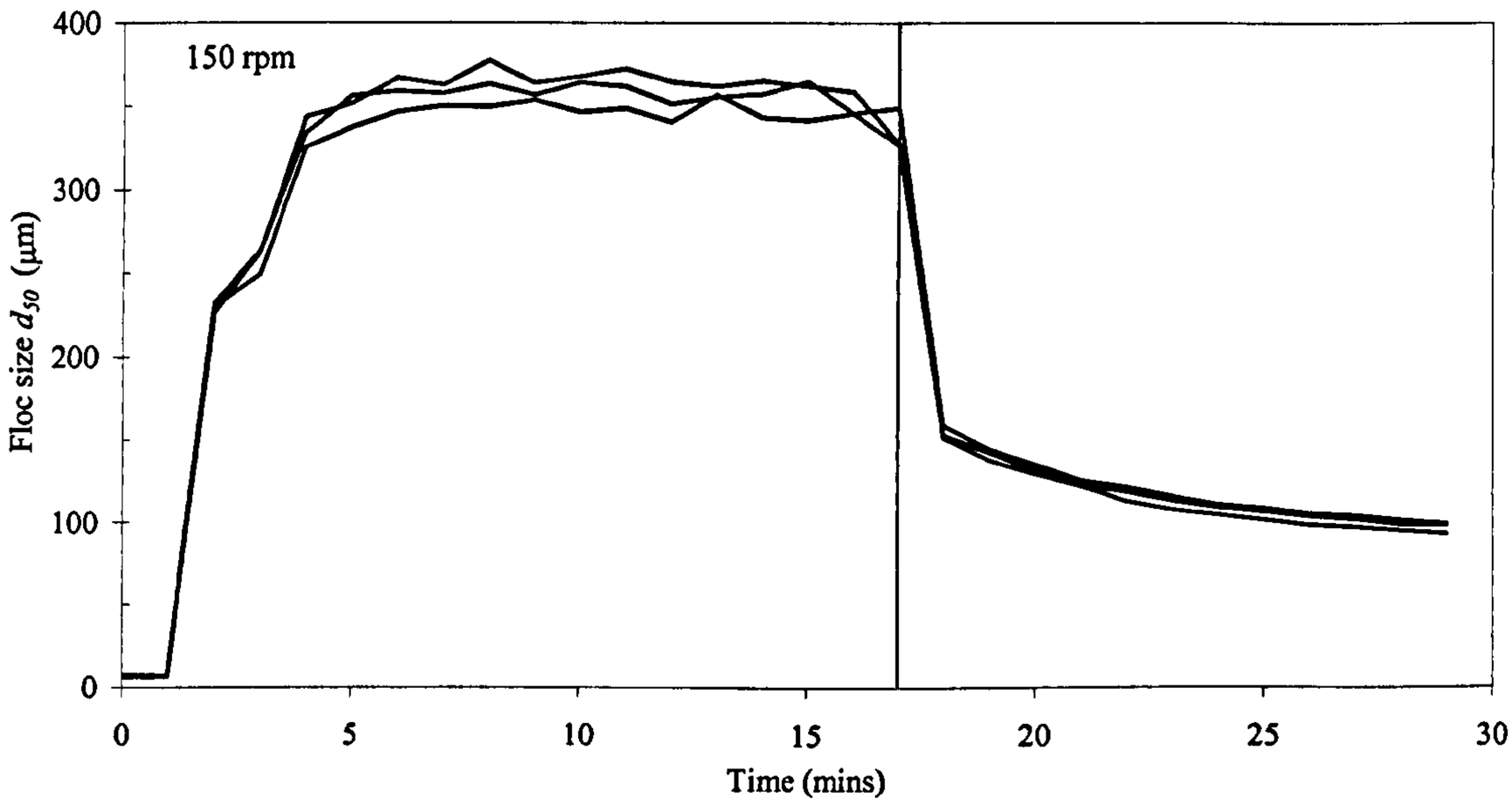

Figure A.5 The reproducibility of floc breakage experiments using the Malvern Mastersizer device. Each line represents a single experiment performed under the same conditions with a breakage at 150 rpm (indicated by the vertical line).

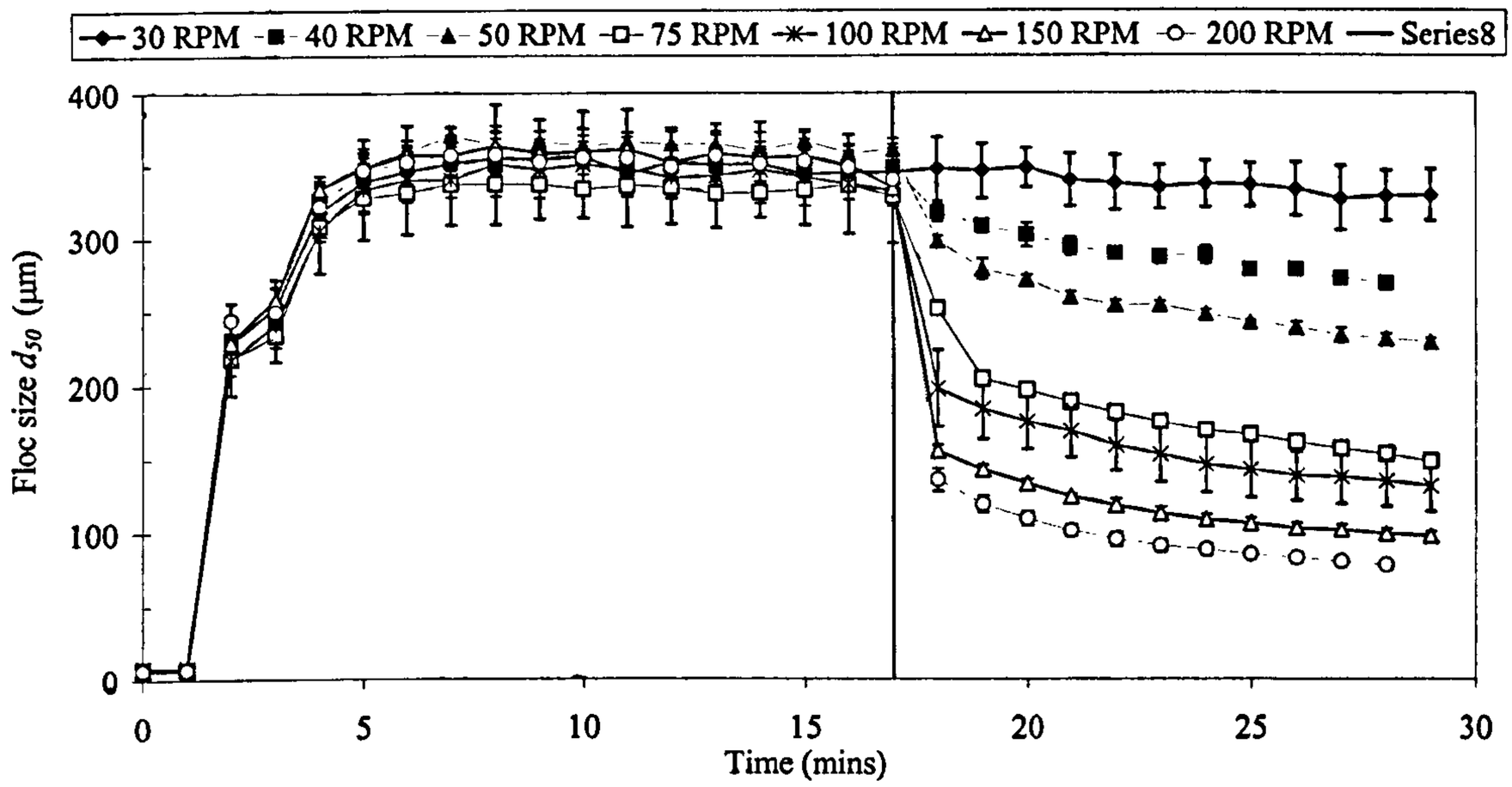

Figure A.6 Kaolin growth and breakage profiles for the median floc size (d_{50}) with increasing rpm for flocs formed at an initial slow stir of 30 rpm. Experiments were repeated three times for each rpm increase (indicated by the vertical line).

The floc sizes given by the laser diffraction instrument were verified using conventional light microscopy and image analysis software. Flocs were transferred from the jar tester using a wide mouthed pipette after the slow stir period (30 rpm) and after increased shear of 50, 100 and 200 rpm. Approximately 100 flocs from each set of rpm conditions were measured using this method.

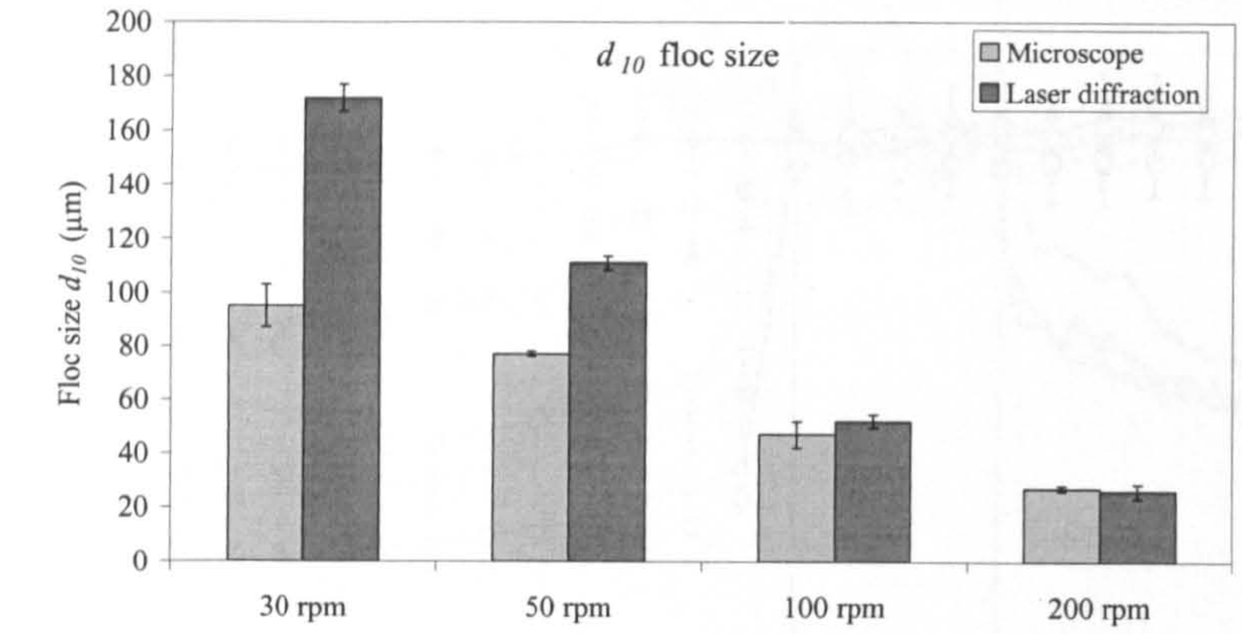

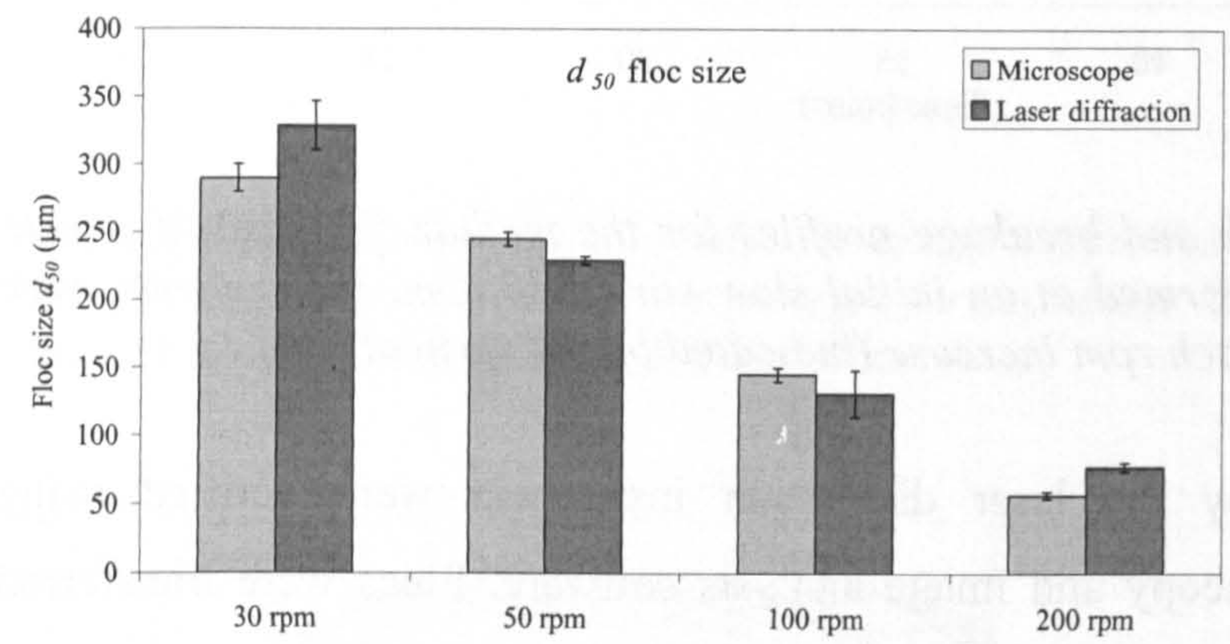

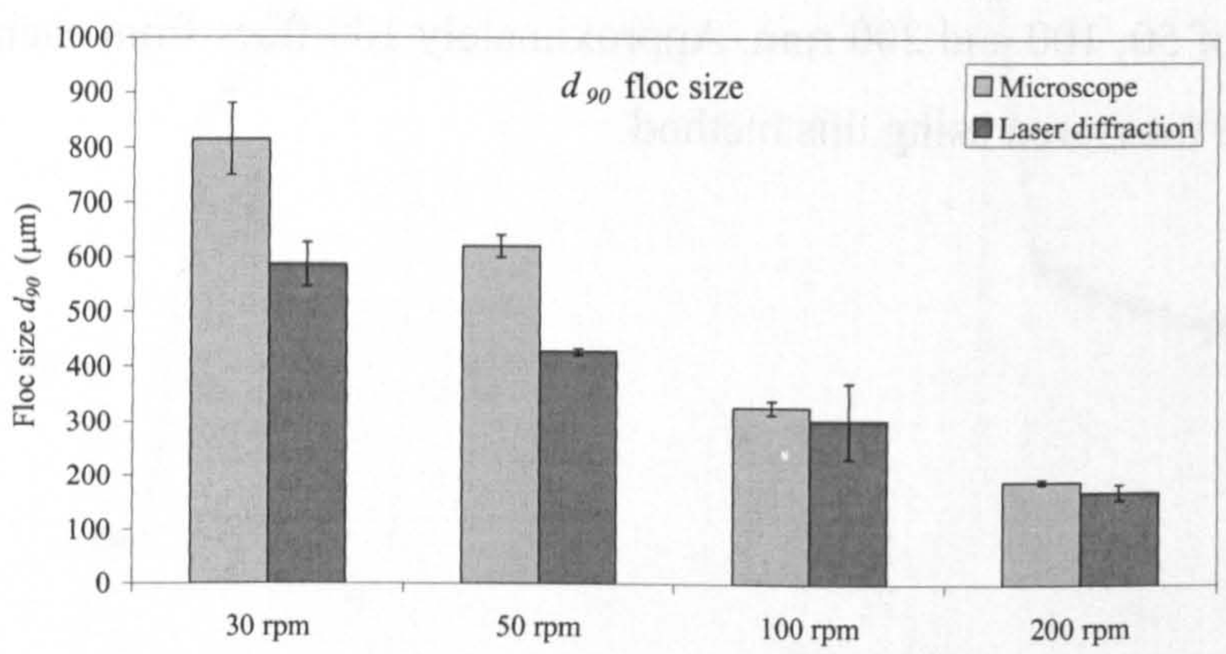

Figure A.7 A comparison of the d_{10}, d_{50} and d_{90} floc size as measured using microscopy and laser diffraction techniques.

As can be seen from Figure A.7 there was reasonable agreement between the two sizing methods. For the small particle sizes (d_{10}) the laser diffraction instrument tended to give an increased aggregate size which was more pronounced at lower rpm. This was likely to be a reflection of the bias of laser diffraction instruments towards larger particles due to the calculation of size from a particle volume. At higher rpm there were fewer larger particles due to floc breakage and hence the bias will be

reduced. The median floc sizes (d_{50}) were of a similar value for each of the techniques. The microscope technique gave floc d_{90} sizes that were larger than for the laser diffraction technique. This was a somewhat surprising result given the natural bias of laser diffraction to larger particle size. However, it was thought that flocs in the microscope cell underwent further aggregation during the transfer procedure or fell on top of one another giving rise to poor discrimination between individual flocs and hence an over estimation of size. These results show that while there were some differences in the resulting particle size using the two techniques, there was good agreement of the median particle size, suggesting that a high degree of confidence can be placed in these median values. Following from this, it was decided that the Mastersizer would be used to evaluate floc size during growth, breakage and re-growth.

The Mastersizer technique was then applied to NOM flocs. The rpm of the peristaltic pump was optimised for NOM flocs in order to insure that flocs were not affected by the pump speed. Flocs were formed using a humic solution at an approximate concentration of 10 mg L^{-1} and using ferric sulphate coagulant at 8 mg L^{-1} and pump speeds of between 4 and 20 rpm were investigated and the resulting floc sizes were compared as given by the Mastersizer (Figure A.8). At rpm of below 5, the flocs settled in the tubing and measuring cell of the system, therefore giving rise to significant under-sizing of the suspension. At 6 rpm the flocs did not settle in the tubes but became stuck in the measuring cell of the Mastersizer instrument, therefore floc matter accumulated giving rise to an over-sizing of the flocs. At 7 rpm, flocs were observed to flow through the system whilst above this rpm, significant floc breakage was seen in the tubing as reflected by the rapid decrease in floc size shown in Figure A.8. It was therefore decided that 7 rpm would be used for NOM flocs.

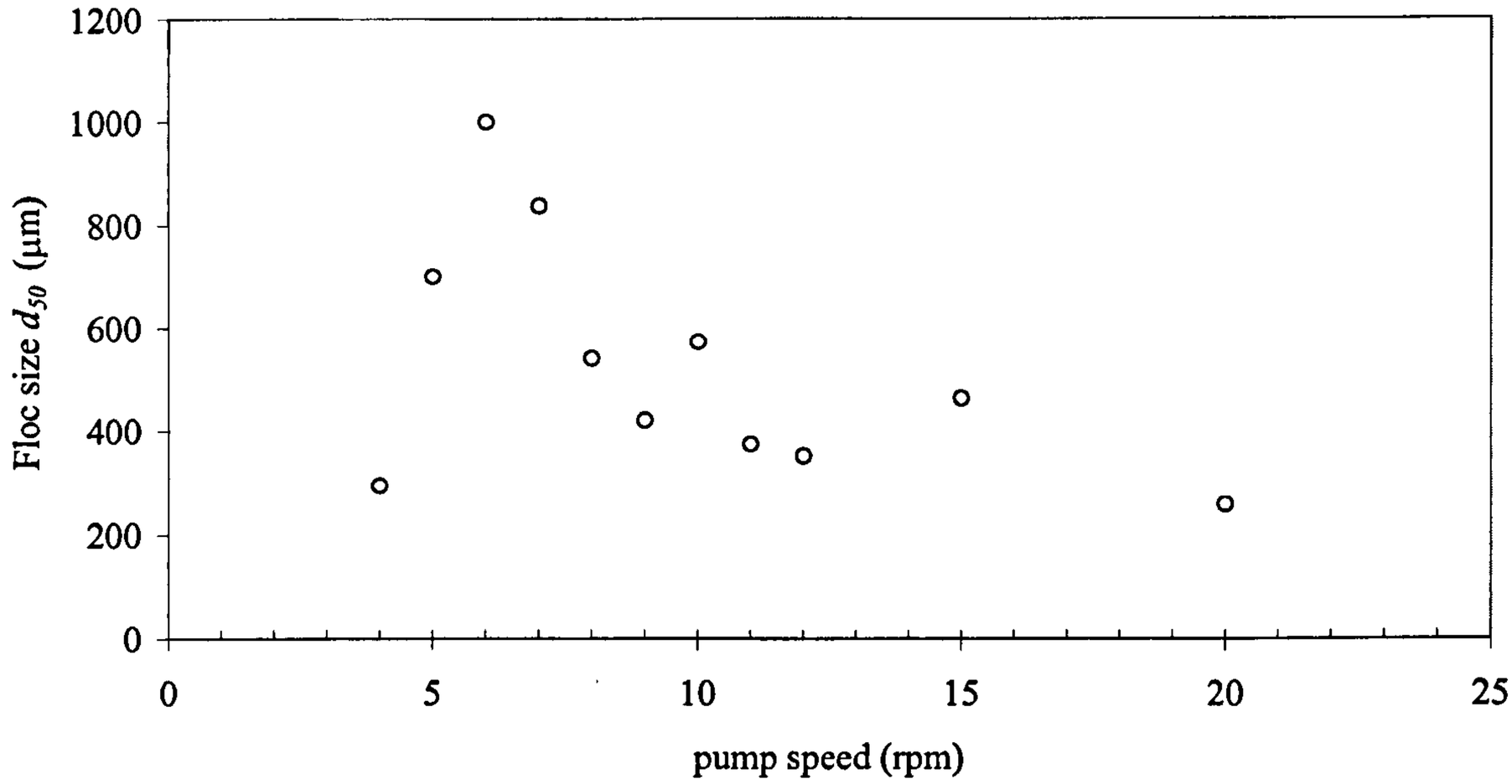

Figure A.8 The optimisation of the peristaltic pump speed for the measurement of NOM floc size.

Finally, as a validation of floc strength experiments for NOM flocs formed from a real NOM rich raw water, floc breakage experiments were performed and repeated three times for all breakage rpm. These experiments were then repeated again three times under the same coagulation conditions (pH 4.5, 12.1 mg L^{-1} as Fe). The resulting relationship between the broken floc size and the applied rpm was then compared. As can be seen from Figure A.9, there was very close agreement between experimental repeats. The equations of the lines were similar with the values of the slopes showing close agreement (-0.48 for trial 1 and -0.49 for trial 2). It was therefore concluded that the floc sizing and breakage technique was very repeatable and subsequent significant differences seen between floc breakage profiles were not as a results of experimental error.

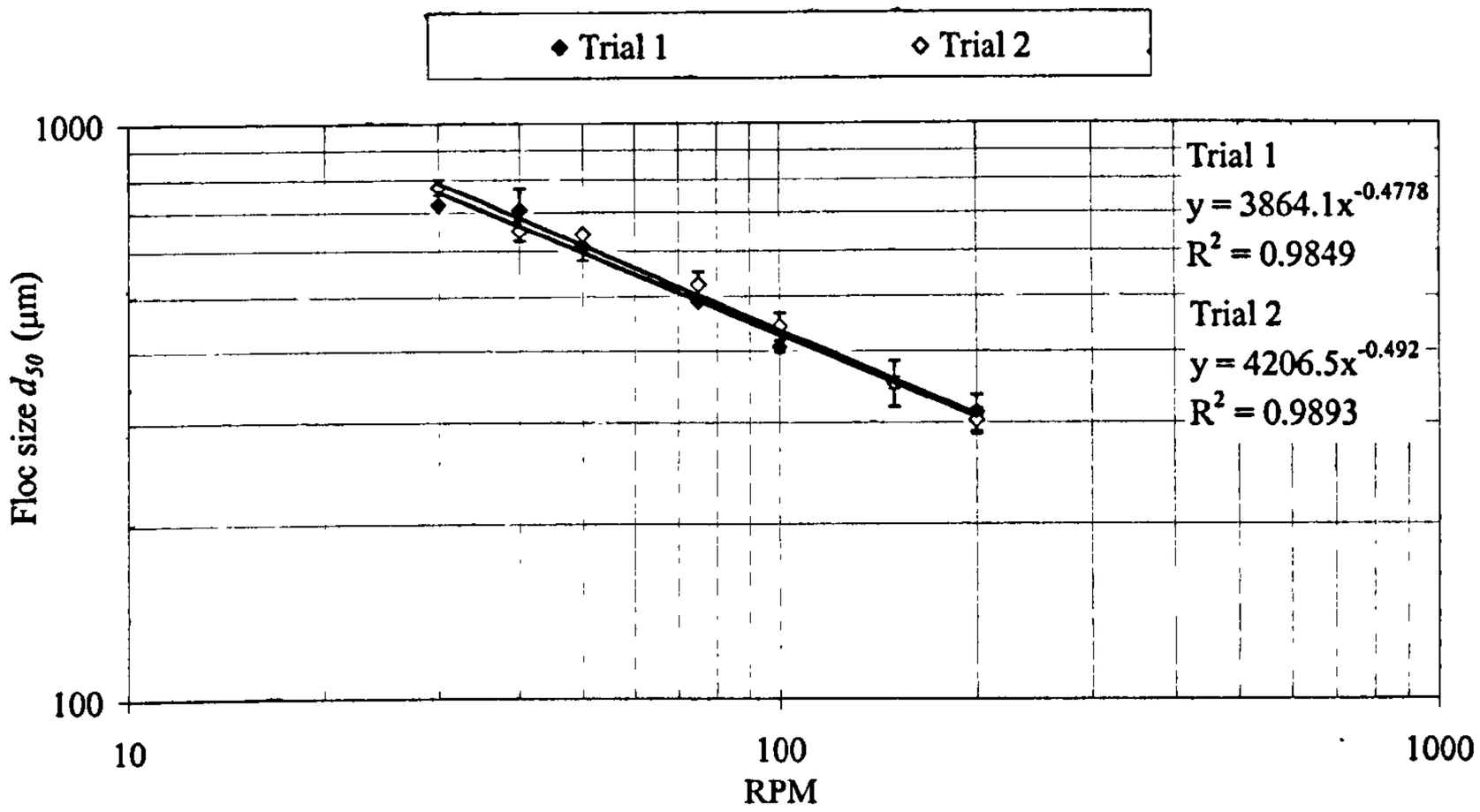

Figure A.9 The reproducibility of floc breakage experiments under the same coagulation conditions and on the same raw water.